ECFA 85/91
CERN 85-07
10 June 1985

THE GENERATION OF HIGH FIELDS for Particle Acceleration to Very High Energies

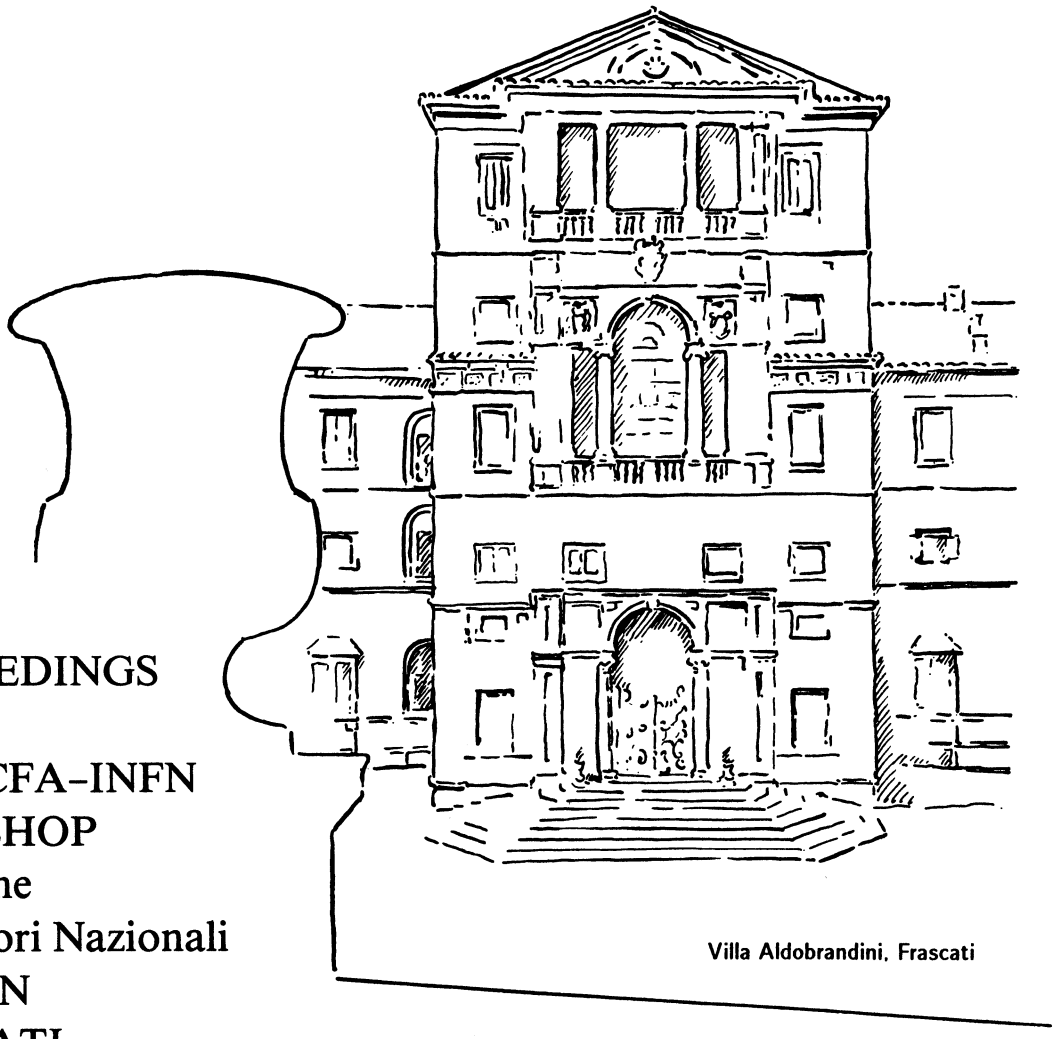

Villa Aldobrandini, Frascati

PROCEEDINGS
of the
CAS-ECFA-INFN
WORKSHOP
held at the
Laboratori Nazionali
dell'INFN
FRASCATI
September 1984

ECFA 85/91
CERN 85-07
10 June 1985

THE GENERATION OF HIGH FIELDS for Particle Acceleration to Very High Energies

PROCEEDINGS of the CAS-ECFA-INFN WORKSHOP Laboratori Nazionali dell'INFN

25 September - 1 October 1984

CERN — Service d'information scientifique-RD/669-3400-juin 1985

ABSTRACT

A Workshop organised by the CERN Accelerator School, the European Committee for Future Accelerators and the Istituto Nazionale di Fisica Nucleare was held at the Frascati laboratory of INFN during the last week of September 1984. Its purpose was to bring together an inter-disciplinary group of physicists to review ideas for the acceleration of particles to energies beyond those attainable in machines whose construction is underway, or is currently contemplated.

These proceedings contain some of the material presented and discussed at the Workshop, comprising papers on topics such as: the free-electron-laser, the lasertron, wake-field accelerators, the laser excitation of droplet arrays, a switched-power linac, plasma beat-wave accelerators and the choice of basic parameters for linear colliders intended for the TeV energy region.

FOREWORD

The Workshop was held at the INFN laboratory, Frascati, between 25 September and 1 October 1984, as a sequel to the ECFA-RAL meeting "The Challenge of Ultra-high Energies" held two years previously at New College, Oxford. The purpose was to bring together physicists from the accelerator, plasma and laser fields to review progress in some of the unconventional approaches to particle acceleration and accelerator power sources, and to define questions deserving further study. At the same time a major objective was to foster increased activity in these areas in Europe, and with this in mind the organisers decided on a mainly 'tutorial' approach through working groups.

Following a day of invited, introductory talks there were four days for the work of the groups, interspersed with special topic seminars, and a half day of summary talks. The programme, including names of speakers and the convenors of the working groups, is shown below. There were 86 active participants of whom about 30% were from the plasma and laser fields, indicating that a reasonably broad distribution of disciplines was achieved. If the interest and enthusiasm generated by the discussions are any guide, there is good reason to hope that additional effort will be applied to the many problems of achieving higher energies.

By its nature, the workshop was not expected to generate much new material for publication in these proceedings and several of the presentations to the working groups and the special seminars were based on material already in course of publication. On the other hand a few papers on topics initiated in discussions at Frascati and pursued further afterwards are included; a notable example is the paper by W. Willis on a switched-power linac.

At Frascati the great technical difficulties which confront the designers of linear-colliders when high luminosity is required, as well as high energy, were much more clearly brought out than at the Oxford meeting in 1982. A range of extremely challenging problems were identified which are independent of the means of acceleration, and which are as demanding of serious effort to reach an understanding of the boundaries of feasibility (on emittance, bunch size, wakefield effects, etc.) as are the ideas for new acceleration methods.

The relationship between energy and luminosity was nicely illustrated by Carlo Rubbia in his 'key-note' address. Unfortunately other pressures on Carlo since Frascati - including such welcome diversions as the award of a Nobel Prize shared with Simon van der Meer - have left him no opportunity to write-up his paper for inclusion in these Proceedings. However the figure on p. viii is from his talk, and shows why he called for a luminosity of 10^{34} cm^{-2} s^{-1} for an e^+e^- collider with a centre of mass energy of 10 TeV. Subsequently it was suggested (by John Rees) that a new unit of luminosity should be coined: 1 Carlo $\equiv 10^{34}$ cm^{-2} s^{-1}.

Finally, on behalf of the organising committee (see below) we should like to thank our generous financial sponsors CERN and INFN, our hosts at Frascati, the speakers, convenors, and participants, our many helpers at Frascati, and in particular Suzanne von Wartburg the CAS secretary, Barbara Strasser, who has worked tirelessly on the proceedings, and Sylvia Giromini of Frascati without whose efforts nothing would have been possible.

P. Bryant
J. Mulvey
Editors

Organising Committee

P. Bryant (CERN), G. Coignet (LAPP), R. Evans (RAL), K. Johnsen (CERN), J.D. Lawson (RAL), J. LeDuff (LAL), J.H. Mulvey (Oxford), W. Schnell (CERN), R. Sigel (MPI, Garching), S. Tazzari (INFN, Frascati), V. Vaccaro (Napoli), G. Voss (DESY), W. Willis (CERN).

PROGRAMME FOR FRASCATI WORKSHOP ON THE GENERATION OF HIGH FIELDS FOR PARTICLE ACCELERATION

WORKING GROUPS AND CONVENORS

1. IFEL and FEL
   A. Renieri
2. Near-field structures
   T. Weiland/
   A. Sessler
3. Plasma beat-waves
   C. Joshi
4. Accelerator considerations
   W. Willis

Time \ Date	Tuesday 25 September	Wednesday 26 September	Thursday 27 September	Friday 28 September	Saturday 29 September		Monday 1 October
09.00	Registration	Organisation of Working Groups	Seminars b) R. Palmer c) W. Barletta	Seminars e) A. Sessler f) A. Kolomensky g) J. Nation		Sunday excursion to Ostia Antica	Working Groups
10.00	Opening Address N. Cabibbo						
10.30	Coffee						
11.00	HEP and HE Accelerators C. Rubbia	Working Groups					Working Group Reports Group 1: A. Renieri Group 2: A. Sessler Group 3: C. Joshi
12.00	Laser Accelerators: Where do we stand? J.D. Lawson						
13.00	Lunch						
14.30	Two-beam, Wake Field & mm Wave Accelerators T. Weiland	Working Groups					Group 4 and Workshop Summary M. Tigner
15.30	Coffee						
16.00	Waves in Plasma J. Dawson	Seminar a) J. Wurtele	Seminars d) R. Evans W. Funk H. Henke W. Bialowans S. Takeda P. Wilson M. Tigner	Working Groups			Concluding Remarks E. Laing
17.00	Survey of Modern Pulsed High-Power Lasers K. Witte						
18.00							

SEMINARS:

a) Microwave radiation from a high-gain FEL amplifier
b) Laser plasma-droplet linac collider
c) Brightness development for induction linac
d) Reports on experiments in progress
e) Optical guiding by an FEL or IFEL
f) Longitudinal field for FEL
g) Space-charge-wave accelerators

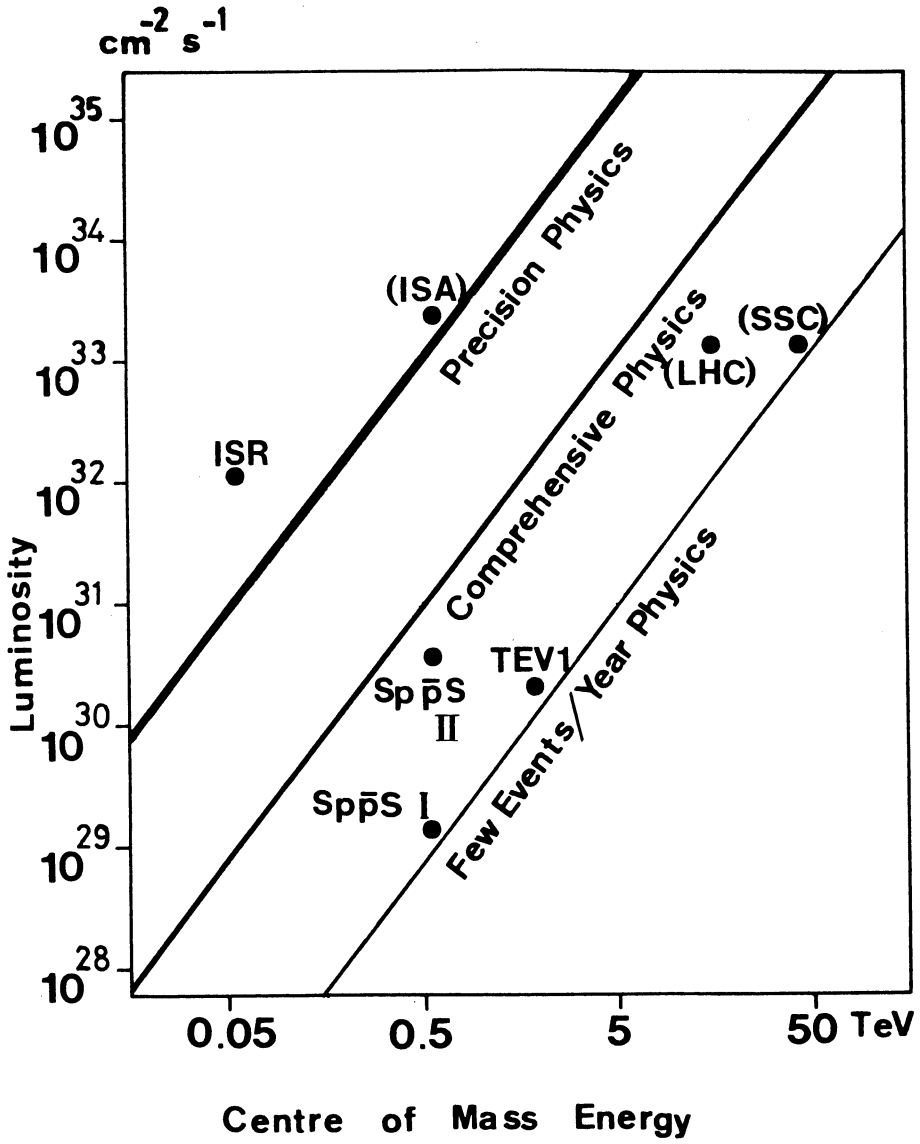
cm-2 s-1
Luminosity
10^35
10^34
10^33
10^32
10^31
10^30
10^29
10^28
(ISA)
Precision Physics
(SSC)
(LHC)
ISR
Comprehensive Physics
TEV1
Sp p̄S II
Sp p̄S I
Few Events/Year Physics
0.05
0.5
5
50 TeV
Centre of Mass Energy

OPENING ADDRESS

N. Cabibbo

Istituto Nazionale di Fisica Nucleare, Ufficio di Presidenza, I-00186 Rome.

I am pleased to be able to welcome you here today to this Workshop. Whenever one speaks about accelerator techniques, at some point one shows the so-called Livingston chart, but today will be an exception because I do not have it with me. This chart shows that the energy of accelerators has been increasing exponentially with time. Now this increase has been made possible by a succession of what one could call "phase transitions", and these transitions are the ways in which we conceive accelerators and accelerator building.

One transition in fact, took place here in Frascati and this was the so-called ADA project, which was the birth of the concept of particle-antiparticle colliding beam accelerators and has not this kind of accelerator dominated our physics in the last fifteen to twenty years? There are other transitions that you may not recognise as transitions in accelerator technology but they are no less important. One of them has certainly been the founding of CERN, which opened the era of international collaboration for accelerator building. Another transition is what you could call the "exo-geographical transition" and it is also connected with CERN. The idea is that you can build an accelerator, such as the SPS, without owning the land on which, or rather under which, the accelerator is built. Now this transition is a new idea in accelerator building, and it is certainly one which has been essential for enabling Europe to remain at the forefront of the accelerator field. We could not build new large accelerators in Europe if we could not build them underground in this way. It is this transition that has rendered possible the next generation of machines such as LEP; machines so large that in order to perceive them you will need a geographical map. Once you accept the dimensions of LEP you have within the next ten to fifteen years the possibility of further increases of energy with the conception of machines of similar dimensions, but machines which are proton-proton machines and not electron-positron machines.

At this point it seems that our ideas end, in the sense that it is difficult to conceive that you could go much beyond LEP dimensions for the next stage. So if we want to explore yet higher energies and if we want to keep pace with this famous Livingston extrapolation of energy versus time, we have to invent something new, something of the kind that you are going to discuss here. I think this Workshop, although it is discussing ideas very far from practical realisation at the moment, is certainly an important step for what we will be doing in maybe twenty to thirty years. So good work, and thank you.

CONTENTS

*) No contribution received.
**) Abstract only.

LASER ACCELERATORS: WHERE DO WE STAND?

J D Lawson
Rutherford Appleton Laboratory, Chilton, Oxon, OX11 0QX, UK

ABSTRACT

Numerous proposals for accelerating particles using laser light have been made over the past twenty years. After a brief historical review the current status of four categories of accelerator is reviewed. These are 1) near field (e.g. grating), 2) far field (inverse FEL) 3) inverse Cherenkov, and 4) beat wave.

1. HISTORICAL INTRODUCTION

It is now twenty—two years since the first published paper, by Shimoda[1], proposing the use of a laser to accelerate particles. The mechanism described was the inverse Cherenkov effect in a gas. In the same year (1962) Lohmann in an unpublished IBM report proposed the use of illuminated gratings to exploit the inverse Smith-Purcell effect[2]. He also considered acceleration in the fields near dielectrics in which total internal reflection is occurring, and noted that the E_z field associated with these surface waves drops to zero as their phase velocity approaches that of light. To overcome this problem he proposed the use of fields midway between two surfaces. In 1980[3] Palmer pointed out that single-sided grating systems can support waves for which E_z is finite when $\beta < 1$ provided that $k_\perp > 0$. This corresponds to waves moving at an angle other than 90° to the grating lines.

Another scheme, now recognised as a form of the 'two wave' interaction used in the free electron laser was proposed by Kolomenskij and Lebedev in 1966[4]. This was again proposed independently by Palmer in 1972[4a]. (Indeed, Palmer suggests the free electron laser, at that time only considered in quantum mechanical terms). The physical principle used is essentially that put forward in connection with microwave tubes by Gorn in 1947[5], and embodied in the ubitron millimetre wave generator[6].

In 1972, Rosenbluth and Liu analysed the setting up of a longitudinal electrostatic plasma wave by two coincident laser beams of frequency ω and $\omega + \omega_p$[7]. A proposal for an accelerator based on this principle, the 'beat-wave accelerator', was made by Tajima and Dawson in 1979[8]. Essential modifications to deal with the problem of phase slip were later made by Katsouleas and Dawson[9].

Many papers on the laser acceleration of particles have by now been written, and other suggestions have been made. Some of these are not sufficiently developed to be readily intelligible, others seem to be

fallacious, and yet others, though maybe of interest, are unlikely to be relevant to ultra high energies.

2. CATEGORIES OF LASER ACCELERATOR

2.1 Introduction

There are many ways of classifying laser accelerators; here the three basic categories identified at the Los Alamos workshop[10] will be used. First, we note that it is not possible in free space to have a wave with phase velocity $v < c$ and an electric field in the direction of propagation. To produce a slow wave, the presence of some matter is required. This can be in the form of a dielectric or plasma medium through which the beam passes. Alternatively, it can take the form of a periodic metal structure, or a dielectric rod or slab. The particles in this case travel in vacuum close to the structure. Conventional synchrotrons and linacs fall into this class, the 'structure' in this case being an array of cavities, (or a few cavities repeatedly traversed).

If no matter is present, two waves of different frequency are required. In the inverse free electron laser one of these 'waves' is the magnetic wiggler, which has finite k but zero frequency. In such schemes the accelerated particles execute transverse as well as longitudinal motion.

In the next sections we examine the possibilities and constraints of these various approaches. The category of 'media' accelerators can be conveniently be divided into two, depending on whether the medium is a dielectric or a plasma.

2.2 Near Field Accelerators

The simplest form of slow-wave, with phase velocity less than c and a component of E in the direction of propagation is the evanescent plane surface wave. This can be supported by a grating or plane dielectric surface. If the phase velocity in the z-direction is βc, then the field decay distance is $\beta\gamma\lambda\!\!\!^{-}$ and the ratio of the field components $Z_o H_x : E_y : E_z$, where y is measured perpendicular to the surface, is $1 : 1/\beta : 1/\beta\gamma$. As $\gamma \to \infty$, $E_z/E_y \to 0$ and so a single wave component is not suitable for acceleration of relativistic particles.

There are two ways out of this difficulty. Waves can be combined in such a way that on a symmetry plane or symmetry axis the transverse fields cancel. In the limit of $\beta \to \infty$, E_z remains, but the transverse fields rapidly grow away from the axis, equalling E_z at a distance of order $\lambda\!\!\!^{-}$.

Such waves are familiar in disc loaded linacs, or fourier components of fields in cavity arrays. The constraint associated with this configuration is that particles must be near the surface. Furthermore, symmetry requires a closed rather than open system.

The second alternative is to retain an open system, but to make k_x non-zero. (This is Palmer's suggestion for a plane grating). In order to contain the field either a boundary must be provided, or a cylindrical system with finite azimuthal mode number used. For example one might use an inside-out disc loaded guide, or washers mounted on a solid rod. Another possibility would be a dielectric coated rod.* A compact transverse pulse on a wide grating will not propagate without dispersion. Lack of symmetry in an open system gives problems in focusing[11].

Both closed and open systems would be physically very small at optical wavelengths. All the criteria for designing conventional linacs apply.

2.3 Far Field Accelerator

Far field accelerators depend on the 'two-wave' interaction, sometimes known as the Compton effect. To demonstrate the physical features of this interaction we consider two oppositely travelling circularly polarized waves, with opposite helicity, interacting in a resonant manner with a relativistic particle. Imagine first a near-relativistic particle moving at velocity $\beta_z c$ in the same direction as a circularly polarized plane wave with frequency ω_1. Viewed in the laboratory frame the particle experiences a constant field $E_1(1 - \beta_z)$ perpendicular to the direction of motion rotating at an angular velocity $\omega_1(1 - \beta_z)$. Suppose now a wave is coming in the opposite direction with frequency ω_2. This will give rise to a rotating force $E_2(1 + \beta_z)$. The effects of the electric and magnetic fields add, and a particle of rest mass m_o moves in a helical orbit of radius $(1 + \beta)eE_2/\gamma m_o\omega_2^2$ and wavelength $2\pi c/\omega_2(1 + \beta)$. This imparts a transverse velocity $2\pi rc/\lambda$, which is equal to $(1 + \beta)^2 eE/\gamma m_o\omega_2$. If, now, the two fields are made resonant, by choosing $\omega_1/\omega_2 = (1 + \beta)/(1 - \beta) \approx 4\gamma^2$, the field from the first wave rotates at the same rate as the particle rotates along the helix. The electric field from the first wave can be resolved into two components, one along the helix and the other perpendicular to it. Particles will then receive continuous acceleration or deceleration according to their phase on the helix. As presented, this analysis is only valid when $\gamma\theta_s$, where θ_s is the spiral pitch, is small; when this is not so the factor $4\gamma^2$ between the two wave frequencies is reduced.

---

*) A further suggestion, a 'structure' consisting of two adjacent rows of spheres was made at the meeting by Palmer.

Since the transverse velocity is much less than $\beta_z c$, the accelerating field and particle motion are almost perpendicular; the interaction is a second order effect and needs very high fields in the short wavelength (laser) beam if a high accelerating gradient is to be achieved.

The second wave could be replaced by a guided wave, furthermore its direction can be different provided that the appropriate resonance condition is fulfilled[12]. In practice it is probably more convenient to replace it by a twisted transverse magnetic field. This is done in the free electron laser. This has the same effect, and forces the particle into a helix of wavelength equal to Λ the twist length. The relation $\omega_1/\omega_2 \approx 4\gamma^2$ is replaced by $\Lambda / \lambda_1 \approx 2\gamma^2$. Sometimes it is more convenient experimentally to replace the twisted magnetic field by a transverse one which alternates in sign. Motion is in one plane only, but the general principle of operation is the same.

Fortunately the theory of free electron lasers is well developed, and may readily be used in assessing the potential of the two wave and wave plus wiggler (IFEL) schemes. Synchrotron radiation imposes a limit for electrons, and the problem of focusing the laser light over long distances is difficult. A waveguide with glancing incidence has been proposed for this[13].

2.4 Inverse Cherenkov Accelerator

In a medium of refractive index n a plane wave at an angle less than $\cos^{-1}(1/n)$ to the z-axis has a phase velocity less than that of light in free space. Furthermore, there is a component of electric field in the direction of propagation. Such a wave will accelerate particles passing through the medium. Obviously this must not be too dense, or the particles will be scattered. If it is too dilute, however, $\cos^{-1}(1/n)$ is small, and the accelerating field is small compared to the transverse fields. As with near field accelerators a cylindrical geometry can provide a pure z-field on the axis, but transverse fields are necessarily large elsewhere. The performance is thus limited both by scattering and breakdown in the dielectric. The problem has been analysed by Fontana and Pantell[14].

2.5 Beat-Wave Accelerator

In a plasma, longitudinal electrostatic waves ('Langmuir waves') can be propagated. The plasma frequency $\omega_p = (ne^2/\varepsilon_o m_o)^{\frac{1}{2}}$ is independent of k, so that the group velocity is zero. The field arises from alternate bunching and rarefaction of the electron density, and has a limiting value when the rarefaction has reduced the local density to zero. Of course the waves are

highly non-linear near the limiting amplitude, and the critical field is

$$E_z = \alpha\, m_o c \omega_p / e = (m_o c^2/\varepsilon_o)^{\frac{1}{2}}\, n^{\frac{1}{2}}$$

where α is a constant of order unity. It is interesting to note that this expression is independent of k, and hence of the phase velocity of the wave. Insertion of quite modest plasma densities yields spectacular values of E_z.

The question is, how can we set up such a wave? Tajima and Dawson's suggestion[8] is to use two lasers with frequencies ω_1 and $\omega_1 + \omega_p$. This sets up a 'beat-wave' with wavelength about $2c/\omega_p$. The gradient of $\langle E^2 \rangle$ associated with this beat-wave represents a ponderomotive force which builds up the plasma wave. For collinear laser beams the group velocity of the laser waves, $c\,(1 - \omega_p^2/\omega_1^2)^{\frac{1}{2}}$, is equal to the phase velocity of the beat wave; it is therefore resonantly driven as the waves pass through the plasma. The physics in a real plasma is very complicated and highly non-linear at field levels of interest. It is not at all clear what happens in practice. To find out, experiments are needed.

The attraction of the scheme is that very much higher fields appear to be possible than in any of the other proposals. It has been suggested that the difference in phase velocity between the particles and the beam be overcome by staging, or not having all three beams (particle and laser) collinear[9,15].

3. PRESENT STATUS AND FUTURE PLANS

3.1 Introduction

In this section the present status of the various concepts is noted. Some suggestions are made with regard to further action. The vital question of objectives is not discussed here, but a series of questions posed to help to define these more clearly is discussed in a companion paper[16]. Although specifically dealing with the beat-wave scheme the first part of the paper is of general relevance.

3.2 Near Field Accelerators

It was argued in 2.2 that near field laser accelerators are essentially miniature linacs. All the same criteria apply for assessing their performance and usefulness. Perhaps a broad general survey, from decimetre to laser wavelengths, would be a more profitable enterprise than looking only at laser wavelengths. It might be of interest to study the implications of open waveguides at longer wavelengths, (this has been

started at Cornell, by Tigner and Pickup).

3.3 Far Field Accelerators

Both two beam and beam plus wiggler schemes were studied at the Los Alamos workshop. Two difficulties were identified; first, that of focusing the laser beam over long lengths, or alternatively of staging, and second, synchrotron radiation loss which becomes very severe at a few hundred GeV for electrons. At Oxford in 1982 a modified design capable of going to higher energies was presented by Pellegrini[17], and the use of a waveguide with transverse dimensions of many wavelengths, operating in the lowest mode was suggested for transporting the laser light. More specific proposals for the waveguide, in which two walls are loaded with a thin dielectric coating, were later given by Pellegrini et al[13].

The basic physical foundation for this concept is sound and well understood. The task is now to arrive at some sort of realistic design that has interesting parameters and acceptable cost. This requires good liaison between laser and accelerator physicists, and a great deal of detailed work. The task should, however, be straight-forward.

3.4 Inverse Cherenkov Accelerator

Relatively little work has been done on the inverse Cherenkov accelerator. Some sketchy ideas for an accelerator were outlined at Los Alamos, and a proposal for some experiments made. The most complete assessment of the concept is in ref.12. Viewed in the light of the requirements for high energy particle physics does this remain a concept worthy of further investigation? The physics is fairly well based, and any study requires the co-operation of laser and accelerator physicists.

3.5 Beat Wave Accelerator

It is in this, the most 'exciting' of the proposals, that the physics is most uncertain. The link between the physical process and some sort of credible 'scheme' has not yet been made. An excellent start in this direction was made by Ruth and Chao, though their work seems to have made little impact[18]. An attempt to follow up their idea and look at some of the requirements for an actual accelerator was made by the RAL study group[19]. This showed formidable problems, but again no comments have been received. If the accelerator community is to make any progress, simple relationships (maybe containing uncertain numerical factors) between the basic parameters must be available. It is important that accelerator physicists acquire some understanding of the plasma physics, and also that the plasma physicists find out what it is that accelerator physicists need

to know and are trying to do. Laser experts must be in close touch to say what can, in principle and in practice, be done with lasers. Some basic questions are set out in a companion paper[16].

4. CONCLUSION

The way ahead for further systematic investigation of the schemes that have been proposed for laser acceleration of particles is clear. It is important now that their potential is measured against the presently perceived requirements for particle physics research in the next century.

* * *

REFERENCES

1. K. Shimoda, Applied Optics 1, 33, (1962).
2. A. Lohmann, "Electron Acceleration by Light Waves", Unpublished IBM Technical Note TN5, San Jose, Oct 3, 1962.
3. R. B. Palmer, Part. Accel. 11, 275, (1980).
4. A. A. Kolomenskij and A. N. Lebedev, Soviet Phys. JETP 23, 753 (1966).

4a. R. B. Palmer, J. App. Phys. 43, 3014, (1972).

5. E. J. Gorn, U.S. Patent 2, 591, 350, filed 1947.
6. R. M. Phillips, IRE Trans. Elec. Devices ED7, 231, (1960).
7. M. N. Rosenbluth and C. S. Liu, Phys. Rev. Lett. 29, 701, (1972).
8. T. Tajima and J. M. Dawson, Phys. Rev. Lett. 43, 267, (1979).
9. T. Katsouleas and J. M. Dawson, Phys. Rev. Lett 51, 392, (1983).
10. P. J. Channell, (Ed) 'Laser Acceleration of Particles', (Los Alamos 1982), AIP Conference Proceedings 91, (1982).
11. K-J. Kim and N. M. Kroll, Ref.10, p.190.
12. R. H. Pantell and T. I. Smith, 'Laser Driven Electron Acceleration by means of Two-Wave Interaction', Stanford University Preprint (1981).
13. C. Pellegrini, P. Sprangle and W. Zakowicz, Proc. 12th Int. Conf. on High Energy Accelerators, Fermilab, p.473, (1983).
14. J. R. Fontana and R. H. Pantell, J. App. Phys. 54, 4285, (1983).
15. T. Katsouleas, C. Joshi, W. Mori and J. M. Dawson, Proc. 12th Int. Conf. on High Energy Accelerators, Fermilab, p.460, (1983).

16. J. D. Lawson, 'The Beat-Wave Accelerator: Twenty Questions', Paper for Frascati Workshop, 1984.

17. C. Pellegrini, 'The Challenge of Ultra-High Energies', 1982 Oxford Meeting, ECFA report 83/68, p.249.

18. R. D. Ruth and A. W. Chao, Ref.10, p.94.

19. J. D. Lawson, 'Beat-Wave Laser Accelerators: First Report of the RAL Study Group', Report RAL 83-057, (1983), and 'Beat-Wave Laser Accelerators, Further Comment Including Note on 'Surfatron' Concept', RAL-84-059, (1984).

Discussion

T. Tajima, Texas

It is very important to reduce the beam area to extremely small values in order to get the necessary luminosity without an enormous increase in the cost of energy input. Perhaps one task in the Workshop should be to examine such a question?

Answer

Agreed; this is one of the items listed in my 'Twenty Questions', in these proceedings.

A.A. Kolomensky, Moscow

I want to remark that along with FEL and IFEL devices based on the application of transverse magnetic field, similar systems can also exist with longitudinal magnetic field. Such systems are based on the auto-resonance effect discovered by A.N. Lebedev and me in 1962. They can be used for laser acceleration of particles and for effective wave generation (in the latter case they are called cyclotron autoresonance masers).

The effectiveness of IFEL depends on the factor K/γ, which can be made large enough by means of increasing the magnetic field $\beta_\perp$. As to the limit of the FEL action it will be finally set by synchrotron radiation.

Answer

You need large B_z for resonance at laser wavelengths; as you say the main application is to cyclotron masers (gyrotrons).

P. Krejcik, Jülich

You seem to have glossed over the importance of laser efficiency as a power conversion device. You mentioned 5% efficiency. Can you comment some more about the fact that the acceleration devices might be small enough to build but the power stations we need to drive them might be the limiting factor.

Answer

This aspect needs further consideration, but of course one hopes for more efficient lasers in the future! There are two aspects to this problem, first getting the energy into the laser-light, and then getting it from the laser-light into the particle; both these efficiencies have to be multiplied together.

P. Krejcik

If we look at present day linear accelerator structures, we could upgrade their energy gradients no end if we could afford the power.

Answer

This is an important point. The first thing that people see about machines is they are too big; the obvious thing to do, then, is to make them smaller by using high fields. But with an ordinary linac that the optimum solution is not the one with the highest gradient, because the power goes up as E^2. The Stanford linac for instance would be less efficient if you went up to a higher field.

R. Evans, RAL

Recent reports have given efficiencies as high as 15% in some of the krypton fluoride lasers, which is putting a new light on the inertial confinement fusion business and it is also relevant for efficiency as far as accelerators are concerned.

L. Hand

What is the acceleration efficiency of the Pellegrini IFEL?

Answer

This certainly needs to be studied; it should be possible to make a good estimate since the IFEL is relatively well understood.

A. Renieri, Frascati

I agree with you and have a personal comment. I believe that laser acceleration must now be investigated but not limiting the consideration to existing lasers. We need a better understanding of possible IFEL systems, and I believe it may be possible to utilise an FEL for driving these accelerators. For example some schemes transform the energy of the primary beam in an FEL and then transfer the energy of the electromagnetic wave into high energy electrons in the IFEL. Of course, it is important to understand if it is possible to accelerate efficiently and then it may be possible to construct an ad hoc system. I believe that the results in electron lasers are now good enough to give us confidence in this.

Answer

I agree that this is a direction which it would be useful to follow.

A. Renieri

If you compare a linear accelerator with a given electric field and an IFEL, the effective field in this laser accelerator is some value of K, the parameter of undulators, divided by γ. K is proportional to the magnetic field, so in principle you can have very high K, but of course γ acts in the reverse direction. I think the most critical factor is the synchrotron radiation which will put a limit on this.

TWO-BEAM, WAKEFIELD AND MILLIMETER-WAVE ACCELERATORS

T. Weiland
Deutsches Elektronen-Synchrotron DESY, Hamburg

INTRODUCTION

The collection of topics addressed in this paper has the common feature that they all are thought of as new techniques for a future high-gradient linear collider. However, apart from the fact that in all the three schemes (Two-Beam, Wakefield and mm-Wave) a metallic structure is used for guiding electromagnetic fields, they have very little else in common. Thus, I will simply describe them sequentially.

The common goal of these new ideas is to enable the construction of 1 TeV (say) linear collider for e^+e^- physics at a reasonable cost, i.e. at a reasonable construction cost (i.e. a short overall length) and at a low operational cost (i.e. high efficiency). From this goal and from particle physics aspects[1] one can derive the main parameters:

center of mass energy	$E_{c.m.} = G \cdot L \approx 1$ TeV
total length	$L \leq 10$ km
accelerating gradient	$G \geq 100$ MeV/m
total wall plug power	$\langle P \rangle \leq 100$ MW
luminosity	$\mathcal{L} \geq 10^{32}\,cm^{-2}s^{-1}$

At this point it is useful to emphasize that it is more important to establish a 10 km long linac with a high average gradient than to try to maximize the achievable gradient for short stretches.

Only recently very high gradients have been achieved at SLAC[2] and Novosibirsk[3] in standard structures using very high power per unit length. Although these schemes demonstrate the technical possibilities, they would be rather expensive when used over a length of 10 km for a TeV collider.

However, standard structures such as the SLAC linac (see figure 1) already provide a good starting point for investigations of how to improve gradients and efficiency.

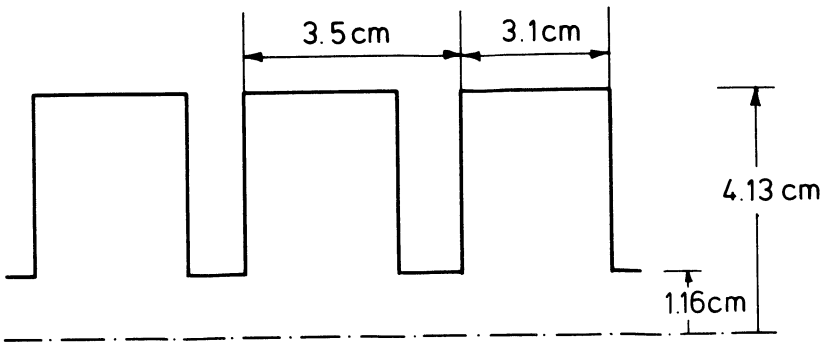

Figure 1: Typical section of the SLAC linac accelerating structure.

MILLIMETER-WAVE ACCELERATOR

The accelerating gradient G in a standard rf structure is given by [4]:

$$G = \sqrt{\hat{P}' R_S'}$$

$\hat{P}'$: peak power per unit length

R_S' : shunt impedance per unit length

In order to improve on G we can make use of the scaling laws for the shunt impedance

$$R_S' = \left(\frac{R}{Q}\right)' Q$$

$$(R/Q)' \propto f$$

$$Q \propto f^{1/2}$$

$$\Rightarrow R_S' \propto f^{3/2}$$

f : rf frequency

Q : quality factor

(R/Q)' : geometric impedance per unit length

These scaling laws favour high frequencies and in themselves indicate no limitation. However, the accelerated electron/positron bunches excite electromagnetic wakefields when they pass through the accelerating cavities. These self-fields are considered today to be the main limiting factor for the luminosity in high energy accelerators. In many existing and future machines (e.g. PETRA, SLC and LEP) these wakefields are and will be a severe problem.

By scaling all dimensions (cavity radius, iris hole radius, bunch length, see figure 1) down as f^{-1} we find that the decelerating self-fields per unit length increase like f^2 (transverse wakefields scale even worse than f^3) and thus the maximum number of particles per bunch scales as f^{-2} when the limitation is given by these fields.

Another limitation is given by alignment errors of long accelerating structures. Transverse self-fields caused by misalignment depend strongly on these errors and are found to be one of the most severe problems for the SLAC collider SLC [5]. Using standard techniques of fabrication the highest frequency currently under consideration is around 35 GHz, 12-times the SLAC linac frequency.

The second ingredient for increasing the gradient is the maximum rf power available. For a 1 TeV linac made out of SLC structures one needs of the order of 200 GW peak power (i.e. some 5.000 SLAC klystrons). The obvious way to overcome this high number is to increase the peak power per klystron to 1 GW (say) and intense investigations towards this goal are under way in SLAC [6] and Japan [7]. A very promising new type of power source is the so-called "photo-klystron" or "lasertron". This idea originated in SLAC and is being investigated there with computer modeling [8]. The results of a small "proof of principle" experiment have already been reported from Japan [7,8]. Figure 2 shows the S-band model of a photo-klystron, for more details see references 7 and 9. Together with the high power klystrons, new accelerating structures have to be developed with a high group velocity in order to allow large distances between klystrons and short pulse duration and the so-called "jungle gym" and "Disk and Washer" structures look promising.

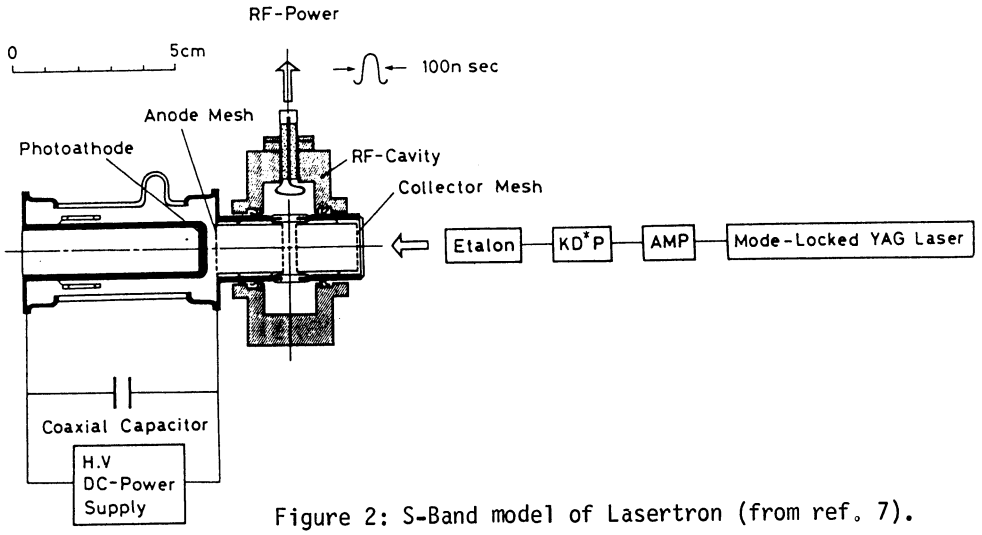

Figure 2: S-Band model of Lasertron (from ref. 7).

Assuming that klystron development and the optimization of rf structures succeeds in the near future, there is still another limitation for high gradients: breakdown effects. (This is, however, not an effect specific to mm-wave structures but also for all schemes described here). For a long time this was considered to be a "big problem", however, recent experiments at SLAC and Novosibirsk showed that it is possible to exceed 100 MeV/m at 3 GHz. Thus, these phenomena appear to be not fully understood. Nevertheless, applying the scaling law [10]:

$$E_{breakdown} \propto f$$

we do not expect any problem in the region around 30 GHz. Figure 3 shows a limitation chart (from ref. 10) with the latest results from SLAC added. It is most important, it seems, that more investigations should focus on break down effects, which are much less well understood than the three other points: shunt impedance considerations, high peak power klystrons, wakefield effects.

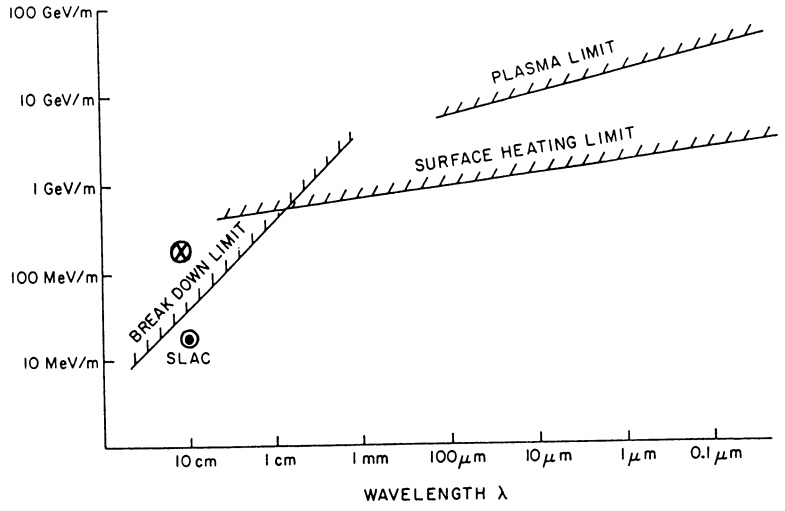

Figure 3: Limitations for surface field strength (from ref. 10) with the latest result from SLAC experiments ⊗ added.

TWO-BEAM ACCELERATOR

This scheme invented by Sessler[11] also employs a more or less standard accelerating structure but scaled to run at about one order of magnitude higher frequency. The difference between the TBA (Two-Beam Accelerator) and a standard linac is that the TBA has two parallel beam lines. Besides the beam channel for the high energy particles there is a parallel low-energy electron beam moving along wiggler fields. These fields cause the particles to move transversely to the direction of the beam line and thus to excite electromagnetic radiation. Such a device is called a Free-Electron-Laser (FEL)[12]. The driving beam looses energy while radiating and has to be reaccelerated. This is done using standard induction units. The essential features of a TBA are shown in figure 4.

Instead of having the two beams separated it has also been proposed to combine them into one waveguide. The three main possibilities are shown in figure 5.

With such a FEL driven high gradient it is claimed that an accelerating gradient of 250 MeV per meter could be reached. A 1 TeV (center of mass) linear collider could then be built within a length of 5 km (say). The average power consumption would be around 500 MW.

Experimental studies with these devices are underway at Berkeley and it is hoped to have rf-power in the 35 GHz cavity in 1985. The cavity is a scaled SLAC[5] structure and has already been built. The FEL is operating successfully.

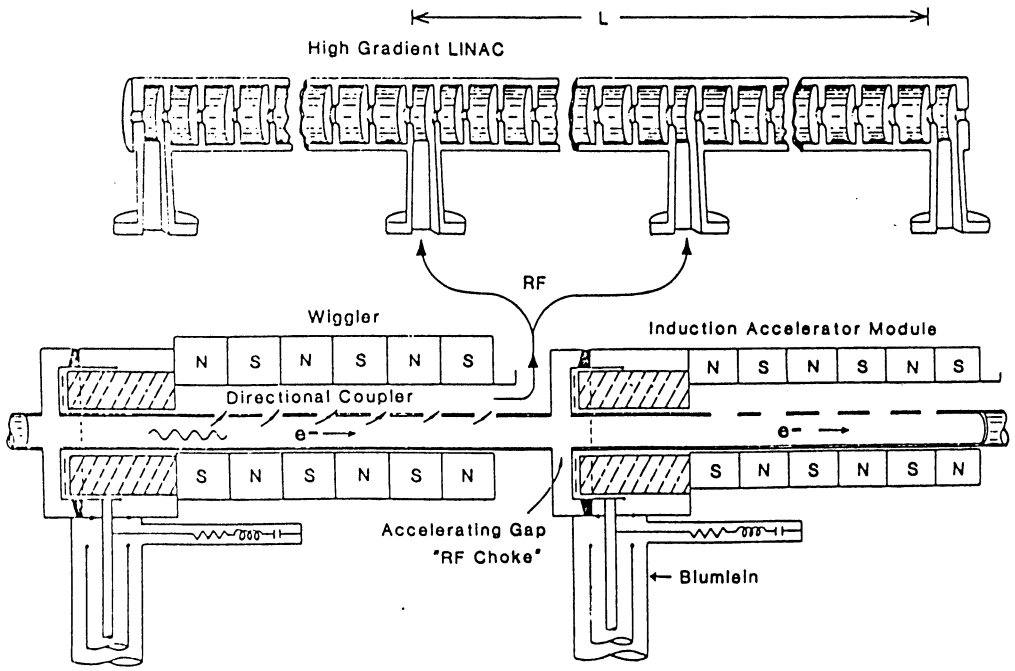

Figure 4: Basic layout of the Two-Beam Accelerator (from ref. 11).

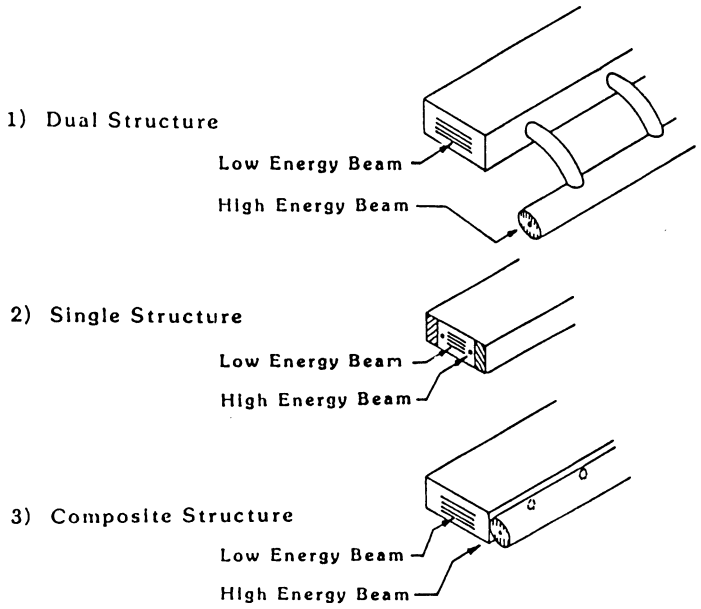

Figure 5: Three principal concepts for a TBA (from ref. 11).

Problems specific for the TBA are 1.) achieving the steady FEL operation, 2.) the coupling of the FEL radiation to the accelerating structure (for the case of separated lines), and 3.) the common waveguide design for the structure where both beams run in one channel. Fig. 6 shows a possible arrangement of a driving beam which excites a waveguide mode inside the accelerating structure for acceleration of two high energy beams. Fig. 7 shows a possible layout of a coupler system to extract FEL radiation and to feed it to a high gradient structure using a single mode waveguide.

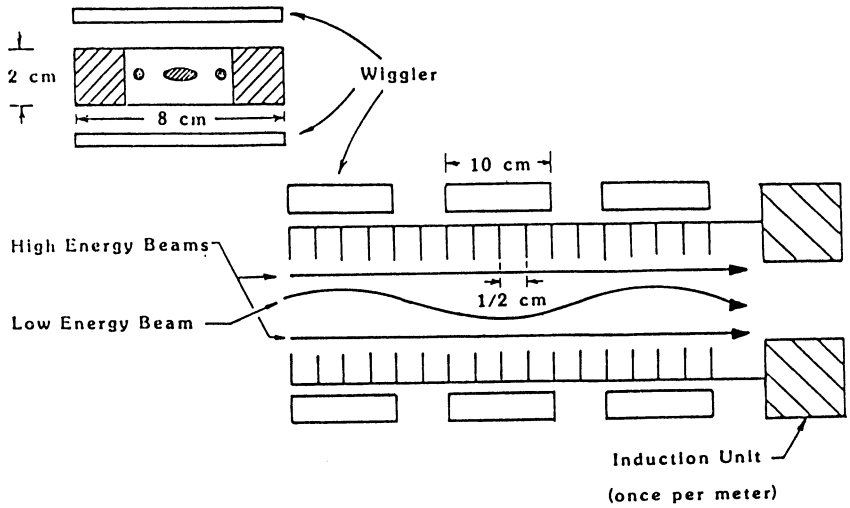

Figure 6: Possible structure of a TBA with both beams in the same waveguide.

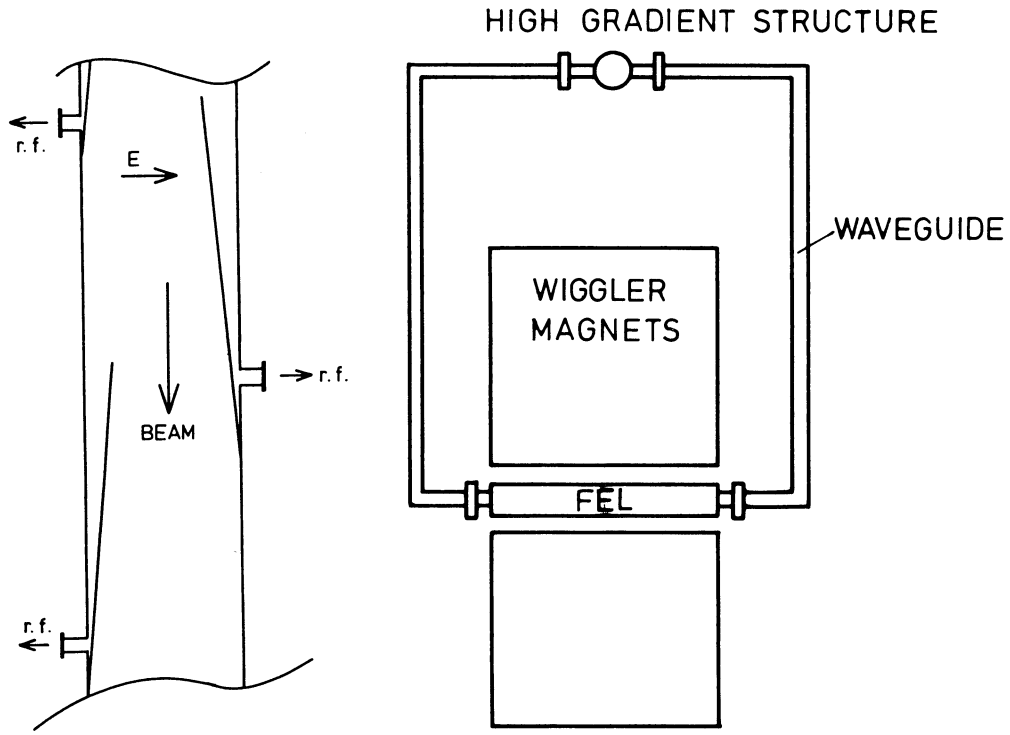

Figure 7: Extraction of rf into the high gradient structure by tapers.

WAKEFIELD ACCELERATORS

When a bunch of charged particles traverses a beam pipe with varying cross-section, electromagnetic waves are excited. Fig. 8 shows a typical example of a bunch passing an iris loaded circular waveguide. These "Wakefields" exert a decelerating and deflecting force on all particles in the bunch while they pass the region around the iris. After the particles are far down stream the transients have settled down and we are left with a net change in longitudinal and transverse momentum. This change (times the particle velocity) is called "Wake Potential". Fig. 9 shows typical wake potentials inside and behind a Gaussian bunch after a passage through an iris loaded pipe. As can be observed, most of the particles are decelerated, i.e. they loose energy due to these self-fields. When the beam does not pass exactly on axis, the particles also experience a net deflection.

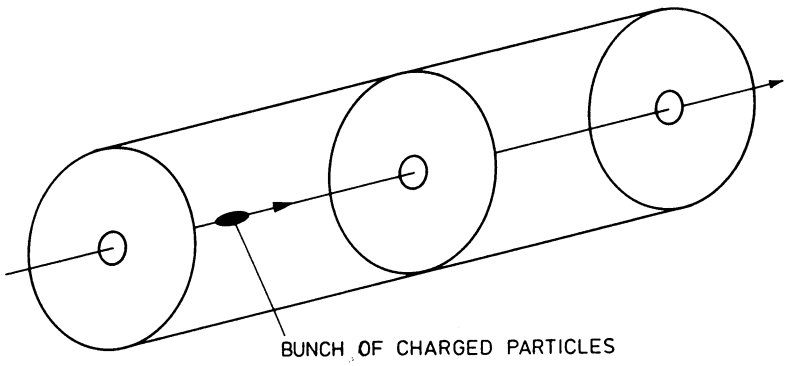

Figure 8: A bunch of charged particles passing through an iris loaded circular waveguide.

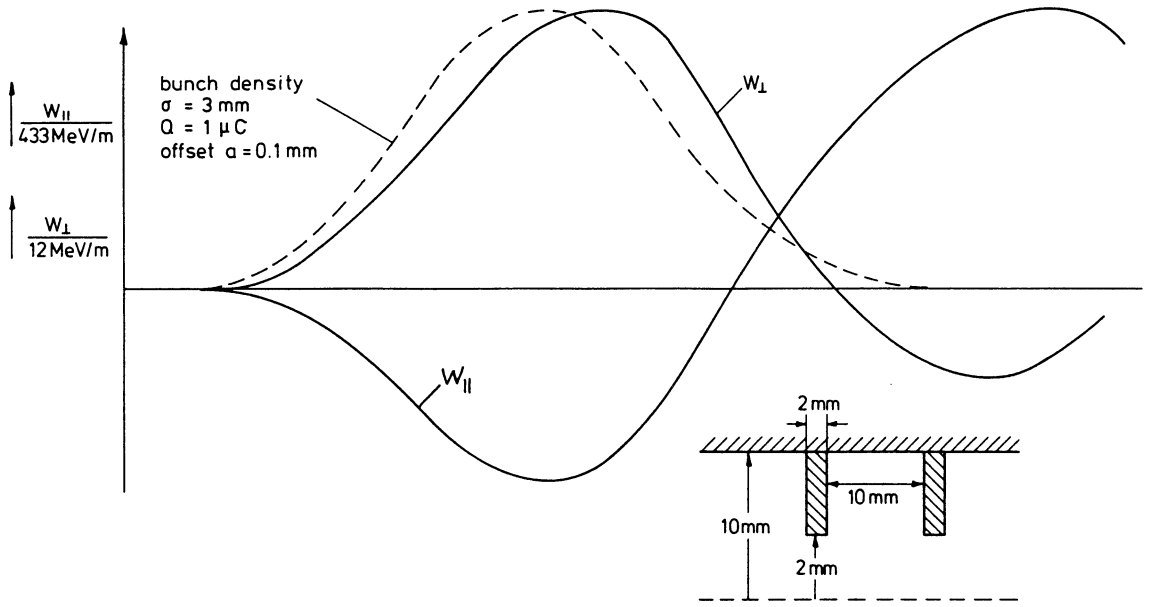

Figure 9: Wake potentials due to an iris loaded waveguide.
σ = 3 mm, Q = 1μC, beam axis offset = 0.1 mm.
$W_\perp$ = deflecting force per unit length
$W_\parallel$ = accelerating force per unit length

However, some particles in the tail of the bunch are in fact accelerated. This effect in which some particles in an ensemble can be accelerated by the scattered self-fields was recognized long before it was possible to calculate these fields and was named "Auto-Acceleration" [13].

It was suggested later that a proton synchrotron could be used for generation of the driving bunched beam and to inject a few electrons behind the protons so that the electrons are accelerated [14]. However, it follows from basic considerations that the maximum energy that can be obtained for the electrons is always less than twice the proton energy (for longitudinally symmetric charge densities). Apart from this rather small transformation ratio ($t \leq 2$) it seems almost impossible to create a very high intensity proton bunch (3×10^{13} particles) with the length of only a few millimeters necessary for creating the gradient of 1 GeV/m as claimed by the authors.

As an extension of these ideas it has recently been suggested that electrons be used to drive the wakefields instead of protons [15].

Common to all these kinds of wakefield accelerators is the problem of transverse stability. The few tail particles (≈2 - 5 %) see the strong deflecting wakefields excited by the whole beam (100 %). Taking into account that transverse stability is already a problem for beams at much lower currents (see e.g. SLC design [5]), it seems unlikely that this type of wakefield accelerator will be used in a future collider. Also, no design has been published yet taking transverse stability considerations into account.

WAKEFIELD TRANSFORMERS

The wakefield acceleration situation can be improved significantly by generating wake potentials as shown in figure 10. As we see there is a late pulse in the potential that is much larger than the decelerating potential inside the driving bunch. As we know from the previous section, such potentials cannot be obtained by sending the two beams (the driving and the accelerated particles) down the same line. Thus, structures that can in fact transform wake potentials to much higher values must have two spatially separated channels.

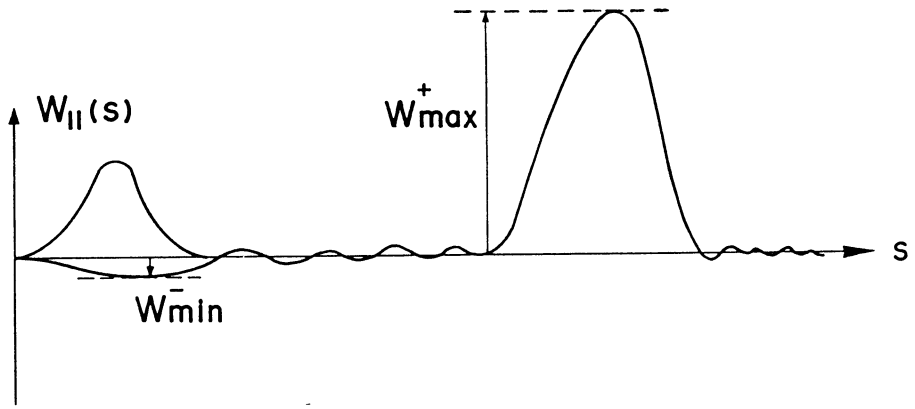

Figure 10: Wakepotential with a higher accelerating pulse than deflecting pulse.

The idea of "Wakefield Transformation" [16] can be understood best by considering the fields generated by a hollow, "wedding ring" shaped bunched beam, see figure 11. Wakefields are generated when the hollow beam enters. Subsequently a collapsing wave packet travels towards the center of the pill box after being reflected at the outside wall (That is why the pulse is positive!). During that time the volume of the wave packet decreases (neglecting dispersion for the moment) and thus increases the field strength.

When we assume that the wave packet has the same length (L) as the driving beam we find a transformation ratio t of the field strength

$$t^2 = \frac{\text{Volume at } r = R}{\text{Volume at } r = 0} = \frac{2\pi R \cdot L}{(\frac{L}{2})^2} = \frac{8R}{L}$$

For L = 5 mm, R = 5 cm we obtain $t \approx 9$. Exact calculations have been performed for the wake potentials shown in figure 8 by the computer code TBCI [17] using the dimensions given above and it was found that a hollow beam of 1μC, R = 5 cm and about 2 mm r.m.s. length can generate wake potentials of the order of 200 MeV/m or more.

At DESY - after a year of theoretical studies - an experiment has been started to test this scheme [18,19].

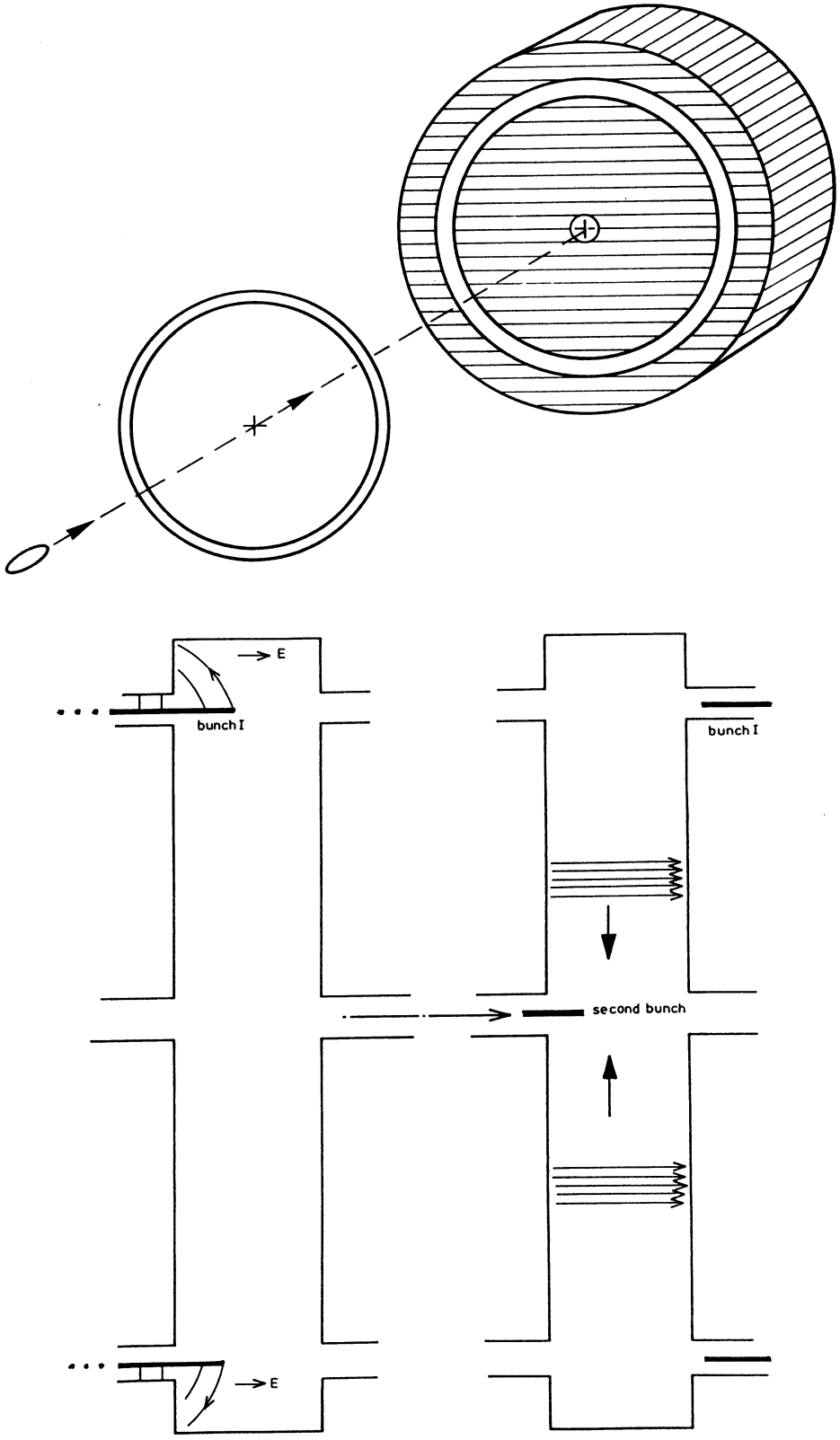

Figure 11: Hollow beam entering a pill box cavity with a slot and qualitative fields showing a collapsing wave packet.

The overall layout of the DESY experiment is shown in figure 12. A hollow electron beam of several hundred amperes and 2ns length in time will be extracted from a laser driven gun. The hollow beam will be bunched and accelerated to 8 MeV in a linac. The accelerating system consists of four 500 MHz-cavities and a 1 MW Valvo klystron (pulsed).

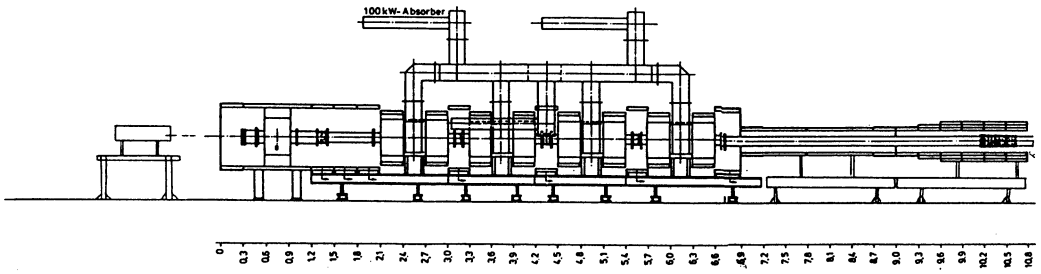

Figure 12: Layout of the Wakefield-Transformer Experiment at DESY.

After acceleration the hollow beam will be further compressed longitudinally and radially before it enters the wakefield transformer.

The entire system is surrounded by solenoid coils which provide the force needed to maintain the hollow beam shape.

In the wakefield transformer (Length ≈ 40 cm) the ring beam will generate a wakefield that will, if it works, accelerate a co-travelling central test beam at a rate above 100 MeV/m. Calculated wake potentials for the transformer are shown in figure 13.

The experiment is well under way and it is hoped to have first results in 1985.

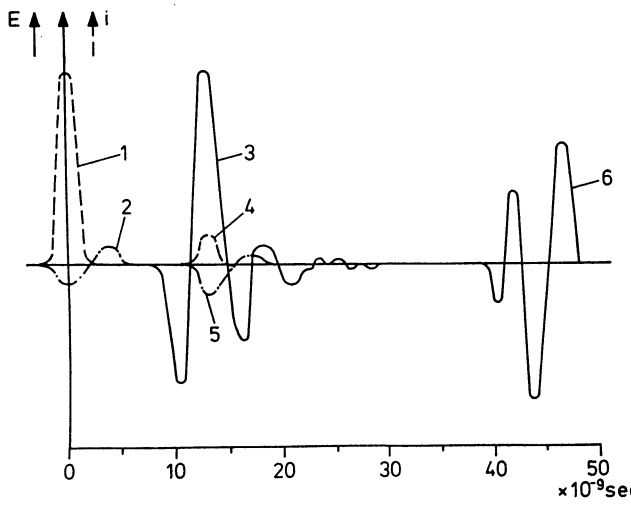

Figure 13: Wakepotentials for the experimental setup as calculated.
1 driving beam density
2 driving beam decelerating potential, W_{min} = 20 MeV/m
3 accelerating wake potential for electrons, W_{max} = 157 MeV/m
4 accelerated beam density
5 decelerating wake potential of the accelerated beam, W_{min} = 7.3 MeV/m
6 accelerating wake potential for positrons, W_{max} = 110 MeV/m
Driving Beam: σ = 2 mm, R = 5 cm, Q = 10^{-6}C
Accelerated Beam: σ = 2 mm, Q = 10^{-8}C

A TeV collider based on the wakefield transformer concept could have two kinds of layout as shown in figure 14. If it is possible to keep the driving ring beam clean and stable over a long transformer section, one would first generate the medium energy driving beam only once at the beginning and then transform its energy to the high energy beam over the whole length. If it turns out that the hollow beam does not survive long transformer sections, a multiple stage system could be used where a fresh driving beam is generated at the beginning of each section.

Theoretical and experimental studies have also been reported from Japan [20], where elliptical [16] tranformers are being tried.

Common to every wakefield transformer accelerator is the problem that the driving beam must be intense (10^{12}-10^{13} particles) and short in time (10 ps) in order to achieve high gradients. Thus the real limitation could well be located in the low energy preaccelerator where space charge forces counteract bunching and focusing.

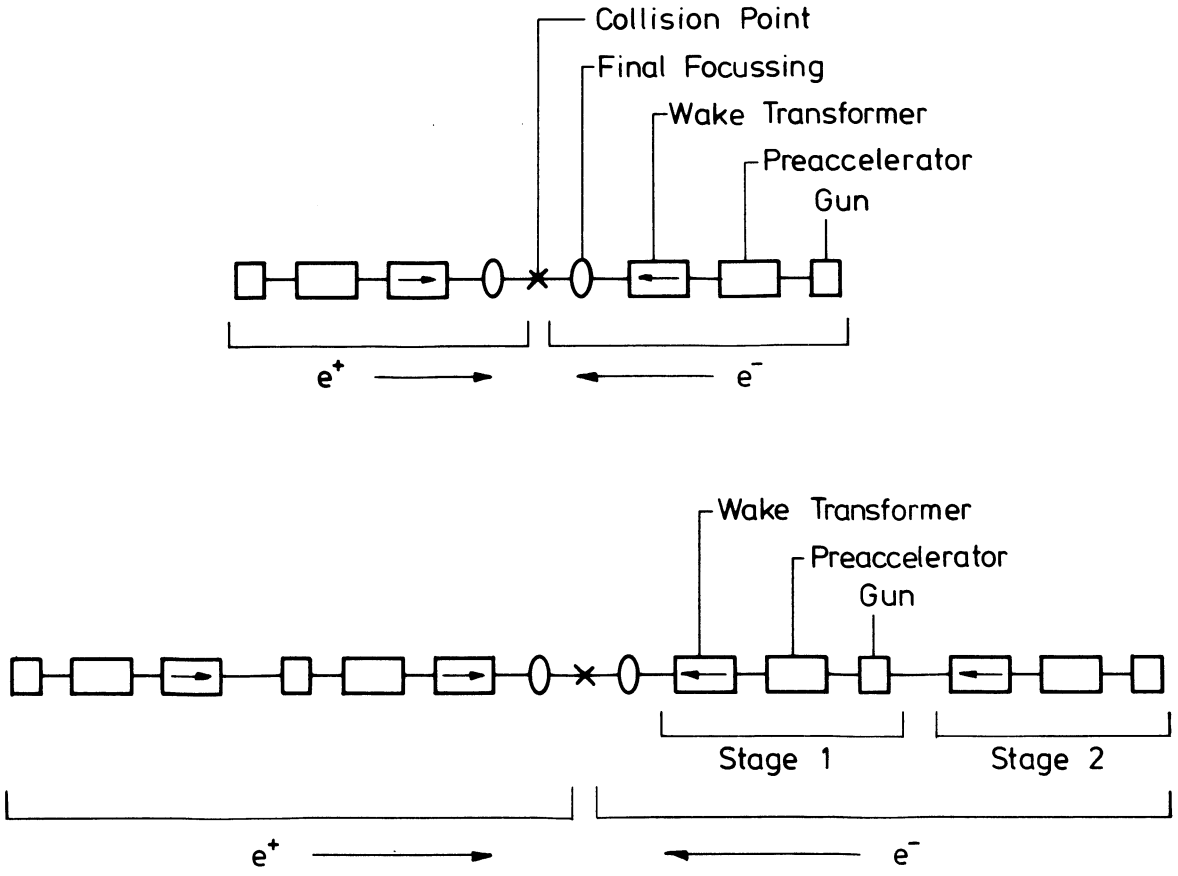

Figure 14: Layout of a large Wakefield-Transformer colliding beam facility with single (top) and multiple stage (bottom) version.

ACKNOWLEDGEMENT

The author wishes to thank D. Barber for careful reading of the manuscript.

REFERENCES

1. C. Rubbia, this Workshop.
2. G. Loew, SLAC private communication (1984)
3. A. Skrinsky, private communication (1982)
4. For definitions see e.g. P.B. Wilson, SLAC-PUB-2884, February 1982
5. SLC Design Report, SLAC-229, June 1980
6. P.B. Wilson and W.B. Herrmannsfeldt, private communication
7. Lasertron study group, INS-490, March 1984, University of Tokyo
8. W.B. Herrmannsfeldt's, SLAC AP21, April 1984
9. S. Takeda, this Workshop.
10. D. Prosnitz, M. Tigner, AIP 91, p. 189
11. D.B. Hopkins, A.M. Sessler, J.S. Wurtele, LBL-178000, April 1984
12. H. Motz, J. Appl. Physics 22 (1951), p. 527
13. A. Kolomensky, private communication
    H. Friedmann, Phys. Rev. Letters 31 (1973), No. 18, pp. 1107
    N.R. Heese and W.R. Randord, Rev. Sci. Instr. 43 (1972), pp. 1594
    I.A. Grishaer and A.M. Shenderovich, Sov. Phys. Thech. 17 (1973), pp. 1871
    L.N. Kazanskii, A.V. Kisletsov, A.N. Lebedev, Atomaya Energyia 30 (1971), pp. 27
    J.R. Briggs, T.J. Fessenden, V.K. Neil, 9th Intern. Conf. on High Energy Accelerators, SLAC 1974, pp. 278
14. E.A. Perevedentsev and A.N. Skrinsky, Proc. of the 6th All-Union Conf. on Charged Particle Accel., Dubna 1978, Vol. 2, p. 272
    V.E. Balakin and A.V. Novokhatsky, Preprint INP 79-86, Novosibirsk 1979
15. John T. Seemann, Cornell Report CBN 82-17, May 1982
16. G.-A. Voss and T. Weiland, DESY M-82-10, April 1982
    G.-A. Voss and T. Weiland, DESY 82-074 (1982), November 1982
17. T. Weiland, NIM 212 (1983), pp 13-21
18. T. Weiland, F. Willeke, 12th Internat. Conf. on High Energy Accel., Chicago 1984, pp 457-459
19. The Wakefield Accelerator Study Group, 12th Internat. Conf. on High Energy Accel., Chicago 1984, pp. 454-456
20. S. Takeda., private communication, 1984

Discussion

J. Nation, Cornell

I would like to make one comment and ask one question. The comment refers to the auto-accelerator configuration of the wakefield accelerator which I think you should not dismiss quite so readily, not because of its promise for high accelerating field gradients, but because it allows a means to recover energy from your beam and if you are worried about power consumption, energy recovery is rather important. The question is that I remember at the Oxford meeting that Burt Richter very succinctly pointed out that when you get up to fields of 100 MV/m near a surface, everything field emits. Clearly, it will help if you are going up to very high frequencies and reduce the duration of the field, but has any further thought been put into this? Is 500 MV/m a realistic goal in a near-field device?

Answer

Let me first reply to your comment: I think energy recovery from a linear collider is not worth the effort.

Now let me answer your question: in practice I think this factor of two is more encouraging than it looks because what counts after all is the total gradient for total length, and even with a factor of two over a short distance you might have a high gradient of the order of 500 MV/m on average. But the reason I am putting it down nevertheless is because it has not been looked at carefully in regard to problems of transverse wake instabilities.

On the breakdown limit: it does not exist even at 3 GHz and 100 MV/m, which is 200 MV on the surface. No more thoughts have gone into that from our side, we just hope we should be much better because our pulse length is just half a wave; there should not be any resonant system that is better than this one.

L. Hand, Cornell

I thought Tom emphasised very well the fact that the main limit is power. In any of these schemes has anyone seriously thought of designing some form of energy storage into the system? What you need is peak power for acceleration and you would like to be able to make the energy available and then store it again in some way. I know there are nebulous schemes for doing this with superconducting rf cavities, but have any of those schemes been examined with respect to linear accelerators of these types?

Answer

In the wakefield accelerators the energy is stored in the ring. You can compare the efficiency, say with a normal accelerating structure limited by some maximum field strength, and then take only a tenth of the structure and add the wakefield transformer. You find out that the efficiency goes up. In percent I do not know what the efficiency is. I do not have an example for a TeV collider.

L. Hand

My point is that for a TeV collider if the efficiencies are the same as they are now it looks very difficult unless we use some form of energy storage. Maybe you get around that with a wakefield but I do not see how.

B. Zotter, CERN

I would like come back to the breakdown problem. It is not the question of just having a single shot device. I think in all linear colliders you need a high repetition rate to get a high luminosity and if you have breakdown you will have plasma formation inside your waveguide. What is the limit on the repetition rate?

Answer

At SLAC 100 MV/m were reached at 3 GHz, and for the assumed law of proportionality to f one could get 1 GV/m at 30 GHz, so I do not see a problem yet.

G. Dôme, CERN

About the peak-field limit due to breakdown, is the dependence on frequency given by Kilpatrick's criterion obsolete? According to Kilpatrick the peak field grows like the square root of the frequency, rather than the first power.

Answer

Clearly more experimental checks are required, that is why we are planning experiments at DESY. We do not know a good theory for pulsed rf breakdown.

D. Chan, Chalk River

This is just a comment on the Kilpatrick limit. It is only a guideline for cw conditions and for pulsed mode it does not apply. SLAC's 110 MV/m is an experimental result.

J. Rees, SLAC

We hear much about peak fields forming the ultimate limits on the acceleration mechanisms we are talking of. The present practical limits on klystron performance at SLAC for the SLC is repetition rate, not peak power. In luminosity the repetition rate is very important and may form the ultimate stumbling block in any scheme, particularly if you want to achieve the unit of luminosity which Carlo Rubbia was talking about this morning, which I suggest we call the Carlo (1 Carlo = 10^{34} cm^{-2} s^{-1}). Our machines are now running at a milliCarlo.

I think many of these new schemes, the wakefield or the two-beam accelerator, have the possibility of greatly increasing the frequency with which you have pulses and therefore the average power. We have to consider how frequently we can make rings, or in our case how frequently you can send pulses of electrons through the FEL and how quickly can you make the induction unit work and so on. We think that both these devices will be rather good as far as the repetition rate is concerned.

A.A. Kolomensky, Moscow

In the seventies in our laboratory, the Lebedev Institute, Moscow, a series of experiments on auto-acceleration has been conducted. In particular we forced an intense pulsed electron beam (0.7 MeV, 10 kA, 40 nsec) to propagate in a waveguide tuned to a wavelength of 10 cm. We found at the waveguide output that about 10% of the electrons had doubled their energy and 2-3% had trebled their initial injection energy. It is worthwhile noting that this process was accompanied by relatively powerful microwave radiation ~ 10 MW at λ = 10 cm. I should also like to draw your attention to the fact that the first theoretical paper on acceleration was published in the soviet journal "Atomnaja energia" by a group of authors from our laboratory in 1971. In this paper, the conception of and the term for autoacceleration were introduced for the first time.

Answer

I apologize for not having made reference to you! About the factor of 3 in energy gain, I should like to mention that my statement about a factor of 2 being the maximum applies only for symmetric short bunches. If you

have a longitudinally asymmetric bunch you can get about any transformation in gradient; but if it is a short symmetric distribution you can never get more than two.

R. Palmer, Brookhaven

While we are talking about power sources I hate to mention lasers again, but of course, one of the attractions of lasers is not just that the wavelength is short, and therefore some of these problems like the breakdown may go down considerably, but the fact that one can relatively easily obtain lasers with powers of 10^{11} watts. And of course, a laser is so attractive because it is a storage mechanism that you put the energy into over a relatively long time and then you can get it out over a picasecond. Although I have always been interested in lasers operating with gradients of 10 GV per metre it is interesting to speculate on what gradients we can get without destroying a grating and it seems quite likely, after what you have said, that one will be able to get up to at least a one GV per metre. Certainly the power is there from the lasers and it would seem likely that breakdown would not occur at those levels. Whether we can get the wakefield effects and things under control is something we have got to look at.

THE BEAT-WAVE AND SURFATRON ACCELERATORS FOR PARTICLES

J.M. Dawson
Department of Physics, Univ. of California, Los Angeles, CA, USA

In the main the work discussed in this talk appears in the Proceedings of the International Conference on Plasma Physics, Lausanne, Switzerland, from June 27 through July 3, 1984, and consequently only an abstract of the highlights will be given here; the interested reader is referred to the above paper for more details.

The possibility of using intense space charge plasma waves to accelerate particles to high energy is considered. These are of interest because of the very strong electric fields that can be generated. Wave breaking theory predicts that fields as large as $E = \sqrt{n_e}$ volts/cm can be achieved; numerical simulations using relativistic particle models of the plasma show fields up to 0.7 of this amplitude. Such plasma waves have phase velocity ω_p/k_p where ω_p is the plasma frequency ($\omega_p^2 = 4\pi ne^2/m_e$) and k_p is its wave number. The phase velocity can be close to that of light. One way to generate such waves is to propagate two intense light beams through the plasma with a frequency difference equal to the plasma frequency. The non-linear $j \times B$ force sets up a plasma wave with a phase velocity equal to the group velocity of the light through the plasma, $V_g = c(1-\omega_p^2/\omega^2)^{1/2}$; if the light frequency is large compared to the plasma frequency, the group velocity (and hence the phase velocity of the plasma wave) is close to c and the plasma wave is very effective at accelerating particles to high energy.

The generation of the beat wave has been simulated using a two-dimensional fully electromagnetic fully relativistic particle code. Two electromagnetic waves of finite width are launched into the plasma. The electromagnetic waves exhibit self-focusing to what appears to be a stable beam width of diameter a few times c/ω_p. The accelerated electrons are also found to self-focus.

There is a maximum energy to which electrons can be accelerated which is $2m_ec^2\omega^2/\omega_p^2$. If a magnetic field is introduced into the plasma perpendicular to the direction of wave propagation, then a particle being accelerated by the wave also experiences an acceleration parallel to the phase fronts of the wave. This acceleration allows a particle to phase lock with the wave and remain in an accelerating phase (a particle moving at c can have the component of its velocity parallel to the direction of wave propagation equal to V_p). In this way the particle can in theory be accelerated indefinitely. This is the Surfatron concept. The phase locking tends to cause all particles to experience the same acceleration and hence it should produce relatively little energy spread.

There is another method of accelerating particles using the beat-wave approach which appears to offer much promise for producing high quality very high energy electrons; it is essentially the method first proposed by Tajima and Dawson with the single modification that preaccelerated electrons are introduced into the plasma for acceleration to high energy so that the background electrons are not picked up. The situation is shown schematically in Fig. 1. An intense laser pulse propagates through the plasma at its group velocity $V_g = c(1-\omega_p^2/\omega^2)^{1/2}$. It generates a wake of intense plasma oscillations. In a frame moving with the pulse the electrons are seen as streaming backwards. The intensity of the laser pulse is chosen so that the plasma wave does not reflect the bulk electrons. However, the preaccelerated electrons in the plasma have a lower velocity relative to the pulse and can be reflected. If the preaccelerated electron beam is of high quality the reflected beam should also be of high quality. Preacceleration to an MeV (or perhaps several) should be sufficient. Since the beam extracts energy at the front of the wake plasma wave there should be no problem with plasma turbulence and the intensity of the wake plasma wave should be able to reach values as near wave breaking. The accelerated particles extract energy early from the plasma wave so it appears probable that they can withdraw a substantial fraction of its energy. If they extract 10% of the plasma waves energy they will decrease its amplitude by 5% which appears quite modest. Extraction of 20-30% of the wave energy does not seem out of the question. Since the laser pulse can be made self-focusing there does not seem to be a problem in propagating such a pulse through tens to hundreds of meters of plasma. A 0.25 μ laser pulse propagating in a 10^{16} density plasma should be able to accelerate electrons to about a TeV.

Editor's Note

The following reference is also relevant.

C. Joshi, W.B. Mori, T. Katsouleas, J.M. Dawson, J.M. Kindel and D.W. Forslund, Ultrahigh gradient particle acceleration by intense laser-driven plasma density waves, Nature Vol. 311, 11 October 1984, p. 525.

Wave Frame

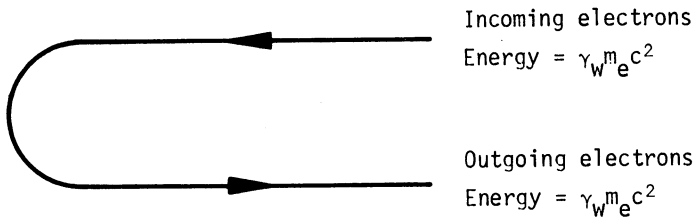

Laboratory Frame

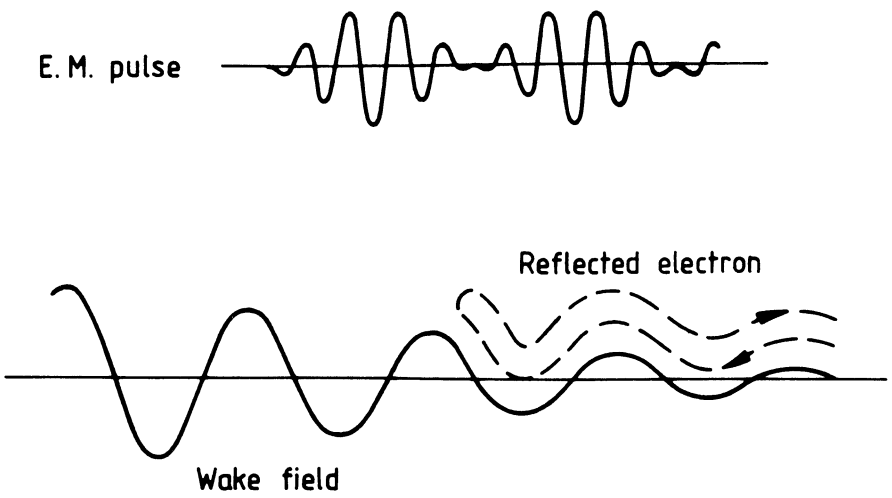

Outgoing electrons have energy = $2\gamma_w^2 m_e c^2 = \frac{2\omega^2}{\omega_p^2} m_e c^2$

where = $\gamma_w = (1 - V_p^2/c^2)^{-1/2} = \omega/\omega_p$

Figure 1

Discussion

B. Montague, CERN

Plasma densities like 10^{16} may seem rather low to plasma physicists, but if they would permit 1 TeV to be reached in a hundred metres this would be very impressive!

Answer

I agree and I think that potentially this is possible if you had a KrF laser and a pulse of about 10 ps. I do not think you can use much more than that because the whole thing becomes turbulent.

Question

In this electron pulse excitation plasma, how short do the electron pulses have to be, sideways?

Answer

I think you want the length and width of the bunch to be something like c/ω_p and so it depends on what plasma density you want, but if you want really high fields then you need high ω_p. If you are satisfied with low plasma frequencies, let us say a fairly modest plasma density of 10^{14}, that already gives you 1 GV/m. The length of the pulse is 0.5 mm, say, and then you have to space your electron pulses so that they come in reinforcing situations. Some of this was done in conjunction with the people at SLAC, in fact that is where the idea first came from. They had bunches of 5×10^{10} in 1 mm by 100 μm, or something like that, and that creates these fields with just 4 or 5 bunches. You do not need many.

A. Renieri, Frascati

Are the qualities of the laser beam critical, that is to say the coherence, phase conservation etc?

Answer

I think they are not so terribly critical because first of all the length of the laser pulse is only something like 10 ps long. You can use the uncertainty principle to figure out how much incoherence you are allowed over that length of time. In fact if you can pack more energy into a short pulse, you can still do it, you can make it 1 ps or even a fraction of a ps, just so that you have enough punch to drive up the plasma

oscillation in that one pulse. Actually that works out to be not too difficult, compared to what people who build lasers do. Also it looks as if it self-focuses, and if you make the beam the proper width it self-focuses into one channel, if you make it too wide it tends to form several filaments and so you do not want to put in too wide a beam. Precisely what that condition is we have not worked out but we have in our simulations formed one channel and then if we doubled the size we found that we had two channels. So there are conditions like that which you have to worry about but I do not think they are so serious. I am more worried about whether the wave itself creates a high quality beam of the kind of brightness that people here are talking about.

B. Zotter, CERN

In your simulations do you always assume that the difference between the two laser frequencies is exactly at the plasma frequency or do you take finite fluctuations of the plasma density into account which with all the long columns you have must be quite severe?

Answer

In the simulations we always choose the difference to be equal to the average plasma frequency, and the fluctuations are not severe in the simulations. It is an experimental problem of how uniform you have to make the plasma density. I frankly think that it is not a serious problem. Well, let me give you an example of a way you might do it. Fill the channel with gas at the density you want and then put a UV flash lamp round it and just suddenly ionise it and there it is and you do not create any big disturbances in that gas. Remember it is a small channel. It depends on whether you have long wavelength fluctuations or short ones. If you have long wavelength effects to worry about then one thing you can do is just put a gentle gradient in it towards the far end and that will do.

C. Joshi, UCLA

We have looked both in simulations and in an experiment to see exactly what kind of density mismatch can be tolerated. It turns out in an experiment you can tolerate a density mismatch of apparently 5%, and at the moment, plasma sources can be made which can produce plasma densities over 10 centimetres with that kind of density tolerance. In simulations we have put both a perturbation of 5-10% and also an almost arbitrary step mismatch and again if you have up to about 5% mismatch then you can still set up a reasonably coherent plasma wave. If it is anything larger than that, then you very rapidly get a plasma amplitude that is both incoherent and also quite small.

W. Willis, CERN

We should remember that we are not just talking about linacs but colliding linacs. So there are two kinds of beam quality that you might think about. One is what kind of beam emittance comes out of the end of the linac, the other is what is its position in absolute space or, if you like, relative to the beam that is coming at you the other way. So that means it would be sad if I had at the end of my 100 metres a quarter of a micron beam and it was not in the same quarter of a micron as the other beam. That must imply a tight tolerance on the plasma uniformity.

Answer

I am sure it does. There are alignment problems and this is a uniformity problem that may affect the alignment.

J. Mulvey, Oxford

The first bunch of particles accelerated is not, you say, troubled by turbulence. How long is it before your plasma is nice and uniform again and you can send another pulse down?

Answer

It only gets turbulent along the channel that you have sent it. You could, for example, make a big plasma and send successive pulses down different channels; or another way is to just blow the plasma gas out and refill, and then I am sure you can do it at kilocycle rates because that is what is now done for high power lasers. What the absolute limit is I do not really know.

SURVEY ON MODERN PULSED HIGH POWER LASERS

K.J. Witte
Max-Planck-Institut für Quantenoptik, D-8046 Garching/FRG

1. Introduction

The requirements to be met by lasers for particle acceleration are partially similar to those already known for fusion lasers. The power level wanted in both cases is up to 100 TW or even more. The pulse durations favourable for laser accelerators are in the range from 1 ps to 1000 ps whereas fusion lasers require several ns. The energy range for laser accelerators is thus correspondingly smaller than that for fusion lasers: 1-100 kJ versus several 100 kJ. Due to the availability of highly efficient frequency conversion processes no real preference at present exists for a certain wavelength: iodine (1.3 μm), Nd:glass (1.06 μm), XeCl (.308 μm) or KrF (.248 μm) can all be used as long as the high repetition rate capability is disregarded. The CO_2 laser plays a special role. Whereas it is well suited for the grating, plasma or inverse free electron accelerators it is not attractive any more for fusion due to the production of hot electrons leading to an unacceptable level of target preheating.

The design criteria of lasers meeting the requirements mentioned above will be discussed in the following. The CO_2, iodine, Nd:glass and excimer lasers will be treated in detail. The high repetition rate aspect will not be particularly addressed since for the present generation of lasers the wanted rates of far above 1 Hz are completely out of scope. Moreover, for the demonstration of principle these rates are not needed.

2. Paraxial Wave Equation

This section is a short review on laser theory. Its intention is to show that the output characteristics of a complex high power laser system can indeed be calculated with a precision of about 10 % and are thus not subject to the caprice of fortune.

The paraxial approximation to Maxwell's equation has been proven to be completely sufficient for the description of the phenomena occurring in large laser systems such as amplification, diffraction, absorption, scattering, self focussing and frequency conversion. The derivation of the paraxial wave equation starts from Maxwell's equation from which it is easy to derive the following wave equation (mks units, E electric field in V/m, P volume polarization in As/m^2, c velocity of light in vacuum in m/s, $\varepsilon_o = 8.86 \cdot 10^{-12}$ As/Vm permittivity of free space)

$$\nabla^2 \vec{E} - \frac{1}{c^2} \frac{\partial^2 \vec{E}}{\partial t^2} = \frac{1}{c^2 \varepsilon_0} \frac{\partial^2 \vec{P}}{\partial t^2} + \text{grad div } \vec{E} .$$

The paraxial wave equation is obtained by writing

$$E(x,y,z,t) = \frac{1}{2} \vec{\mathcal{E}}(x,y,z,t) \exp\{i(\omega t - kz)\} + \text{c.c.},$$

$$P(x,y,z,t) = \frac{1}{2} \vec{\mathcal{P}}(x,y,z,t) \exp\{i(\omega t - kz)\} + \text{c.c.},$$

making the slowly varying enveloppe approximation ($\partial^2/\partial z^2$, $\partial^2/\partial t$ of $\vec{\mathcal{E}}, \vec{\mathcal{S}}$ negligible) and by assuming grad div $\vec{\mathcal{E}} \cong 0$. The last requirement is the condition that the $\vec{\mathcal{E}}$-field must be approximately perpendicular to the propagation direction (z-axis here) /1/. If the retarded time $\tau = t - z/c$ is used as the reference frame one obtains with $c = \omega/k$, $\vec{\mathcal{E}} = \mathcal{E}\vec{e}_y$ and $\vec{\mathcal{S}} = \mathcal{S}\vec{e}_y$ ($\vec{\mathcal{E}}, \vec{\mathcal{S}}$ are assumed to be linearly polarized along the y-direction with unit vector $\vec{e}_y$)

$$\frac{\partial \mathcal{E}}{\partial z} - \frac{1}{2ik}\nabla_\perp^2 \mathcal{E} = \frac{k}{2i\epsilon_0}\mathcal{S}. \tag{1}$$

The corrections to this equation are of the order $f^2 = (\lambda/2\pi w_o)^2$ and $g\lambda$ (g gain). w_o is a characteristic transverse beam dimension (not necessarily the beam diameter). Typically, f^2 is $\leqq 10^{-4}$ and $g\lambda \leqq 10^{-3}$ so that eq. (1) is an accurate laser analysis tool (λ laser wavelength).

2.1 Free Space Propagation

In free space eq. (1) becomes particularly simple since $\mathcal{S} = 0$ holds. Free space propagation is very important to know in high power lasers since due to diffraction resulting from hard edges or due to gain inhomogeneities the intensity profile may become heavily structured in the near field, usually the region where passive elements like lenses, beam splitters etc. or the entrance window of an amplifier are located. In order to avoid material damage the intensity peaks have to be known precisely. Soft aperture or image relaying can be used to minimize the unwanted intensity fluctuations.

There are various ways of solving eq. (1) with $\mathcal{S} = 0$. One method which is now frequently used is based on a 2-dimensional Fourier analysis (plane wave decomposition) represented by the Fourier transform of $\mathcal{E}$ /2/

$$\mathcal{F}\{\mathcal{E}\} = \mathcal{E}_F(z,\tau,a_x,a_y) = \int_{-\infty}^{+\infty}\int \mathcal{E}(x,y,z,\tau)\exp\{-2\pi i(xa_x + ya_y)\}\,dx\,dy \tag{2}$$

and the inverse Fourier transform /2/

$$\mathcal{F}^{-1}\{\mathcal{E}_F\} = \mathcal{E}(x,y,z,\tau) = \int_{-\infty}^{+\infty}\int \mathcal{E}_F(z,\tau,a_x,a_y)\exp\{+2\pi i(xa_x + ya_y)\}\,da_x\,da_y \tag{3}$$

where a_x, a_y are spatial frequencies. $\mathcal{E}_F\,da_x da_y$ is the complex amplitude of a plane wave propagating with direction cosines λa_x, λa_y and $[1-(\lambda a_x)^2-(\lambda a_y)^2]^{1/2}$. If the angular spectrum of the beam ($\mathcal{E}_F$) is not too widely spread, the angle between the $\vec{k}$-vector of an individual plane wave component and the z-axis is approximately given by λa with $a^2 = a_x^2 + a_y^2$.

Introducing eq. (2) into eq. (1) leads to the propagation equation of the angular beam spectrum $\mathcal{E}_F$

$$\frac{\partial \mathcal{E}_F}{\partial z} - i\pi\lambda a^2 \mathcal{E}_F = 0$$

which has the solution

$$\mathcal{E}_F(z,\tau,a) = \mathcal{E}_F(0,\tau,a)\exp(i\pi\lambda a^2 z). \tag{4}$$

Free space propagation is therefore easily carried out by inserting eq. (4) into eq. (3). The formalism is readily handled with numerical methods on computers by using FFT-routines (Fast-Fourier-Transforms). The propagation of a pulse between two amplifiers is thus rapidly calculated (see Fig. 1). In cross section 1 $\mathcal{E}_{F,1}$ is firstly determined from $\mathcal{E}_1$ yielding immediately the spectrum $\mathcal{E}^{in}_{F,2}$ on mirror M (position 2) by means of eq. (4). Going back to the physical space by using eq. (3) the field distribution $\mathcal{E}^{in}_2$ impinging on the mirror is calculated. Losses and phase changes introduced by the mirror can now be taken into account by writing

$$\mathcal{E}^{out}_2 = M\,\mathcal{E}^{in}_2$$

where M is the mirror transmission function. Moving to the $\vec{k}$ - space again $\mathcal{E}^{out}_{F,2}$ and $\mathcal{E}_{F,3}$ are obtained from eqs. (2) and (4) and then finally from eq. (3) the field distribution $\mathcal{E}_3$ in the entrance plane of amplifier B. Usually the transverse intensity profile changes along the pulse which then has to be cut in several pieces. Each of these is treated according to the procedure just described. At position 3 they are put together to yield $\mathcal{E}_3$. Even with this additional complexity FFT is much faster than a direct integration of eq. (1).

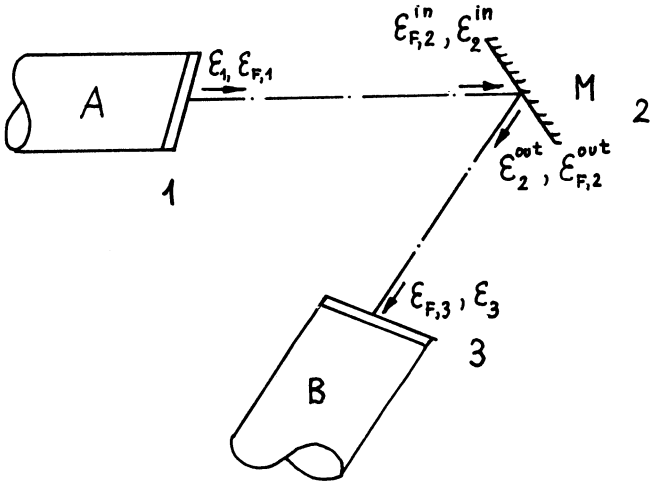

Fig. 1: Free space propagation between two amplifiers.

2.2 Propagation in Polarized Media

Outside free space the polarization $\mathcal{P}$ is not zero and in general nonlinear in the electric field $\mathcal{E}$ so that the Fourier formalism is not favourable any more. It is convenient to distinguish between two cases. In the first only a single wave is present, whereas in the second two or more waves may be present simultaneously.

Single Wave. Here $\mathcal{P}$ can be written as a power series in odd powers of $\mathcal{E}$ according to

$$\mathcal{P} = \epsilon_0 \{ \chi_1 \mathcal{E} + \chi_3 \mathcal{E}^3 + \cdots \} \tag{5}$$

where χ's denote susceptibilities. The real part of χ_1 represents the refractive index, whereas the imaginary part is either exponential loss (Beer's law) or gain as in an amplifier. The term $\chi_3 \mathcal{E}^3$ accounts for two processes. The real part of χ_3 represents self focussing and the imaginary part multiphoton processes.

Two or More Waves. This case includes various processes. Frequency mixing involves the interaction of three waves at different frequencies, ω_1, ω_2 and ω_3 obeying the relation $\omega_3 = \omega_1 + \omega_2$. A special case is second harmonic generation where $\omega_1 = \omega_2$ and thus $\omega_3 = 2\omega_1$ holds; ω_1 is then the pump wave. Frequency conversion is now commonly used in all large fusion laser systems in order to increase the fraction of laser light absorbed by the plasma. Stimulated Brillouin and Raman scattering are also three wave interaction processes with two light waves at frequencies ω_p, ω_s (ω_p pump light, ω_s scattered light) and a sound wave or a molecular vibration, respectively, either at frequency Ω. In laser systems only the Stokes-case is of importance where $\omega_s = \omega_p - \Omega < \omega_p$ holds. The scattered wave amplitude can be made the phase conjugate of the pump wave amplitude if the pump and scattered waves travel in exactly opposite directions (back scattering). Phase conjugation or wave front reversal enables the cancellation of static aberrations acquired by the pulse if the medium in which they occur is traversed first by the pump wave and then by the scattered wave /3/. Phase conjugation can also be achieved by degenerate four wave mixing (DGFW) where the frequencies of the two counter propagating pump waves and the signal and reflected waves are equal. Brillouin, Raman and DFWM-mirrors can also be used for amplifier isolation in order to avoid parasitic chain oscillations and, in addition, to a certain extent for pulse shortening, especially for pulses originally several or more ns long.

Amplification. As already mentioned, the imaginary part of χ_1 is responsible for amplification. For the following discussion it is sufficient to consider only the incoherent approximation, $T_2 \ll T_{pulse}$, where T_2 is the dephasing time and T_{pulse} the pulse duration. In this case the polarization is simply given by (two level system, no detuning)

$$\mathcal{P} = \epsilon_0 \, \mathrm{Im}(\chi_1) \, \mathcal{E} = i \epsilon_0 \Delta N \sigma \mathcal{E} / k \tag{6}$$

where σ is the induced emission cross section at line centre and ΔN the inversion density defined as

$$\Delta N = N_u - \frac{g_u}{g_l} N_l \, . \tag{7}$$

$N_{u,\ell}$ are the population densities of the upper and lower laser levels with the degeneracy factors $g_{u,\ell}$. σ can be calculated from the relation

$$\sigma = \frac{A_{u,\ell}\ \lambda^2}{4\pi^2 n^2\ \Delta\nu} \tag{8}$$

where $A_{u,\ell}$ denotes the Einstein coefficient of spontaneous emission for the transition under consideration, $\Delta\nu$ the medium bandwidth and n the refractive index. If eq. (6) is inserted in eq. (1) and diffraction is neglected in the amplifier which is a reasonable assumption when the amplifier is not too slender ($\frac{d^2}{4\lambda\ell} \geqq 10^2$ with d,ℓ diameter and length of the amplifier) the electric field can be replaced by the intensity

$$I = \frac{1}{2}\,\epsilon_0 c n\, \mathcal{E}\mathcal{E}^* \tag{9}$$

thus yielding the differential equation

$$\frac{\partial I}{\partial z} = (\sigma\Delta N - \gamma) I. \tag{10}$$

Here a loss term γI has been added phenomenologically. For small signal amplification (SSA) ΔN can be considered as constant and the integration of eq. (10) readily yields

$$I(z,\tau) = I(0,\tau)\exp\{(\sigma\Delta N - \gamma) z\} \tag{11}$$

whereby $\sigma\Delta N$ is usually referred to as the gain coefficient

$$g = \sigma\Delta N. \tag{12}$$

If medium saturation (large signal amplification, LSA) occurs ΔN is no longer constant and the wave equation must be supplemented by two rate equations for the determination of the population densities $N_{u,\ell}$ of the upper and lower levels. These equations are

$$\frac{\partial I}{\partial z} = (\sigma\Delta N - \gamma) I, \tag{10}$$

$$\frac{\partial N_u}{\partial \tau} = -\sigma\Delta N I/h\nu - \frac{N_u}{\tau_u} + P, \tag{11}$$

$$\frac{\partial N_\ell}{\partial \tau} = +\sigma\Delta N I/h\nu + \frac{N_u}{\tau_{u,\ell}} - \frac{N_\ell}{\tau_\ell}. \tag{12}$$

$h\nu$ is the photon energy, τ_u the actual upper level life time, $\tau_{u,\ell} = 1/A_{u,\ell}$ the life time of the upper level regarding the radiative transition to the lower level and τ_ℓ the actual life time of the lower level. P is the pump rate of the upper laser level ($cm^{-3}s^{-1}$). τ_u is defined by

$$\frac{1}{\tau_u} = \sum_j A_{u,j} + \frac{1}{\tau_q} \tag{13}$$

where $\sum_j A_{u,j}$ counts for radiative transitions from the upper level to lower lying levels and τ_q for non-radiative transitions (quenching). τ_u is an important parameter. It allows for the distinction between storage and non-storage media. For a storage medium the pulse duration T_{pulse} is small compared to τ_u, $T_{pulse} \ll \tau_u$. CO_2, iodine and Nd are examples of a storage medium. A non-storage medium is characterized by the opposite condition, $T_{pulse} \geq \tau_u$; usually the excimer lasers XeCl and KrF belong to this category when T_{pulse} is in the ns-regime. However, these lasers can also support the propagation of ps-pulses and are then storage lasers ($\tau_u \sim 5$ ns). As it will become clear later the architectures of a storage and a non-storage laser are completely different.

Storage Medium: $T_{pulse} \ll \tau_u$. We consider a lossless medium with $\gamma = 0$, $T_{pulse} \ll \tau_{u,\ell}$, τ_ℓ and with $P = 0$ after excitation. Eqs. (11,12) can then be combined to an equation for the inversion density

$$\frac{\partial \Delta N}{\partial \tau} = - \frac{\Delta N I}{e_s} \tag{14}$$

whereby the saturation fluence e_s has been introduced

$$e_s = \frac{h\nu}{\left(1 + \frac{g_u}{g_\ell}\right)\sigma} . \tag{15}$$

If the beam loading exceeds e_s the energy e_{st} (J/ℓ) stored in the medium can be effectively extracted provided the damage threshold of either the laser medium or the output window is nowhere exceeded. In the SSA-case characterized by ($e = \int I dt$ beam fluence)

$$\Delta N \simeq \text{const.}; \; e_{in}, e_{out} \ll e_s$$

where e_{in}, e_{out} are the beam fluences at the amplifier entrance and exit the relations

$$\begin{aligned} I_{out} &= A_{ss} I_{in}, \\ e_{out} &= A_{ss} e, \\ A_{ss} &= \exp\{\sigma \Delta N \ell\} \end{aligned} \tag{16,a,b,c}$$

hold with A_{ss} being the small signal amplification. The pulse shape is conserved under these conditions. In the LSA-case the integration of the eqs. (10,14) yield the famous Frantz-Nodvik formula /4/

$$e_{out} = e_s \ln\left\{1 + A_{ss}\left(e^{\frac{e_{in}}{e_s}} - 1\right)\right\}. \tag{17}$$

The value of A_{ss} is to be taken prior to extraction. In opposite to the SSA-case strong pulse compression may occur in the LSA-case. The extraction efficiency is determined from

$$\eta_{ex} = \frac{e_{out} - e_{in}}{e_{st}} \leq \frac{1}{1 + g_u/g_\ell} \tag{18}$$

where

$$e_{st} = \Delta N h\nu \tag{19}$$

is the stored energy density, usually measured in J/ℓ. The extraction efficiency comes close to its maximum value $(1+g_u/g_\ell)$ if $e_{in} \geqq e_s$ holds.

Non-storage-Medium: Due to $T_{pulse} >> \tau_u$ the time derivatives in eqs. (11,12) can be neglected. If it is further assumed that the lower laser level is practically not populated, $N_\ell \cong 0$, due to its small life time τ_ℓ what is valid for XeCl and KrF the steady state population of the upper level reads

$$N_u = \frac{P\tau_u}{1+I/I_s} \tag{20}$$

whereby the saturation intensity

$$I_s = \frac{h\nu}{\sigma\tau_u} \tag{21}$$

has been introduced. I_s is the counterpart to e_s. The paraxial wave equation can be transformed to

$$\frac{dI}{dz} = \gamma \frac{I/I_s}{1+I/I_s}\left(I_{Max} - I\right) \tag{22}$$

where the loss coefficient γ has been retained (necessary for XeCl and KrF) and I_{Max} is the maximum possible intensity achievable by the pulse. I_{Max} reads

$$I_{Max} = I_s\left(g/\gamma - 1\right) \tag{23}$$

with

$$g = P\sigma\tau_u$$

as the stationary small signal gain. I_{max} is the maximum possible intensity achievable by the pulse. This can be easily seen by realizing that a pulse with an input intensity equal to I_{Max} is not amplified because of dI/dz = 0 so that $I_{out} = I_{in} = I_{Max}$ holds. For $I_{in} > I_{Max}$ the pulse is attenuated since dI/dz is negative. Amplification is thus only possible for $I_{in} < I_{Max}$. When the amplifier is long enough the pulse intensity eventually reaches I_{Max}. The SSA-case, $I << I_s$, has the simple solution

$$I_{out} = I_{in}\exp\{(g-\gamma)\ell\} \tag{24}$$

where ℓ denotes the amplifier length. The general solution (LSA-case) of eq. (22) can only be given in an implicit form firstly derived by Schulz-Dubois /5/

$$\left(\frac{I_{out}}{I_{Max}-I_{out}}\right)^\delta \frac{1}{I_{out}} = \left(\frac{I_{in}}{I_{Max}-I_{in}}\right)^\delta \frac{\exp(\gamma\ell)}{I_{in}} \tag{25}$$

with

$$\delta = \frac{1}{1-\gamma/g}\,. \tag{26}$$

The extraction efficiency is defined as

$$\eta_{ex} = \frac{I_{out} - I_{in}}{P\tau_u h\nu l} \,. \tag{27}$$

It is not difficult to see that η_{ex} must have a peak. η_{ex} is zero for $I_{in} = I_{Max} = I_{out}$ and almost zero for the SSA-case, $I << I_s$. At some value of $I_{in} < I_{Max}$ η_{ex} must thus show a maximum. For high power excimer amplifiers one typically finds $\gamma l \sim 1$, $\gamma \cong 5\text{x}10^{-3}\text{cm}^{-1}$, $g/\gamma \cong 15$, $I_s \cong 2$ MW/cm^2 and $I_{Max} \cong 28$ MW/cm^2. For an input intensity of $I_{in} = 0.1$ MW/cm^2 an extraction efficiency of 40 % is thus possible.

Although the model presented here is a rather simple one it is sufficient for an approximate judgement of the performance of excimer amplifiers. Improvements would result from a more accurate consideration of the kinetics and the V,R dynamics of the various molecules involved.

Amplified Spontaneous Emission (ASE). Due to the radiative life of the upper laser level of only a few nanoseconds amplified spontaneous emission is a serious problem for excimer lasers; in iodine and CO_2 it is of little importance since the Einstein coefficients are much smaller compared to those of KrF or XeCl. Nd:glass is somewhere in between these two extremes; blocking of ASE occurring during the end of the pumping period is usually necessary here to prevent premature target damage.

A rough estimate of the ASE-intensity can be made if one considers a cylindrical amplifier with perfectly absorbing walls so that no reflections have to be taken into account (see Fig. 2). With the inclusion

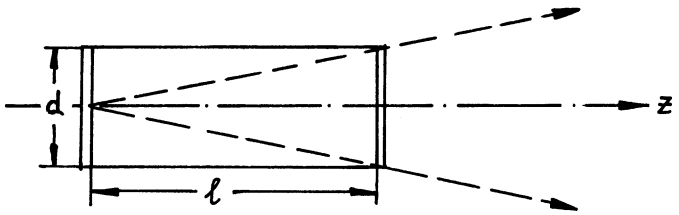

Fig. 2: Beam geometry for an estimation of ASE

of spontaneous emission the paraxial wave equation reads

$$\frac{\partial I}{\partial z} = gI + \frac{N_u h\nu}{\tau_{u,l}} \frac{\delta\Omega}{4\pi} \tag{28}$$

which when integrated on the assumptions g = const., N_u = const. and on the boundary condition I (z = 0) yields

$$I_{ASE} = I(z=\ell) = \frac{\delta\Omega}{4\pi} \frac{h\nu}{\sigma\tau_{u,\ell}} \frac{N_u}{\Delta N} \left(e^{g\ell} - 1\right) \simeq \frac{\delta\Omega}{4\pi} \frac{h\nu}{\sigma\tau_{u,\ell}} A_{ss} \cdot \tag{29}$$

In eqs. (28,29) $\delta\Omega/4\pi = \frac{(d/\ell)^2}{4\pi}$ is the fraction of spontaneously emitted photons moving in the "right" direction. In eq. (29) the inversion ΔN was set equal to the upper level population density N_u ($N_\ell \sim 0$). It was further required that $A_{ss} >> 1$ holds.

For storage lasers (CO_2, Nd:glass, iodine) the important criterion is that ASE should not damage the target. This may either occur by too much power or energy. The latter can be obtained by the integration of eq. (29) over the pumping time. In any case, the need to avoid premature target damage puts an upper bound on A_{ss} which in a chain is to be understood as the amplification resulting from all amplifiers belonging to the chain. If A_{ss} turns out to be too large saturable absorbers, Pockels cell shutters or Brillouin/Raman mirrors must be introduced in the chain to decrease the ASE gain.

For non-storage media or cw-system, like the long pulse excimer lasers, the main concern is that all the pump power may be converted to ASE and will thus not be available for the pulse to be amplified. In order to prevent this from happening the condition $I_{ASE} < I_s$ must be met or with the help of eqs. (21) and (29)

$$A_{ss} \frac{\tau_u}{\tau_{u,\ell}} \frac{\delta\Omega}{4\pi} < 1. \tag{30}$$

This condition connects the geometry of the amplifier, $\delta\Omega$, with the gain of the medium, A_{ss}. More realistic calculations take wall reflections /6,7/ into account. They show that cuboid-shaped amplifiers have attractive properties.

3. Laser Media

In this section the most important laser medium parameters will be firstly reviewed followed by a presentation of the damage threshold of bare and coated surfaces of various materials and their dependence on wavelength and pulse duration. After that the excitation scheme, performance and overall efficiency achievable in reality will be discussed for the CO_2, iodine, Nd-glass and excimer lasers.

3.1 Survey on Characteristic Laser Medium Properties

In section 2.2 the fundamental properties of a laser medium were introduced. These are wavelength λ, induced emission cross section σ, medium line width $\Delta\nu$, actual upper level life time τ_u, Einstein coefficient $A_{u\ell}$, saturation fluence e_s, saturation intensity I_s, stored energy density e_{st}, inversion ΔN and, for gas lasers, the pressure. These data are collected in Table 1 for the CO_2, iodine, Nd:glass, KrF and XeCl lasers.

Table 1: Laser Medium Properties

Laser Medium	λ μm	σ cm^2	ΔN cm^{-3}	$\Delta\nu$ GHz	$A_{u,\ell}$ s^{-1}	τ_u μs	I_s $\frac{MW}{cm^2}$	e_s $\frac{J}{cm^2}$	e_{st} $\frac{J}{\ell}$	p bar	Ref.
CO_2 *	10.6	6×10^{-19}	6×10^{16}	13	.21	4	/	.23	17	2.4	8
CO_2 **	9.4	1.6×10^{-19}	1.3×10^{17}	$\frac{75}{>10^3}$		.4	/	.70	35	10	9,10
Iodine	1.32	1×10^{-19}	1×10^{17}	20	8	100	/	.5	15	5	11
Nd: glass	1.06	3×10^{-20}	2×10^{18}	10^4	2.800	300	/	5	375	/	12
XeCl †	.308	6.4×10^{-16}	3×10^{14}	5×10^3	9×10^7	5×10^{-3}	.2	1×10^{-3}	~5	5	13,34
KrF #	.248	2×10^{-16}	4×10^{14}	$\sim10^4$	1.4×10^8	4×10^{-3}	1-2	/	10	1-3	6,7

* The data given in this line refer to the 40 kJ/1 ns ANTARES system. $\Delta\nu$ is the width of a single line. The inversion ΔN pertains to the P(20) line only. $e_{st}=(N_{001}-N_{100})\ h\nu$ is the energy difference between the energies stored in the 001 and 100 vibrational modes, thus $\Delta N \cong \mathcal{R}(J)e_{st}/h\nu \cong 0.07\ e_{st}/h\nu$. $\mathcal{R}(J)$ is the rotational partition function. Note that $e_s = h\nu/\{2\sigma\mathcal{R}(J)\} \cong 7\ h\nu/\sigma$ holds.

** In /9/ 3 ps-pulses at 9.4 µm were amplified. 75 GHz is the width of a single line. The R-branch at 9.4 µm has a total width of > 10^3 GHz.

\+ The data correspond to the experimental conditions of /34/ where 2 ps-pulses of 300 GHz bandwidth were amplified. σ is the cross section of the 4 main B-X transitions. τ_u is the actual life time of the B-state. e_{st} is the energy difference between the B- and X-states whereas ΔN is the inversion pertaining to the 0-2 transition only (B → X).

\# The data refer to long pulses > 1 ns. Regarding ΔN, e_{st} see footnote for XeCl. σ is a transition averaged cross section.

Together with the pulse duration T_{pulse} the upper level life time τ_u not only determines the type of laser, storage or non-storage, but also the technical realization of the pumping process. The larger τ_u the more economical can the power supply be built. In this sense the short upper level life times of the excimer lasers are somewhat unfavourable.

The Nd-glass laser and the iodine laser are optically pumped. In both cases τ_u is large enough that relatively cheap flashlamp technology can be used. Large volume CO_2 lasers need e-beam sustained discharges. This technique is now rather well understood and established.

Saturation fluence or saturation intensity are important for the extraction efficiency. If they are much smaller than the damage threshold of the various materials occurring in a complex laser system the energy stored in the active medium can be efficiently extracted by the pulse (saturation regime). This is true for the excimer, iodine and CO_2 lasers. Due to the high value of $e_s = 5\ J/cm^2$ only long pulses of several ns duration enable a good energy extraction in Nd:glass lasers; short pulses (< 1 ns) are more or less restricted to the small signal regime with low extraction efficiency.

The column of the stored energy density shows that Nd:glass is the most compact laser system. All the gas lasers roughly need twenty times more volume for the same amount of stored energy. At the first glance this figure is very much in support of glass lasers but falls off importance if it is realized that the amplifiers constitute only a minor fraction of the total volume required by a large laser system.

For gas lasers the pressure determines the strength of the mechanical structure and the thickness of the amplifier windows. Large size amplifiers with a volume of about $1\ m^3$ or more can only tolerate a few bar; high pressure devices as those needed for the generation of ps CO_2-laser pulses can only be built for small volumes of a few liter.

The medium line width $\Delta\nu$ determines the shortest pulse duration which can be realized. Since the pulse bandwidth cannot become larger than $\Delta\nu$, T_{pulse}^{Min} is given by $1/\Delta\nu$ provided the pulse is Fourier-limited. In high pressure CO_2-lasers, in Nd:glass and excimer lasers $\Delta\nu$ is $\geqq 10^3$ GHz so that ps-pulses can be amplified. In iodine lasers the shortest pulse duration practically achievable is ~ 50 ps.

3.2 Damage Thresholds

With almost no exception the performance of high power lasers is limited by laser-induced damage occurring either on bare or coated surfaces or within the material supporting the pulse propagation. Since surface damage usually precedes volume damage only surface damage will be considered in the following.

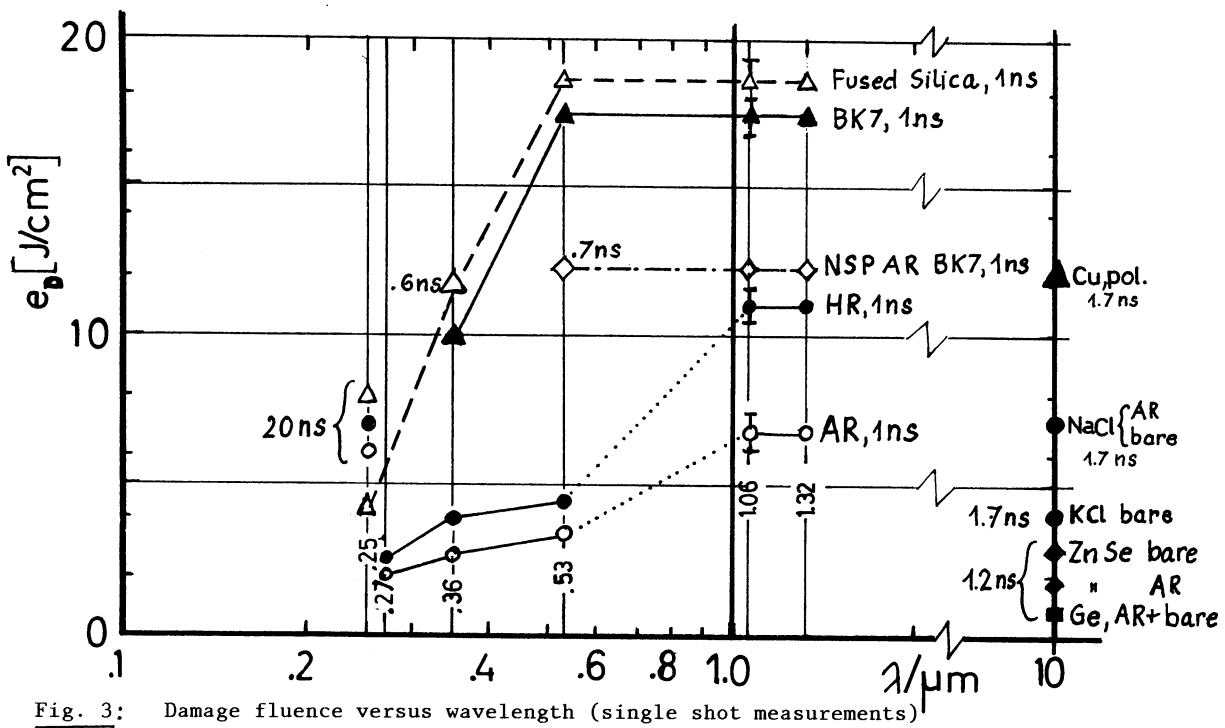

Fig. 3: Damage fluence versus wavelength (single shot measurements)
HR High reflectivity coatings, AR antireflective coatings, NSP AR Neutral-solution processing gradient index AR BK7 surfaces

The morphology of surface damage to transparent dielectric materials indicates that damage is caused by absorption of energy from the laser pulse which heats a small volume of material to the point of stress fracture or melting. Sources of absorption depend on the substrate and coating material and the way they are processed and on the wavelength and pulse width of the laser. The most important mechanisms for damage by pulses in the range of 100 ps to 20 ns duration are absorption by particle impurities of submicron diameter or by small volumes of critical-density plasma generated by avalanche ionisation at impurity sites. Details of the absorption mechanisms are subject of continuing debate and not yet fully clarified. Models used to predict the parametric dependence of the damage threshold on pulse width, wavelength and beam diameter are still at a very early stage. For the purpose of this review article it is sufficient to say that damage is related to impurities and defects rather than to intrinsic properties of the materials.

In Fig. 3 damage threshold data which have been recently published in the literature are collected; the pulse durations are between 0.6 and 20 ns. Measurements are available at 10 μm (CO_2)/14,15/,1.32 μm (iodine), 1.06 μm (Nd), .53 μm, .355 μm, .266 μm and .248 μm (KrF). A large body of the material at the Nd wavelength of 1.06 μm and of its second, third and fourth harmonics as well as that at the KrF wavelength of .248 μm comes from the Lawrence Livermore Laboratory where a big Nd:glass laser program (SHIVA,NOVA) and a smaller KrF laser program is being conducted /16,17,18/. For iodine (1.32 μm) our own measurements have shown (not yet published) that the damage threshold are very much the same as those found for 1.06 μm. Additional data have been found in /12,19,20/.

The largest thresholds are obtained for bare or uncoated surfaces regardless whether they are fused silica, BK7-glass, polished copper, NaCl or KCl. Coated surfaces have a much lower damage threshold. Noticable is the difference between the high reflective (HR) and anti-reflective coatings (AR). The reason for that is not yet clear. Attempts to correlate this phenomenon with the different standing wave field distributions in both cases have not been conclusive. In /16/ it is argued that the higher thresholds of the HR coatings is due to the fact that the interface between the coating and the substrate is not exposed to the laser energy. This is just opposite to the situation occurring in AR coatings where the damage originates at the coating-substrate interface which can be affected by polishing, cleaning and residual surface contamination.

Common to all thresholds is their decrease with decreasing wavelength, especially at short wavelengths. This trend probably results from the increase in absorption at uv-wavelengths of both transparent dielectric materials and common molecular or particulate contaminants.

The neutral-solutions processing gradient index anti-reflective BK7 surfaces (NSP AR BK7) deserve special attention since their damage threshold is even higher than that of HR-coatings /17/. Especially attractive is the independance of the threshold on the wavelength down to .5 µm just opposite to the behaviour of AR-coatings. Unfortunately,

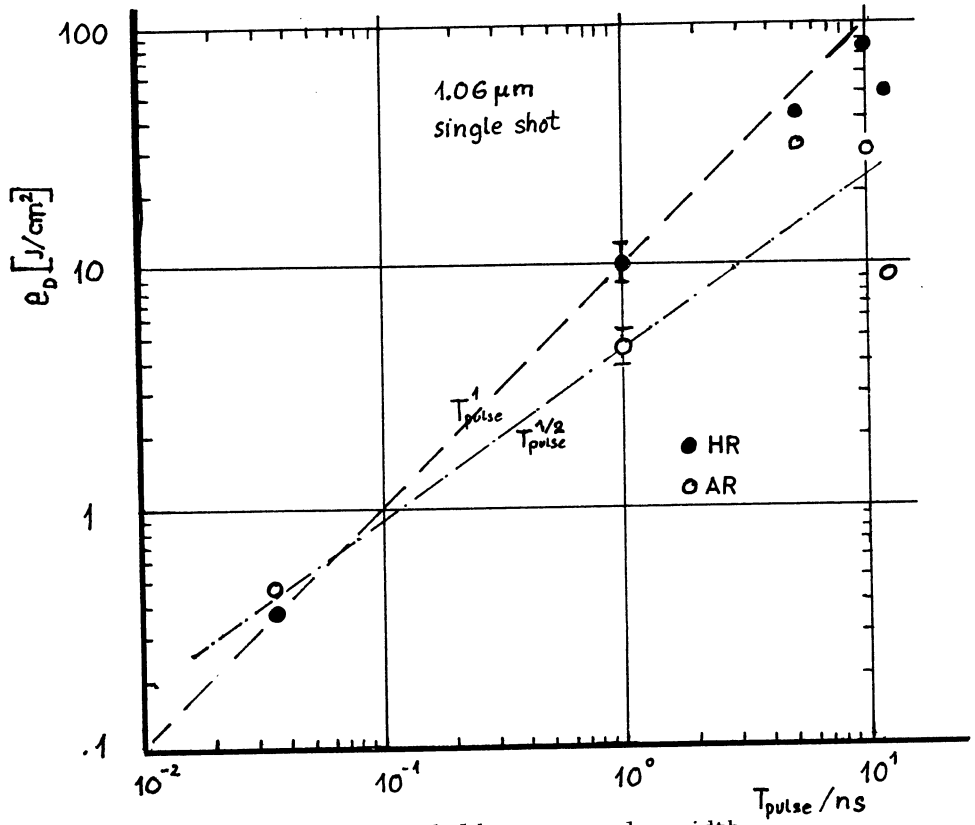

Fig. 4: HR- and AR-damage thresholds versus pulse width

the NSP process does not produce AR surfaces on fused silica which is the only material presently capable of transmitting high intensity pulses below .35 µm. The Sol-Gel Technique /18/ is presently viewed as the most promising method to fabricate porous silica coatings which might have higher damage thresholds than those achievable with AR coatings.

The dependance of the damage threshold on pulse duration is as complex as that on the wavelength. Fused silica and BK7 approximately obey the square root law on the pulse duration

$$e_D \cong \text{const.}\ T_{pulse}^{1/2} \tag{31}$$

in the pulsewidth range from .17 ns to 5 ns /16/ and in the wavelength range from .5 to 1.3 µm. In the UV the exponent (fused silica) appears to be much smaller, .25 versus .5. For HR-and AR-coatings experimental material is only available at 1.06 µm /20/. Fig. 4 shows the damage threshold dependance on T_{pulse} from 35 ps to 12 ns for single shot operation. HR- and AR-coatings appear to follow the square root law only to some extent: $e_D^{HR} \sim T_{pulse}^{0.8}$ and $e_D^{AR} \sim T_{pulse}^{0.7}$. These relations are, however, just a rough estimate, since the data scatter too much at ~ 10 ns. Moreover, the physics responsible for damage at 35 ps is not known and might be different from the mechanisms active at ~ 1ns. The possible role of nonlinear processes such as two photon absorption, harmonic generation or Raman scattering is also not yet identified which all might lower either the reflectivity of HR-coatings or the transmission of AR-coatings and that of the substrate. This field is rather unexplored, especially in the region of ps-pulses.

Finally, it should be pointed out that damage threshold for multiple shot operation are much smaller than those for 1 shot operation. A reduction by a factor of 10 is very likely to occur if the same coating is exposed to $\geqq 10^4$ laser shots /20/.

3.3 CO_2 - Laser

The CO_2 level diagram is shown in Fig. 5 /8/. For a typical gas composition of 4:1:1:He:N_2:CO_2 (at 1 bar) the lifetime of the upper laser level 00°1 is about 8 µs. The main factor in de-exciting this level is CO_2-CO_2 collisions populating other CO_2 excited states. Owing to the Fermi-resonance for the 100-020 levels the equilibration time between them is very short, ~ 4 ns. The complex of levels is then seen to decay to the 01^10 level with a lifetime of ~ .13 µs. The 01^10 level is the "bottle-neck" in the CO_2 laser; in pure CO_2 the lifetime is quite long, ~ 10 µs at a CO_2 pressure of 600 mbar. It has been found that the addition of He to CO_2 preferentially de-excites the 01^10 level, for the cited gas composition the deactivation time is reduced to .2 µs. For pulses longer than a few hundred nanoseconds helium thus improves the extraction efficiency; for operation in the nano- or picosecond regime it has, however, no effect on the extraction efficiency but can be used to control the discharge parameter E/N (E electric field, N molecules per cm^3).

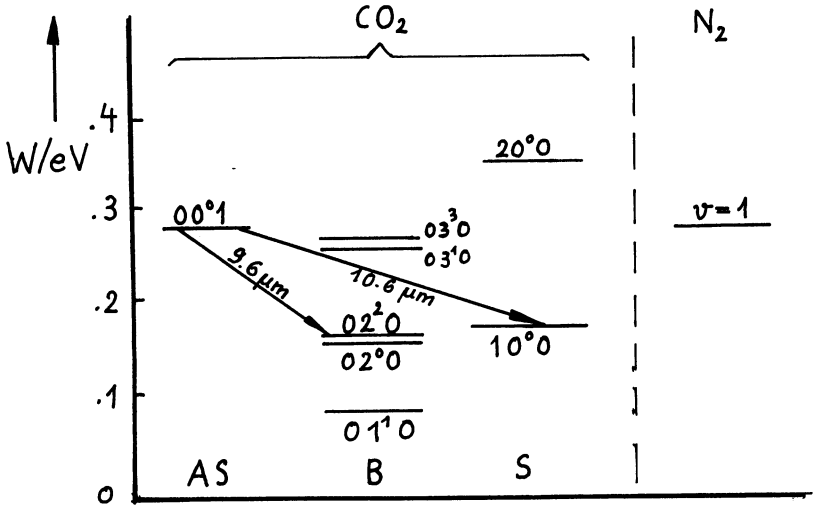

Fig. 5: Energy level diagram of CO_2 and N_2
(AS Asymmetric Stretching Mode, B Bending Mode, S Symmetric Stretching Mode)

Large amplifier volumes can only be pumped by means of e-beam sustained discharges. Self-sustained discharges are inherently unstable and quickly degenerate into constricted, low impedance arcs destroying the electrical and thus optical uniformity of the laser medium. The "trick" of the e-beam controlled discharges relies on the separation of electron production from the electric field which is optimum for the excitation of the CO_2 vibrational level which is due to inelastic e-CO_2, e-N_2 and N_2-CO_2 collisions. The excitation cross sections for CO_2 and N_2 are such that they correlate with different positions of the electron energy spectrum.

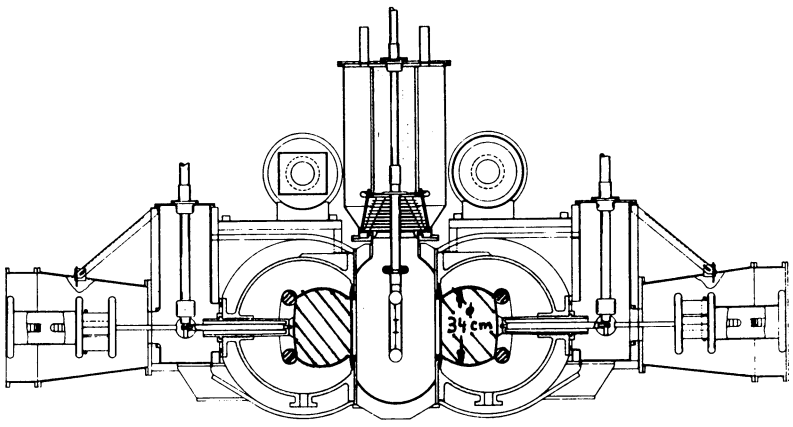

Fig. 6: Cross Section of a HELIOS dual beam module

Fig. 6 is a cross section of one of the four final HELIOS dual beam amplifiers /8,21/. HELIOS is an eight-beam facility delivering altogether 10 kJ in .5 ns into calorimeters. The electron gun is the central assembly suspended from a high voltage vacuum feed through bushing. The cathode structure has a pair of emitter blades on each side of the backing plate and emits a beam of electrons towards thin titanium windows to the left and to the right of the cathode. Each e-beam has a cross section of about 40 x 200 cm^2 and has a current of 5000-7000 A at -300 kV. A rather similar amplifier design is used in the Japanese LEKKO VIII laser system /22/.

The presently biggest CO_2-laser is ANTARES which can deliver an energy of 40 kJ in ~ 1 ns. Fig. 7 shows a photograph of one of the two final modules during the construction period. It clearly demonstrates the enormous size and space requirement of high energy lasers.

The overall efficiency η_{tot} is determined by a product of several fundamental and engineering factors

$$\eta_{tot} = \eta_{ex} \cdot \eta_E \cdot \eta_P \tag{32}$$

where η_p is the pump efficiency, η_{ex} the extraction efficiency and η_E an engineering factor. η_p is defined by /8/

$$\eta_P = \frac{e_{st}}{\int \vec{E} \cdot \vec{j}\, dt} \leq 7\% \tag{33}$$

where $\int \vec{E} \cdot \vec{j} dt$ is the energy input to the laser medium. η_{ex} is calculated from

$$\eta_{ex} = \frac{e_{out} - e_{in}}{e_{st}} \simeq 50\%. \tag{34}$$

Although due to the low value of the saturation energy density the energy stored in the 00°1 vibrational mode can be fairly well extracted, η_{ex} is limited to 50 % since on ns-time scale ground state depletion by helium is ineffective. η_E counts for various engineering limitations resulting from the e-beam generation, pumping power transmission and deposition in the laser medium, incomplete discharge volume utilization, reflection losses of mirrors and windows etc. A reasonable value for η_E is 0.5 so that

$$\eta_{tot} \leq 1.8\%. \tag{35}$$

η_{tot}-values of up to 1.6 % have been achieved in HELIOS.

As already noted, ps-CO_2 lasers need rather large pressure of $\geqq$ 10 bar to achieve a sufficient degree of overlap of the rotational lines. The active volume which can thus be pumped is small; in the devices described in /9,10/ 40 and 32 cm^3 are reported. Under these circumstances a normal discharge with either UV-preionization /9/ or with e-beam preionization /10/ can be used. In /9/ a 2 ps-pulse could be amplified to a power of

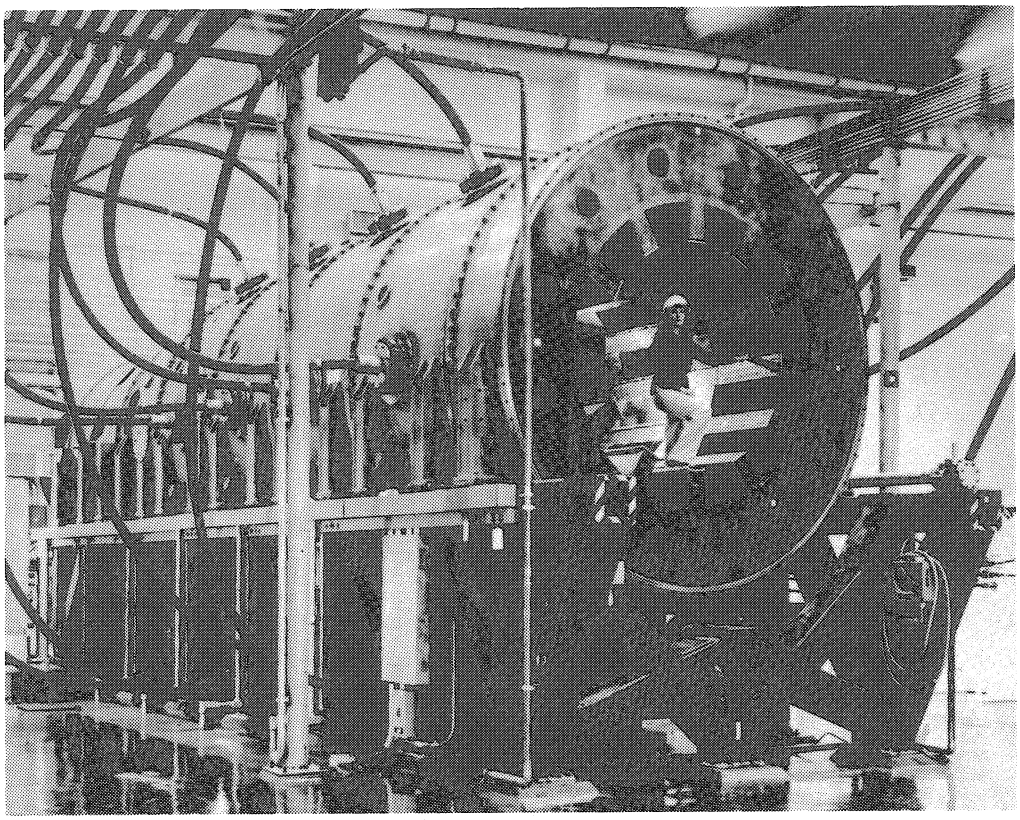

Fig. 7: Final Amplifier Module of ANTARES

10 GW. Hence, if the discharge volume could be scaled to the liter-region which technically appears to be feasible the power level reaches the TW-range thus shortening the gap regarding the power demands of laser grating accelerators.

The generation of ps-CO_2 laser pulses - although straight-forward - requires some effort /9/. It needs a single longitudinal mode CO_2-laser delivering a long output pulse of typically ~ 100 ns duration and a ps-dye laser which is used to switch out a ps-portion from the long CO_2-laser pulse. Switching elements which are activated by irradiation with the dye laser pulse are either polycrystalline CdTe (in reflection) or silicon slabs (in transmission). The power level of the ps-CO_2 pulse achievable with this technique is in the 100 kW-range.

The CO_2 laser is also an interesting candidate for laser plasma accelerators. In this case the pulses don't have to be that short as for laser grating accelerators; durations ~ 50 ps are currently viewed at as an acceptable choice. Such pulses can be effectively generated with the optical free-induction decay /23/. Amplification of 50 ps-pulses needs a medium linewidth of ~ 10 GHz corresponding to a pressure of 2.5 bar. This is just the range in which the high energy amplifiers of ANTARES are operated. This laser is thus

ideally suited as a driver for the plasma accelerator. Since the pulse should have two carrier frequencies (two line operation) amplification has to be controlled in such a way that the two pulse components are intensified by the same amount, i.e. they have to experience the same gain. This requirement puts some restriction on line selection and separation.

3.4 Iodine Laser

Three different pumping mechanisms of the atomic iodine laser radiating at a wavelength of 1.32 µm are known /11/. Two of them are based on the dissociation of fluorinated alkyliodides as CF_3I, C_2F_5I, C_3F_7I etc. either by irridiation with UV-light centred around 270 nm or by electron impact. The third method is chemical pumping and relies on resonant energy transfer between molecular oxygen and atomic iodine according to

$$O_2^*(^1\Delta) + I(^2P_{3/2}) \rightleftharpoons O_2(^3\Sigma) + I^*(^2P_{1/2}) . \tag{36}$$

Chemical pumping is well suited for cw-operation and also for high repetition rate operation. However, its potential for pulsed high-power operation is very limited since the energy is mainly stored in the excited oxygen molecules and too a far less extent in the iodine atoms thus requiring inefficient multiple pass operation for energy extraction.

Dissociation by electron impact produces ground state $^2P_{3/2}$ and excited state $^2P_{1/2}$ iodine atoms with an almost equal amount and is thus not very attractive. Only the photodissociation of fluorinated alkyliodides according to

$$RI + h\nu\,(\sim 270\ nm) \longrightarrow R + I^*(^2P_{1/2}) \tag{37}$$

has proven to generate preferentially excited iodine atoms and is therefore presently the only pumping method used for high power applications. i-C_3F_7I is the most commonly used compound; it has an I*-yield close to 1 and its radical C_3F_7 has a large rate constant for recombination with a ground state iodine atom to the parent molecule C_3F_7I.

Since high energy photons are needed to crack the C-I bonding of the alkyliodides the quantum efficiency of the iodine laser

$$\eta_q = \frac{h\nu_{IR}}{h\nu_{UV}} = \frac{1.5\times10^{-19}\,J}{7.2\times10^{-19}\,J} = 0.21 \tag{38}$$

is not very high.

The lifetime of the upper, metastable laser level is 125 ms. Actually, due to quenching processes by I_2, RI, CO_2, SF_6, Ar it is much shorter and lies for high power amplifiers between 100 µs and 1 ms depending on the kind of gas mixture used which is composed of C_3F_7I + buffer gas (either Ar, SF_6 or CO_2) with a ratio of RI: buffer gas of 1:50 up to 1:1000 at a total pressure of a few bar /11/.

The detailed spectroscopy of the iodine $^2P_{1/2}$ - $^2P_{3/2}$ transition is of importance for the extraction efficiency. The nuclear spin (I = 5/2) splits the excited state in 2 levels with F_u = 3,2 (see fig. 8) and the ground state in 4 levels with F_ℓ = 4,3,2,1. According to the selection rules $\Delta F = 0, \pm 1$ six transitions (magnetic dipole) are possible; however, under usual conditions, i.e. in the absence of strong magnetic fields, only the 3-4 line which has the highest gain is emitted by an oscillator. The upper state level mixing time is about 30 ns whereas for the ground levels it is much faster, of the order of the dephasing time T_2, ranging from 10 to 60 ps. For a several hundred picosecond or longer pulses the ground state levels can thus be replaced by one level with an effective

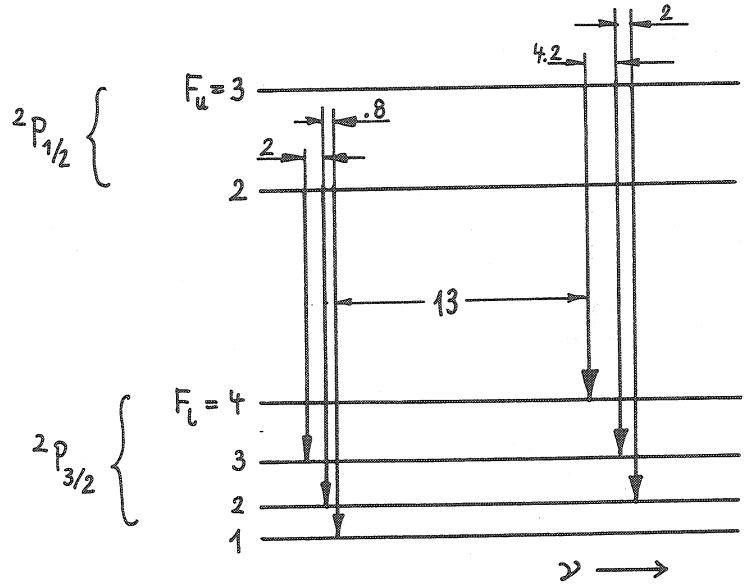

Fig. 8: Hyperfine spectrum of the iodine laser transition (The line separations are in GHz).

degeneracy factor of 24. If the medium linewidth $\Delta\nu$ is $\geq$ 15 GHz (single transition) which is typical for high power amplifiers line overlapping becomes sufficiently strong that a pulse whose carrier frequency is coincident with the centre frequency of the 3-4 transition also has access to the energy stored in the upper F = 2 hyperfine level. In this case the maximum possible efficiency reads

$$\eta_{ex}^{Max} = \frac{1}{1+12/24} = 67\%. \qquad (39)$$

If there is no line overlapping at all ($\Delta\nu \leq 3$ GHz) η_{ex} drops to 45 %. Practically achievable values lie between 50 and 55 % and are connected with strong medium saturation leading to a considerable pulse compression and distortion. This not only means that the chain input pulse duration has to be much longer than that wanted for the exit pulse (up to a factor of 10) but also complicates pulse shaping.

Photodissociation pumping can be done by flashlamps or open discharges. Fig. 9a shows an amplifier based on flashlamp pumping. Pump source and laser medium are completely

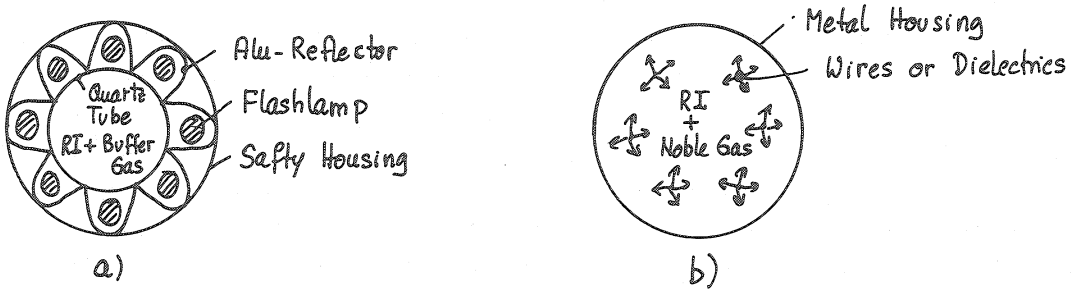

Fig. 9: Amplifier pumped by flashlamps a) or open discharges b)

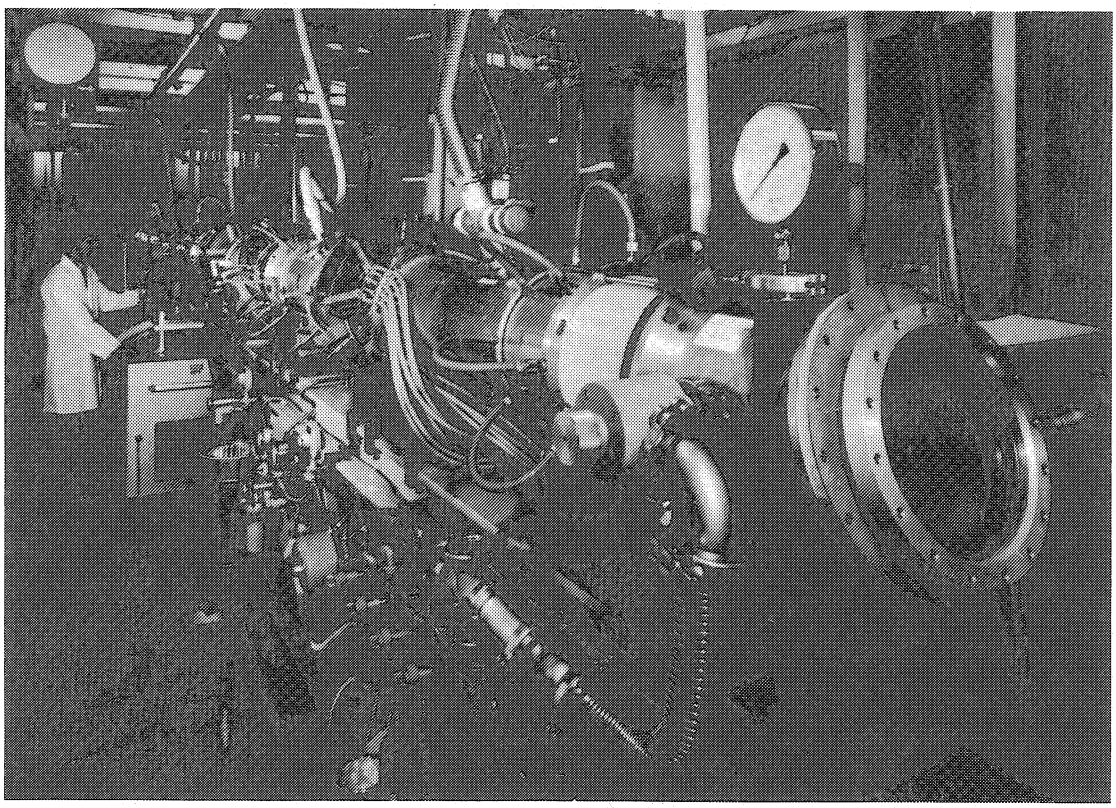

Fig. 10: Final amplifier of the ASTERIX III iodine laser system

separated from each other. With no flashlamps embedded in the laser medium the stored energy density e_{st} scales inversely with the tube diameter d, $e_{st} \sim 1/d$; at d = 30 cm e_{st} = 10 J/ℓ is achievable. For larger diameters external and internal pumping (flashlamps in the laser medium) have to be combined in order to keep e_{st} at a level of 10 J/ℓ.

An alternative to flashlamp pumping is open discharges favoured in russian iodine lasers. An amplifier using this scheme is shown in Fig. 9b. In this case no quartz tubes are needed since the discharge takes place in the laser medium itself. Stored energy densities of up to 20 J/ℓ have been realized for large diameter amplifiers (42 cm).

The advantage of a simple design and a good scalability to large volumes is, however, opposed by the disadvantage of contamination problems; the windows f.e. have to be cleaned after a few shots so that high repetition rate operation is principally difficult to achieve.

The overall efficiency is given by

$$\eta_{tot} = \eta_q \cdot \eta_{ex} \cdot \eta_E \tag{40}$$

where η_E is an engineering factor and counts for flashlamp efficiency (8 % of the energy stored in the capacitors can be converted into UV-light falling in the absorption bandwidth of the fluorinated alkyliodides), optical losses connected with the radiation transfer from the flashlamps to the laser medium and incomplete utilization of the pumped volume. For the present generation of lasers $\eta_E \leq 0.03$ holds. Accepting a value of .5 for η_{ex} the overall efficiency η_{tot} becomes 0.3 % which is to be considered as a kind of upper bound. In the ASTERIX III system /11/ a η_{tot}-value of about .1 % has been realized. Fig. 10 shows a photograph of the final amplifier of the 1-Beam-ASTERIX III-system which can deliver a power of 1 TW at a pulse duration of 250 ps. The repetition rate is 1 shot each 10 minutes.

At a medium linewidth of 20 GHz (single transition) corresponding to an Ar pressure of 5 bar amplification of 50 ps-pulses is possible. Due to the small overall linewidth of only 40 GHz two line operation as required by the beat wave plasma accelerator /24,25/ and characterized by a separation of $> 10^3$ GHz between the two carrier frequencies of the pulse cannot be realized. The iodine laser is thus only useful for that version of the plasma accelerator /24/ which is based upon a pulse with only one carrier frequency.

3.5 Nd:glass Laser (1.06 μm)

Glass has many beneficial properties as a laser host. It can be fabricated in large pieces of variable shape and size (rods up to 11 cm in diameter, disks up to 30 x 60 cm, see Figs. 11,12) with high optical quality and low loss coefficient (0.001 cm^{-1}). It is isotropic, durable and moderate in cost.

Nd goes into the glass as the Nd^{3+} ion each with a different site due to the amorphous glass structure. The absorption and emission lines (see Fig. 13) are therefore inhomogeneously broadened from 20 $cm^{-1} \hat{=}$ 600 GHz to 200 $cm^{-1} \hat{=}$ 6000 GHz for the glass as a whole. This permits amplification of short and long laser pulses. In the 24-Beam-

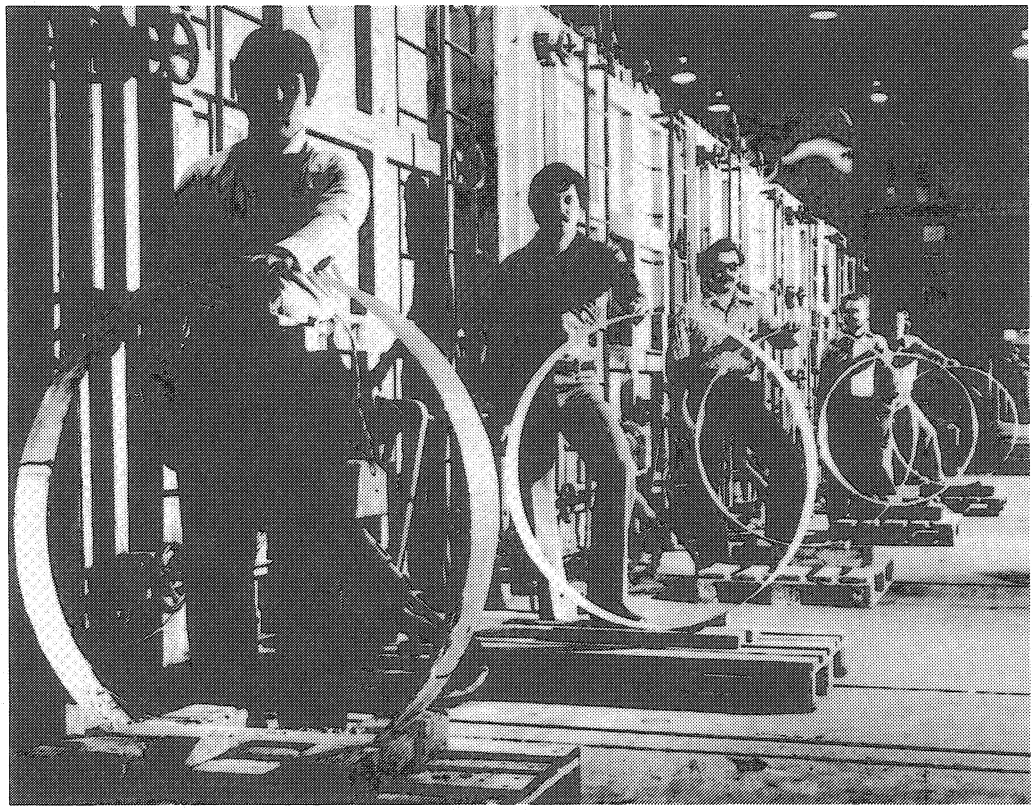

Fig. 11: Large diameter BK7 disks with graded-index antireflective surfaces

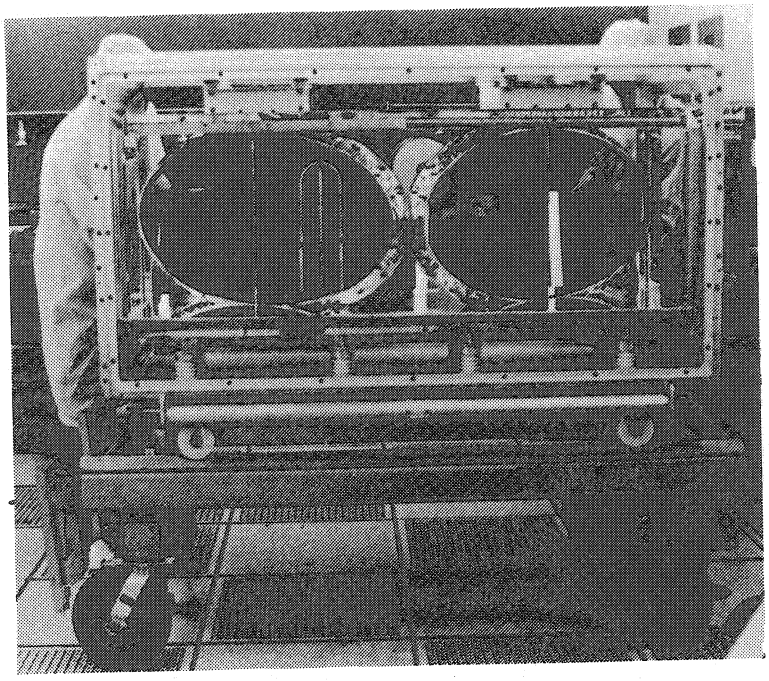

Fig. 12: 46 cm diameter disk amplifier of NOVA

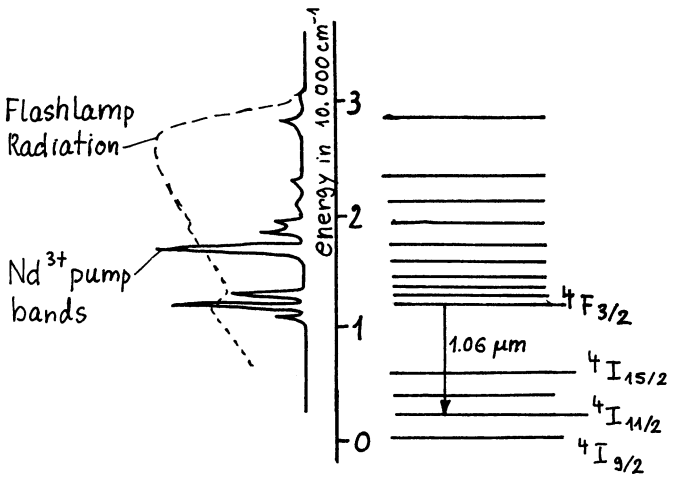

Fig. 13: Absorption spectrum and energy level diagram for Nd^{3+} ions in glass

OMEGA-facility /26/ 50-300 ps-pulses are generated with total powers ranging from 10 TW to 6 TW. The 10-Beam-NOVA-facility /27/, which will be the largest laser in the world after completion by the end of 1984, can amplify pulses with duration from 100 ps to 5 ns with corresponding total powers from 120 TW to 25 TW.

Nd^{3+} ions are optically pumped by flashlamps whose radiation matches the absorption spectrum of the Nd^{3+} ions quite well. Absorbed energy is rapidly accumulated in the $^4F_{3/2}$ atomic levels, which are about 12.000 cm^{-1} above the ground state. These levels have a lifetime of 200 to 700 µs, determined both by radiative and ion-ion non radiative transitions. The dominant fluorescence and highest gain laser action is from the $^4F_{3/2}$ level to the $^4I_{11/2}$ level, which is ~ 2000 cm^{-1} above ground state. Peak gain is at a wavelength from 1.045 to 1.065 µm, depending upon the refractive index of the glass-host composition. The terminal laser level is rapidly depopulated (< 1 ns) and it is far enough above the ground state ($^4I_{9/2}$) that it is thermally almost empty.

At normal doping levels the deposition profile of the pump light in the glass is non-exponential with a characteristic depth of a few cm. This enables a spatially rather uniform excitation which is important for the generation of a beam with a low transverse intensity modulation. The efficiency of transfer from the absorption lines to the upper level $^4F_{3/2}$ is near unity in most glasses. However, the effective energy utilization is η_q ~ 60 % (for a Xenon spectrum) because of the difference between the energy of the absorbing levels and the upper laser level. The lost energy is taken away by phonons heating the glass. 80 % of the energy stored in the capacitor bank is converted to photons by the flashlamps. But not all of these photons are absorbed by the Nd^{3+} ions; the majority goes somewhere else and shows up as heat. Only ~ 3 % is accumulated in the absorbing levels lying above the upper laser level $^4F_{3/2}$. The engineering factor η_E, already introduced when treating the CO_2 and iodine lasers, is thus ~ 0.03. Since the quantum efficiency η_q equals .6 not more than ~ 2 % of the capacitor energy is trans-

ferred into useful inversion of the Nd^{3+} ions. This figure has been found for disk amplifiers and is also approximately valid for rod amplifiers /28/.

At short pulse length of ≦ 100 ps Nd:glass lasers have to be operated in the small signal regime thus showing a low extraction efficiency η_{ex}. Consequently, the overall efficiency $\eta_{tot} = \eta_E \cdot \eta_q \cdot \eta_{EX}$ is also small, fractions of a per mil . Only for long pulses (≧ 1 ns) gain saturation is possible to some extent, yielding η_{tot} values of ≦ .2 %.

Due to its pulse width flexibility, broad amplification bandwidth enabling two line operation with a frequency separation of ~ 10^3 GHz or more and its scalability to very high powers the Nd-glass laser appears to be an appropriate candidate for the plasma and inverse free electron accelerators /29/.

3.6 Excimer Lasers

Excimer lasers like XeCl (308 nm) and KrF (248 nm) have a broad medium linewidth of approximately 5.000 GHz $\widehat{=}$ 1.5 nm thus allowing the amplification of short (ps) and long (ns) pulses as well as two line operation with a frequency separation of up to a few THz. If pumped by e-beams both systems are scalable to large energies; f.e. in /30/ a conceptual design of a 50 kJ KrF amplifier for inertial confinement is presented. The overall efficiency of e-beam pumped excimer lasers is estimated to be at least a few percent and is thus much higher than that of the lasers discussed above. These properties make them interesting candidates both for fusion and particle acceleration.

Up to now the main effort has gone to the KrF laser because its intrinsic efficiency of ~ 12 % (laser output energy over e-beam energy deposited in the laser medium) is approximately twice as high as that of XeCl. This difference has recently become smaller. In /31/ a XeCl laser using an Ar/Xe/HCl mixture achieved an intrinsic efficiency as high as 8 %. Because of its ability to propagate a higher fluence, higher damage thresholds and cheaper optics an XeCl driver system offers significant advantages from a system's viewpoint and has thus become an alternative to an KrF driver.

For large volume amplifiers the pump time has to be several hundred nanoseconds; shorter pump times lead to unattractively expensive devices. Because of the short excited state lifetime of excimer lasers efficient operation is then only possible if energy is extracted during the entire duration of the pump pulse, i.e. the laser pulse has to be as long as the pump pulse. Since fusion needs pulse durations of only a few ns schemes have been devised (see sect. 5.2) allowing a pulse compression from several hundred ns down to some ns. In this case excimer lasers are operated in the non-storage mode.

If the pulse duration is, however, in the ps-range, $T_{pulse} \leqq 50$ ps, excimer lasers have to be treated like storage - lasers, since $T_{pulse} \ll \tau_u$ holds. Pumping times large compared to τ_u can then only be tolerated if the energy is extracted by a series of

ps-pulses separated in time by ~ τ_u. This could be achieved by a modelocked pulse train generated by frequency doubling the output of an appropriately chosen w-modelocked dye laser. For single pulse operation what includes repetition rates up to several KHz the pumping time has to be of the order of τ_u to maintain a reasonable efficiency. This is possible with discharge lasers. Their low intrinsic efficiency of only 1-2 % is, however, offset by their ability to enable repetition rates in the KHz-range. Their most serious limitation arises from the fact that the discharge volume cannot be scaled to large sizes; at present, volumes of ~ 1 liter appear to be an upper bound when uv-preionization is used. However, with the recently developped x-ray preionisation technique /32/ volumes larger by a factor of 10 can be homogeneously pumped without arcing. Moreover, by additionally employing magnetic switching in the electric circuit the power deposition time can be shortened to less than 10 ns /33/. Such a system is ideally suited for amplification of a single ps-pulse.

Recently a ps-pulse was amplified to a power of 20 GW in a conventional uv-preionized XeCl laser /34/. With the new generation of discharge lasers this result can be scaled to the TW-level. This is still not quite that what is wanted, but nevertheless a big step forward. It appears conceivable that with further work it may be possible to gain another factor of 10 what would then be sufficient to reach the 100 TW-level with a 10-beam facility.

In the following the XeCl laser will be treated first. Emphasis will be on the aspects connected with the amplification of ps-pulses (storage mode). For the KrF-laser the non-storage mode of operation will be mainly dealt with.

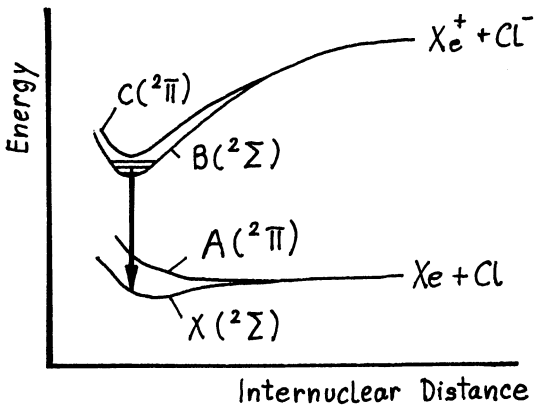

Fig. 12: Schematic potential energy diagram of XeCl

Xenon-chloride (308 nm): The kinetics of XeCl like that of all excimers are rather complicated and will not be discussed here (for details see, f.e. /35/). In high pressure mixtures of Ne, Xe, HCl (typically 4.5 bar Ne, 20 mbar Xe, 4 mbar HCl) which are used in

e-beam controlled and uv-preionized discharges /31,35/ the excited XeCl molecule is predominantly formed by ionic recombination

$$Xe^+ + Cl^- + Ne \rightarrow XeCl^* + Ne. \qquad (41)$$

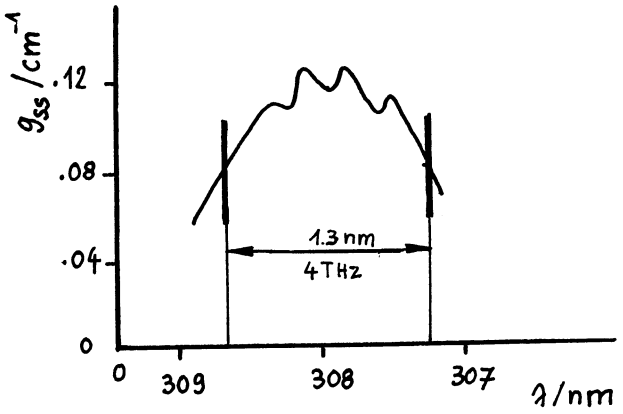

Fig. 13: Spectral gain profile in a He/Xe/HCl/H_2-mixture after /34/

A fast three body charge exchange process produces X_e^+ from N_e^+ which itself is indirectly generated by electrons. Cl^- is formed by dissociative attachment of vibrationally excited HCl.

The ground state of XeCl is covalently bonded /36/ and actually consists of two states (see Fig. 12). Of these, the $^2\Sigma$ has the lowest energy; it forms the ground state and is referred to as the X-state which is weakly bound (255 cm^{-1}). The $^2\pi$ state of the ground state manifold is always repulsive as indicated. Since it is the first state above the ground state it is referred to as the A-state.

The upper laser level is ionically bound and also a manifold with the $^2\Sigma$ state lying lowest. By convention this is referred to as the B-state. The other state is a $^2\pi$ state and is usually designated with C.

The emission spectrum consists of several bands. The strongest band is assigned to the $B(^2\Sigma) \rightarrow X(^2\Sigma)$ transition and gives rise to the laser transition observed to date. All other bands are weaker by at least a factor of ten and are of no importance here. Fig. 13 shows the spectral gain profile of XeCl in a mixture of 3 bar He, 4 mbar H-Cl, 20 mbar Xe and 1.3 mbar H_2. Four bands due to the transitions between the v' = 0 vibrational level in the B-state and v" = 0,1,2 and 3 vibrational levels in the X-state are clearly resolved. It is clear from Fig. 13 that XeCl has sufficient bandwidth for amplification of ps-pulses. In fact, amplification bandwidth-limited pulses as short as ~ .15 ps should be possible, provided that it is bandwidth and not dispersion or something else that

imposes a lower limit on the pulse duration. Fig. 13 also shows that two line operation with the two carrier frequencies separated by 1.3 nm ≙ 4 THz is possible at an equal and reasonable gain for the two components.

The asymmetric structure of the vibrational bands shown in Fig. 13 is due to rotational transition. It is, however, very likely that the discrete nature of the rotational lines will have little effect on the small signal gain profile at high pressure due to pressure broadening and isotopic blending.

In /34/ the energy saturation parameter e_s was measured by combining small signal and large signal gain measurements. For 2 ps-pulses with a bandwidth of 1 Å ≙ .3 THz e_s = 1 mJ/cm^2 and from that using the relation $e_s = h\nu/\sigma$ $\sigma = 6.4 \times 10^{-16}$ cm^2 were found. These values are given in table 1 and are valid for the four main lasing transitions. From gain recovery measurements an upper level life time of about 5 ns could be deduced.

One severe problem in all excimer lasers is the control of ASE. For any amplifier, there is a minimum input signal below which ASE, and not the pulse, will dominate the output of the amplifier. There is also a maximum amplifier gain for a given module geometry above which ASE will saturate the gain by parasitic oscillations. This situation is similar to that known from dye lasers. The maximum tolerable gain g of a XeCl amplifier module with length ℓ and diameter d can be estimated from the relation /34/

$$g \lesssim \frac{1}{\ell} \ln \left\{ \frac{1.9 \times 10^{-4} \ell^2 I_s}{d^2} \right\} \qquad (42)$$

where I_s is in W/cm^2 and ℓ,d in cm. F.e. with $\ell/d = 20$, ℓ = 80 cm and $I_s = 2 \times 10^5$ W/cm^2 g should be kept smaller than 10 % per cm. For an amplifier chain removal of ASE from the beam is essential. This requires either suitable saturable absorbers and/or spatial filters.

Finally, a few words will be said regarding the generation of ps-pulses. Because of the short B-state life time modelocking is not an appropriate technique. For this reason another, unfortunately rather complicated method has been developped /34,37/. Single ps-pulses are switched out from a synchronously pumped cw-modelocked dye laser, amplified in an excimer-laser pumped dye amplifier chain to high peak powers and then frequency shifted to serve as an input for an excimer amplifier chain. Achieving and maintaining exact synchroism between several excimer lasers, the mode-locker, pulse selector and resonator length stabilizing feedback circuit is thus quite complex. Recently a much easier scheme has been successfully demonstrated /38/ which avoids the synchronisation problem. It consists of two excimer laser heads switched by one thyratron so that the operation is jitterfree and a simple dye laser (not modelocked) pumped by one of the excimer lasers. This dye laser is designed such that it produces a single ps-pulse which is then amplified, frequency doubled to 308 nm and amplified in the second excimer laser.

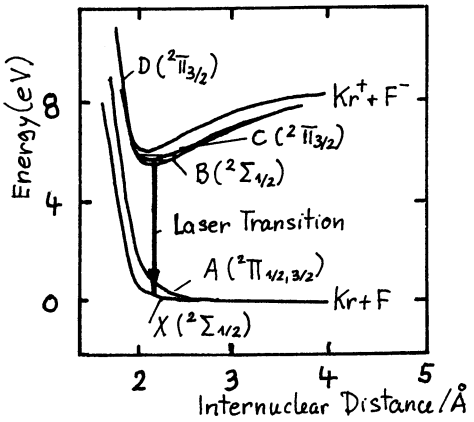

Fig. 14: Potential energy diagram of KrF /36/

Krypton-fluorine (248) nm. Fig. 14 shows the potential energy diagram of KrF which is very similar to that of XeCl except for the fact that the ground state $X(^2\Sigma_{1/2})$ is unbound. The basic kinetics of $Ar/Kr/F_2$ laser mixtures are presently well understood /39/ and will not be repeated here. As already mentioned for large volumes efficient excitation can only be achieved by means of e-beams. The predominant energy transfer is then through the formation of ionic species. In particular, the KrF molecule is formed primarily via the ionic recombination reaction

$$Kr_2^+ + F^- + Ar \longrightarrow KrF^* + Kr + Ar. \qquad (43)$$

The production efficiency η_{KrF} of KrF* can be quite high, up to 25 %, since 65 % of the e-beam energy is converted to ions and excited states finally forming KrF*. There are, however, also losses the major of which are due to spontaneous emission, electron collisional deactivation and photoabsorption. The latter consists of two contributions, saturable and non-saturable losses. The saturable losses mainly arise from Kr_2F trimer formation according to

$$KrF^* + Ar + Kr \longrightarrow Kr_2F^* + Ar. \qquad (44)$$

This represents not only a reduction of the KrF* number density but also a propagation extraction loss because the trimer molecule Kr_2F^* absorbs radiation at 248 nm. This is counteracted to a certain extent by saturation through the action of strong KrF* radiation reducing the KrF* concentration and thus also that of Kr_2F^*. The non-saturable losses result from the absorption of KrF* radiation by F_2, F^- and excited states of the rare gases and are about $5 \times 10^{-3} cm^{-1}$. They limit the output intensity of an amplifier to ≤ 30 MW/cm^2. The total photoabsorption losses have the consequence that only 50 % of the energy stored in the KrF* molecules can be converted to excimer radiation, $\eta_{ex} \leq 50$ %.

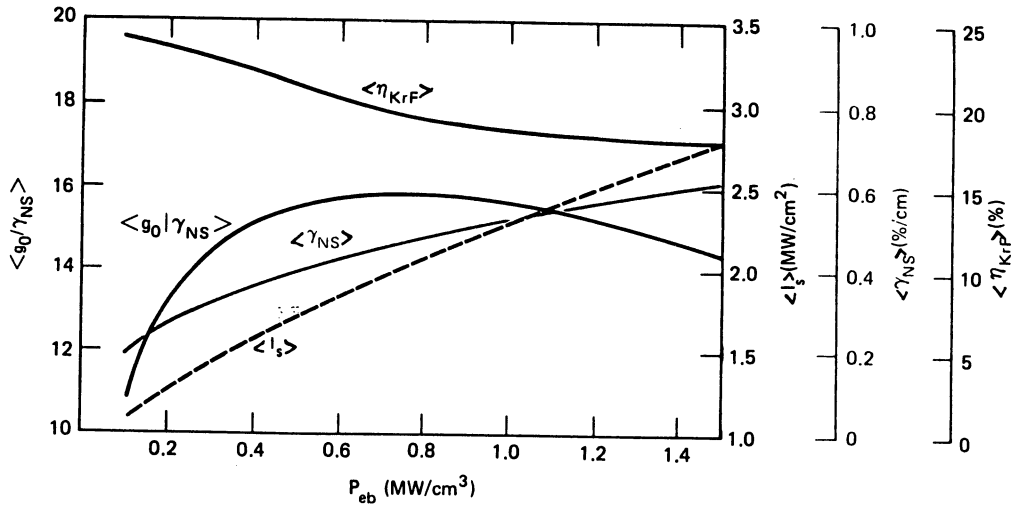

Fig. 15: Dependence of KrF amplifier parameters on e-beam pump power P_{eb} deposited in the medium /7/. η_{KrF^*} is the molecule production efficiency, g_o the small signal gain, γ_{NS} the non-saturable loss coefficient, I_s the saturation intensity. All parameters plotted are average values over fluorine burnout time τ.

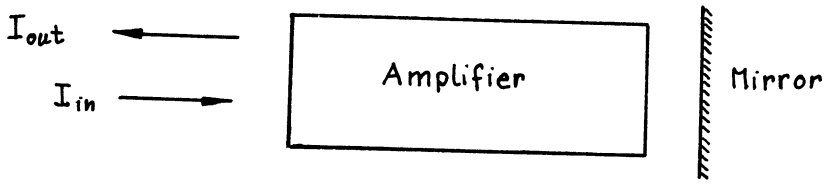

Fig. 16: Bidirectional amplifier

For best laser performance the medium is usually composed of argon (≧ 90 %), krypton (3-8 %) and fluorine (< 1 %) at total pressures between 1 to 3 bar. Fig. 15 shows the characteristics of a mixture consisting of 93.7 % Ar, 6 % Kr and 0.3 % F_2 at a pressure of 1 bar /7/. The laser parameters are average values over the fluorine burn out time τ. This is to be understood in the following sense.

At constant volumetric pump power, P_{eb} (MW/cm^3), deposited in the mixture the laser medium parameters g_o/γ_{NS}, and I_s vary with time. The gain-to-loss ratio g_o/γ_{NS} (NS:Non-saturable losses) changes most rapidly. It at first increases as the KrF* molecule is begun to be formed. However, as time passes by, the F_2 present in the original mixture is depleted by attachment and dissociation kinetic processes. Consequently, g_o/γ_{NS} achieves a maximum and then declines. As the F_2 is consumed, the electron loss mechanism changes from dissociation attachment to dissociative recombination whose rate is slower so that the electron density rises. This changes both the saturation intensity I_s and the non-saturable loss coefficient γ_{NS} as the dominant kinetic processes and composition of the medium change. The usefulness of the medium is determined by the time over which g_o/γ_{NS} remains large. This time period is taken as the fullwidth at 80% of maximum g_o/γ_{NS} and can be considered as a measure of the fluorine burnout time τ. The dependance of τ on the power deposition rate P_{eb} is such that $P_{eb}\tau \cong 0.1\ J/cm^3$ holds for the mixture given above.

Detailed calculations such as those shown in Fig.15 and calculations taking into account finite aperture effects such as parasitic oscillations and ASE (amplified spontaneous emission) show that the bidirectional amplifier (see Fig. 16) is probably an optimum solution. It enables a near uniform fluence gain along the amplifier axis at a sufficiently high level of about 10. Non-saturable losses force tradeoffs between intrinsic efficiency ($= \eta_{KrF^*} \cdot \eta_{ex}$) and energy per aperture. ASE limits extraction efficiency in large aspect ratio amplifiers when the ratio radius over length exceeds a value of 0.15. Parasitic oscillations limit aperture scaling and require diffuse electron beam foil reflectivities ≦ 2 % (current values are ~ 5 %). Achievement of high amplifier energies > 100 kJ within parasitic constraints requires long pump times ≧ 400 ns /6,7/. If parasitic oscillations are controlled, KrF amplifiers appear scalable to an output energy of several hundred kJ at an intrinsic efficiency of ~ 8 % provided the KrF* pulse injected in the amplifier is as long as the e-beam pump pulse (~ 400 ns).

In the western world there are presently two major efforts regarding high power KrF lasers. One is at the Los Alamos Scientific Laboratory/USA where an amplifier module is being constructed whose output energy is expected to be between 10-20 kJ. The other effort is at the Rutherford Appleton Laboratory/England and concerns the high power KrF Laser SPRITE /41/. It is smaller than the LASL-system but more advanced in the sense that experimental results are already available. Fig. 17 shows a cross-sectional view of SPRITE. The laser chamber has a circular cross section. The medium is pumped by by means of 4e-beams. This device has delivered an output pulse of 220 J in 45 ns at a deposited e-beam energy of 2.7 kJ thus yielding an intrinsic efficiency of 8.2 % /41/. The main

efforts are now directed towards solving the problem of pulse compression and associated power multiplication. The aim is to get a 1 ns-pulse with 50 % efficiency, i.e. with an energy ≧ 100 J.

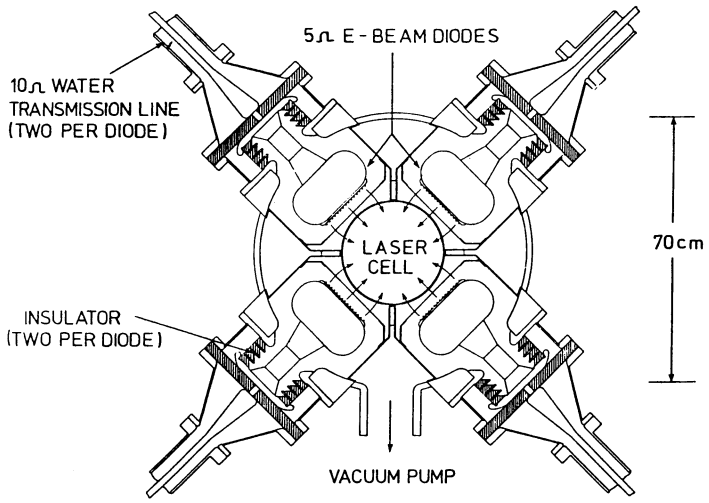

Fig. 17: Cross-sectional diagram of SPRITE

4. Beam Quality

High intensity beams can only be amplified and transmitted over long distances if their angular spectrum is not significantly enlarged upon propagation through the amplifier chain. There is, however, a variety of beam quality impairing processes which will be shortly covered in the following paragraph. The second and third paragraph of this section deals with the cure of these unwanted effects.

4.1 Beam Quality Impairing Process

Optical elements like windows, lenses, mirrors, beamsplitters, polarizers, crystals etc. are not perfect. They have either surface defects such as scratches or attached dust particles or bulk inhomogeneities or both. Since there are many elements of this kind in an amplifier chain it is clear that the beam quality is affected by these inhomogeneities. Moreover, glass plates at Brewster angle put astigmatism on the beam. In addition, there are air paths of 100 m length or even more. Air turbulence - even if it is small - may thus also degrade the beam quality. Processes like scattering, diffraction, non-circular and arbitrary phase variations convert an originally smooth intensity profile to a heavily structured one which is equivalent to a broadening of the angular beam spectrum. This has the unwanted consequence that the beam loading and thus the overall

efficiency cannot be made as large as in the case of a flat profile since otherwise material damage will occur.

Beam quality impairing processes are also possible in the amplifiying medium itself. Of main concern are the deposition of the pump energy, medium saturation and self focusing. If the pump energy is not homogeneously deposited acoustic disturbances are generated since always a significant fraction of the pump energy is directly converted to heat. Another source of such perturbations is the boundary between the pumped and unpumped portions of the laser medium. These problems are mainly encountered in gas lasers with pumping times of about 10 µs or more since the disturbances have then sufficient time to develop and propagate. In the iodine laser these effects limit the pumping time to 10-20 µs. Pumping by e-beams yields a rather uniform medium excitation. Moreover, since the pumping time is usually less than or not more than a few µs acoustic medium perturbations are negligible. This has been verified in e-beam pumped CO_2 and excimer lasers. The acoustic disturbances occurring in high repetition rate discharge lasers do not influence the discharge by which they were generated but perturb the medium for the next following shot when no damping measures are taken. These have turned out to be absolutely necessary if diffraction limited beams are aimed at.

Medium saturation may affect the beam quality in connection with anomalous dispersion. When the carrier frequency ν_p of the pulse does not coincide the centre frequency ν_c of the laser transition and the on-axis portion of the pulse is more strongly amplified than its edges (what is the usual case) the refractive index can be changed in such a way that either focusing or defocusing occurs depending on the relative position of the pulse carrier frequency to the central transition frequency, $(\nu_p-\nu_c) \gtrless 0$. This effect is possible in any of the four high power lasers and needs quantitative consideration when the detuning $\nu_p-\nu_c$ is of the order of the medium linewidth $\Delta\nu$.

Self focusing is a nonlinear process and occurs whenever the refractive index increases with the local intensity of the laser beam according to

$$n = n_0 + n_2 \langle E^2 \rangle = n_0 + \bar{\gamma} I \tag{44}$$

where n_o is the intensity independent part of the refractive index. Thus, the more intense parts of the beam propagate more slowly. An intensity bump on a beam therefore forms a converging lens in the medium, and consequently intensifies itself to a spike. This spike may eventually become so narrow that diffraction balances further self-focusing. However, the involved intensities are so high that any material will be damaged. The filamentation is thus not a feasible solution to the problem of beam propagation.

In order to maintain a good beam quality the bump or ripple growth which is proportional to e^B whereby B is the so-called Beam Break-up Integral /12/

$$B = \frac{2\pi}{\lambda} \int_{\text{chain}} \bar{\gamma}(z)\, I(z)\, dz \tag{45}$$

Table 2 : Nonlinear refractive index for various gases and BK7

Medium	Air (1 bar)	Ar (1 bar)	SF_6 (1 bar)	C_3F_7I (10 mbar)	BK7
$\bar{\gamma}x10^{10}cm^2/MW$	10	5	10	1	4000

has to be controlled. Catastrophic beam break-up can be avoided if B does not exceed a value of about 3 [12]. Self focusing limits the performance of Nd:glass lasers below pulse duration of 300 ps. Gaseous media suffer less from self focusing than solids (see Table 2). However, at gas pressures of ~ 5 bar and short pulses (≦ 200 ps) self focusing is no longer negligible although not as severe as in glass lasers. This conclusion has been confirmed in the iodine laser ASTERIX III. In ps-excimer lasers no experimental material has been reported so far. Self focusing will certainly become evident when the intensities are further increased. Non-storage excimer lasers are not subject to self-focusing since the involved intensities of ~ 30 MW/cm^2 are too small to cause any appreciable effect. In ns-CO_2 lasers self-focusing is also unimportant since the wavelength is too long. In ps-CO_2 lasers the long wavelength advantage may be offset by the very high beam intensities (> 10^{11} W/cm^2). This conjecture remains, however, to be verified.

Self focusing like the other beam quality impairing processes mentioned above broaden the angular beam spectrum. This is to be understood in the sense that upon propagation more and more beam energy is transferred from the central plane wave component moving along the laser axis to components making a more or less large angle with the laser axis. These components can be removed from the beam by spatial filtering. In case of self focusing this means that after each spatial filter B is reset equal to zero. How such a filter "works", will be explained in the following paragraph.

4.2 Spatial Filtering and Image Relaying

A spatial filter is a combination of two positive lenses separated by the sum of their focal lengths. At their common focus a pinhole of radius R is placed (see Fig.18). Thus only rays having an angle with the filter axis

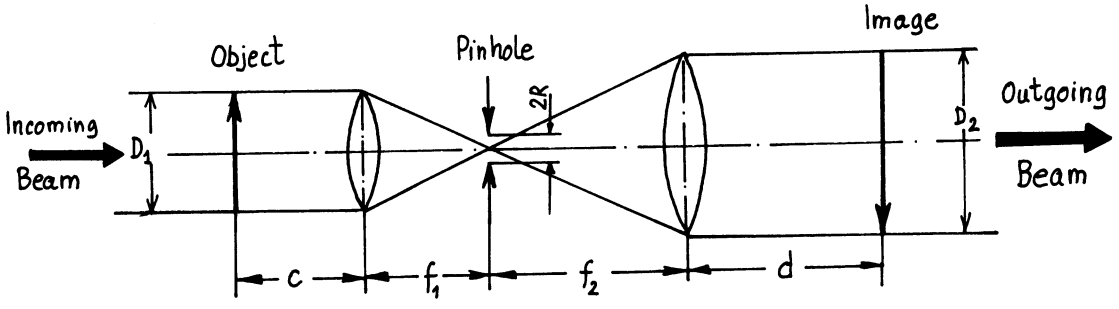

Fig.18: Spatial filter

smaller than R/f_1 (in front of the first lens) will pass through the filter; any other ray will be rejected by the pinhole. In this way a broad angular beam spectrum can be narrowed down so that the intensity profile of the beam emerging from the filter becomes smoother.

A spatial filter is also an image relaying device. An object placed in the front focal plane of the first lens will have its image in the rear focal plane of the second lens. This feature is especially attractive when the "object" is the exit window of an amplifier and the "image" the entrance window of the following amplifier. It is then possible to maintain a smooth intensity profile and thus a good fill factor and high beam loading. However, to understand the image relaying property of the spatial filter more precisely, diffraction must be taken into account.

The electric field distribution $\mathcal{E}_{o,Foc}$ of the object in the common focus of both lenses is given by /2/

$$\mathcal{E}_{0,Foc} = \mathcal{F}\{\mathcal{E}_0\}\,\frac{1}{i\lambda f_1}\exp\left\{\frac{ikr^2}{2f_1}\left(1-\frac{c}{f_1}\right)\right\} \tag{46}$$

where $\mathcal{F}\{\mathcal{E}_0\}$ is the Fourier transform of the object defined by

$$\mathcal{F}\{\mathcal{E}_0\} = \mathcal{F}_0\left\{\frac{x}{\lambda f_1}, \frac{y}{\lambda f_1}\right\} = \iint_{-\infty}^{+\infty}\mathcal{E}_0(x_0, y_0)\exp\left\{-\frac{2\pi i}{\lambda f_1}(x_0x + y_0y)\right\}dx_0\,dy_0$$

with $x^2 + y^2 = r^2$.

Similarly, the electric field distribution $\mathcal{E}_{I,Foc}$ of the image in the common focus of both lenses reads

$$\mathcal{E}_{I,Foc} = \mathcal{F}\{\mathcal{E}_I\}\,\frac{1}{i\lambda f_2}\exp\left\{-\frac{ikr^2}{2f_2}\left(1-\frac{d}{f_2}\right)\right\} \tag{47}$$

with $$\mathcal{F}\{\mathcal{E}_I\} = \mathcal{F}_I\left\{\frac{x}{\lambda f_2}, \frac{y}{\lambda f_2}\right\} = \iint_{-\infty}^{+\infty}\mathcal{E}_I(x_I, y_I)\exp\left\{-\frac{2\pi i}{\lambda f_2}(x_Ix + y_Iy)\right\}dx_I\,dy_I\,.$$

In the pinhole plane the relation

$$\mathcal{E}_{0,Foc}\cdot P_H = \mathcal{E}_{I,Foc} \tag{48}$$

must hold where P_H is the pinhole transmission function. Introducing the magnification factor

$$m = f_2/f_1\,, \tag{49}$$

the "detuning" distance

$$l = (f_1 - c)\frac{f_2^2}{f_1^2} + (f_2 - d) \tag{50}$$

and the new coordinate

$$\xi = r/\lambda f_2 \tag{51}$$

one arrives at a formula relating the Fourier spectrum of the object, $\mathcal{F}_0$, and to that of the image, $\mathcal{F}_I$, in the form

$$\mathcal{F}_I(\xi) = m\,\mathcal{F}_0(m\xi)\,P_H(\xi)\exp\{i\pi\lambda l\xi^2\}\,. \tag{52}$$

In the special case that the "detuning" distance ℓ is zero i.e. the location of the object plane and that of the image plane are related by the laws of geometrical optics and that there is no pinhole, $P_H = 1$ everywhere in the pinhole plane, eq. (51) reduces to

$$\mathcal{F}_I(\xi) = m\,\mathcal{F}_0(m\xi) \tag{53}$$

or transformed back to the physical space

$$\mathcal{E}_I(r_I) = \frac{1}{m}\,\mathcal{E}_0\left(\frac{r_I}{m}\right). \tag{54}$$

Perfect image relaying is thus only possible if the pinhole is removed. If this condition is not met the image will display Gibbs modulation even if the intensity profile in the object plane is smooth. Image relaying and spatial filtering ($P_H = 1$ only in a small area of the pinhole plane, but not everywhere) are thus conflicting claims. In the compromise realized in practice the pinhole diameter 2 R is usually chosen ten times larger than the diffraction limited spot size diameter of the object. This choice only removes those plane wave components from the beam responsible for the worst ripples but has the advantage that image relaying is only weakly blurred by Gibbs modulation. In addition, amplifier isolation is also provided to a certain extent.

4.3 Phase Conjugation

Phase conjugation by stimulated Brillouin-backward scattering (SBBS) was discovered independently by two groups in 1972: in the USSR by Zeldovich, Nosach and coworkers /42,43/ and at Garching by Eidmann and Sigel /44,45/. Zeldovich and Nosach observed phase conjugation using a Ruby laser and CS_2 as the Brillouin-Medium. They already gave a rather detailed explanation of the effect. Eidmann and Sigel found phase conjugation when investigating SBBS from ion-acoustic waves in laser-produced plasmas.

Since then a large body of material has been published /3/. It could be demonstrated that besides SBBS also stimulated Raman or Rayleigh backward scattering (SRaBS, SRayBS) and degenerate four wave mixing (DFWM) can produce phase conjugated waves. Their use in high power laser systems is illustrated in Fig. 19 . A small auxiliary laser illustrates a broad area and some of the scattered light is gathered by the lens and amplified in the

gain medium. The phase conjugation acting like a mirror returns the beam to pass again through the gain medium and onto the target. Any static phase aberrations picked up by the beam on his first passage through the amplifier will be cancelled on his second passage so that the beam hitting the target has perfect quality.

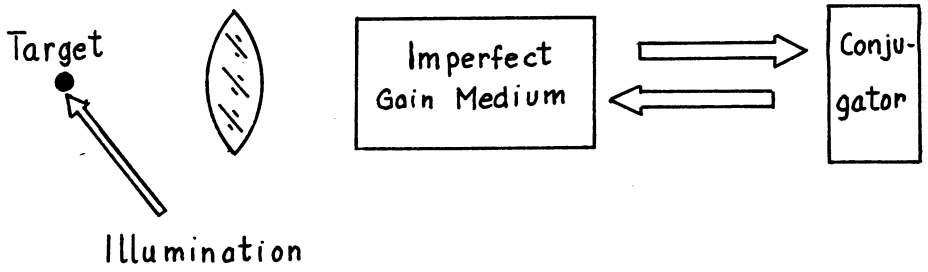

Fig. 19: Laser with phase conjugating mirror

Complete cancellation of static phase aberrations requires zero frequency shift between the incoming and the reflected wave. This is only possible with DFWM. This scheme has, however, the disadvantage that it needs a rather strong pump beam of good beam quality to set up the grating for the reflection of the probe beam. This property together with the low reflection coefficient (relative to the pump beam) makes DFWM not very attractive for an application in a high power laser.

The stimulated backward scattering processes are conceptually much simpler since they don't need additional pump beams. The smallest frequency shift occurs in SRaBS. However, significant phase conjugation has not yet been demonstrated. Many experiments have been reported using either SRaBS or SBBS as the phase conjugating process. The results clearly show that SBBS is superior to SRaBS. SBBS when properly done can produce reflected waves with a high degree of phase conjugation and with reflectivities close to 1. Moreover, the frequency shifts associated with Raman scattering are much larger than those occurring in Brillouin scattering. This is prohibitive for SRaBS when the carrier frequency of the reflected wave falls outside the amplification bandwidth of the amplifying medium.

As already noted, phase conjugation can only cancel static phase aberrations. Wave front distortions resulting from self focusing cannot be compensated. In an amplifying medium the gain must be constant over the beam cross section. If not, the angular beam spectrum is changed upon amplification and this change cannot be canceled by phase conjugation. Wave front perturbations caused by medium saturation are thus not correctable.

Many papers have been published demonstrating the principal ability of SBBS for the correction of wave front distortions occurring in high power laser systems due to thermally induced optical inhomogeneities or poorly fabricated amplifier rods (see f.e. /46/). This should make it possible to reduce the enormous costs of present high power

laser systems substantially since the requirements to be met by the laser materials regarding optical quality can be relaxed.

Besides phase conjugation SBBS and also SRaBS can be used for prepulse suppression and amplifier decoupling since weak pulses experience a very low reflection, $R \leqq 10^{-10}$. Another interesting property concerns the ability for significant pulse compression at high efficiency. This can be exploited in non-storage excimer lasers and is currently investigated /41/.

For present research lasers the principle quantity to be minimized in the design process is the ratio of capital cost over focusable output energy or power. The capital cost involve not only those for the mechanical, electrical and optical components but also those for the building and support facilities. This design strategy may lead to the result that the cheapest laser is not that with the highest overall efficiency. Looking at present and projected laser systems a fair estimate of the optimization parameter appears to be 10^3-10^4 DM/J whereby the smaller numbers refer to the larger laser systems. The price of a 1 MJ system could then be expected at a level 10^9 DM. This estimate only holds for long pulse systems (~ 1 ns); for short pulse sytems (~ 1 ps) no cost estimates are available at present.

5. System Design

5.1 Storage Laser Architecture

Large fusion lasers have until now all employed the master-oscillator power-amplifier (MOPA) configuration (see Fig. 20). In MOPA a low-level pulse (usually ~ 1 mJ) is injected in a chain of amplifiers of increasing size and energy. Sizes and gains are adjusted to maintain a fluence level high enough for efficient energy extraction without causing material damage. The MOPA design shown in Fig. 20 is a conceptually simple approach in

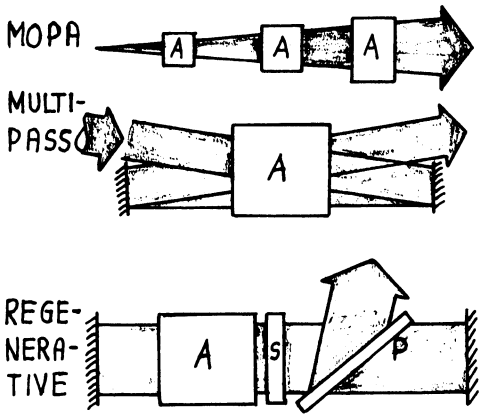

Fig. 20: Three different laser architectures; A amplifier, S switch, P polarizer

the sense that it uses the natural beam divergence for beam expansion so that no beam expanding optics is necessary. An angle of about 1 mrad is required to avoid an excessive chain length. This design is especially convenient for laser media with a low saturation fluence like CO_2 or I since then all the amplifiers except for the very first can be operated in the saturation regime. Very long amplifiers (> 10 cm) should be avoided because the beam divergence of 1 mrad then leads to an incomplete utilization of the pumped volume. A disadvantage of the natural beam divergence concept is that it does not provide for image relaying so that the beam loading is not as close to the damage threshold as it could be.

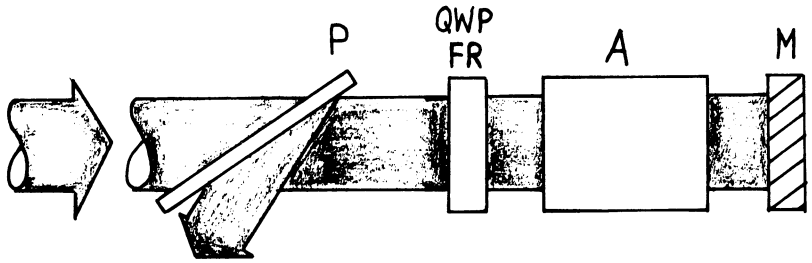

Fig. 21: Double pass amplifier (P polarizer, QWP quarter wave plate, A amplifier, M Mirror: conventional or SBBS

For laser media with a high saturation fluence like Nd the simple MOPA architecture is not as attractive since the chain would have mainly to be operated in the small signal regime. Alternatives are the multipass amplifier and the regenerative amplifier (see Fig. 20). Multipass systems are only technically feasible for short amplifiers. Even in this case long propagation paths are required to reduce beam vignetting at the amplifier aperture. The regenerative amplifier is a larger version of the usual oscillator geometry used for the generation of low power pulses. The major problem in this concept is the requirement for a large diameter optical switch that has a rapid switching time, low leakage (no prepulses) and the need for low-loss optical components. Due to these difficulties the regenerative amplifier concept has not been used so far in a high power system. Similar holds for the multipass amplifier arrangement with the exception of the double pass configuration shown in Fig. 21. Since beam separation is effected by polarization control this configuration is also applicable to long amplifiers. The mirror can be of conventional or SBBS-type. In the first case a saturable absorber or an electrooptic shutter is necessary to avoid parasitic chain oscillations. An advanced MOPA configuration is shown in Fig. 22. By means of expanding telescopes the growth of the beam diameter is optimized to extract energy from the amplifiers in a more efficient way, than it is possible with the simple MOPA arrangement. Moreover, spatial filtering and image relaying can be easily incorporated so that a smooth beam profile and high fill factor can be transported all along the laser chain. Each stage also contains the necessary components for isolation to avoid premature target damage by prepulses, ASE or

parasitic oscillations of the entire chain. When the advanced MOPA architecture is properly designed the beam loading approaches the damage threshold in each stage at a corresponding position or everywhere (isofluence), i.e. in each component of each stage the fluence is at the damage level.

The advanced MOPA architecture is the arrangement for present Nd:glass laser systems like NOVETTE and NOVA and also for the 2 kJ ASTERIX IV system to be put into operation by 1986.

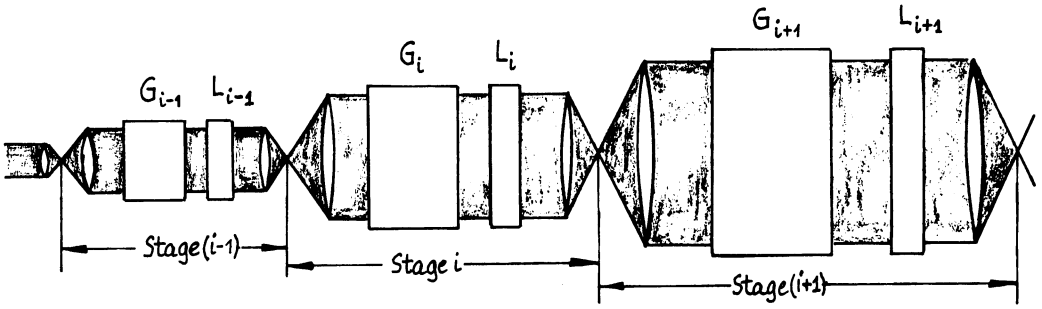

Fig. 22 : Advanced MOPA architecture (G Gain, L loss dur to scattering, reflection, absorption and filtering)

5.2 Non-Storage Laser Architecture

As already pointed out KrF excimer lasers are efficient and scalable to sizes interesting for inertial confinement fusion. The main characteristic is the short excited state life time so that efficient operation is only possible if energy is extracted during the entire duration of the pump pulse of ~ 400 ns duration; shorter pump times are unattractively expensive for large amplifiers. Since fusion requires pulse durations of a few nanoseconds an efficient method for pulse shortening of KrF pulses from 400 ns down to at least 10 ns is necessary.

One technique for this purpose is staged multiplexing shown schematically in Fig. 23 . The large aperture KrF amplifier is e-beam pumped for a time interval of 4 τ and energy is sequentially extracted by two angle encoded

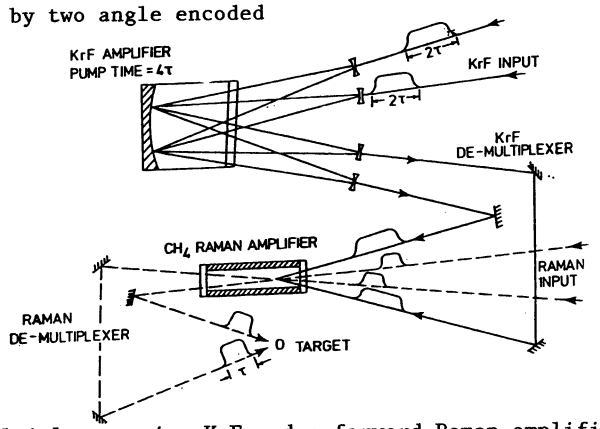

Fig. 23 : 2x2 Staged multiplexer using KrF and a forward Raman amplifier (——— KrF beams, - - - 1st Stokes Raman beams)

KrF laser pulses each of duration 2 τ one delayed from the other by 2 τ. The first KrF pulse enters the amplifier at the start of the e-beam and the second leaves the amplifier at the end of the e-beam. After amplification the two KrF pulses (248 nm) are decoded and appropriately delayed to simultaneously pump a forward Raman amplifier with a pump time of 2 τ. This amplifier is itself optically multiplexed by two pulses of duration τ at a wavelength of 268 nm (corresponding to the Raman shift in CH_4). These two new pulses are then decoded and directed on target in synchronism. A pulse compression factor of 4 has thus been achieved with an intensity gain probably approaching 4 since the conversion efficiency from the pump beam to the stokes beam is close to unity even if both beams travel at an angle to each other. Using this principle a 5 x 12 staged multiplexing scheme is being designed for SPRITE /41/ to compress the expected 60 ns/300 J output pulse into a 1 ns pulse at 268 nm.

A second technique for compressing a long pulse is that of backward wave Raman scattering /47/ whereby also large compression ratios can be achieved. The conversion efficiency is, however, about inversely dependent on the ratio of T_p/T_R where T_p denotes the duration of 248 nm pump pulse and T_R that of the Raman shifted pulse; at $T_p/T_R = 5$ a conversion efficiency of 60 % may be achievable. In spite of this disadvantage combination of backward wave Raman scattering and multiplexing appears to be attractive since then each technique has not to be exhausted up to its technological limits.

A third method is SBBS, as already mentioned. Conceptually it is the simplest of all but not yet fully explored in the sense that its limitations have still to be determined.

In the design of these non-storage systems proper consideration of suppression of prepulses due to ASE or parasitic oscillations is also an important task.

5.3 Optimization

Because the performance of each component in a chain depends on the laser-pulse duration a laser system can only be optimized at one pulse duration. Three regimes of system design can be clearly distinguished: a) the short pulse region below a few hundred picoseconds where self focussing is the limiting process; b) the intermediate regime from a few hundred picoseconds to several nanoseconds where surface damage controls the laser performance and c) the long pulse regime above several nanoseconds where the stored energy determines the laser performance. Short pulse Nd:glass lasers (≦ 100 ps) and short pulse iodine lasers (≦ 200 ps) belong to category a). CO_2 lasers and iodine lasers both operating at ~ 1 ns are examples of category b). The nonstorage KrF laser has a typical pulse duration of several nanoseconds or longer; it is stored-energy limited and thus falls under category c). For ps-CO_2 and excimer lasers the processes limiting the system performance have still to be identified. ps-excimer lasers will probably be stored energy limited.

The optimization procedure starts with the desired laser output energy E and assumes a number of beams M. The output energy per beam or chain is then E/M. The number of stages

per chain is determined by working backwards using as a first approximation the concept of isofluence and obeying the limitations on the small signal amplification such that ASE, prepulses and parasitic oscillations are not harmful to the target. By varying the number of beams and thus the number of stages per chain the design yielding the lowest value for the capital costs per unit focusable output energy can be found. Usually the laser system with the technologically still feasable smallest number of beams, i.e. with large-diameter final stages, minimizes the total costs.

5.4. Isolation

As already pointed out protection of the target from damage due to ASE, prepulses or parasitic oscillations of the amplifiers require a careful isolation of the chain from the oscillator delivering the chain input pulse and from the amplifiers among each other. In addition the chain has to be protected from the light backreflected from the target.

a) Oscillator-Chain: The shutter is usually a polarizer-Pockels cell arrangement. If a mode-locked oscillator is used it also acts as a pulse selecting system. If the oscillator emits a long pulse the shutter simultaneously acts as pulse cutter i.e. it cuts out a short pulse from the long pulse. In any case, however, the contrast ratio of the shutter defined as the ratio of the transmitted intensity to the incident intensity at closed shutter has to be $\sim 10^3$ smaller than the inverse of the effective small signal amplification of the chain. Only then prepulses are kept at a level that they don't damage the target. If the chain input pulse is generated by frequency shifting the pulse from another laser decoupling is perfect.

b) Stage-Stage: Isolation from stage to stage is necessary to avoid parasitic amplifier oscillation and build-up of ASE. Several measures can be taken for this purpose. Saturable absorbers are applied in the CO_2 laser (gas mixtures) and in the iodine laser (dyes or hot iodine cells). Equally well suited are polarizer-Pockels cell arrangements. They are used in Nd, I and KrF lasers, but only for diameters $\leq$ 10 cm. Spatial filtering is also an isolation technique, but of course not as effective as the others already mentioned. SBBS mirrors are especially attractive for KrF (long pulse) and to a certain extent also for iodine; their potential has not yet been fully evaluated.

c) Target Backreflection: For diameters up to 20 cm Faraday rotators are efficient in protecting the chain from the light retroreflected from the target. They are usually placed in front of the final amplifier. This technique has been widely employed in Nd and I and may also be used in KrF. For large diameters (> 20 cm) Faraday rotators become too expensive. Then the plasma shutter is the more favourable solution. It is placed between the chain exit and the target and can be used for any laser.

6. References

/1/ Lax M., Louisell W.M., Mc Knight W.B.: Phys. Rev. A 11, 1365 (1975)

/2/ Goodmann J.W.: Introduction to Fourier Optics. Mc Graw-Hill Book Company, San Francisco - New York - London, 1968

/3/ Optical Phase Conjugation, (ed. R.A. Fisher), Academic Press, New York - London - Toronto, 1983

/4/ Frantz L.M., Nodvik S.J.: J. Appl. Phys. 14 (1963), 2346

/5/ Schultz-Dubois E.O.: Bell System Techn. J. 43, 625 (1964)

/6/ LLL Annual Report UCRL - 50021-78, Vol. 3, Sect. 8, pp. 10-48 (1971)

/7/ LLL Annual Report UCRL - 50021-79, Vol. 3, Sect. 7, pp. 1-45 (1980)

/8/ Singer S., Elliot C.J., Figuereira J., Libermann I., Parker J.V., Schappert G.T.: High-Power, Short-Pulse CO_2 Laser Systems for Inertial-Confinement Fusion. In "Proc. Int. School of Physics Enrico Fermi, Course LXXIV," (ed. C. Pellegrini), North Holland Publishing Company, Amsterdam - New York - Oxford, 1981

/9/ Corkum P.B.: Opt. Lett. 8 (10), 514 (1983)

/10/ Chong-Yi W., Schwab C., Fuss W., Kompa K.L.: Opt. Commun. 46, 311 (1983)

/11/ Brederlow G., Fill E., Witte K.J.: The High Power Iodine Laser, Springer Series in Optical Science, Vol. 34, Springer Verlag, Berlin - Heidelberg - New York, 1983

/12/ Brown D.C.: High Peak Power Nd:Glass Laser Systems, Springer Series in Optical Sciences, Vol. 25, Springer Verlag, Berlin - Heidelberg - New York, 1981

/13/ Maeda M. et al.: Appl. Phys. Lett. 36, 636 (1980)
Reksten G., Varghese T., Bradley D.J.: Appl. Phys. Lett. 38, 513 (1981)

/14/ Carlsson R.L. et al.: IEEE J. Quant. Electron QE-17 (9), 1662 (1981)

/15/ Figueira J., Thomas S.: IEEE J. Quant. ELectron. QE-18 (9), 1381 (1982)

/16/ Lowdermilk W.H., Milam D.: IEEE J. Quant. Electron. QE-17 (9), 1888 (1981)

/17/ LLL Annual Report 82, UCRL-50021-82, section 7, pp. 7.24-7.33

/18/ LLL Annual Report 83, UCRL-50021-83, section 6, pp. 6.31-6.40

/19/ Bennet H., Guenther A., Milam D., Newnam B.: Appl. Opt. 22 (20), 3276 (1983)

/20/ Guenther K. et al.: Appl. Opt. 23 (21), 3743 (1984)

/21/ Comley J.C. et al.: IEEE J. Quant. Electr. QE-17 (9), 1786 (1981)

/22/ Yamanaka C. et al.: IEEE J. Quant. Electron. QE-17 (9), 1678 (1981)

/23/ Mukherjee P., Kwok H.S.: Appl. Phys. Lett. 44 (2), 180 (1984)

/24/ Tajima T., Dawson J.M.: Phys. Rev. Lett. 43 (4), 267 (1979)

/25/ Katsouclas T., Dawson J.M.: Phys. Rev. Lett. 51 (5), 392 (1983)

/26/ Bunkenburg J. et al.: IEEE J. Quant. Electron. QE-17 (9), 1620 (1981)

/27/ LLL Annual Report UCRL-50021-83, section 2, pp. 2-5

/28/ Martin W.E. et al.: IEEE J. Quant. Electron. QE-17 (9), 1744 (1981)

/29/ Pellegrini C.: The Challenge of Ultra High Energies - Proc. of the ECFA-RAL Meeting, Oxford Sept. 1982, p. 249

/30/ Loewenthal D.D. et al.: IEEE J. Quant. Electron., QE-17 (9), 1861 (1981)

/31/ Moody St. et al.: IEEE J. Quant. Electron. QE-17 (9), 1856 (1981)

/32/ Sandström R.L., Levatter J.I.: CLEO'83, Techn. Digest, paper WF 2, p. 100, May 17-20, 1983, Baltimore /Md.

/33/ Smilanski I., Byron S.R., Burkes T.R.: Appl. Phys. Lett. 40, 547 (1982)
" - ": CLEO'83, May 17-20, 1983, Baltimore /Md., Techn. Digest, paper FE 4, p. 22

/34/ Corkum P.G., Taylor R.S.: IEEE J. Quant. Electron. QE-18 (11), 1962 (1982)

/35/ Taylor R.S. et al.: IEEE J. Quant. Electron QE-19 (3), 416 (1983)

/36/ "Excimer Lasers", ed. Ch. K. Rhodes, Springer Series "Topics in Applied Physics", Vol. 30, Springer Verlag, Berlin · Heidelberg · New York, 1979

/37/ Egger H. et al.: Appl. Phys. Lett. 41, 1032 (1982)

/38/ Szatmari S., Schäfer F.P.: Opt. Commun. 48 (4), 279 (1983)

/39/ Rokni M., Jacob J., Mangano J.: Phys. Rev. A 16, 2216 (1977)

/40/ Rutherford Appleton Laboratory, Annual Report 1982, Ch. 2

/41/ Rutherford Appleton Laboratory, Annual Report 1983, Ch. 2

/42/ Zeldovich B.Ya., Popovichev V.I., Ragulskiy V.V., Faizullov F.S.:
Sov. Phys. JETP 15, 109 (1972)

/43/ Nosach O.Yu., Popovichev V.I., Ragulskiy V.V., Faizullov F.S.:
Sov. Phys. JETP 16, 435 (1972)

/44/ Eidmann K., Sigel R.: Int. Conf. on Laser-Matter Interaction, Marly-le-Roi /France, 9-13. October, 1972

/45/ Eidmann K., Sigel R. in "Laser Interaction and Related Plasma Phenomena", ed. H.J. Schwarz and H. Hora, Plenum Press, Vol. 3B, 667 (1974)

/46/ Horn D.T.: Optical Engineering 21 (2), 252 (1982)

/47/ Murray J.R. et al.: IEEE J. Quant. Electron QE-15, 342 (1979)

Discussion

R. Palmer, BNL

I want to remind you that at least in some cases the specifications for laser powered acceleration are really very, very far from the specifications for fusion studies. The things that we have been looking at are, say, 3 ps CO_2 laser pulses, where an entire accelerator going up to several TeV would not require more than something like a 1000 joules a pulse. So that when you talk about already having tens or hundreds of kilojoules and wanting to go higher, I have to remind you that at least in some cases that is far above what we want. In another way we are far from having what we want, because we want to run at something like a kiloherz instead of once every ten minutes. We want high efficiency much more than capital cost. For instance if I calculate from your beautiful formula what the cost of a thousand joule laser would be I would come to only 10^7 deutschmarks, which is of course a bargain. On the other hand when I say that I want it to run at a kiloherz you are going to take back that offer.

Answer

This is certainly true. The lasers which I have been talking about are single pulse lasers. I do not think you can get a kiloherz with the kind of lasers which are now used for fusion studies. You would need a laser which is pumped differently.

R. Palmer

I've been talking to people who were interested in isotope separation and there are a number of kiloherz lasers about in the States which could be modified to work at CO_2 wavelengths. In fact when you discuss with these people they can imagine a 3 cm aperture providing something like 10 joules at a kiloherz for a not completely ridiculous cost and efficiencies which could be as high as 10%. So the story I get from the isotope separation people does not discourage me completely although the laser to the necessary specification does not exist. One of the reasons why they believe that it may be possible is that by operating at 10 atmospheres you exhaust the energy from all the lines simultaneously so the efficiency is much higher than you get from a nanosecond pulse.

Answer

But you should not overlook that such a laser cannot be operated in saturation; it will be small signalled. So the gain which is due to the line broadening is partially offset by the decrease in efficiency.

K.W. Chen, Texas

To increase laser repetition rate, I believe that high power magnetic switching can be used. Could you comment on this?

Answer

This could indeed be used but so far I do not know of any laser where it has been employed. It is certainly a possibility which should be exploited.

Remark

Magnetic switches have been operated at several hundred Hz at companies such as MSNW. Also at Los Alamos there is work on laser switching.

SUMMARY REPORT OF THE WORKING GROUP 1 ON FEL AND IFEL

A. Renieri
ENEA, Dip. TIB, Divisione Fisica Applicata, Centro Ricerche Energia Frascati, C.P. 65, 00044 Frascati, Rome, Italy

Participants in Working Group

W.A. Barletta, M. Biagini, M. Castellano,
E.D. Courant, A. Cutolo, S. Kawasaki,
A. Kolomensky, J. Nation, M. Placidi,
M. Preger, A. Renieri, W. Schnell, J.S. Wurtele
H. Zyngier

The two topics, FEL as accelerator driver and IFEL as accelerator, have been investigated in this working group by taking into account, as starting points, the conclusions of the Oxford Workshop[1] for the IFEL and the Castelgandolfo Conference[2] for the FEL. In this short note I summarize the main conclusions derived during the four days work. A more detailed analysis can be found in other articles submitted to these proceedings.

In particular the FEL as accelerator driver has been discussed by A. Renieri, the transverse stability in IFEL by E.D. Courant and A.A. Kolomensky, and, finally, the problems connected with laser beam handling and laser-electron beam coupling by A. Cutolo and M. Placidi.

The main conclusions we derived can be summarized as follows:

a) FEL sources are quite suitable for laser acceleration apart from the IFEL. Indeed the typical FEL peak electric field, which can be of the order of some GV/m, is too low for driving an efficient IFEL device in which the gradient is only a small fraction of the laser electric field (10^{-2}-10^{-3}).

b) The IFEL, which is not a linear accelerator but a circular one, is not suitable for colliders operating at an energy of the order of the TeV. Namely synchrotron radiation losses limit the maximum energy at about 300 GeV. In principle it is possible to operate up to 1 TeV but in this case, the gradient is comparable with that obtained in standard accelerating structures[3].

c) Some preliminary estimates seem to require additional focusing (with quadrupoles or strong focusing undulators) for the IFEL. The effects of focusing on the acceleration mechanism must be carefully analyzed.

d) Laser beam handling is a very crucial point for a multistage IFEL accelerator. In particular tolerances on phasing between the various stages are very critical, but it seems that the state of the art will allow a correct timing for a few tens of stages at least. Various schemes have been suggested for the coupling between laser and electron beams. The most promising one seems to be that based on the utilization of a hollow mirror, or a mirror with a very thin (few microns) reflecting foil in the centre which allows the passage of the electron beam, followed by a metallic waveguide. We stressed that this topic requires a more careful theoretical and experimental investigation.

ACKNOWLEDGEMENTS

The Group 1 participants acknowledge a very fruitful and interesting discussion with K.J. Witte.

* * *

REFERENCES

1) Proceedings of the ECFA-RAL meeting "The Challenge of Ultra-High Energies" Oxford, Sept. 1982, Report ECFA 83/68 (1983).

2) Proceedings of the "1984 FEL Conference" Castelgandolfo, Sept. 1984, J.M.J. Madey and A. Renieri Eds (to appear in Nucl. Instrum. and Meth. in Phys. Res.).

3) C. Pellegrini, Proc. of 12th Int. Conf. "High Energy Accelerators", Fermilab 1983, p. 473.

Discussion

W. Schnell, CERN

I should like to comment that the expression for maximum energy in an IFEL (balancing acceleration rate against radiation loss) is the same as for a storage ring if one replaces the storage-ring voltage-per-turn by the IFEL "transverse-voltage-gain" per wiggler period and the storage ring bending radius by the wiggler bending radius.

MICROWAVE RADIATION FROM A HIGH-GAIN FREE ELECTRON LASER AMPLIFIER*)

T.J. Orzechowski, B. Anderson, W.M. Fawley, D. Hopkins, A.C. Paul, D. Prosnitz, E.T. Scharlemann, A.M. Sessler, J. Wurtele, and S. Yarema

Lawrence Livermore National Laboratory, Livermore, CA 94550 and Lawrence Berkeley Laboratory, Berkeley, CA 94720

ABSTRACT

A high-gain, high-extraction efficiency, linearly polarized free electron laser amplifier has been operated at 34.6 GHz. At low signal levels exponential gain of 13.4 dB/meter has been measured. With a 30 kW input signal, saturation was observed with an 80 MW output and a 5% extraction efficiency. The results are in good agreement with linear models at small signal levels and non-linear models at large signal levels.

*) Submitted to Phys. Rev. Lett.

OPTICAL GUIDING BY A FREE ELECTRON LASER*)

E.T. Scharlemann
University of California, Lawrence Livermore National Laboratory, Post Office Box 808/L-321, Livermore, CA 94550

A.M. Sessler and J.S. Wurtele
Lawrence Berkeley Laboratory, One Cyclotron Road/58-101, Berkeley, CA 94720

ABSTRACT

The coherent interaction between an optical wave and an electron beam in a free electron laser (FEL) is shown to be capable of optically guiding the light. The effect is analyzed using a two-dimensional approximation for the FEL equations, and using the properties of optical fibers. Results of two-dimensional (cylindrically symmetric) numerical simulations are presented, and found to agree reasonably well with the analytically derived criterion for guiding. Under proper conditions, the effect can be large and has important application to short wavelength FEL's and to directing intense light.

*) To be published in "Proceedings of the Workshop on Coherent and Collective Properties in the Interaction of Relativistic Electrons and Electro-magnetic Radiation, Como, September 1984" which will form a special issue of Nuclear Instruments and Methods in Phys. Res. (1985).

PERSPECTIVES ON FREE-ELECTRON LASER DRIVEN VERY HIGH GRADIENT PARTICLE ACCELERATORS

A. Renieri

ENEA, Dip. TIB, Divisione Fisica Applicata, Centro Ricerche Energia Frascati, C.P. 65, 00044 Frascati, Rome, Italy

ABSTRACT

The prospects on the possible utilization of FEL sources for laser acceleration are reviewed.

1. INTRODUCTION

The possibility of realizing very high gradient accelerators is strongly dependent on the availability of reliable, efficient, high power and high repetition frequency electromagnetic radiation sources operating in the more convenient wavelength region (related to the chosen accelerating scheme). Under these aspects the free-electron laser (FEL)[1] is one of the most promising sources. Indeed for the FEL the following general features can be outlined,

a) FEL performance mainly depends on low energy accelerator technology, which now presents a good level of reliability.

b) FEL overall efficiency can be, in principle, of the order of some percent.

c) Repetition frequency is not limited by heating of the active medium, as in gas or solid state lasers, and, with the present technology, can be of the order of many kHz.

d) The FEL radiation is now tunable from millimiter waves down to visible. In the near future VUV and, later, X-rays radiation would be obtained from this kind of source.

In order to have a better general insight into all these features and, in particular, into the power output which is possible from this source, we shall outline in section 2 the state of the art of FEL technology and, in section 3, the prospects for the near future. Finally, section 4 is devoted to some comments on the possible utilization of FEL sources for laser acceleration.

2. STATE OF THE ART OF FREE-ELECTRON LASERS

After the first succesful FEL experiment[2] performed in 1977 at the Stanford University, a noticeable theoretical and experimental effort has been made in many laboratories. All the main theoretical problems are now well clarified as well as many experimental aspects (for example the undulator magnet technology) have reached a remarkable level of development. The scenario of the operating devices[3] is reported in Table 1. The more special feature of the FEL source, i.e. the tunability, is displayed in Fig. 1, where the output peak power is reported versus wavelength. In Table 1 the intracavity peak power for the TRW oscillator is also reported. Indeed we can eventually utilize the intracavity beam itself, which can be extracted with a fast optical switching system. The value of the intracavity peak power (P_i) is just given by the ratio between the output one (P_o) and the total cavity losses Γ, i.e.

$$P_i = P_o/\Gamma. \tag{1}$$

TABLE 1

State of the Art for FEL Oscillators

Laboratory	Accelerator	$\mathscr{E}$ (MeV)	λ (μm)	P_i (W)	P_o (W)	E_i (MV/m)	E_o (MV/m)
Livermore	Induction Linac	4.5	8×10^3		8×10^7		
S. Barbara	Pelletron	3	400		5×10^{-3}		
Los Alamos	Linac	20	9-11		10^6		6
Stanford	Superconducting Linac	43	3.3		10^6		10
TRW	Superconducting Linac	66	1.6	1.7×10^8	5×10^5	200	10
ORSAY	Storage Ring	160	0.65		1		0.024

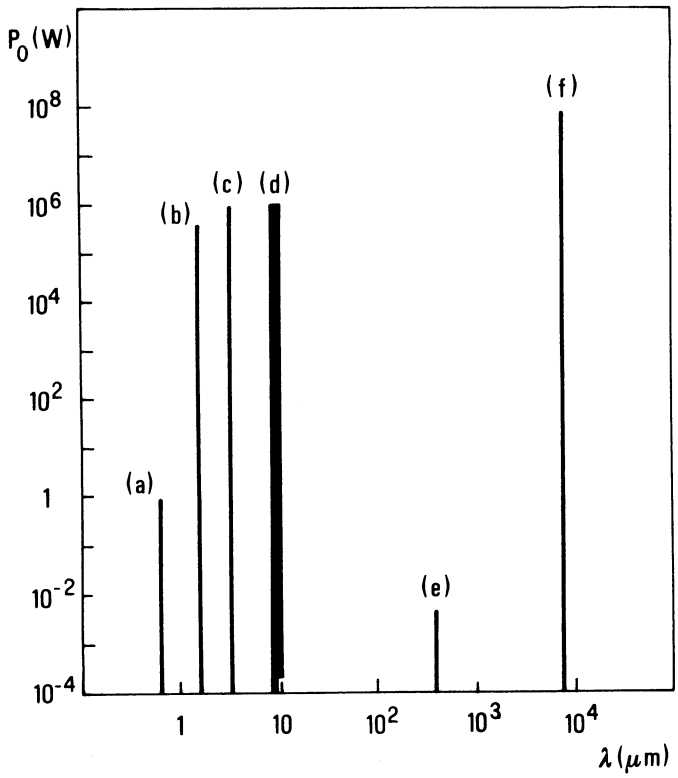

Fig. 1 Peak power vs wavelength for the operating FEL devices
(a) ORSAY
(b) TRW
(c) STANFORD
(d) LOS ALAMOS
(e) S. BARBARA
(f) LIVERMORE

In the first case we have a lower power laser beam, whose duration is of the same order as the electron beam, apart from the transient pulse rise time (typically many microseconds). In the second case the laser power is higher, but its maximum duration is roughly given by the round trip optical cavity transit time (some tens of nanoseconds).

Finally, in the last two columuns of Table 1, laser electric fields for Infrared FELs ($\lambda \lesssim 10$ μm) for a focalization corresponding to a Rayleigh length of four meters are reported for both output and intracavity laser beams.

Namely the electric field in the beam waist is given by,

$$E = \left(\frac{2PZ_o}{\pi w^2}\right)^{\frac{1}{2}} = \left(\frac{4PZ_o}{\lambda L}\right)^{\frac{1}{2}} \tag{2}$$

where we have defined

P = peak power

$w \doteq \sqrt{L\lambda/2\pi}$ = waist radius

λ = wavelength

L = Rayleigh length

$Z_o = 377\ \Omega$

3. PROSPECTS FOR FEL PERFORMANCE

It is not a simple task to foresee the best performances that will be possible to have in the future with a radiation source like the FEL one, whose development started only few years ago and where very few devices (only six!) up to now have been able to lase (see Table 1). However we can take advantage (for the near future) both from the well established electron accelerator technology and from the fact that the experimental FEL performances are in very good agreement with the previously derived theoretical predictions.

Let us start from some general considerations. Namely the output laser power P_o in a FEL is related to the electron beam current I and energy $\mathscr{E}$ by the relationship,

$$P_o[W] = \eta \frac{\Gamma_T}{\Gamma} I[A]\ \mathscr{E}[eV], \tag{3}$$

where η is the efficiency in delivering energy from the electron beam to the laser one and

Γ_T = output cavity mirror transmissivity

Γ = total cavity losses

The intracavity power is given by (see eqs (1) and (3)),

$$P_i\ [W] = \eta \frac{1}{\Gamma} I[A]\ \mathscr{E}\ [eV]. \tag{4}$$

As example, the main parameters for two FEL devices, operating at 10 and 100 μm wavelength respectively, are reported in Table 2. We focus our attention on these infrared devices mainly because for 10 μm the optical components technology is well developed (for CO_2 laser systems) while the wavelength of 100 μm (where high power standard sources are not available) appears very promising for some laser acceleration schemes (e.g. grating linac). In the examples of table 2 the efficiency is estimated of the order of 10%. This is a quite large value, if compared with that obtained up to now (~ 1%). However, theoretical considerations[4] and recent experimental results[5] show that this efficiency can be obtained in "tapered" or, in general, "multicomponent" FEL devices. The electron beam current (10 kA at 50 MeV) is that obtained in ATA[6]. We must stress, however, that the actual beam emittance of ATA is not enough good for an efficient FEL operation, so that further improvements of electron beam brightness are needed.

Table 2

Future Prospects for FEL Performance

I (A)	(MeV)	λ (μm)	η (%)	Γ_T (%)	Γ (%)	P_i (GW)	P_o (GW)	E_i (GV/m)	E_o (GV/m)
10^4	50	10	10	1	2	2.5×10^4	25	10	1
10^4	50	100	10	1	2	2.5×10^4	25	3	0.3

4. FEL AS A LASER ACCELERATOR DRIVER

The convenience of utilizing a laser wave for particle acceleration is related to the possibility of realizing very high gradients, with respect to conventional linacs, by taking advantage of the very high electric field that is possible to obtain in the laser radiation. Under this aspect we can put, as a lower limit, a gradient of the order of 100 MV/m. The electric field of the laser wave must be of the same order of magnitude or more (apart high Q resonating structure accelerators, which are not easy to realize for short wavelengths, e.g. in the infrared). In particular the IFEL accelerating scheme[7] requires an electric field which is many order of magnitude larger than the requested accelerating gradient. Indeed, in this case, the gradient G is just a small fraction of the laser electric field E_L

$$G \sim \frac{k}{\gamma} E_L, \qquad k = \frac{eB\lambda_u}{2\pi mc^2}, \qquad \gamma = \mathcal{E}/mc^2 \tag{5}$$

where k/γ is the pinch angle of the electron in the IFEL, which is roughly given by

$$\frac{k}{\gamma} \sim \sqrt{\frac{2\lambda}{\lambda_u}}$$

λ = laser wavelength

λ_u = IFEL undulator period.

From eq. (1), (5) and (6), we obtain,

$$G = \left(\frac{8PZ_o}{\lambda_u L}\right)^{\frac{1}{2}} \quad . \tag{7}$$

From table 2 and eq. (7) we derive the IFEL gradient for both infrared sources

$$G \sim \begin{cases} 7 \text{ MV/m (intracavity beam)} \\ 0.7 \text{ MV/m (output beam)} \end{cases} \tag{8}$$

in the case

$$\lambda_u \sim 0.25 \text{ m}, \qquad L \sim 4 \text{ m} \quad . \tag{9}$$

From Tables, 1, 2 and eq. (8) we can outline the following conclusions,

a) the actual FEL sources (Table 1) can provide suitable electric field (> 100 MV/m) for laser acceleration only using intracavity beam,

b) future generation devices can, in principle, generate very large electric fields, both in intracavity and output beams, suitable for driving near field accelerators, where a large fraction of the laser electric field is utilized for acceleration;

c) for IFEL devices the situation is quite different from near field ones; indeed the gradients corresponding to the electric fields we hope to obtain from FEL sources in the future are very low (see eq. (8)). So that we can conclude that FEL devices are not suitable sources for IFEL accelerators.

ACKNOWLEDGEMENTS

I like to acknowledge all the collegues of the group FEL-IFEL and in particular J.S. Wurtele for fruitful discussions and suggestions.

REFERENCES

1) See, for example, Proc. of the "Bendor Free Electron Laser Conference". J. de Physique (Colloque C1, Suppl. n. 2) 44 (1983).

2) D.A.G. Deacon, L.R. Elias, J.M.J. Madey, G.T. Ramian, H.A. Schwettman and T.I. Smith, Phys. Rev. Lett. 38, 892 (1977).

3) Proceedings of the "1984 FEL Conference" 3-7 September 1984, Castelgandolfo (Italy), A. Renieri and J.M. Madey Ed., to appear in Nucl. Instrum. and Meth. in Phys. Res.

4) N.M. Kroll, P. Morton and M. Rosenbluth, in "Free Electron Generators of Coherent Radiation" (Addison-Wesley, Reading, 1980) Vol. 7, p. 89.

5) G.R. Neil, J.A. Edighoffer, S.W. Fornaca, C.E. Hess, T.I. Smith and H.A. Schwettman "The TRW/Stanford Tapered Wiggler Oscillator", to appear in ref. 3).

6) W.A. Barletta, J.K. Boyd, A.C. Paul, D.S. Prono "Brightness Limitations in Multi-kiloampere Electron Beam Sources" to appear in ref. 3).

7) See, for example, C. Pellegrini, Proceedings of the ECFA-RAL Meeting "The Challange of Ultra-High Energies" Oxford, p. 249, Sept. 1982.

HIGH POWER RADIATION GUIDING SYSTEMS FOR LASER DRIVEN ACCELERATORS

Antonello Cutolo

Istituto Nazionale di Fisica Nucleare - Sezione di Napoli

Dipartimento di Elettronica, Via Claudio 21 80125 Napoli (Italy)

Salvatore Solimeno

Dipartimento di Fisica Nucleare, Struttura della Materia e Fisica Applicata

Mostra d'Oltremare, Padiglione 20 80125 Napoli (Italy)

ABSTRACT

This paper reviews the main problems encountered in the design of an optical system for transmitting high fluence radiation in a laser driven accelerator. Particular attention is devoted to the analysis of mirror and waveguide systems.

I INTRODUCTION

The main conclusions of the workshops held in the last three years and dedicated to laser driven accelerators can be summarized in the fact that, while the performances of the different schemes proposed till now are clear enough, serious doubts have been cast on the possibility of handling efficiently the required high fluence laser beams over distances of the order of a few kilometers [1-3]. This paper is aimed to review critically the wealth of problems connected with the transmission of high power laser beam in a laser driven accelerator (LDA).

The first thing to bear in mind in the design of high power laser systems is the fact that refractive optical components must be excluded wherever possible and, reflective components must be preferred by virtue of their higher optical damage threshold [4]. As an example, we note that in high power lasers the cavity is made of totally reflecting metallic mirrors, the external coupling being ensured by either an unstable configuration or a small hole in one of the mirrors.

An additional reason for excluding refractive lenses wherever possible, is

that they produce large losses due to the transition radiation given off by the fast electrons passing through the lenses.

For the above reasons the choice is limited, as a rule, to one of the following schemes:

1. **Free space propagation**
2. **Mirrors**
3. **Waveguides**
4. **Hybrid configurations**
5. **Self-focusing**

The first four schemes will be carefully analyzed in the next sections. With regard to the self-focusing of the laser beam into the electron bunch [5] proposed by Sessler et al., we limit ourselves to remark that, when it can be efficiently exploited, it seems to be the best approach for solving the problem of the confinement of the radiation in an LDA. However, it is limited by the requirement of high values of the e-beam current intensity.

In conclusion, the main problems we shall deal with are:

1. **Damage threshold**
2. **Coupling of the radiation with the e-beam**
3. **Absorption and diffraction losses**
4. **Manufacturing**

II DAMAGE THRESHOLD IN OPTICAL MATERIALS

Here we give only a short summary of the problems of optical damage, it being assumed that the reader can obtain details from the listed references if desired.

The laser effects induced in optical devices can be either reversible or irreversible. Among the first ones the most important consists in a change of the profile of the surface of the device. These deformations are responsible for the so-called thermally driven abberrations [6]. As they are characteristic of metal surfaces, they will be analyzed in full detail in the next section. Here we prefer to focus our attention on the irreversible damage with reference to dielectric materials, whose importance descends from the fact that a laser beam entering the vacuum chamber of the e-beam, must pass through a transparent window.

In regard to dielectric devices the main possible sources of damage

are melting, thermally induced plastic strains and electric breakdown. The first two classes of damage are characteristic of high average power. In the case of an LDA very high peak intensities (> Gw cm^2) with average intensities less than 1kw/cm^2, are usually required. In these conditions the main mechanism responsible for the damage is simply the electric breakdown.

The problem of an exact definition of the threshold electric field (E_t) for the electric breakdown is quite involved. In fact, while from a theoretical point of view the definition of E_t is straightforward, many experimental factors contribute to prevent the attainment of reproducible values of E_t. Among them, we list the following:

1. Irreproducibility of the temporal and spatial behaviour of the laser field
2. Presence of absorbing inclusions
3. Poor knowledge of the device surface conditions.
4. Self-focusing.

In comparing different experimental results it is customary to define the breakdown threshold as the value at which breakdown occurs in 50% of the pulses. In a well-designed optical system, it is convenient to use electric fields smaller than E_t. In fact, when an electric breakdown occurs a small fraction of the material can be removed from the surface thus generating small irregularities. As pointed out by Bloembergen [7] and Giuliano [8] any kind of surface irregularities as cracks, pores, digs, contribute to reduce the value of E_T. This reduction is a sharp function of the refractive index of the material. As an example, the reduction factor of E_T, due to surface imperfections, is estimated to lie between 2 and 4 for low index materials such as alkali halides, glass and sapphire, while it can be considerably larger in highly refractive materials such as ZnSe and CdTe [7]. This decrease of E_T is not only in inclusion-free materials, where the damage mechanism is electron avalanche breakdown, but also in materials with bulk inclusions, where the damage is due to thermal stresses around the absorbing inclusions.[9]

In general, a good finishing of an optical surface, is obtained by final polishing of the surfaces with ion beams. Fortunately, this results in a marked increase of surface damage threshold compared with that of abrasively polished samples. As an example, we can recall the results obtained by Giuliano,[8] who, after polishing sapphire windows with energetic Ar^+ ion beams, obtained an increase of a factor four in the damage threshold.

The physical mechanism governing optical breakdown in solids is basically the same as in gases. The conduction electrons here play the role of free electrons

and excitation of valence electrons to the conduction bands is essentially equivalent to ionization of atoms in a gas. These features lead to a dependence of the damage threshold on the frequency similar to that of gases excited with microwaves

$$E_T(\omega) \approx E_T(\omega=0)\sqrt{1+\omega^2\tau^2} \qquad (1)$$

where τ is the collision lifetime. In solids τ is estimated to be of the order of 10^{-15} sec[11]. This value of τ gives $\lambda \approx 2\mu m$ for $\omega^2\tau^2 = 1$, which means that, at the wavelengths of pratical interest for LDAS ($\lambda > 1\mu$), E_T is pratically independent of the wavelength and equal to the dc value.

Now, since the breakdown process depends on thermal diffusion (particularly for long-duration pulses) or on plasma growth by electron diffusion from an initial location, we can expect a square root functional form ($\sqrt{\tau_L}$) of the time dependence of the breakdown process (τ_L is the laser pulse length). This leads to predict that the breakdown threshold electric field E_T will scale like $\tau_L^{-1/4}$

In tables I, II, III we have reported some measured values of the damage threshold for different materials with different materials under different irradiation conditions.

Wavelength (μm)	Laser	Transmittance (%)	Damage Threshold
0.694	Ruby	99.0	2.0 G watts/cm^2 in 30 nsec. pulses
0.730	Alexandrite	99.0	1.5 G watts/cm^2 in 100 nsec. pulses
1.053	Nd	99.0	5 joules/cm^2 in 1 nsec. pulses
1.064	YAG	99.0	5 joules/cm^2 in 1 nsec. pulses
1.315	I_2	99.0	5 joules/cm^2 in 1 nsec. pulses

TAB. I Main parameters of windows with **antireflection** coatings on both sides and working at normal incidence.

Wavelength (μm)	Laser	Reflectance	Damage Threshold
0.694	Ruby	99.6	2 G watts/cm^2 in 30 nsec. pulses
0.730-.790	Alexandrite	99.4	1 G watt/cm^2 in 100 nsec. pulses
1.053-.60	Nd	99.5	5 joules/cm^2 in 1 nsec. pulses
1.064	YAG	99.5	5 joules/cm^2 in 1 nsec. pulses

TAB. II Main properties of some dielectric coated mirrors for 45° incidence.

Wavelength (μm)	Laser	Reflectance	Damage Threshold
0.730-.790	Alexandrite	99.5	2 G watts/cm^2 in 100 nsec. pulses
1.053-.60	Nd	99.5	10 joules/cm^2 in 1 nsec. pulses
1.064	YAG	99.5	10 joules/cm^2 in 1 nsec. pulses
1.315	I_2	99.5	10 joules/cm^2 in 1 nsec. pulses

TAB. III Main parameters of some dielectric coated mirrors for normal incidence

III. METALLIC MIRRORS

A small and well shaped focal spot remains the ultimate goal for a good design of a beam-handling system. The thermal deformations of the mirrors used for focusing on or simply directing a laser beam cause distortions of the wavefronts which result in an increased focal spot. This circumstance reduces the peak irradiance with prejudice for the efficiency and overall performance of the laser apparatus.[12,13]

The reflective optics used in high power laser systems undergo severe thermal cycles when subject to high fluence beams. Even a small percentage of power absorbed can lead to damage and possibly destruction of the mirrors under high power loadings. Although the precautions adopted by the manufacturers are sufficient to prevent destruction, in time the surface of the mirror partially loses its reflectivity because of oxidation. This effect assumes a particular relevance when a laser beam undergoes many reflections, and severe reductions of the power transfer efficiency of the optics may result.

The occurrence of hot spots on the mirrors due to the nonuniform absorption of the oxidized areas may result in a strong deformation of the surface and, consequently, in an aberrated wavefront. This results in an aberration function which depends on the mirror's thermal load. Two classes of aberrations, known as power driven aberrations, can be generally found. One is characterized by low spatial frequencies and is due to the slow intensity variation over the beam diameter. The second class exhibits high spatial frequencies (Fresnel ripples). The presence of these aberrations contrasts with the fact that a small and regularly shaped focal spot is the ultimate goal for a well designed laser beam handling system. All these effects are in general enhanced by the large number of mirrors used for shaping and handling the beams. The control of the exposure cycles of a target to the laser beam requires an exact knowledge of the power falling on it.

We will discuss, now, some analytical results obtained by solving exactly the thermoelastic equations for a water-cooled finite-size mirror illuminated by a c.w. doughnut shaped laser beam. No restrictive hypothesis will be made on the intensity distribution and full account will be taken of the cooling process together with the elastic constraints imposed on the mirror. The mirror will be modelled as a cylinder of finite size (radius R and thickness d) cooled by forced convection as a result of the water flowing at temperature T inside a rigid support to which the inner face of the mirror is stiffly constrained. The thermoelastic

equation will be solved and the results of some numerical calculations will be presented, together with the quantitative evaluation of the influence of the deformations on the peak irradiance.

Consider a metallic mirror (cf. fig.1) exposed on the outer face to a laser beam producing an illumination $I(r,\phi)$. In many cases the beam is collimated and axial-symmetric. We shall ignore temperature transients by considering steady-state distributions. Accordingly, the temperature field inside the mirror $T(r, z, \phi)$ will be found among the solutions of the heat equation

$$\nabla^2 T(r, z, \phi) = 0 \qquad (3.1)$$

subject to the boundary conditions

$$k \frac{\partial}{\partial z} T = A I(r, \phi) = A I_{max} I(r, \phi) \quad \text{for } z = 0 \qquad (3.2a)$$

$$k \frac{\partial}{\partial z} T = h (T - T_c) \quad \text{for } z = -d \qquad (3.2b)$$

$$\frac{\partial}{\partial r} T = 0 \quad \text{for } r = R \qquad (3.2b)$$

with A the absorption coefficient of the mirror (1-5%), k the thermal conductivity ($\sim$380 W/m for copper), h the thermal convection coefficient ($10^2 \div 10^4$ W/m^2 °C) and T_c the temperature of the cooling water. By the variable separation technique we get the results plotted in fig.2 [4,12].

The temperature field $T(r, z, \phi)$ induces a deformation of the mirror described by a displacement vector $u(r, z, \phi)$. Assuming an axial symmetry the thermoelastic equation can be solved to give the results plotted in fig. 3 [12].

The effect of the thermal deformation on the focusing properties of the mirror can be summarized in the function I/I*, where I is the peak intensity in the focus of our mirror when the deformations of its surface are taken into the right account while I* is the same intensity when these deformations are absent.

In fig. 4 we have plotted the thermal coefficient h as a function of the cooling water flow rate while I/I* is plotted in fig. 5 as a function of the thermal coefficient h.

Oxide films, presumibly cuprous oxide,form as a rule on copper after exposure to air. This explains the spread of the optical reflectivity values measured by several authors (see table IV). According to Roberts [15] the absorption

coefficient attains its lowest value (0.7%) for a copper specimen thoroughly annealed in hydrogen, electropolished to produce a finished surface, and made clean by heating it to 277°C in a vacuum chamber at a pressure of less than 10^{-5} mm. The other listed values refer to specimens exposed to the atmosphere. The absorption coefficient A $\approx$ 1.3%, measured with the technique of ref.16, for a Spawr mirror LCuW-081 having a diameter of 5 inches and a guaranteed reflectivity higher than 99% (at delivery)[16] is slightly higher than the above referred values.

Table II reports some measurements carried out on some steel SAE 1045 samples irradiated with a 500 W CO_2 laser delivering about 250 watts.

Then a polished steel sample exposed to the atmosphere almost twice as much as a film of pure iron evaporated on a substrate at a pressure of about 10^{-6} mm. This confirms the importance of the oxide films forming on the surface of metallic specimens exposed to air as already discussed for the copper mirrors.

TABLE IV OPTICAL DATA FOR SEVERAL COPPER SAMPLES

Author	Ref.	k'[a]	k"[a]	n[b]	k[b]	100(1-R)[c]
Beattie et al.	19	-2500	750	7.422	50.52	1.13
Shkliarevskii	20	-3406	1248	10.96	59.22	1.20
Roberts						
(bare copper)	15	-5274	1386	9.46	73.24	0.69
(same with						
40 Ä film)	21	-3988	902	7.09	63.54	0.69
Spawr et al.						
(Spawr mirror						
LCuW-081)	16					0.8

a) k'+ik" is the relative dielectric constant

b) n + ik indicates the complex refractive index

c) R represents the reflectance

TABLE V ABSORPTION COEFFICIENTS OF SOME SAE 1045 STEEL SAMPLES WITH DIFFERENT SURFACE CONDITIONS AND FINISHING.*

Surface Condition	Incident Power (W)	Absorbed Power (W)	Absorption Coefficient
Polished	257	29	0.11
Blasted	257	88	0.34
As it is	257	95	0.37
Blackened	257	132	0.51
Phosphate Coated	257	239	0.93

* Chemical composition, % in weight: 0.45 C; 0.8 Mn, 0.3 si, 0.1 Cr, 0.02 S

IV METALLIC AND DIELECTRIC COATED WAVEGUIDES

A number of metallic waveguides have been studied [21] in the search for flexible systems able to deliver the output of CO_2 lasers. All these devices, the best understood being rectangular, helical and circular waveguides [22, 23], share the feature of transmitting efficiently the low-order modes only. This circumstance, together with the fact that their dimensions (height for rectangular guides or curvature radii for the helical and circular ones) are many wavelengths large, limit the divergence of the delivered beams. Reciprocally, the alignment and the matching of an incoming beam with the geometry of the guide input section are very critical. These features have been limiting factors in using these devices in laser metal-working system[4].

In more recent years, various types of midinfrared optical fibers have been developed. Reports have been given of $ZnCl_2$ glass fiber and of polycristalline and single crystal of thallium and silver halides.[24, 25] Hidaka et al [26] have also proposed a new type of fiber in which oxide glass is used as the cladding material to define a hollow core. Some of these structures are currently employed in hollow waveguide lasers[26].

As an outgrowth of these developments, it is interesting to analyze structures combining the main characteristics of metallic and hollow dielectric waveguides, that is ruggedness and low losses. Some authors [28] have studied the propagation characteristics of circular waveguides with dielectric load for increasing the bandwidth of a gyratron. In their analysis they did not account for the finite resistivity of the metals, which becomes an important factor in the midinfrared. In addition, the coating thickness was much smaller than a wavelength. So they did not point out at some special features of these structures occurring when the optical thickness of the coating assumes values close to odd multiples of $\pi/2$.

Coated guiding structures can be made by depositing a dielectric film on metallic strips cut to form the top and the bottom walls of the waveguide.

In this section we are going to review the main properties of both metallic [29] and dielectric coated waveguides [30] for high power laser transmission [31].

With reference to the geometry illustrated in fig. 6 we can express the mode function $u(x, z) = E_y(H_y)$ relative to a TE(TM) mode in the form [30]

$$u = e^{i(\beta + i\alpha)z} \begin{cases} \left\{ \begin{matrix} \cos \\ \sin \end{matrix} \right\} (K_x X), & |x| < b \\ A_+ \left\{ \begin{matrix} \cos \\ \sin \end{matrix} \right\} (K_{x1} X + \phi_+) + A_- \left\{ \begin{matrix} \cos \\ \sin \end{matrix} \right\} (K_{x1} + \phi_-) & \\ b < |x| < b + \delta & \end{cases} \tag{2}$$

where a time dependence $\exp(-i\omega t)$ is understood and suppressed and k_x and k_{x1} satisfy the dispersion relations

$$K_x^2 + (\beta + i\alpha) = K^2 \tag{3}$$

and

$$K_{x1}^2 + (\beta + i\alpha) = n_1^2 k^2,$$

n_1 being the generally complex refractive index of the coating and $k = \omega/c$ the wavenumber. The two boundary matching conditions can be both satisfied if k_{x1} and k_x comply with the eigenvalue equation for the transverse propagation constants

$$K_x \tan\left(K_x b + (m-1)\pi/2\right) = \begin{cases} -\left(n_1^2/K_{x1}\right) \tan\left(K_{x1} + \psi\right) & \text{TM modes} \\ K_{x1} / \tan\left(K_{x1} + \psi\right) & \text{TE modes} \end{cases} \tag{4}$$

with $m > 0$ integer, and

$$\psi = \begin{cases} \tan^{-1}\left(i K_{x1} \tilde{n}_2 / K\right) & \text{TM modes} \\ \tan^{-1}\left(i K_{x1} / \tilde{n}_2 k\right) & \text{TE modes} \end{cases} \tag{5}$$

Equation (4) has been solved numerically with respect to k_x and plots of $\mathrm{Re}(k_x b)$ and $\mathrm{Im}(k_x b)$ for the TE_{01}, TE_{02}, TE_{03} modes are presented in fig.7 for $n_1 = 3$, $\tilde{n}_2 = i60$ (full lines), $\tilde{n}_2 = 7 + i60$ (dotted lines) and $kb \approx 150$ ($b = 0.25$ mm at $\lambda = 10\,\mu$m). Notice that $\tilde{n}_2 = 7 + i60$ is the complex refractive index of copper surfaces at $10\,\mu$m.

The loss factor α_m^{TE} of the mth TE mode can be calculated by solving the eigenvalue equation (4) for the transverse propagation constant, by taking into account the imaginary part of n_1 and the real (β) and imaginary (α) components of k_z. Following Nishihara et al. [32] we can use the reflection coefficient r_{TE} of the dielectric coated metallic surface for an incidence angle $\phi_0 = \sin^{-1}(k_x/k)$

$$r_{TE} = \left[1 - \frac{K_x}{n_e K} - i \left(\frac{K_{x1}}{\tilde{n}_e K} - \frac{K_x}{K_{x1}} \right) \tan \left(K_{x1} \delta \right) \right]$$

$$\cdot \left[1 + \frac{K_x}{n_e K} - i \left(\frac{K_{x1}}{\tilde{n}_e K} + \frac{K_x}{K_{x1}} \right) \tan \left(K_{x1} \delta \right) \right]^{-1} \qquad (6)$$

to calculate α_{TE}

$$\alpha_{TE} = - K_x \left(\ln |r_{TE}| \right) / 2 Kb \qquad (7)$$

Equation (7) holds true for values of the dielectric thickness far from the transition regions, where the eigenvalue equation (eq.(4)) must be solved numerically. Figure 3 shows the loss α_{TE} for a metallic waveguide with kb = 150 and loaded with a dielectric film with n_1 = 1.5,3.

The radiation pattern and the coupling of a cylindrical gaussian beam into the uncoated metallic waveguide modes have been calculated by many authors (see e.g. refs.21,32) by assuming the field on the open end coincident with the mode itself. This corresponds to neglecting the reflection caused by the waveguide truncation. While this assumption is in practice correct for metallic waveguides, the same does not hold true when there is a coating. In fact, in this case a surface wave can be excited, which, travelling backward inside the dielectric substrate, can detract power from the forward scattered wave. In this case the analysis of the diffraction at an open end is a very difficult problem, which can be approximately solved by assimilating the waveguide walls to a half-plane with two face impedances defined, as usual, by $Z_s = E_y / H_z$.

Relying on the method proposed by Maliunzhinets [33] the following expression on the field diffracted by the dielectric coated waveguide has been obtained in ref. 30

$$u_d (\rho, \phi) = - \frac{\exp \left(i k \rho + i \pi / 4 \right)}{\left(2 \pi \rho / b \right)^{1/2}} \exp \left(i \phi \right) \frac{\operatorname{sinc} \left(\phi + \phi_o \right) + \operatorname{sinc} \left(\phi - \phi_o \right)}{\sin \phi_o + i \left(\phi / \phi_o \right) \cos \phi_o} \qquad (8a)$$

where

$$\phi_o = Kb \sin \phi_o = K_x^{(m)} b, \quad \phi = Kb \sin \phi \qquad (8b)$$

Now, taking advantage of the reciprocity theorem the coupling effieciency F_m (defined as the ratio between the power coupled into the mth mode and power of the input beam) can be easily calculated [30] thus giving the results plotted in fig.9.

Now, it is worth discussing briefly some problems relevant to the manufacture of these waveguides. As in high efficiency LDA the laser beam must be kept well focused over distances of several hundred metres, we believe that dielectric coated waveguides would not be the best choice. In fact, the thickness of the dielectric coating should be controlled with a very high precision to avoid the mode coupling, which could easily reduce the coupling efficiency between the radiation and the e-bunch.

After these considerations a metallic waveguide seems to be the best choice and so in the next part of this section we shall focus our attention on these devices. We start by analyzing the loss factor α_m (m being the index of the mode) by a simple ray-optical analysis. In fact, a mode TE_{mo} or TM_{mo} is formed by two plane waves travelling at angle $\vartheta_m = \lambda m \pi / 2d$ with respect to the waveguide axis. Then, each ray travels a distance $d_m = a/\tan\vartheta_m$ between two reflections on upper and lower plates. Let $A(\vartheta)$ the loss per reflection at the incidence angle $i = \pi/2 - \vartheta_m$, the mode undergoes an attenuation per unit length equal to

$$\alpha_m = \frac{m \lambda A(\vartheta)}{2 d^2} \tag{9}$$

A being the absorptance of the metal at the grazing angle ϑ.

For grazing incidence $A(\vartheta)$ is given by (see f.i. Ref.17):

$$A^{TE}(\vartheta) = 4 Re\left(n^{-1}\right) \sin\vartheta \cong 4\vartheta Re\left(n^{-1}\right), \tag{10a}$$

$$A^{TM}(\vartheta) = \frac{4 Re(n) \sin\vartheta}{1 + 2 Re(n) \sin\vartheta + |n^2| \sin\vartheta} \tag{10b}$$

n being the generally complex refractive index of the metal. Consequently,

$$\alpha_m^{TE} \sim \frac{m^2 \lambda^2}{a^3} Re\left(n^{-1}\right), \quad \alpha_m^{TM} \sim \frac{m^2 \lambda^2}{a^3} Re(n) \tag{11}$$

A transmission of more than 95% per meter in a straight aluminium waveguide having a cross section of 0.5 x 7 mm has been measured at $\lambda = 10\mu$.

It is noteworthly that α^{TE} scales with the inverse cubic power of the waveguide height. Consequently, using a waveguide 5 mm high the attenuation reduces to $5 \times 10^{-5}\ m^{-1}$.

Another factor to be considered is the ratio between the electric fields on the walls and in the middle of the waveguide for the TE_{10} mode, which exhibits the

lowest losses,

$$\frac{E_{wall}}{E_{centre}} = \frac{1}{2}|A| = \frac{1}{2} 4 Re\left(n^{-1}\right)\frac{\pi\lambda}{2a} = \frac{\pi\lambda}{a} Re\left(n^{-1}\right) \qquad (12)$$

Since n oscillates between 60 and 70 for Al, Cu or Au, the above ratio is of the order of:

$$\frac{E_{wall}}{E_{centre}} \sim \frac{0.5 \cdot 10^{-3}}{a} \qquad (13)$$

with "a" expressed in mm. With a spacing of a few millimeters the field on the walls reduces to $10^{-3} \div 10^{-4}$ of the value in the middle. This reduction is of the same order of magnitude as the reduction which can be reasonably achieved in a hollow dielectric waveguide.

If we assume that E_{centre} can reach values of the order of a few GV/m, a rough estimate of the field inside the metal yields $E_{metal} \sim$MV/m. This field corresponds to a flux density of $\sim 10^5$ W/cm^2. The same intensity can be reached by illuminating the metal almost at normal incidence with a flux density of $\sim$10 Mw/cm^2, having assumed a reflectivity a 99 ÷ 98%. Good quality copper mirrors can withstand such high flux densities for a few nanoseconds.

If we illuminate a metallic waveguide with a well focused beam, we can excite a few modes in such a way as to keep the field on the walls below the damage threshold value. This means that the most critical stage of this system is represented by the coupling of the input beam with the waveguide.

In case of Gaussian beams, the percentage of the power channeled through any waveguide mode can be calculated by assimilating the beam to that irradiated by a source located at a complex point. In so doing it is possible to apply the geometrical theory of diffraction (GTD) which can account very accurately for the geometry of the metal [29]. In fig.10 we have plotted the coupling coefficients for different parameters of a Gaussian beam. These plots show how critical the coupling with these structures is.

The reader is justified in questioning how well founded is the suggestion of using dielectric or metallic waveguides for confining and guiding the very powerful laser beams required by laser accelerators, over distances of some hundred meters. Inquiry of the laser damage literature to date indicates that wide-bandgap insulators can withstand rms optical electric fields ranging from 1 MV/cm to 10 MV/cm depending on the pulse duration. These field breakdown thresholds correspond

to flux densities of $10^{-3} \div 10^{-1}$ Tw/cm^2.

The experimental data refer to the case of normal incidence. In case of grazing incidence we can expect a notable increase of the damage threshold. If we assume that the damage originates in the bulk of the dielectric the above quoted values of electric field will modify as

$$\frac{E_{normal}}{E_{grazing}} = \left(\frac{T_{graz}}{T_{nor}}\right)^{1/2} \tag{14}$$

where $T_{nor} = 4n(n+1)^2$ is the transmission coefficient for normal incidence while T_{graz} refers to the case of grazing incidence.

For optical quality surfaces satisfying Fresnel's equations of the reflectivity we have at grazing incidence

$$T^{TE} = \frac{4\vartheta}{n} \quad , \quad T^{TM} = 4\vartheta n \tag{15}$$

so that

$$\begin{aligned} E_{threshold} &\sim \vartheta^{-1/2}\,(1 \div 10)\ \text{MV/cm} \quad (TE) \\ &\sim \frac{\vartheta^{-1/2}}{n+1}\,(1 \div 10)\ \text{MV/cm} \quad (TM) \end{aligned} \tag{16}$$

If we assume that our dielectric waveguide is used to confine a gaussian beam having a spot size ω_o, we obtain a rough estimate of the incidence angle in the above relation by equating ϑ to the far field aperture, i.e.

$$\vartheta \sim \frac{\pi\lambda}{\omega_o} \tag{17}$$

being the waist spot size. Accordingly,

$$E_{threshold} \sim \left(\frac{\omega_o}{\pi\lambda}\right)^{1/2}(1 \div 10)\ \text{MV/cm} \tag{18}$$

If we consider that the field on the wall is equal to that on the axis times $\exp(-a^2/w^2)$, we obtain a rough estimate of the highest rms field obtainable in the centre of a hollow dielectric waveguide

$$E_{max} \sim \left(\frac{w_o}{\pi\lambda}\right)^{1/2} e^{a^2/w_o^2} \quad (1 \div 10) \quad HV/cm \tag{19}$$

As an example, if we choose a = 1.5 mm, λ = 10.6 μm, we obtain

$$E_{max} \sim 8 \div 80 \quad GV/m \tag{20}$$

These values are of the correct order of magnitude compared to laser fields considered for acceleration where useful gradients of 0.1 ÷ 1 GeV/m, are assumed.

Figure 10 shows that the coupling is a very sharp function of the orientation and of the parameters of the laser beam. Unfortunately, flared waveguides as well as compound parabolic concentrators [31] cannot be used in our case. This is due to the fact that they increase the coupling efficiency between the input laser beam and the waveguide, but the coupled power is shared between several modes thus reducing the acceleration gradient.

ACKNOWLEDGEMENTS

Useful discussions with Dr. A. Renieri and Dr. M. Placidi and the assistance of Mrs F. Candiglioti are sincerely acknowledged.

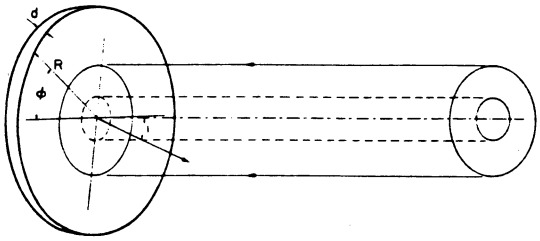

Fig. 1 The metallic mirror in its reference system

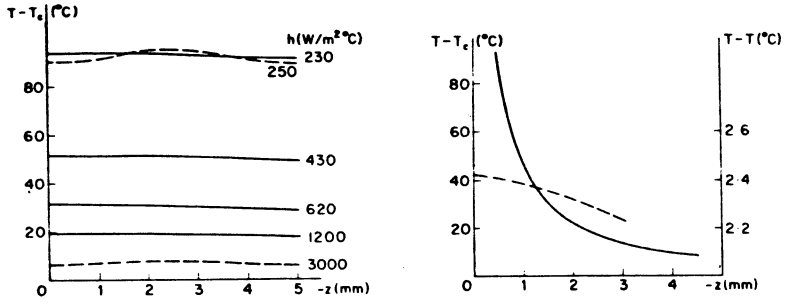

Fig. 2 Plot of the temperature T-Tc (Tc is the reference temperature set equal to zero in our calcolations) of the exposed face of the mirror with R = 10 cm, d = 5 mm, A = 0.05 for different value of h and k = 384 W/m °C (copper, continous lines) and k= 3.84 W/m °C (dotted lines). An incident laser beam with a continous power of 10 Kw has been assumed (after ref. 12).

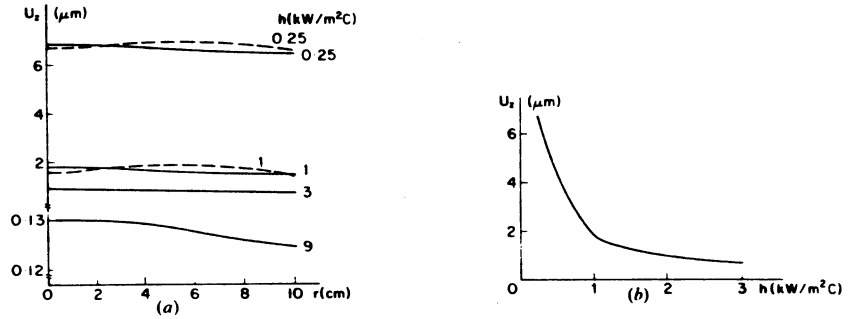

Fig. 3 Normal displacement of the exposed face of the mirror described in fig. 2 (on the top) and of the centre of the same exposed face (on the bottom).

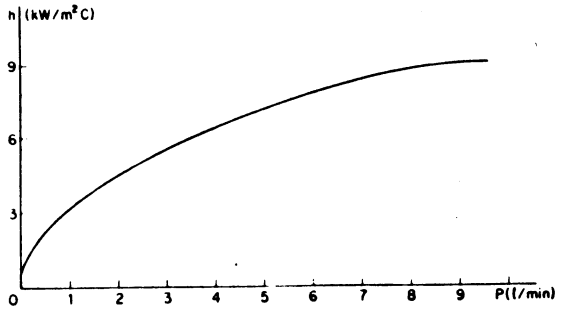

Fig. 4 Plot of the thermal coefficient h as a function of the flow rate of the cooling water.

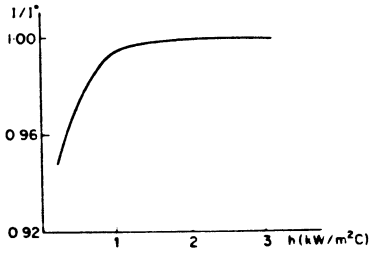

Fig. 5 The ratio I/I^* versus the thermal coefficient h.

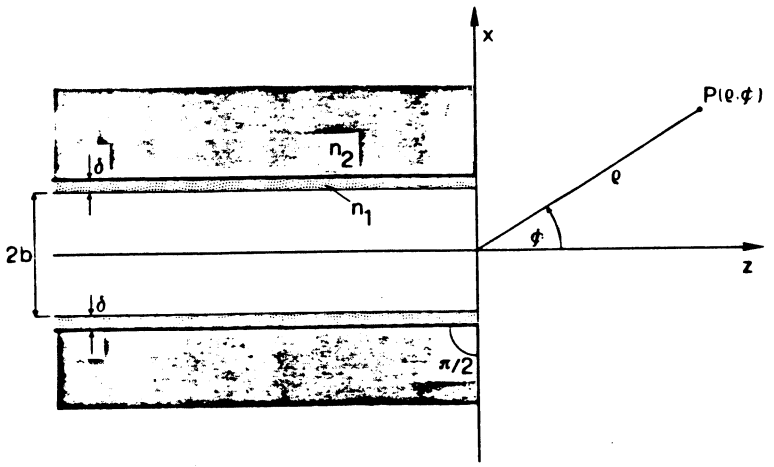

Fig. 6 The dielectric coated metallic waveguide.

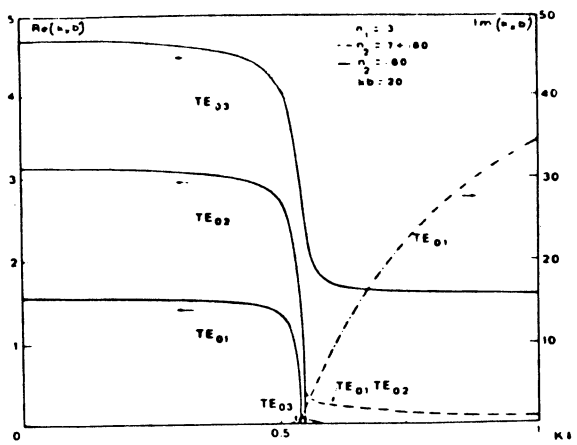

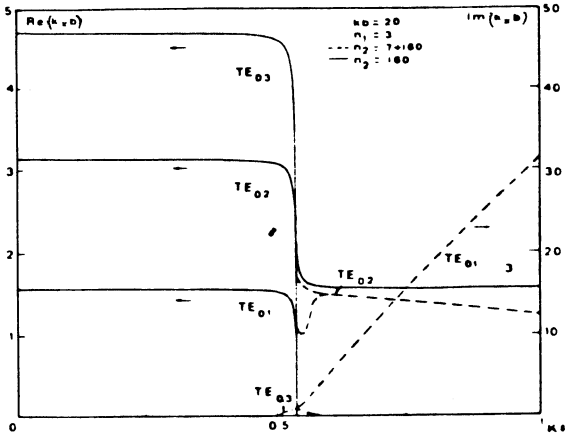

Fig. 7 Plots of $Re(k_x b)$ and $Im(k_x b)$ for TE_{01}, TE_{02}, TE_{03} modes versus $k\delta$ for a waveguide with kb = 20 (fig.7a) and kb = 150 (fig.7b). In both cases $n_1 = 3$ and $\tilde{n}_2 = i60$ (___) and $\tilde{n}_2 = 7 + i60$ (---).

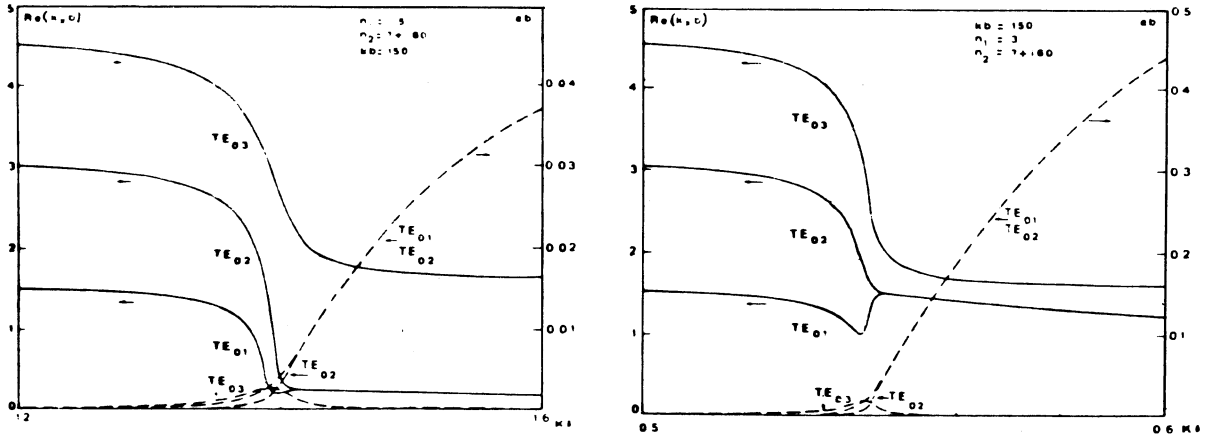

Fig. 8 Plots of $Re(k_x b)$ (full lines) and the loss factor α (dotted lines) for the TE_{01}, TE_{02}, TE_{03} modes of the waveguide with kb = 150 and $\tilde{n}_2 = 7 + i60$, $n_1 = 1.5$ (fig.8a) and $n_1 = 3$ (fig.8b).

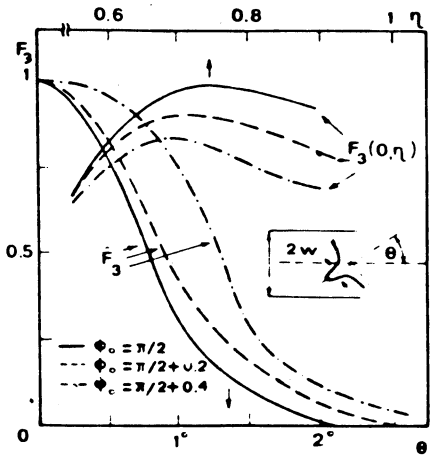

Fig. 9 Coupling efficiency $F_3(0, \eta)$ of a cylindrical gaussian beam versus $\eta = w/b$ and $F_3 = F_3(\theta, \eta_{opt})/F_3(0, \eta_{opt})$ for different values of Φ_0. Θ is the angle between the waveguide and the laser beam axis. Note that the dielectric coating decrease the sensitivity of the coupling efficiency to the alignment.

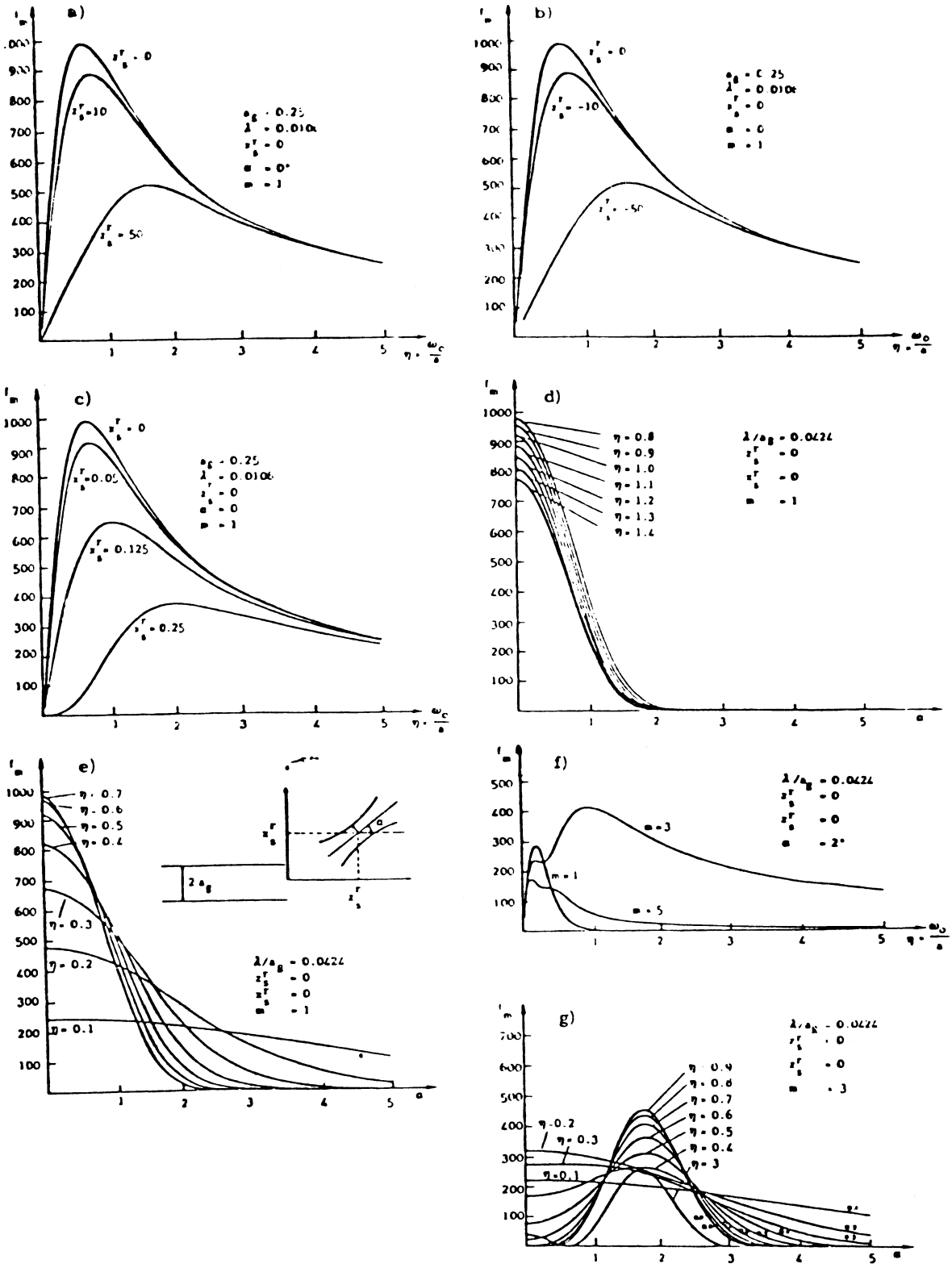

Fig. 10 Coupling coefficient of a Gaussian beam with the fundamental (m = 1) and third (m = 3) modes of a metallic waveguide as a function of $\eta = w_o/a$, and the coordinates x_s^r, z_s^r, of the waist, α the angle formed by the propagation axis of the beam with the waveguide.

REFERENCES

1. P.J. Channel Ed., Laser acceleration of particles AIP (N.Y. 1982)
2. The Challenge of Ultra High Energies, Proc. of the ECFA-RAL meeting, Oxford (1982)
3. These proceedings
4. V. Bartiromo, A. Cutolo, S. Solimeno in "Laser Matter Interaction" ed. by M. Bertolotti, Plenum Press (1984)
5. A. Sessler, these proceedings
6. P.V. Avizonis in "Adaptive Optics and short wavelength sources" eds. S.F. Jacobs, M. Sargent III and M.O. Scully, Addison Wesley (1978)
7. N. Bloembergen, Appl. Opt. 12, 661 (1973)
8. C. Giuliano, Appl. Phis. Lett., 21, 39 (1972)
9. N. Bloembergen, IEEE J. of Quant. Electron., QE-10, 375 (1979)
10. Shen, The principles of non-linear Optics, J. Wiley and Sons, N.Y. 1983
11. S.A. Ramsden, W.E.R. Davis, Phis. Rev. Lett. 13, 227 (1964)
12. A. Cutolo, P. Gay, S. Solimeno, Optica Acta 27, 1105 (1980)
13. A. Cutolo, Alta Frequenza, LXIX, 261 (1980)
14. F. Crescenzi, A. Cutolo, P. Gay, S. Solimeno, Opt. Engeneering 21, 511 (1982)
15. S. Roberts, Phys. Rev. 118, 1509 (1960)
16. W.J. Spawr, R. Pierce, SPAWR Opt. Res.; Rept. 74-004 (1976)
17. Landolt, Börstein, Eigenschaften der Materie in Ihren Aggregatzustanden, 8. teil, Springer Verlag; Berlin (1962)
18. F. Bueche, J. Opt. Soc. of 38, 806 (1948)
19. J.R. Beattle, C.K. Conn, Phylos Mag. 46, 989 (1955)
20. I.N. Shkharevskii, V.G. Padalka, Opt. Spektrosk. 6, 78 (195
21. E. Garmire, T. McMahon and M. Bass, IEEE J. Quant. Electron. QE-16 (1980) 23
22. L. Casperson, IEEE Quant. Electron. QE-15 (1979) 491
23. H. Krammer, Appl.Optics 17 (1978) 316
24. S. Sakuragi, M. Saito, Y. Cubo, K. Imagawa, H. Kotami, T. Marikawa and J. Shimada, Optics Lett. 6 (1981) 629
25. T.J. Bridges, J.S. Hasiak and A.R. Struad, Optics Lett. 5 (1980) 85
26. R.L. Abrams, and W.B. Bridges, IEEE J. Quant. Electron. Q9 (1973) 940
27. T. Hidaka, T. Marikawa and J. Shimada, J. Appl. Phys. 52 (1981) 4467
28. S.Y. Choe, H.S. Ulm and S.A. Chu, J. Appl. Phys. 52 (1981) 4508
29. F. Crescenzi, P. Gay, A. Cutolo, I. Pinto, S. Solimeno, Proc. of 1980 Europ. Conf. on Opt. Systems, SPIE vol. 236, 365 (1981)
30. A. Cutolo, S. Solimeno, Opt. Comm. 43, 323 (1982)
31. S. Solimeno, in ref. 1
32. K.D. Laakmann, W.H. Steier, Appl. Opt. 15, 1334 (1976)
33. G.D. Malinzhiuets, Soviet Phys. Dokl. 3, 752 (1958)

Discussion

R. Evans, RAL

I have a question concerning the maximum intensity in the waveguide mode. The number quoted was 80 GV/m. Is that experimentally measured or is it a theoretical limit?

Answer

It is an extrapolation depending on how the damage threshold varies with the pulse length. It should be possible for pulses with a length between 5, 10, or at the most 50 ps. For longer pulses this damage threshold goes down inversely proportional to the square root of the pulse length.

H. Lengeler, CERN

An experimental value given to me by K. Witte is about 1 GV/m for a 1 ns single-shot pulse, at 10 μm.

SUMMARY REPORT OF THE WORKING GROUP 2 ON NEAR FIELD ACCELERATORS

T. Weiland
Deutsches Elektronin-Synchrotron DESY, Hamburg

Participants in Working Group

W. Bialowons, D. Chan, J. Claus, G. Dôme, K. Frank, L.W. Funk, J.P. Girardeau-Montant, H. Haseroth, H. Henke, H. Klein, P. Krejcik, H. Lengeler, R. Palmer, L. Palumbo, A.G. Ruggiero, K. Rustagi, A. Sessler, R. Sigel, S. Takeda, V.G. Vaccaro, T. Weiland, B. Zotter

Group 2 considered three types of accelerators:
- Wake Field Accelerators (WFA)
- Two-Beam Accelerators (TBA)
- Laser Droplet Accelerators (LDA)

Most of the workshop was spent on presenting these three types of accelerators in detail. Only a small amount of time was left to actually "work" on any of these subjects. However, during the presentations a number of "weak" points were discussed. For each acceleration scheme a list of the problems was made that urgently need more theoretical and/or experimental work.

General problems common to all three types of accelerators were found to be:

Overall efficiency,
Wake Field effects/limitations,
Breakdown limit on gradients,
Bright sources.

But no time was left to do much more than prepare this list and identify the problems. Thus, here we will simply list these points and not repeat a description of the three schemes.

WAKEFIELD ACCELERATORS (WFA)

A major problem common to all types of wakefield accelerators is that the essential ingredient is a very short high-density driving beam of protons or electrons. Peak currents around 50000 amps or more are necessary to create sufficiently high wakefields to accelerate particles at a rate above the magic figure of 100 MeV per meter. In terms of bunch size one needs millimeter long bunches carrying 10^{12} to 10^{13} particles ($\approx$ 1μ Coulomb). The generation of such short high density bunches may possibly be the real limitation for the wakefield schemes since space charge effects in the low energy region will counteract external bunching forces. Furthermore, the preacceleration of such beams is itself a very difficult problem since the wakefield effects mainly do harm, especially to high density short bunches.

If a TeV collider is based on the wakefield effect without transformation, then one has to provide about 1μ Coulomb at 500 GeV (or 10 times 50 GeV if built in 10 stages (say)) in a bunch of a few millimeters in length. No reasonable scheme is known for realizing this, whether one uses protons or electrons. If one uses the Wakefield-Transformer the situation looks better since only 50 GeV (or ten times 5 GeV if built in 10 stages (say)) have to be provided as acceleration of the 1μC bunch.

TWO-BEAM ACCELERATORS (TBA)

The TBA problems are mainly centred around the operation of an FEL that generates the rf-power for the high gradient standard type accelerating structure.

Steady state FEL operation was one of the problems considered and - as usual - the problem of tolerances on the wiggler field and in the period length. Also the slippage between the high energy beam and the low energy beam can become a problem. For a 3 MeV beam the slippage amounts to a few percent, i.e. some ten meters after one kilometer.

For successful operation the power output per unit length also has to be around 500 MW/m, a number which is not far from the results achieved at Berkeley (50 MW/m).

A second kind of problem occurs in the accelerating structure where wakefield effects will be a major limitation. These effects are common to all accelerating schemes which use metal near the beam, and thus they must be considered in all wakefield accelerator schemes.

LASER DROPLET ACCELERATOR (LDA)

The laser droplet accelerator is a quite unusual device and this implies that problems will be more difficult to forsee. However, the proper generation of droplets is an obvious problem as well as the wakefield effects and the determination of useful modes for acceleration. The fact that it is a scheme that is fully threedimensional makes the analysis quite cumbersome. 3D-codes will have to be used for studying these effects which are, after all, again very similar to those occuring in the WFA and TBA.

The laser providing the accelerating field will have to have some extreme properties such as 1 Joule per pulse, repetition rate of a few KHz, efficiency a few percent, ... etc. This is probably the most expensive part of the scheme and it was considered that this could provide the main obstacle to a realization.

It is somewhat difficult to compare the three schemes WFA, TBA and LDA since the first two promise gradients of some hundred MeV/m and the LDA of some GeV/m. This difference in gradient is also reflected in the different levels of practicability of the concepts. Whereas the WFA and TBA are being studied experimentally and appear to provide a possible solution for the next generation, the LDA is not yet at a stage where an experiment can be mounted (?). On the other hand, the LDA is destined to be used in the next but one generation of accelerators and so there is more time available for R&D.

GENERAL PROBLEMS

Breakdown:

Measurements at SLAC were reported that removed any fear that breakdown could be a problem. Field strengths of more that 100 MeV/m have been achieved at 3 GHz. If one believes the frequency scaling laws, there will be no problem for the TBA nor for the WFA. The WFA is in all cases considered the concept with the highest possible field strength since the pulses are much shorter than in a TBA or a standard pulsed linac. However, the general feeling was that no-one in the group knew very much about this area.

Wakefield effects:

Here we address the wakefield effects that do harm to the beam and not those that are used for acceleration. These wakefield effects lead to energy loss and spread, to transverse blow-up and beam break-up. General scaling laws are not easy to give since the collective effects depend strongly on the detailed geometry of the structure and on all the beam parameters. However, from scaling, it is already clear that there will be a severe problem for the WFA and the TBA. Experimental and detailed theoretical studies are under way and the effects are well understood, though not completely analyzed yet. Less obvious, since it is so different from the ordinary linac, are the wakefield problems in the LDA. Here one could use the same techniques as are usually used in standard structures for beam dynamics calculations, i.e. wakefield calculations, mode computations and tracking studies.

SUMMARY

As a result from this week's work one could see that far too few accelerator people actually work for most of their time on new accelerator schemes.

If one compares the technology of LEP with that of PETRA/PEP and the technology of PETRA/PEP with that of DORIS/SPEAR one finds a more or less continous development and essentially only a change in scale but not in basic principles.

The next generation however, whether it is a WFA, TBA or LDA or even an extended SLC version, will be very much different from the existing accelerators. In spite of that, the amount of work currently being dedicated to the subject of the workshop was considered to be much too little.

The discussions during the week illuminated a large number of basic physical problems that have to be investigated both theoretically and experimentally.

Editor's note

Following the workshop W. Willis developed his proposal for a Switched Power Linac and his paper is included in this section.

Discussion (following Working Group 2 Summary presented by A. Sessler)

M. Tigner, Cornell

Could you make some further comment on the problem of the transverse wakes?

A. Sessler, LBL

We can discuss the transverse displacement in terms of the quantity

$$A = x(z)/x_0 \ ,$$

where $x(z)$ is the transverse position at the back-end of a bunch for which the initial displacement off-axis is x_0. If x_0 is zero then everything is fine, but this is not the case in general.

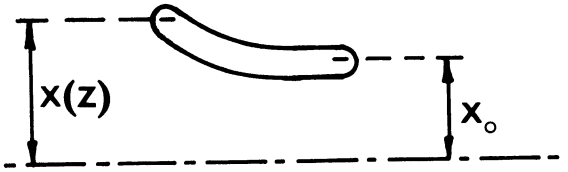

Following P. Wilson, who analysed this effect at the Los Alamos Conference:

$$A = \frac{q}{4E_a} \cdot w_T \cdot \beta$$

where q is the charge, E_a the accelerating field, w_T is proportional to the transverse wake potential, and β is the betatron amplitude function. We can put

$$w_T = \frac{W(\sigma)}{\lambda \pi a^2}$$

where $W(\sigma)$ is a function of bunch length only, and a is the <rad.> of the field; so this gives the correct $1/\lambda^3$ behaviour.

Then

$$A = \frac{1}{4} \ \frac{q}{E_a} \ \frac{W(\sigma)}{\pi a^2} \ \frac{\beta}{\lambda} \ ,$$

and this suggests that going to smaller λ can be compensated by enlarging the aperture, a. But then the efficiency of the accelerator goes down, so we try some more manipulation.

The efficiency can be written:

$$\epsilon = \frac{E_a q}{\omega} = \frac{E_a q}{E_a^2 \pi a^2} ,$$

where ω is the stored energy per unit length.

Thus

$$A = \frac{\epsilon}{4} \cdot W(\sigma) \cdot \frac{\beta}{\lambda} .$$

So, as we discussed at Los Alamos, if β/λ is constant, that is more focusing as you decrease the wavelength, then A is proportional to the efficiency; again we find a result driving us towards lower efficiency.

But is A really the quantity of interest? What we should be asking is how much the back is displaced compared to the width of the bunch. So we have defined

$$\alpha = x(z)/\sigma_x ,$$

and introduce the emittance, via

$$\sigma_x = \sqrt{\frac{\varepsilon_x \beta}{\gamma}} .$$

Next we decided that the initial displacement of the bunch should be measured in units of the wavelength:

$$\delta_x = x_0/\lambda .$$

Then

$$\alpha = \sqrt{\frac{\gamma}{\varepsilon\beta}} \cdot \lambda \delta_x A ,$$

or

$$\alpha = \frac{\epsilon}{4} \delta_x \sqrt{\frac{\gamma\beta}{\varepsilon}} \cdot W(\sigma_z) .$$

For fixed δ this is again independent of λ; it improves as $\sqrt{\beta}$ decreases, but gets worse for high γ. But this has to be put into some big optimisation programme with lots of other factors; and, for example, it could be re-written as:

$$\alpha = \frac{\mathcal{E}}{4}\,\delta_x\, W(\sigma)\sqrt{\frac{\beta}{\varepsilon}}\sqrt{\frac{f\sigma_z\delta_B}{L}}\ ,$$

where δ_B is the beamstrahlung parameter, f the frequency and L the luminosity; now there is no overt γ dependence.

J. Mulvey, Oxford

Presumably the wakefield generated by the driving beam can also disturb succeeding bunches of the driving beam itself. Is this a serious problem?

Answer

We have always envisioned that such effects are small because you have enough separation between bunches. Therefore the repetition rate is sort of limited, say to ~ 10 kHz.

MULTI-STAGE WAKEFIELD ACCELERATORS

Bruno ZOTTER
CERN, Geneva, Switzerland.

ABSTRACT

Large field-gradients for ultra-high energy accelerators can be achieved in structures excited by intense, short particle bunches. In order to extract the energy from the driver at the fastest possible rate, it should be sent through a high-impedance aperture, just as the beam to be accelerated. It then has to be replaced periodically in short stages, which also minimizes the reduction of gradients due to blow-up or particle loss occuring in a driver interacting with the structure over a long distance.

1. INTRODUCTION

Acceleration by wakefield transformers, first proposed in 1981[1], is based on the idea that high accelerating gradients can be obtained in an aperture of a structure if it is excited by a beam passing through a different aperture which has lower impedance than the one used for acceleration. In this manner, the energy loss (per particle) in the strong "driving" beam can be kept small, while the energy gain (per particle) in a weaker accelerated beam may be larger by the impedance ratio of the two beams.

At present, it appears that the largest impedance ratios can be obtained in a concentric device : the driver passes through an annular slot with large radius and the accelerated beam along the axis of a small central hole of a disk-loaded waveguide with rotational symmetry. Impedance ratios of 10, 20 or more can be obtained in this manner. An experimental verification of this scheme is presently being prepared at DESY[2].

Unfortunately, the practical realization of such a device meets with some difficulties. The generation of very short annular rings with high charge is already not easy, but is rendered more complicated by the requirement that the rings should not rotate when they pass through the annular slot because of the supports necessary to hold the inner disks in place. Actually, these supports destroy the rotational symmetry of the device and will make slots in the driving beam which will thus become more vulnerable to transverse instabilities. This lack of rotational symmetry also makes field computations and simulation of particle motion very difficult, and only results neglecting this effect have so far been published.

Because of the very short accelerating structure ($\sim$40 cm), these considerations are only of limited impact on the experiment which is presently being assembled at DESY. However, they could become quite restrictive in a full-length structure where the beams have to be accelerated over several kilometers in order to reach TeV energies. Due to the concentric geometry, staging (i.e. accelerating in short sections) does not appear very

attractive, as it requires disposing of the spent annular driver and introducing a new one without disturbing the accelerated beam. Re-acceleration of the decelerated driver has been proposed[4], but will probably not restore the beam once it has been blown-up by instabilities.

Also the alternative of replacing the annular driver by a number cylindrical beamlets disposed symmetricaly around the slot has been discussed. Again there are problems of transverse stability of the driver, and in addition exact synchronism is required in order to avoid reducing the acceleration and to minimize transverse deflection of the accelerated beam.

Other embodiments of the wakefield transformer have ben proposed, but have in general lower impedance ratios. In particular, elliptical cavities with unequal apertures around the two focal points were already mentionned in the original proposal[1]. A single elliptic cavity (with equal apertures around the foci) has been tested recently in Japan[3]. Unfortunately, the experiment was abandonned because the beam to be accelerated was strongly deflected and did not pass the cavity.

It should be easy to overcome the deflection of the accelerated beam simply by increasing the injection energy, which was only a few tens of kilovolts in the experiment. The overall deflection could also be cancelled by disposing groups of cavities with two drivers alternating on two sides[1]. However, the impedance ratios in elliptic cavities are rather limited. The impedances can be estimated with a special 3-dimensional computer program for wakefields in elliptical cavities [4].

2. MULTI-STAGE ACCELERATORS

High accelerating gradients in a structure can be achieved also when the driving beam passes through a high-impedance aperture but is replaced periodically. Since the driver then only provides the acceleration of a single stage, it may loose its energy at a high rate. One no longer needs to rely on the gain in accelerating field due to impedance transformation, although it could be combined with it.

The elliptic cavity geometry appears particularly well suited for such a scheme : by rotating subsequent groups of cavities, the spent drivers can be easily disposed and new ones introduced in the next stages (see Fig. 1). The driver pulses may all be created as a single pulse train, which have to be split, e.g. by a time-dependent deflection, into single bunches which are steered to the various accelerating stages. By proper timing one can obtain correct synchronism and even overcome any "slippage" problem between driver and accelerated beam if one of them is not fully relativistic.

Because of this possibility, one may also use proton beams as drivers for the acceleration of electrons. In this it resembles the "proton klystron"[5] which, however, has driver and accelerated beam in the same aperture and therefore is difficult to stage. In addition, it is limited by just this slippage problem.

For colliding beams, only much lower energy electrons are required to obtain the same experimental results, compared to protons which distribute the energy amongst their constituents. Hence, it would be sufficient to accelerate electrons to the same energy as that of the driving proton beam and still gain a large advantage. If one can increase the gradient, one obtains furthermore a shortening of the structure required to obtain this energy.

The principal limitation to achieving a high acceleration rate by particle excitation of a structure is due to breakdown and electrical discharges which may damage the metallic surfaces. However, we shall not concern ourselves with this problem here about which only little is known yet. Another difficulty is the production of very short pulses with high charge, i.e. the achievement of extremely high peak currents. Normal RF linacs may have difficulties in reaching these values, but there are a number of studies using laser-excited cathodes to obtain extremely short pulses. It may furthermore be possible to use induction linacs or storage rings to reach the peak current levels required. Other limitations are caused by the total power requirements of a full-scale accelerator which makes high efficiency desirable. Both heating by energy dissipation and total energy requirements can be controlled by reducing the repetition rate, which on the other hand should be kept high in order to obtain a large interaction rate in colliding linacs.

3. A NUMERICAL EXAMPLE

As a simple illustration, we shall use the computed values of the loss-factor in a disk-loaded waveguide to show what gradients could be achieved. The total energy loss per unit length of a Gaussian bunch of RMS-length σ can be written

$$\Delta U' = - k'(\sigma) \cdot Q^2$$

when Q is the total charge in the bunch. The energy gain per unit charge and length, also called gradient, is then simply $G = k' \cdot Q$. The loss factor per unit length for disk-loaded waveguides of various radii and periods is shown in Fig. 2. Over a reasonable range of parameter values it can be approximated by

$$k' = \frac{1}{4\pi\varepsilon_0} \frac{1}{4a^{1/2}\,\sigma^{3/2}}$$

and reaches typically values of a few hundred V/pCm for a few millimeters beam-hole radius. In order to achieve an energy gain of several hundred MeV/m, one thus needs charges of the order of micro Coulombs in a bunch length of a few millimeters RMS. For example, a structure with an inner radius a = 2 mm, an outer radius b = 20 mm, a gap length g = 5 mm and a period p = 6 mm has about k' = 450 V/pCm for σ = 2 mm. Hence a charge of 1 μC which corresponds to about 6×10^{12} particles per bunch or a peak current of nearly 60 kA, would yield a gradient of 450 MV/m.

4. CONCLUSIONS

A particle-driven wakefield accelerator not relying on the impedance-transformer principle appears possible if short stages are used with new driving pulses in each stage. This has the distinct advantages that the degradation of beam quality due to interaction of the driver with the structure is of little concern, and furthermore permits re-adjustment of the acceleration phase in each stage so that (slower) protons could be used as drivers. However, one does require quite high charges in short bunches for the driver which exceed the values which can be obtained in present RF linacs by quite a large factor. However, peak currents of the required amount have been achieved in induction linacs, and may also be obtainable in circular machines. The development of laser-pulsed cathodes, which is actively pursued in several laboratories around the world, may allow a simpler solution to this problem.

* * *

REFERENCES

1. G.-A. Voss, T. Weiland, DESY M-82-10 (1982), DESY 82-074 (1982).
2. DESY Group, Proc. 11th Accel. Conference (1983).
3. S. Takeda, these proceedings.
4. Y. Chin, KEK Report 83-19 (1983).
5. A.N. Skrinsky, The Challenge of Ultra-High Energies, Proceedings of ECFA-RAL meeting held at New College Oxford, Sept. 1982, ECFA 83/68.

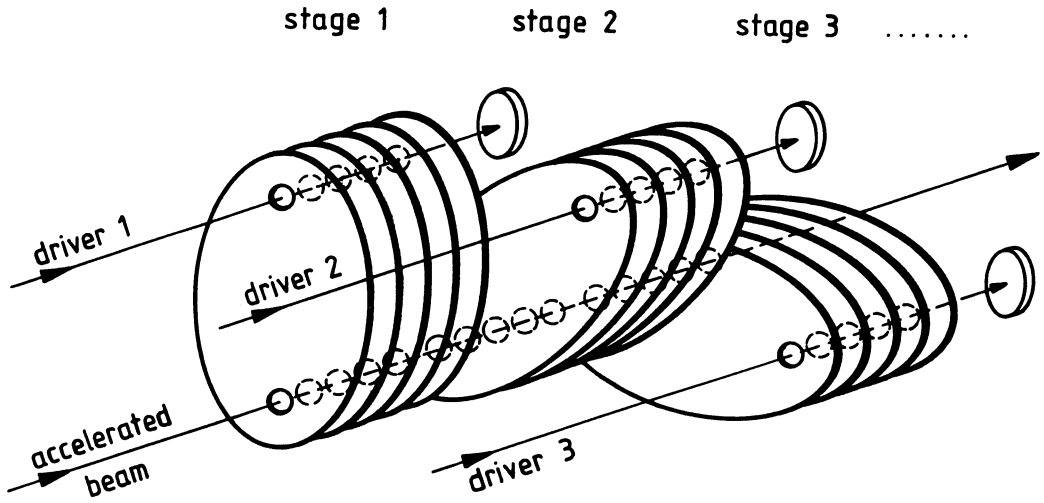

Fig. 1 Schematic geometry of staging accelerator with elliptical cavities.

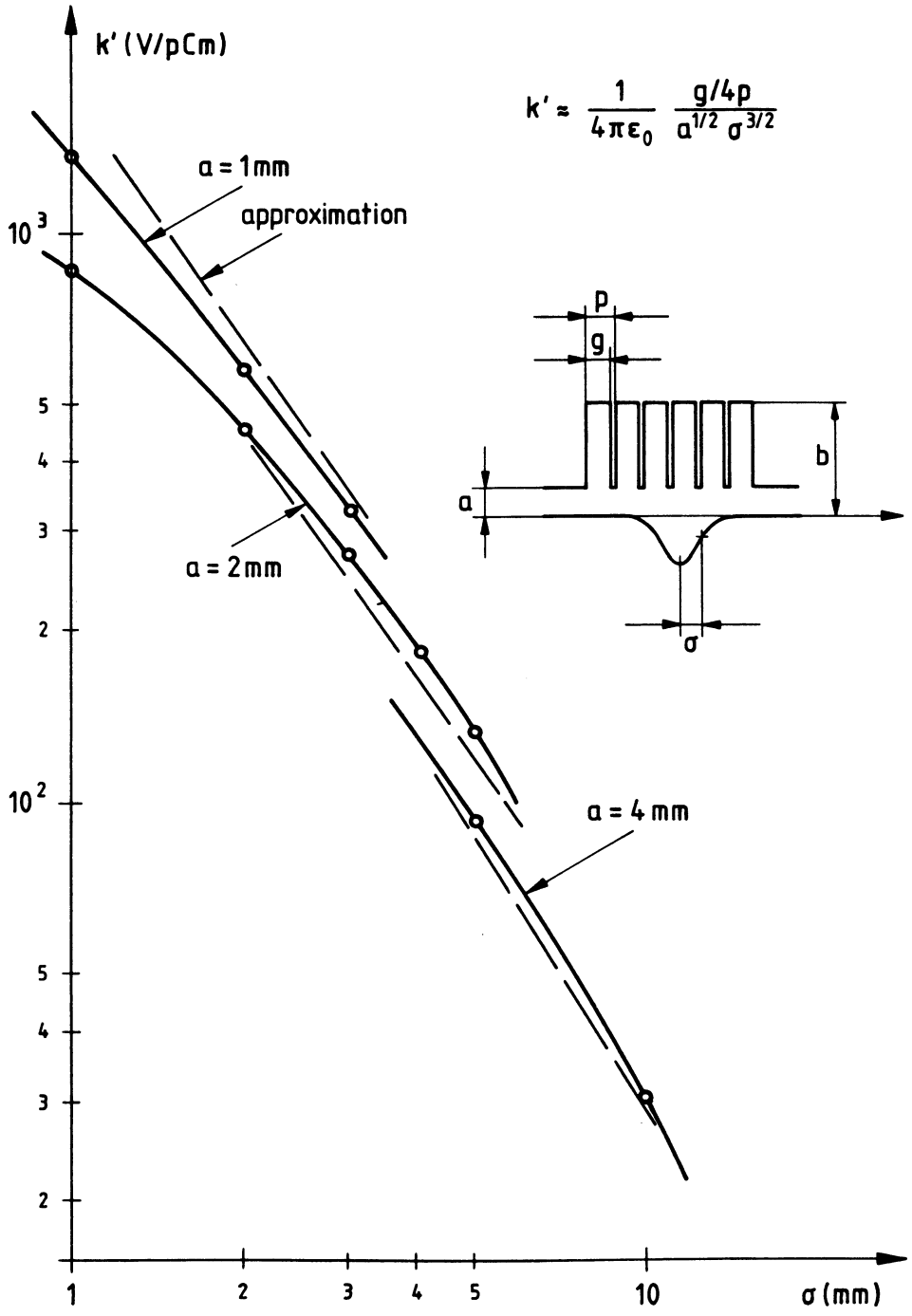

Fig. 2 Loss-factor as function of bunchlength for disk-loaded waveguide.

THE WAKEATRON: ACCELERATION OF ELECTRONS ON THE WAKE FIELD OF A PROTON BUNCH

A.G. Ruggiero

Fermilab, P.O. Box 500, Batavia, IL 60510

ABSTRACT

We expose in this note an idea of how to accelerate a low intensity electron or positron bunch, travelling through a linear rf structure, following at short distance an intense proton bunch which leaves behind a wake field. This device acts like a transformer where two beams are involved: one, made of protons, at high current and low energy, the other, made of either electrons or positrons, at low current and high energy. The two beams are coupled electromagnetically to each other by a specially designed rf structure made of a long sequence of cavities. We discuss the use of this device for the design of an electron-positron linear collider at 1 TeV energy per beam and luminosity 10^{32} cm^{-2} s^{-1}.

Introduction

It has been known for quite some time that a bunched beam in an accelerator, when crossing an rf cavity, leaves behind a wake field along the gap which oscillates at the same frequency (or frequencies) the rf cavity resonates at. This wake field in general persists long enough, especially in the case of cavities with extremely large figures of merit, to affect the motion of subsequent bunches and eventually the next turn around the same bunch that induced it. This phenomenon is called "beam loading". It is well understood and effectively present and visible in all major accelerators or storage rings.

In the case of perfectly conducting rf cavities with no dissipative media, the wake field left behind by a bunch of charged particles is made of energy that will never vanish but will simply oscillate between the inductive and capacitive components (electric and magnetic forms), trapped between the walls of the cavity. A fraction of it will eventually escape by leaking through the opening at the sides of the cavity into the neighboring sections of the vacuum chamber, but most of it will be effectively trapped. There are only two ways the energy can be dissipated so that the wake field will decay at some rate. If the walls are made of resistive material and dissipative media is introduced, currents will be induced in the metal by the wake field and dissipation will occur as consequence of the ohmic relations. Eventually the energy dissipated from its original electro-magnetic form will be all converted in thermal form with a rise in the temperature of the surroundings. This phenomena is also well understood and the figure of merit (Q) of the cavity gives a measure of the size of the effect and therefore of the

---

Editor's Note

In a paper to be published in A.I.P. Conf. Proc. for the UCLA Workshop on Laser Acceleration of Particles, Dr. A. Ruggiero gives reasons why the wakefield acceleration mechanism described here is not subject to the limitation on transformation ratio (i.e. ≤ 2) mentioned by T. Weiland.

decay of the wake field.

It is also possible though that a fraction of the wake field energy, before it has been dissipated considerably, can be recovered by a new bunch of particles following a short distance the one that has generated the wake field. If we call longitudinal the direction along the axis of the rf cavities, and we assume both bunches are travelling at relativistic speed in this direction, a longitudinal electric field must also be generated within the wake field. At the right time interval the phase of this field component will be right to apply an energy impulse to the second bunch, that is to accelerate it.

It has also been known for some time that a bunch of charged particles going across a sequence of rf cavities loses energy by diffraction radiation. An extensive work and research has been done during the sixities and early seventies.[1,2] A computer code (KN7C) has also been generated to make estimates and analysis was carried out for a variety of cavity geometries. In particular one calculated the energy loss per unit length and per particle and the longitudinal electric field extending behind the bunch of particles. It was found that both these quantities depend linearly upon the total charge of the bunch.

At the same time these calculations were done the question was raised by many people whether it is possible to accelerate other particles following the exciting bunch at some distance by reabsorbing at least a fraction of the energy lost. The idea has been around for quite sometime until Perevedentsev and Skrinsky wrote a paper[3] on the subject and called the device a "Proton Klystron". Among other things, they proposed to accelerate electons on the wake field of protons, both of them moving in the same direction through a sequence of rf structure. They proposed several configurations on the best use of a beam of protons to load the structure and their idea is still valid and we encourage the reader of this note to read their paper. Nevertheless we believe the reference to a klystron is not really appropriate. Here we give a look on a different approach on how to design a device which accelerates electrons on the wake field of proton bunches. We prefer to call this device a Wakeatron.

General Idea

Before going in too much detail let us first clear a point that must already appear obvious to the reader. Each proton in the leading bunch will lose an amount of energy per unit length that we can write

$$U = \frac{e^2}{\lambda_{Lp}^2} N_p \qquad (1)$$

where N_p is the number of protons in the bunch, e the charge either of a proton or an electron, disregarding the sign, and λ_{Lp} an effective length which describes the loss to the rf structure and which depends on the cavities geometry and on the proton bunch dimension and shape. An electron which follows at a convenient distance will gain some energy from that lost by the protons, but will lose also some for the same reason and which will be proportional to the total number N_e of electrons in the bunch. Therefore we can write for the energy gain per unit length

$$W = \frac{e^2}{\lambda_G^2} N_p - \frac{e^2}{\lambda_{Le}^2} N_e \qquad (2)$$

Here λ_G is an effective length which describes the energy gain and depends on the geometry of the structure, on the proton bunch dimensions and shape and on the distance of the electrons from the proton bunch. The two lengths λ_{Lp} and λ_{Le} are equivalent and the same, except that the dependence on the proton bunch dimensions and shape is replaced by the dependence on the electron bunch dimensions and shape. It is seen that in order to have an effective (positive) energy gain for the electrons there is a limit on the number N_e of electrons that can be accelerated, that is

$$N_e < \frac{\lambda^2_{Le}}{\lambda^2_G} N_p - \frac{W_o}{e^2/\lambda^2_{Le}} \qquad (3)$$

where W_o is the required energy gain.

In the following we will give some very approximate expressions for λ_G and λ_L. They are very crucial for the design of the Wakeatron and to estimate its performance and efficiency. Clearly a lot of work is in progress and more will be done in the future for their estimate and optimization.

An inspection of both (1) and (2) clearly shows the Wakeatron as a transformer rather than an amplifier (as in the case of a Klystron). Some kind of energy is released to a medium and transformed to another kind, the transformation ratio not possibly exceeding unity. Nevertheless the two lengths λ_G and λ_L have different physical meanings and in principle, with the proper configuration of both bunches and with a

proper choice of the cavity geometry, it is possible to accelerate electrons at a rate higher than the rate at which protons lose their energy. Of course not only (3) has to be satisfied but also the conservation of energy: the total power absorbed by the electron bunch cannot be possibly larger than the total power lost by the protons. We can then introduce a transformation efficiency as the ratio of the total energy gained by the electron bunch to the total energy lost by the proton bunch

$$\alpha = \frac{N_e}{N_p} \frac{\lambda_{Lp}^2}{\lambda_G^2} \qquad (4)$$

At the very best $\alpha = 1$, which, among other things, assumes perfectly conducting material with no thermal losses. Therefore we like to emphasize again that the careful estimate of λ_G and λ_L, which is not really the scope of this note, is essential.

Outline of the Device

The Wakeatron which we describe next is intended as a linear collider for electron and positrons beams each with energy of 1 TeV and luminosity of $10^{32}cm^{-2}s^{-1}$. We believe, as we shall also argue next, that aiming for this performance is reasonable and that it should not really be too difficult to attain. A higher performance is though questionable, but larger energies are certainly possible, the main limitation probably being the amount of real estate one is willing to invest in.

A possible lay-out of the Wakeatron is given in Fig. 1. It is made of two parts identical to each other but arranged symmetrically to each other around the crossing point where the two beams collide. One part is to accelerate electrons and the other positrons. Each part is made of a proton source which generates tight bunches in a conventional way. There is an electron beam source at one side and a positron beam source at the other. The acceleration of electrons and positrons takes place in the two sections of the Wakeatron itself which are identical to each other of the same rf structure. The mode of operation we conceive is that one proton bunch is extracted from each side injected in their respective section of rf structure immediately followed by either an electron or a positron bunch. This will occur at some repetition rate to which all the sources are to be adjusted.

The Proton Source

Each proton source is made of a linac, a booster ring, an accelerator ring and a shuttle ring. The parameters for the components are given in Table I. The accelerator ring has a cycle of one ramp per second and will deliver 4000 proton bunches to the shuttle ring where they will be stored for a period of one second during which they will be extracted one by one until the shuttle ring is empty and ready to receive a new load of 4000 bunches from the accelerator ring. This mode of operation will provide a constant rate of f = 4000 encounters/second. The separation of bunches in the ring though will be 5 nsec and this obviously is of some concern for the design of an extraction kicker. The proton sources have to deliver for obvious reasons very intense and short bunches. We believe that 10^{11} protons per bunch should be possible with an rms bunch length σ_p = 1 cm. For comparison the CERN-SPS has obtained 1.3×10^{11} protons in a bunch with σ_p < 10 cm. The short bunch length can be achieved by raising the transition energy and choosing large accelerating rf frequency and voltage. The proton beam energy has been set to 100 GeV according to the following criterion. As we shall see a luminosity figure of 10^{32} cm^{-2} s^{-1} will require a power of about 1 MW in either electron or positron beam with a repetition rate of f = 4000 s^{-1}; for efficiency consideration the proton beam power ought to be much larger than this and we have chosen 10 MW which yields the energy we have selected for the protons as shown also in Table I. From this point of view, the minimum proton beam energy is 10 GeV, unless one is willing to increase the number of particles per bunch well beyond what we believe is practical. On the other hand it is obvious that larger energies are even more desirable because not only more power would be made available, but also the bunch dimensions can be furtherly reduced. We believe that the energy of 100 GeV represents a good compromise when one also considers cost, magnets and required repetition rate. The parameter list given in Table I is intended as an example. The design of the whole proton source clearly awaits a more detailed study which will make some of these parameters change in order to meet the beam specifications. In particular we believe that an individual bunch area of 0.5 eV-s is large enough for the beam to be stable against microwave coherent excitation, assuming a coupling impedance $|Z/n|$ ~1 ohm. Also the rms emittance, the same in both planes, $\varepsilon = \sigma^2/\beta_L = (10^{-6})/\gamma$ is consistent with the assumptions for other projects of the moment (SSC, LHC).

The Source for Electrons and Positrons

The electrons and positrons sources are each made of a linac and a damping ring. To generate positrons a target is inserted between the two devices. Parameters are given in Table II, and are intended as just an example. A more careful analysis is required to optimize the design of the two sources. Anyway, in principle, the linac will generate bunches at the rate f = 4000 per second. To produce positrons efficiently an energy of 1.0 GeV should be more than adequate and the linac could be made operating in the S-band mode like SLAC which would give an overall length of about 100 m at a gradient of 10 MV/m.

The electron/positron bunches are then transferred into the damping ring where they are kept circulating for a while. The main function of the damping ring is to hold the beam until it is "cooled" effectively by synchrotron radiation. We propose that there are 100 bunches at any one time circulating in the ring; since bunches are to be extracted at the rate of f = 4000 per second, the time each bunch will spend in the ring is 100/f = 25 msec. For the radiation effects to take over effectively we require the typical radiation damping time corresponds to a fraction of the circulating time, for example 1/3 which is 8 msec. The parameters given in Table III would yield roughly an equilibrium rms emittance $\varepsilon = \sigma^2/\beta_L = (10^{-6}\text{m})/\gamma$ similar to the proton beam. For the electron/positron bunch length we have taken an rms value σ_e = 1mm smaller than the length of the proton bunches. The design of these sources should be rather straight-foward and conventional.

The Wakeatron

Fig. 2 shows the geometry of the rf structure that makes the two sections of the Wakeatron. It is made of a sequence of a very large number of identical cells with cylindrical geometry. Both beams go through a central circular opening of diameter 2a. The outer radius is b and assumed to be much larger than the gap width g. The walls of the cavities are taken to be perfectly conducting with no thermal losses and their thickness negligible compared to the gap width. The interior of the cavities is filled with good vacuum.

A bunch of N particles each with electric charge e, rms longitudinal length σ_l and practically no transverse dimensions loses an amount of energy when traversing the rf energy, that is given by eq. (1) when expressed per unit length and per particle. It has

been estimated by several people[1] that the effective length is

$$\lambda_L = \sqrt{2}\, a \exp(\sigma^2_1/2g^2) \qquad (5)$$

where we have also introduced an exponential factor to take into account the longitudinal extension of the bunch. Similarly it is also possible to estimate the amplitude of the wake field.[2] It is speculated that the energy gain for a particle following the primary bunch has a form given by (2), with the effective length λ_G given by

$$\lambda_G = \frac{a}{\varepsilon} \exp\,(\sigma^2_1/4g^2) \qquad (6)$$

In both (5) and (6) σ_1 is the rms length of the bunch inducing the wake field. They are expected to be valid in the limit $b \to \infty$, that is for the case each cavity is made of two infinite parallel planes. In eq. (6), ε is a form factor which depends on the cavity geometry, the distribution of the primary bunch and on the distance between this and a following particle to be accelerated. It is expected $\varepsilon < 1$, but this factor still requires a better analysis and it is certainly one of the major parameters for investigation. In particular it is possible that ε depends somewhat on the gap width g and on the opening radius a, also in the limit $b \to \infty$. For the time being we will consider this constant as such and independent of all other parameters; a point that waits crucially for verification.

Inspection of both (5) and (6) already shows some results:

(i) Since one requires λ_G and λ_L small, it is seen that a small opening is more effective. In principle this requires the smallest beam dimensions. The emittance for both beams are given in Tables I and II and vertical as well as horizontal focussing has to be provided along the Wakeatron, eventually with external means. Obviously the proton beam has the largest transverse dimension; one can achieve an rms cross-section $\sigma = 0.3$ mm if the maximum value of the amplitude lattice function $\beta_{max} = 10$ m, which is not impossible. The electron/positron bunch transverse dimensions are expected to be smaller. Of course extreme care must be taken so that all the beams involved are kept stable against coherent excitation from beam loading and transverse modes, and that their eventual emittance growth can be effectively controlled to the desired value. To

allow enough room for the proton beam we propose here a = 1 mm. It is possible for instance to make the rf cavities as a stack of a large number of conducting, parallel plates and let the proton beam itself drill a hole through the structure.

(ii) A very weak dependence on the energy is expected for both λ_L and λ_G as long as the two beams are travelling at relativistic velocities.

(iii) It seems that the gap width g enters only in the exponential factor where it is compared to the rms bunch length σ_1. One requires $\sigma_1 < g$ in which case both the energy loss and the energy gain per unit length and per particle do not seem to depend on the gap width g, at least as long b >> g. This is a point that requires verification and intensive study and it could be connected to the definition of the form factor ε.

(iv) It may seem that the exponential factors introduced in eqs. (5) and (6) are ad hoc. Actually they can be explicity derived.[1,2] Observe the different dependence on the exponent in the two equations; the dependence on σ_1 is weaker for the energy gain. This can be easily explained by recalling that the energy loss is an integral over the cavity volume of the square of the electric field, whereas the energy gain is the electric field itself.

With (5) and (6), the transformation coefficient (4) becomes

$$\alpha = 2\varepsilon^2 \frac{N_e}{N_p} \exp\left(\sigma^2{}_1/2g^2\right) \qquad (7)$$

As we have said at the most $\alpha = 1$; in reality a fraction of the energy left behind by the proton bunch will be dissipated in other ways. We assume here $\alpha = 0.4$; an assumption that ought to be confirmed. Since, as we shall see later $N_e = 3\times10^9$ particles per bunch are required for a luminosity of $10^{32}\text{cm}^{-2}\text{s}^{-1}$ at 1 TeV we need

$$\varepsilon^2 \exp\left(\sigma_1{}^2/2g^2\right) = 6.7 \qquad (8)$$

The rf cavities ought to be designed with a gap g so that (8) is fulfilled. This remains to be proven. For the moment we can guess and propose

$$g = 1 \text{ cm}$$

$$\varepsilon = 2.0$$

and then it is proper to take for instance b = 20 cm. The thickness of the material can be taken to be 1 mm or less. All the other parameters can be esily derived and they are listed in Table III. In particular the energy gain expected is 350 MeV/m which corresponds to a length of almost 3 Km to achieve an energy 1 TeV. The protons would lose about 26.5 MeV/m, that is a final energy of about 25 GeV at the end of the Wakeatron.

A problem at this point arises. It is necessary that the two beams have as equal velocities as possible so that the distance between the two bunches does not change more than a fraction of the electron bunch length over the length of the accelerating structure. If this is 3 Km, synchronism between the two beams is completely lost. A simple argument is the following: in the case $\gamma_e >> \gamma_p$ and both are constant, the relative difference for the lengths travelled is

$$\frac{\Delta L}{L} \sim \frac{1}{2\gamma_p^2}$$

Even if we take $\gamma_p = 100$ and L = 3000 m we obtain $\Delta L = 15$ cm, which is too large. To cope with this problem the scheme outlined in Fig. 1 should be changed; a possibility being to divide the Wakeatron into several short stages next to each other. Each stage should have a length short enough to preserve synchronism between the two beams. Synchronism is then restored from one stage to another with either multiple bunch operation,[3] or by adjusting the path length of the two beams.

Another problem also of very serious concern is to keep both beams moving right on the axis of the rf structure. Doing so one avoids excitation of transverse modes and the possible instabilities that these can cause. It is certainly crucial to preserve the normalized emittance generated by the electron/positron damping rings. We assume that this is possible.

The performance of the linear collider is described in Table IV. With the present scheme where the energy of the protons is 100 GeV it is not possible to raise the energy of the electrons or positrons beyond 1 TeV. To do this larger proton energy is required. For instance to generate a 10 TeV e± beam it seems that a 1 TeV proton beam is required.

To preserve the repetition rate of 4000 pulses per second the proton source dimensions have also to increase correspondingly ($R \sim 10$ km). If one can do this then also the luminosity will increase if one assumes that the chosen normalized emittance is truly invariant. For instance a linear collider of 10 TeV x 10 TeV could generate a luminosity of $10^{33} cm^{-2} s^{-1}$.

Efficiency and Cost Considerations

We expect the following requirements for the power needed to operate the collider.

Each Proton Source:	
Beam Power	10 MW
Magnet Power	10 MW
RF Power	10 MW
TOTAL	30 MW
Each Electron Source:	
Linac	3 MW
Damping Ring	3 MW
TOTAL	6 MW

Few MW will be also required for focussing and transport along the Wakeatron. Therefore we estimate a total of 2x40 = 80 MW to operate the entire device with the exclusion of the detector. The electron or positron beam we have described above is equivalent to a power of 2 MW (for each beam) and the efficiency can be estimated as the ratio (2x2 MW)/80 W = 1/20, which is not a bad figure at all.

One can make also a very rough estimate for the cost of the entire device (again, excluding the detector, in the following way):

Each Proton Source	200 M$
Each Electron Source	25 M$
Each Section of RF Structure	100 M$
Transport, Transfer and Focussing for Each Side	25 M$
TOTAL	350 M$
	x 2
TOTAL PROJECT	700 M$

free of any contingency and escalation.

References

1. E. Keil, Proc. Intern. Conf. High Energy Accelerators, II (Yerewan, 1969), p. 551. Also Nuclear Instr. and Methods 100 (1972), p. 419.

2. A.G. Ruggiero, Fermilab Notes FN-219, FN-220, and FN-230. Fermilab 1970-1971.

3. E.A. Perevedenstev and A.N. Skrinsky. Proc. of the 6th All-Union Conference on Charged Particles Accelerators (Dubna, 1978), Dubna, 1979, v. 2, p. 272. Also: Proceed. of the 12th Int. Conf. on High-Energy Accelerator. Fermilab, Aug. 11-16, 1983, p. 508.

Table I Parameters for the Proton Source

Components:	Energy	Radius
Linac	1 GeV	-
Booster	1-10 GeV	100 m
Accelerator Ring	10-100 GeV	1000 m
Shuttle Ring	100 GeV	1000 m
Cycle Rate:		
Booster	30 Hz	
Accelerator Ring	1 Hz	
RF	Frequency	Voltage
Booster	175-200 MHz	2 MV
Accelerator Ring	200 MHz	7 MV
Shuttle Ring	200 MHz	10 MV
Beam Parameters in the Shuttle Ring:		
No. of bunches (= rf harmonic no.)		4000
Bunch-to-bunch separation		5 nsec
Rms bunch length		1 cm
Long. phase space area (95% of beam)		0.5 eV-sec
No. of protons/bunch		10^{11}
Normalized emittance (H and V) σ^2/β_L (rms)		10^{-6} m

Table II Electron Positron Beam Sources

Linac:	
Output Energy	1 GeV
RF	3 GHz
Damping Ring:	
Energy	1 GeV
Average Radius	10 m
Packing Factor	50%
Dipole Field	8 kg
Betatron tune, $\nu_{H,V}$	~15
No. of bunches circulating	100
No. of particles/bunch	3×10^{9}
Radiation damping time	8 msec
σ^2/β_L (H and V, assuming full coupling)	$10^{-6}m/\gamma_e$
Rms bunch length	1 mm
Time internal between individual bunch extraction	25 msec
Energy Loss	20 KeV/turn
RF:	
Frequency	500 MHz
Voltage	100 kV

Table III The Wakeatron RF Structure

Cavities:	
Gap width, g	1 cm
Iris radius, a	1 mm
Outer radius, b	20 cm
Wall thickness (copper)	<1 mm
Effective loss length, λ_{Lp}	2.33 m
Effective gain length, λ_G	0.642 mm
Transformation coefficient, α	0.4
Form factor, ϵ	2.0
Energy Loss per proton	26.5 MeV/m
Energy Gain per electron/positron	350 MeV/m
Energy Loss per electron/positron	1.3 MeV/m
Total length of the rf-structure	2x3 km

Table IV Collider Performance

Luminosity	$10^{32} cm^{-2} s^{-1}$
Repetition rate, f	4 KHz
No. of particles/bunch, N	$3x10^9$
$\beta_{H,V}^*$	5 mm
Rms β-emittance, σ^2/β_L	
H and V, assuming full coupling	$10^{-6} m/\gamma_e$
Energy per beam	1 TeV
Rms beam spot, $\sigma_{H,V}^*$	500 A°
Rms bunch length, σ_e	1 mm
Disruption parameter, D	1
Energy spread due to Beamstrahlung	3%
Power in each beam	2 MW

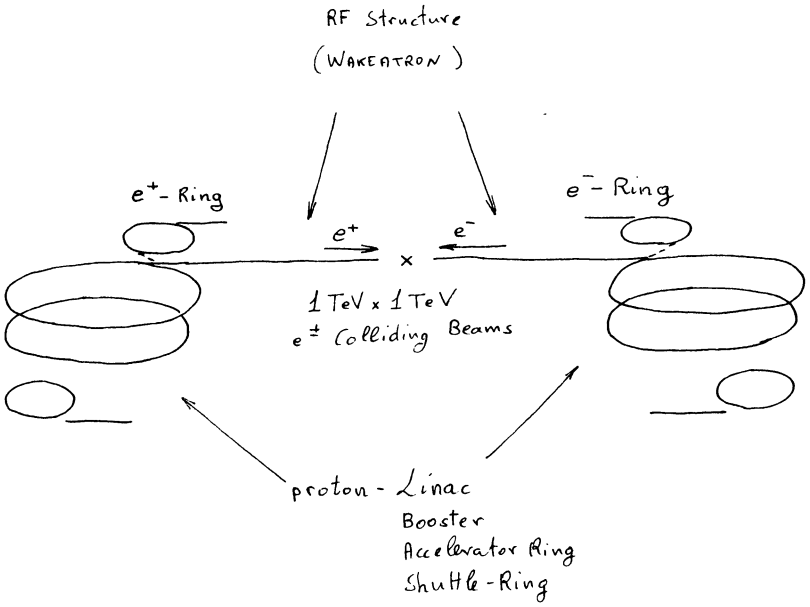

FIG. 1 LAY-OUT OF AN ELECTRON-POSITRON LINEAR COLLIDER WHICH MAKES USE OF THE IDEA OF ACCELERATING ELECTRONS AND POSITRONS ON THE WAKE FIELD OF INTENSE PROTON BUNCHES.

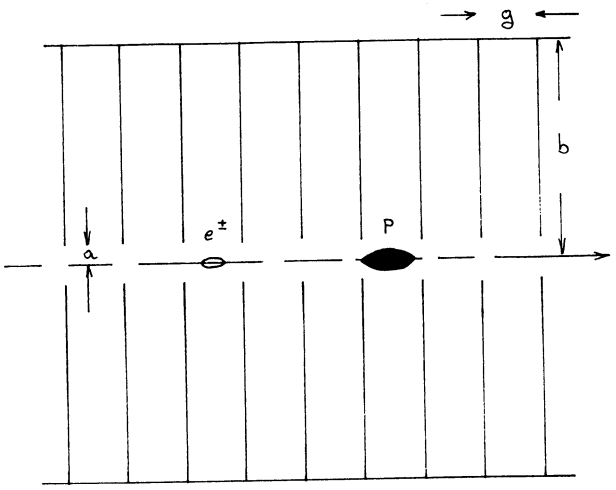

FIG. 2 CONCEPTUAL DESIGN OF AN RF STRUCTURE TO ACCELERATE ELECTRONS OR POSITRONS ON THE WAKE FIELD OF AN INTENSE PROTON BUNCH (PROTON KLYSTRON, WAKEATRON).

THE BNL*)-NRCC**)-AECL***) LASER GRATING ACCELERATOR EXPERIMENT

L.W. Funk
Accelerator Physics Branch, Atomic Energy of Canada Limited, Research Company, Chalk River Nuclear Laboratories, Chalk River, Ontario, Canada

ABSTRACT

A collaboration has been set up to take advantage of the unique capabilities of a laser developed by NRCC to explore the feasibility of acceleration of particles in the electric fields established over the surface of a grating by a laser beam. This report will review the history of the collaboration, discuss the characteristics of the equipment which is available to conduct the experiment, and present a timetable for experimental activities.

INTRODUCTION

In the course of his early investigations into the use of lasers for particle acceleration[1,2], Palmer identified the need for a high-energy picosecond laser. At the time, no such laser existed, but in 1983, Corkum reported[3] on a technique to generate and amplify picosecond laser pulses at 10.6 μm. The laser is rather complex and immobile, and it became clear, during a visit to the NRCC laboratory by Palmer in the spring of 1984, that any experiment which sought to make use of this unique facility would have to be located in close proximity to the laser. A relatively small, portable electron linac would therefore be required as an injector to a grating accelerator.

A suitable linac was available, manufactured in Ottawa by Atomic Energy Canada Radiochemical Company. Further inquiries with AECL Research Company's Chalk River Nuclear Laboratories interested members of the Physics Division in the proposed experiment, and contributed a second possible injector linac and a sophisticated detector to the rapidly maturing collaboration. All elements necesary for a successful experiment seemed to be present, and the first formal meeting of the collaboration was held in Ottawa on September 6-7, just prior to this workshop. The principal investigators are, from BNL: R.B. Palmer and J. Claus; from NRCC: P.B. Corkum and N.K. Sherman; and from AECL: J.W. Knowles and L.W. Funk.

---

*) Brookhaven National Laboratory, Upton, New York
**) National Research Council of Canada, Ottawa, Ontario
***) Atomic Energy of Canada Limited, Ottawa and Chalk River, Ontario

OBJECTIVES

The objectives of this experiment, shown in schematic outline in Fig. 1 are as follows:

(1) determine the intensity threshold for damage to a copper grating with picosecond 10.6 μm pulses,

(2) demonstrate electron acceleration while keeping the laser intensity below the damage threshold,

(3) study the performance of the grating accelerator as a function of various laser and injector parameters,

(4) increase the optical intensity to, and beyond, the damage threshold,

(5) examine plasma physics issues relating to formation and development of a plasma grating, and

(6) accelerate electrons over a plasma grating to determine the maximum achievable accelerating gradient.

The objectives are listed in order of increasing difficulty, and naturally the later objectives may be modified by experience from the earlier ones.

LASER

The laser is shown schematically in Fig. 2, taken from Ref. 3. The picosecond pulse is switched out of a 100 ns pulse from a hybrid CO_2 oscillator using fast semiconductor switches energised by a picosecond pulse from a synchronously mode-locked dye laser. The 10.6 μm picosecond pulse is then regeneratively amplified in a high pressure TE CO_2 laser. The pulse length is continuously variable from 2 to 60 ps, and an output pulse energy of 10 mJ has been achieved. An additional high pressure CO_2 gain module has been ordered which is expected to increase the pulse energy to 100 mJ. The amplified short pulse can be focused down to a diffraction limited spot.

This laser is capable of generating accelerating gradients of 300 MeV/m over a grating area of 0.2 cm^2, even if there is no gain from resonant interaction of the laser beam and the surface, while remaining below the threshold for surface damage. The pulse repetition frequency is 0.5 s^{-1}, limited by thermal dissipation in the final amplifier.

INJECTOR

Two different linacs are being considered as possible injectors for the experiment. The first of these is a 10 MeV standing-wave electron linac built by Atomic Energy Canada Radiochemical Company, who are in the business of providing products for the radiotherapy market. This linac is identical to that used in the THERAC-25 [4], a 25 MV x-ray, 5-25 MeV electron beam cancer therapy unit, but operated in a different mode and at higher currents, since only 10 MeV is required. It has the advantage that it can be obtained as a complete package, with rf system, cooling and controls.

The second choice is a 6 MeV standing-wave electron linac designed and built by CRNL[5]. This is a slightly more compact unit, but it has the disadvantage that more work would be necessary to assemble the auxiliary packages, although it would still be possible to plug the smaller linac into the 10 MeV unit package. In addition the higher energy unit promises to allow a slightly longer acceleration distance before the electrons fall out of synchronism with the accelerating fields.

Both linacs operate at an rf frequency of 3 GHz, and are driven by 2.5 MW magnetrons with a nominal pulse length of 5 μs and a pulse repetition frequency of up to 300 s^{-1}. The operating pulse repetition frequency for the experiment will be 1 s^{-1}, to match the laser capability. With their standard thermionic diode guns, both linacs have unnormalised transverse output emittances of about 0.1 π cm•mrad.

There exists a possibility that a high-current ($\approx$ 5 A), short pulse ($\approx$ 3 ns) thermionic triode gun of the SLAC design[6] could be incorporated in either accelerator, which would improve the transverse matching by reducing the output emittance from the figure quoted above, and enormously improve the signal-to-noise ratio by increasing the fraction of electrons injected which are illuminated by the laser beam.

In spite of such efforts at improving the transverse and longitudinal match between the injector linac and the grating, the grating acceptance is likely to be so small that nearly all the injected electrons will collide with the grating, or cross the grating before or after the accelerating laser pulse arrives, or suffer deflection or deceleration, rather than acceleration. These considerations impose severe constraints on the resolution and noise rejection of the detector.

DETECTOR

The detector which is being made available for this experiment is a bremsstrahlung monochromator[7], designed and built by a CRNL-University of Toronto-University of Illinois collaboration. It is based on the original University of Illinois design and has been used with the Illinois cw microtron for (γ,γ) and (γ,f) measurements. It consists of a dispersive 90° bending magnet (see Fig. 3 from Ref. 7) followed by an analysing magnet operated in the energy loss mode for tagged photon studies. For the laser grating accelerator experiment, the grating will be substituted for the radiator in the figure and the analyser will be operated in the energy gain mode. The limit of energy resolution is 14 keV for 3.5 MeV electrons[7] and is not expected to be much more than 30 keV at 10 MeV. Experiments on the cw microtron are coming to a halt in preparation for a major facility upgrade, and the detector could be made available early in 1985.

TIMETABLE

The installation and commissioning of the new laser amplifier module is expected to be completed late this year. The linac and detector are expected to be available in January 1985. We expect that installing, commissioning and linking of all these systems should be complete by April 1985, at which point the experimental program could begin. We have allocated a period of six months for the first series of experiments, after which time progress would be assessed, and plans for further work reviewed.

* * *

REFERENCES

1) R.B. Palmer, "A Laser-Driven Grating Linac", Particle Accelerators 11, 81 (1980).

2) R.B. Palmer, Laser Acceleration of Particles, Ed., P.J. Channell, AIP Conference Series 91 (1982).

3) P.B. Corkum, "High-power, Subpicosecond 10-μm Pulse Generaton", Optics Letters 8, 514 (1983).

4) T. Taylor, G. Van Dyk, L.W. Funk, R.M. Hutcheon and S.O. Schriber, "THERAC-25: A New Medical Accelerator Concept", IEEE Trans. Nucl. Sci., NS-30, 1768 (1983).

5) R.M. Hutcheon, L.W. Funk, B.A. Gillies, S.B. Hodge, P.J. Metivier and S.O. Schriber, "A Compact 6 MeV Pulsed Electron Accelerator", IEEE Trans. Nucl. Sci., NS-30, 1418 (1983).

6) R.F. Koontz, "CID Thermionic Gun System", Proceedings 1981 Linear Accelerator Conference, Eds. R.A. Jameson and L.S. Taylor, LA-9234C (1982).

7) J.W. Knowles et al., "A High-Resolution Bremsstrahlung Monochromator for Photo-Nuclear Experiments", NIM 193, 463-483 (1982).

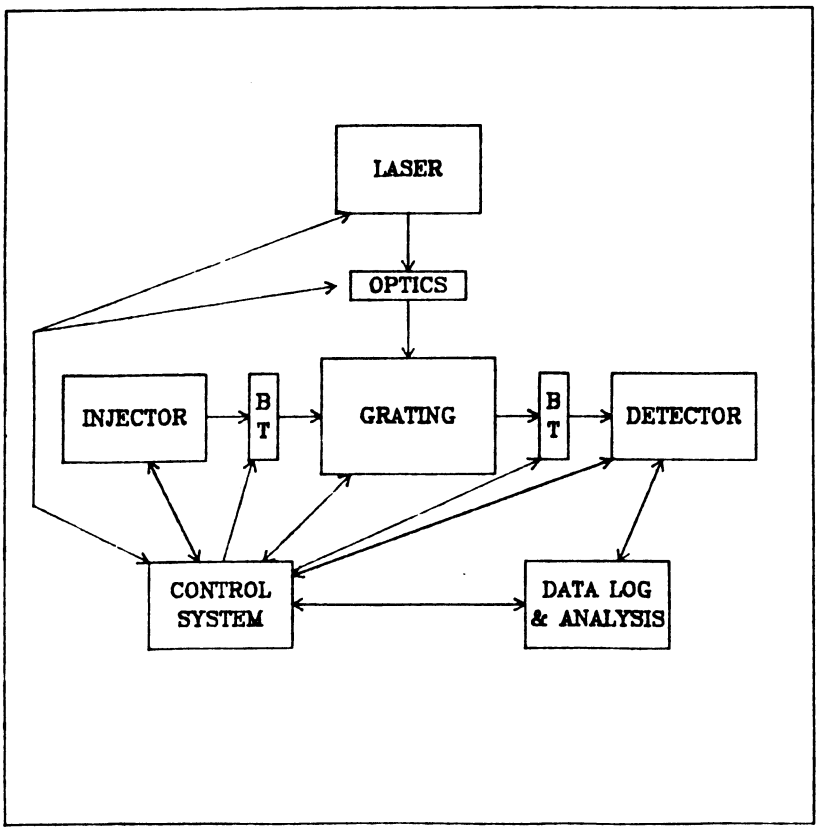

Fig. 1 : Experiment schematic

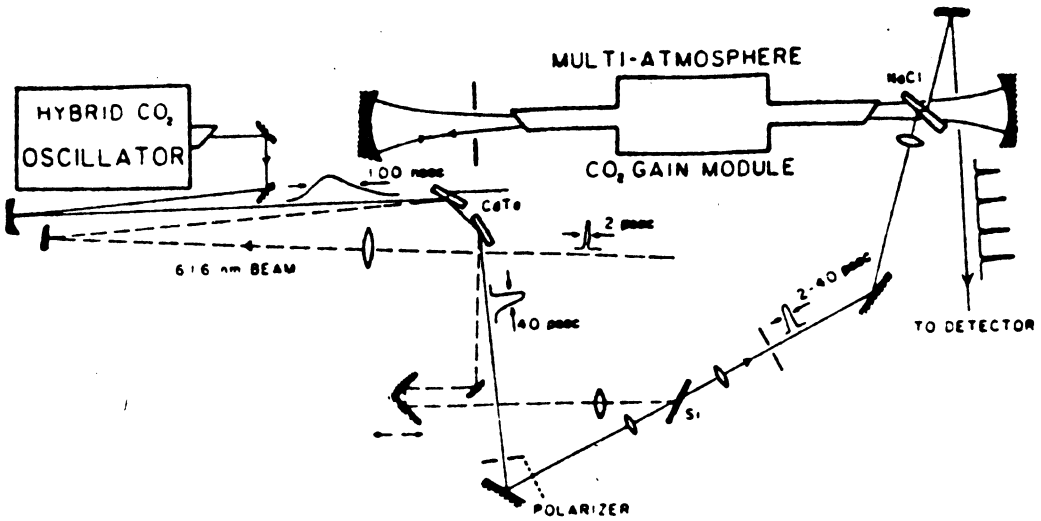

Fig. 2 : Schematic of the laser configuration

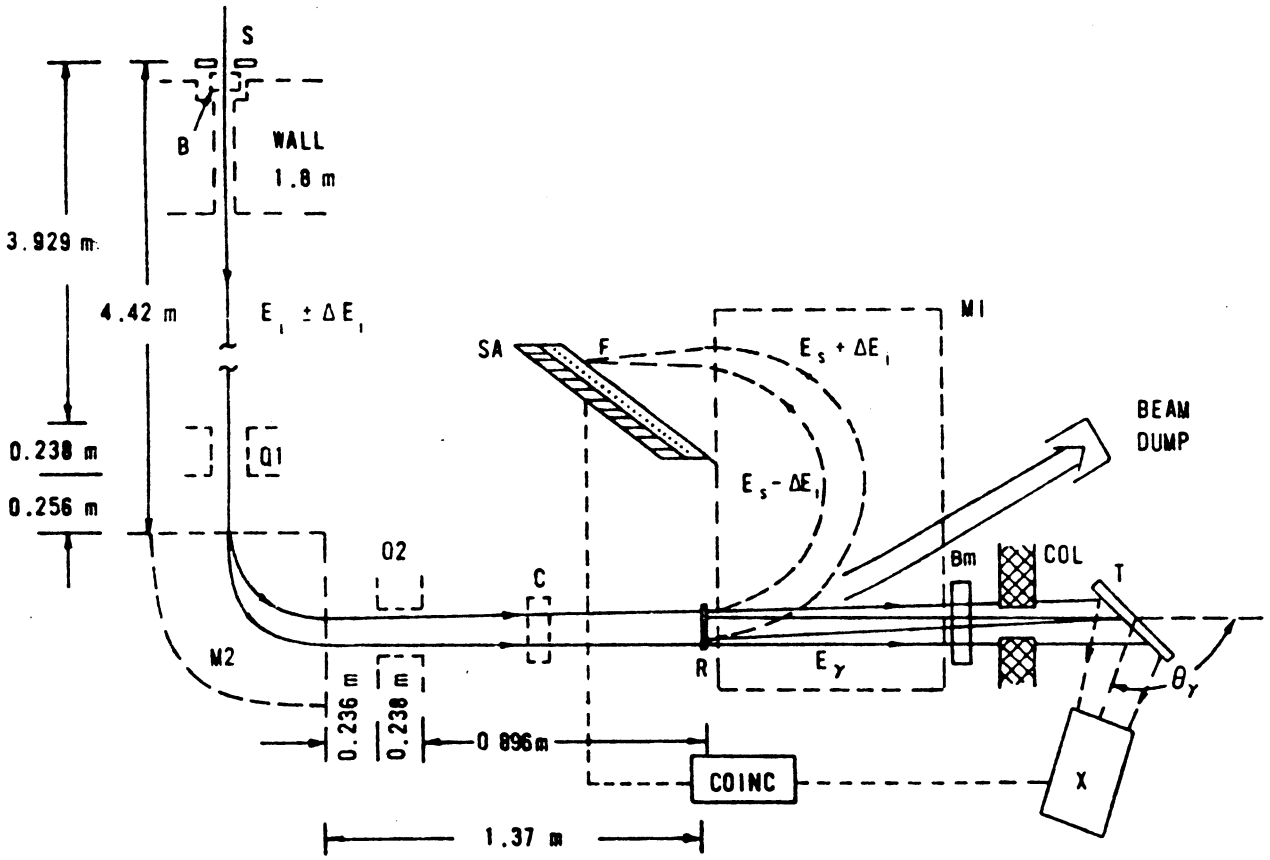

Fig. 3 : Schematic of the photon monochromator, as used for tagged photon experiments, showing reference slit S behind a shielding wall; a beam transport consisting of quadrupoles Q1, Q2, 90° magnet M2 and steering coils B and C. Electrons of energies $E_i \pm \Delta E_i$ are incident on a converter foil R. The bremsstrahlung from R proceeds through a lead collimator COL and a photon flux monitor B_m and is incident on a target T. Radiation emitted by T is detected in a NaI (Tl) counter X shown at $\theta_\gamma \approx 135°$ to the incident beam. Scattered electrons of energies $E_s \pm \Delta E_i$ are focused by magnet M1 at F onto the detector, a multi-wire proportional chamber in front of an array of scintillators (SA). In this experiment, the conventer foil R would be replaced by the grating and the flux monitor, collimator, target NaI(Tℓ) counter and coincidence detector would be removed.

LASER PLASMA LINAC*

R.B. Palmer, N. Baggett, J. Claus, R. Fernow, A. Ghosh, S. Giordano, V. Radeka, I. Stumer, P. Takacs, J. Warren

Brookhaven National Laboratory, Upton, New York 11973

ABSTRACT

The grating accelerator concept is reviewed. The use of a double row of conducting droplets instead of a conventional grating constrains the fields to a narrow band. The use of droplets also allows fields that will destroy the structure. RF modelling results are presented together with a simple theory of the fields. Coupling to incoming radiation is described. A possible laser specification is also given.

1. Introduction

The concept we describe is essentially that of a conventional linear accelerator (LINAC), but with a laser instead of a klystron as the RF power source. The most suitable laser would use CO_2 because of its high energy efficiency (10%) and relatively long wavelength (10 microns). Even 10 microns is very small compared to the wavelength used in conventional linacs (10 cm) and as a result the structure used to couple the radiation to the particles must be small, and of necessity much simpler, than that of a linac. If the available power of CO_2 lasers is employed it should be possible to attain accelerating gradients as high as 10 GeV/m (as high as in a plasma beat wave accelerator). In this case the structure surfaces will become layers of plasma. This will still be an accelerating structure since the plasma layer will be conducting, but it does mean that the entire structure will be destroyed after each pulse. A "disposable" grating is required.

Before describing this "disposable" grating, we will introduce the subject by a brief digression on the history of "grating" accelerators, since they were the historical source of the idea.

2. The Grating Accelerator

Any linac structure must convert incoming radiation into slow modes, since only a slow mode contains longitudinal electric fields and can couple energy to a relativistic particle. In order to do this the structure must, if not containing a dielectric, be periodic. The simplest such periodic structure is a grating. It had been demonstrated in 1953 that when particles travel over the surface of a grating, light is emitted (Smith Purcell, Ref. 1). It seemed reasonable, therefore, that in 1968 Takeda and Matsui should propose what they believed to be the inverse of this effect as an accelerator (Ref. 2). Unfortunately, however, Lawson in 1975 proved that the proposed geometry would not work for relativistic particles (Ref. 3). It was not until 1980 that Palmer (Ref. 4) showed that it was only for the particular geometry of Takeda and Matsui that Lawson's theorem applied and that for skew or otherwise more three dimensional geometries acceleration could indeed be obtained. It was shown further that the grating, if given one half lambda periodicity, could act as a true "cavity". That is, it had accelerating modes that were restricted to the surface and did not radiate energy away from that surface (Fig. 1a). These surface fields are composed of four slow "evanescent" waves crossing the grating surface diagonally (Fig. 1b). The resulting interference pattern provides fields periodic not only along the beam direction but also across it. Acceleration thus occurs within a sequence of channels across the grating. M. Tigner and M. Pickup have experimentally studied this structure using 3 cm radiofrequency fields (Ref. 5). In order to excite these surface fields with incoming radiation some modification to the half lambda periodicity is introduced (Fig. 2). The incoming radiation is then brought onto the grating as two interfering plane waves coming down from either side of the vertical.

Two difficulties remain with this grating accelerator. Firstly, as was pointed out by Tigner and Lawson (Ref. 6), the field must inevitably extend over the entire grating surface. Walls or some other agency are needed if the accelerating fields are to be confined to a narrow strip. The second problem is to invent a way of generating a

*Work performed under the auspices of the U.S. Department of Energy.

disposable grating. Both of these challenges seem to have been solved in the following proposal.

3. The Droplet Structure

The idea is to form a narrow "grating" out of two rows of conducting droplets that have been ejected from appropriate rows of ink-jet-printer like jets (Fig. 3). The droplets could be intrinsically conducting if formed of mercury or another liquid metal, but at high fields any surface will become coated with a conducting plasma and thus any liquid could be employed. The structure would obviously be disposable. Does it have the required properties?

We have made models of such a structure using two 10 cm spheres between square conducting planes that, acting as mirrors, reproduce the fields of an infinite double row of such spheres. With radiofrequency at a wavelength of about 30 cm we were able to study the fields in detail. A cavity-like accelerating solution was found in which the individual spheres act approximately as dipole oscillators, each with its direction of polarization facing in towards the axis. The fields from the two rows add along the axis to provide the required acceleration (Fig. 4a). Particles with Phase $\pi/2$ ahead or behind that needed for acceleration will experience an RF quadrupole field (Fig. 4b). Figure 5 shows the measured accelerating fields along the axis compared with their calculated values assuming that the spheres act as simple dipoles. Clearly this is a good assumption.

Coupling to incoming radiation, as in the grating case, requires some perturbation of the structure. In this case the most effective arrangement seems to be to displace alternate droplets above or below the plane containing their initial centers (Fig. 6). Assuming again that the spheres act as point dipoles we can calculate the azimuthal distribution of incoming radiation that would perfectly couple into the required mode. This (Fig. 7) turns out to be peaked towards the directions perpendicular to the plane, with a half width at half height of about 35 degrees.

With the above information we can now sketch a conceptual design of an accelerating section (Fig. 8). Windows above and below allow the entry of the laser light. Jet assemblies are on both sides to place the droplets in the required positions; micro position controllers are provided to align the droplets with the exact beam axis. Assuming that a volatile liquid, such as water, is used, large vacuum pumps would be provided to remove the vapour between pulses.

4. Jet Construction

Jets, for ink jet printer use, have been discussed in the literature for some time. Already in 1977 Bassous et al. (Ref. 7) had described the production of precision jets whose size was 13 microns and whose precision was such that the resulting droplets were ejected with an angular accuracy of 1 milliradian. Such an accuracy is adequate for our use. For 10μ radiation 3 micron diameter droplets are needed and the holes must then be about 1.5 microns instead of 13μ. Although we know of no liquid jets this size, holes for other purposes have been made as small as .4 microns (Ref. 8).

To pump the liquid out to form the single droplets, either piezo electric pumps or tiny heaters can be used. Either a single pump could be used for a line of jets, or, if needed, a separate pump provided for each jet allowing control of individual droplet positions.

5. Laser Requirements

In order to demonstrate high gradient acceleration with a droplet structure, one needs a single 10-100 millijoule pulse of diffraction limited 10 micron radiation with pulse length of a few picoseconds. The very short pulse is needed both to generate a surface plasma and accelerate particles before the plasma can grow to distort the original droplet geometry. A laser with such characteristics has been run at NRC in Canada (Ref. 9). It employs semiconductor switches to cut a few-picosecond micro-pulse from a conventional CO_2 laser output. The switch is operated by a dye laser amplified mode locked 600 μm laser pulse. The 10 μm micro pulse is amplified regeneratively in a 10 atmosphere CO_2 gain module to approximately 15 millijoules, sufficient for an experiment.

For an accelerator of interest to high energy physics, however, one would require similarly short pulses but at a high repetition rate (a few kilohertz) and with total power of a few kilojoules per pulse. Table I gives an example of parameters for a 5 TeV accelerator suitable for use as a collider (two such accelerators would be required, one facing the other). In this example it is rather arbitrarily assumed that 150 10 joule lasers would be used in preference to one 1500 joule unit.

TABLE I. "Typical" Laser Requirements

Final beam energy	5 TeV	
Accelerator length	500 meters	(× 2 for collider)
Accelerated particles per pulse	$4\ 10^8$	
Repetition rate	3 kilohertz	
Luminosity (when used as collider)	$10^{33}\ cm^{-2}\ sec^{-1}$	
Average beam power	1 M watt	(× 2 for collider)
Average laser power	5 M watts	(× 2 for collider)
Average wall plug power	50 M watts	(× 2 for collider)
Number of lasers	150	
Individual laser specifications		
Wavelength	~10 μm	
Power	10 joules	
Pulse length	5 pico seconds	
Watts	2 TW	
Repetition rate	3 kHz	
Efficiency	10%	

The conceptual design of lasers capable of meeting such a specification is the subject of an ongoing study by Math Sciences Northwest.

References

1. S.J. Smith and E.M. Purcell, "Visible Light from Localized Surface Charges Moving Across a Grating," Phys. Rev. 92, 1069 (1953).

2. Y. Takeda and I. Matsui, "Laser Linac with Grating," Nucl. Instrum. Methods 62, 306 (1968).

3. J.D. Lawson, Rutherford Lab. report RL-75-043 (1975); IEEE Transactions on Nuclear Science, NS-26, 4217 (1979); P.M. Woodard, Journal IEE 93, Part III A, 1554 (1947).

4. R.B. Palmer, "A Laser-Driven Grating Linac," Particle Accelerators II, 81 (1980).

5. M. Tigner and M. Pickup, private communication (1983).

6. M. Tigner and J.D. Lawson, private communication (1984).

7. E. Bassous, IEEE Trans. Electron Devices ED-25, 1178 (1978).

8. H. Bohler, U. Behringer, J. Keyser, P. Nehmiz, W. Zapka, W. Kulcke, "High Throughput Submicron Lithography with Electron Beam Proximity Printing," Solid State Technology Vol. 27, 210 (1984).

9. P.B. Corkum, "High Powered, Subpicosecond 10 μm Pulse Generation," Optics Letters 8, 514 (1983).

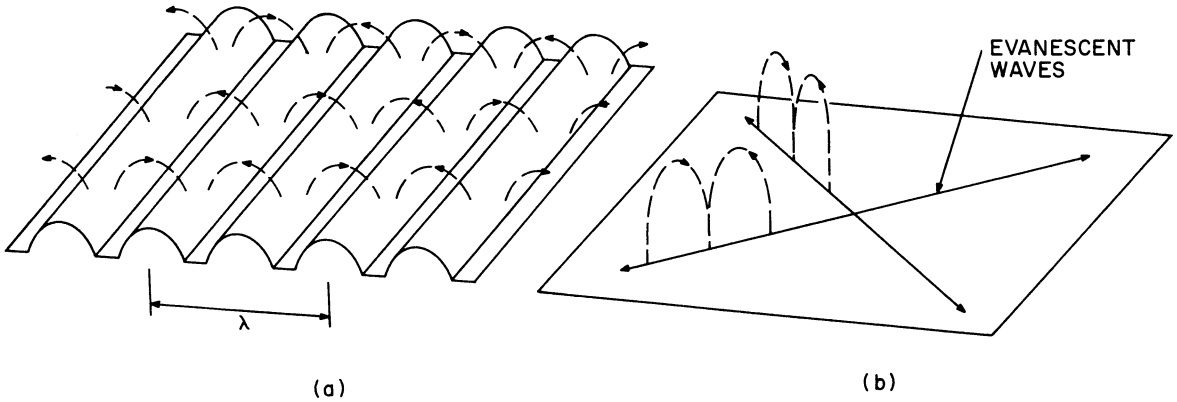

Fig. 1 (a) Fields over a resonant grating. (b) Components of these fields.

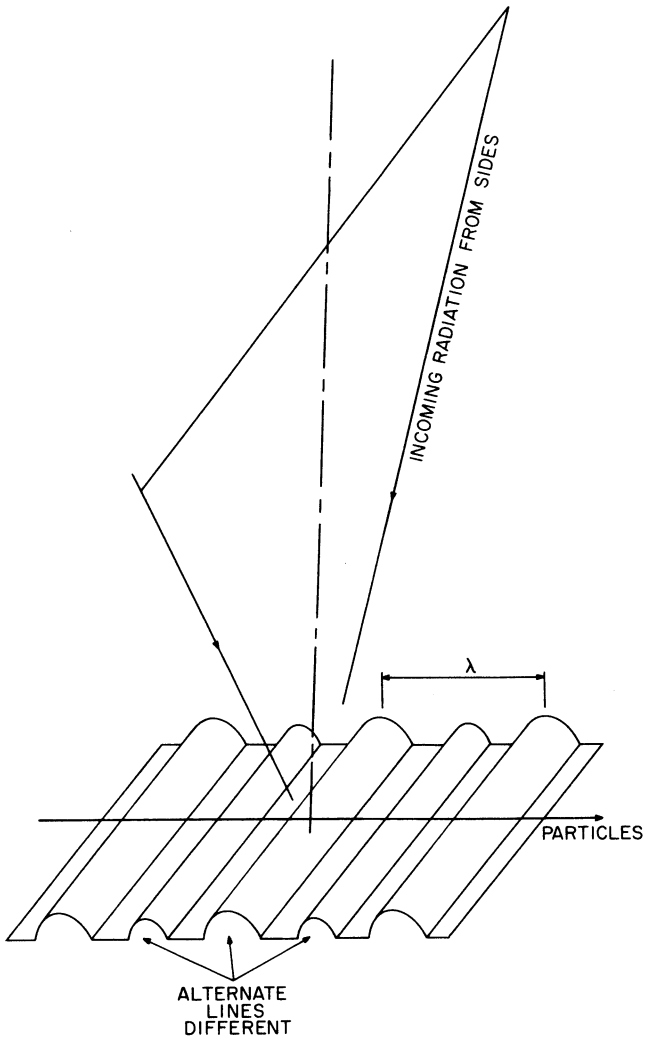

Fig. 2. Modified grating coupling to incoming radiation.

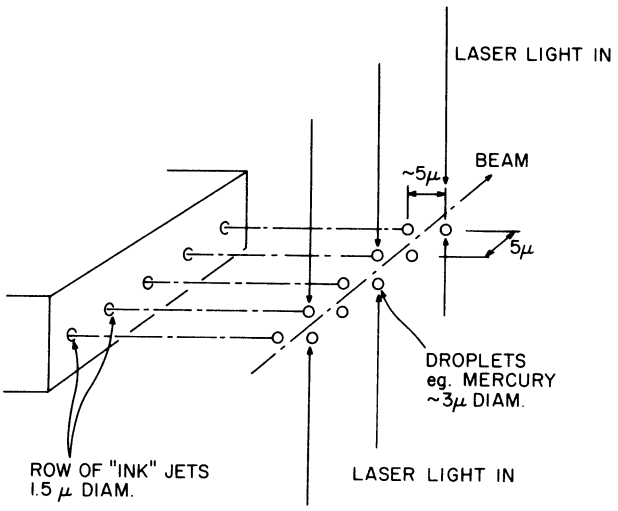

Fig. 3. The droplet accelerator concept.

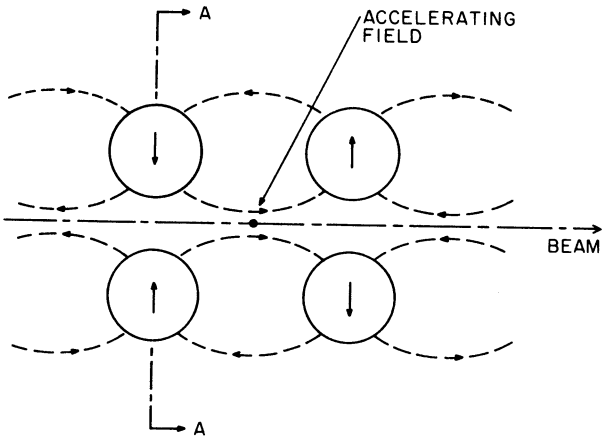

(a)

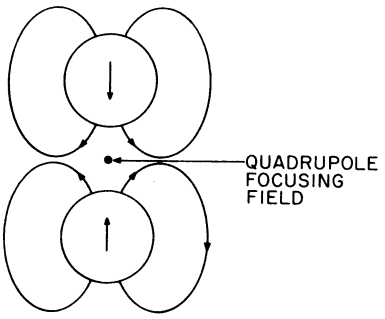

(b) SEC A-A

Fig. 4. Fields in resonant droplet structure; (a) viewed from above, (b) section across the beam.

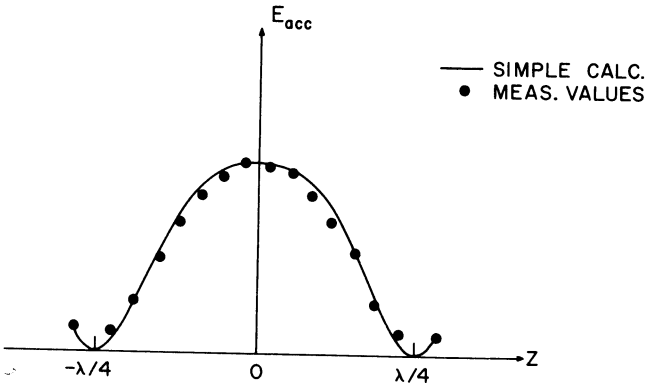

Fig. 5. Measured and calculated accelerating fields along the axis of a droplet structure.

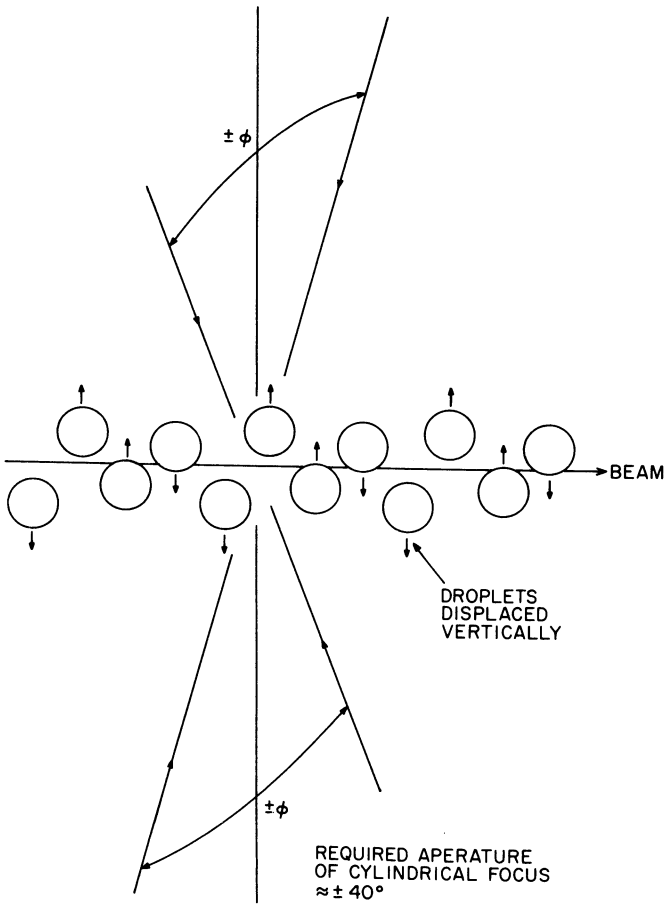

Fig. 6. Modified droplet structure to couple to incoming radiation.

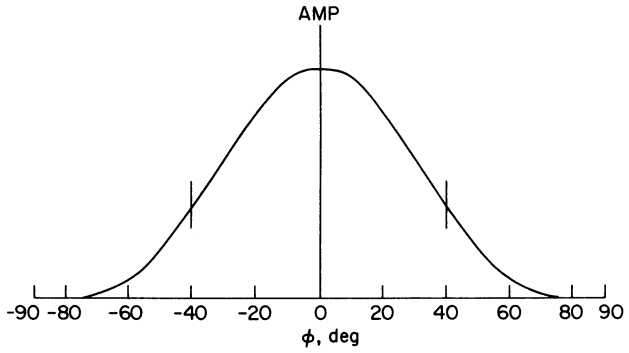

Fig. 7. Azimuthal distribution of incoming light that will 100% couple to the droplet structure.

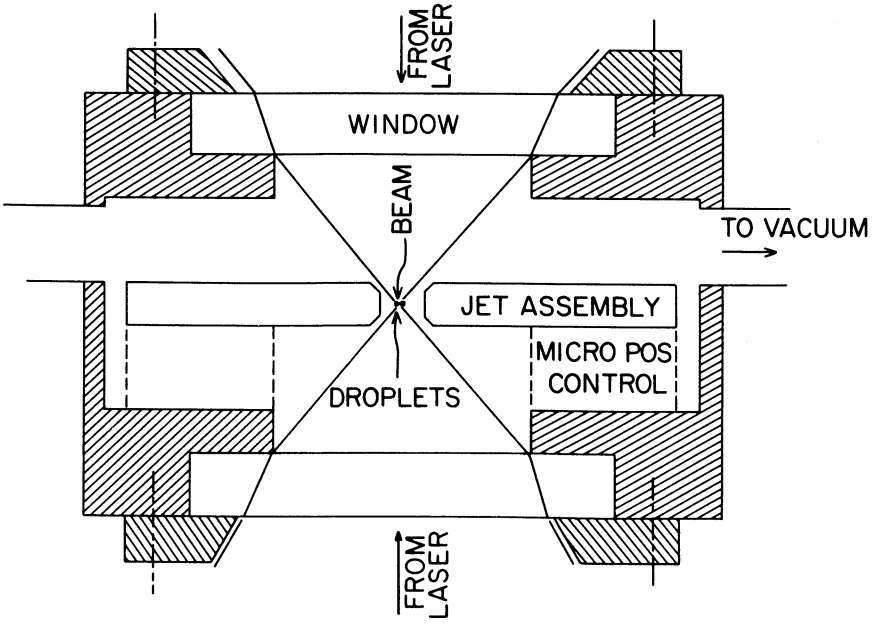

Fig. 8. Conceptual design of accelerator section.

Discussion

J.D. Lawson, RAL

I should like to comment that it is interesting to regard this as a receiving antenna. Matching to the beam impedance will be essential if power from the laser is not to be reflected.

B. Zotter, CERN

Breaking up a long bunch into a series of microbunches does not help to reduce the wakefield unless the memory of the structue is extremely short.

Answer

By keeping the Q smaller than 10, the wakefield should be small after 10 wavelengths. I might add that, according to Perry Wilson at Los Alamos, the transverse wakefield depends on the fraction of stored energy you try to take out and is independent of size. Perhaps he would like to comment.

P. Wilson, SLAC

In answer to your statement that dipole wakefield effects also scale if the fraction of the stored energy removed by the bunch is kept constant, that is correct if the focusing strength is also increased (betatron wavelength reduced in proportion to λ).

K. Witte, Garching

How precise is the estimation of the laser energy? Did you take into account engineering factors like incomplete coupling of the laser radiation to the droplet structure or losses in the laser structure?

Answer

No. We have made only very rough estimates to get an idea of the orders of magnitude involved.

J. Mulvey, Oxford

Would one of the plasma experts like to comment on the lifetime of one of your droplets?

J. Dawson, UCLA

The droplet lifetime depends on temperature. No experiments exist in this range. One can estimate the plasma temperature in the 10's of KeV and expansion sound speed in the neighbourhood of 10^8 cm/sec. The total laser energy is modest so the whole drop cannot be heated to very high values. The drop will disassemble at the sound speed ~ 10^8 cm/sec so that in 1 psec it will move 1 μ.

EXPERIMENT ON 30 nm SPOTS

W. Willis,
CERN, Geneva, Switzerland.

In this Working Group there were long discussions on the feasibility of very small beam spots for colliding beams, smaller even than those of the SLC. One can make general studies on ground motion and surveying (and since the Workshop I have had valuable discussions with J. Gervais and received from J. Rees the most comprehensive notes from G. Fischer), but our Group felt that actual experiments on small beam spots would be most valuable in developing a feeling for what is possible with the type of equipment we are used to, genuine quadrupoles etc.

I'm sure a case can be made for carrying out such studies with the SLAC beam, benefiting from its extremely small intrinsic emittance, but I chose to design an experiment based on a special SPS beam, H8, being built by H. Atherton and N. Doble for experiment NA34. This has the advantage that the momentum, 450 GeV, is in the range in which we are actually interested, and that the collimation has been carefully designed to reduce the intrinsic emittance and end up with a flux allowing one to detect individual particles.

When the SPS is tuned for maximum brightness, it could give about $\sim 10^{12}$ protons in an emittance of $\sim 10^{-6}$m. The H8 beam now provides three stages of collimation and clean-up with sextupole corrections to produce at a fourth focus a beam of $\sim 10^{8}$ particles with an emittance of $\sim 10^{-8}$m in each axis. That emittance is not itself small enough to be very interesting for us, but I propose to add one more stage to the beam, increasing the number of collimating and clean up stages by one. I would cut the number of particles per pulse to 10^{2}, with a vertical emittance of 5×10^{-13}m and a horizontal emittance of 2×10^{-10}m. The last focus should have $\beta_y = 2$ mm, $\beta_x = 12.5$ mm. The rms beam sizes would then be:

$$\sigma y = 30 \text{ nm}$$

$$\sigma x = 1.5 \ \mu\text{m}$$

The aspect ratio of the image, 50:1, is large but I have once dealt with the same value in a separated beam without great alignment problems.

I would detect the position of individual particles by making an array of strips of different elements each 20 nm wide in the y direction and 20 μm along the beam. The characteristic X-rays excited by the particle would then be detected in a nearby Ge crystal, and the ability to distinguish individual elements would allow a measurement of y to ±10 nm. I would measure the auto-correlation function of y(t) during the beam pulse. This would tell me the spectrum of motions in y, the desired goal of the experiment.

LASERTRON FOR A LINEAR COLLIDER IN TeV REGION

S. Takeda
The Institute of Scientific and Industrial Research, Osaka University
Mihogaoka, Ibaraki, Osaka 567, Japan

Y. Fukushima, T. Kamei, H. Matsumoto, H. Mizuno, S. Noguchi, I. SATO, T. Shidara, T. Shintake and K. Takata
National Laboratory for High Energy Physics
Oho-machi, Tsukuba-gun, Ibaraki 305, Japan

H. Kuroda, N. Nakano, H. Nishimura and K. Soda
The Institute for Solid State Physics, University of Tokyo
Roppongi, Minato-ku, Tokyo 106, Japan

M. Mutou and M. Yoshioka
The Institute for Nuclear Study, University of Tokyo
Midori-cho, Tanashi, Tokyo 188, Japan

M. Miyao
Research Institute of Electronics, Shizuoka University
Jyohoku, Hamamatsu, Shizuoka 432, Japan

Y. Kato and T. Kanabe
Institute of Laser Engineering, Osaka University
Yamada-oka, Suita, Osaka 565, Japan

ABSTRACT

Research and development on a new type of rf source "LASERTRON" have been started for an electron-positron linear collider in the multi-TeV energy region. In the LASERTRON, bunches of electrons are emitted at the photocathode with a mode-locked laser modulated at the microwave frequency. A prototype LASERTRON Mk-I has been developed and the rf power of 1.6 kW has been generated at the frequency of 2884 MHz.

1. INTRODUCTION

A linear collider[1,2] seems to be one of the most appropriate accelerators on the order of 1 x 1 TeV in an electron-positron colliding beam-machine in the future. In the linear collider the particles are accelerated to high energies after passing through the half length of the collider, and they are thrown away after collision. The total length of the linear collider is given by the ratio of the center-of-mass energy and the average accelerating gradient in the linear accelerator . In order to make

such large linear accelerators economically feasible, an accelerating gradient greater than 100 MeV/m should be realized. Pulsed rf sources with a peak power of the order of 1 GW are required to generate such high gradients. This rf power is much beyond the level which can be obtained by the conventional technique, and the development of high power rf sources is required.

The LASERTRON[3,4] is a new type of rf source for generating very high peak rf power. Figure 1 shows a conceptual drawing of the LASERTRON. When a photocathode is irradiated by a mode-locked laser modulated at the desired rf frequency, bunches of electrons are emitted from the photocathode during the burst of the laser. The bunches are accelerated by the high voltage applied on the photocathode, and they travel through a cavity gap after passing through an anode. As the electrons are emitted in bunches from the photocathode, the long drift distance required by conventional klystrons for bunching at the relativistic velocity is eliminated. The pulse length of each of the bunches is sufficiently shorter than the rf wavelength, that it is expected to make efficient coupling to the fields in the rf output cavity.

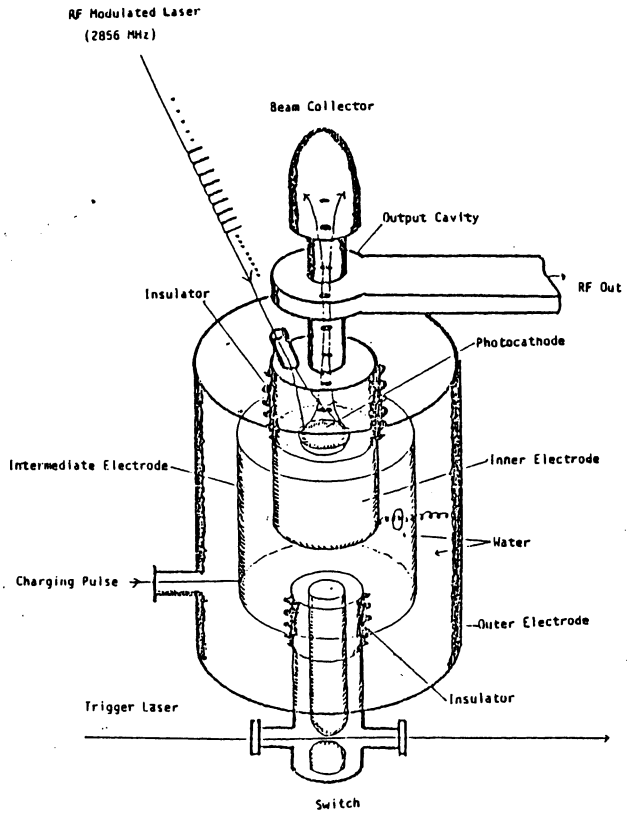

Fig. 1 A conceptual drawing of the LASERTRON.

A prototype LASERTRON Mk-I has been developed, and the rf power of 1.6 kW has been generated by applying the cathode voltage of 30 kV. In order to attain the peak power on the order of 1 GW, many problems over the wide fields in physics and engineering must be solved. Except for the problems in relation to the photocathode material and to the mode-locked laser, the problems seem to be very much like the conventional klystrons. There remains, however, some quite different potential problems on beam dynamics.[5,6]

2. CONVENTIONAL KLYSTRONS

In the conventional klystron , the transit time of electrons between

cathode and anode is shorter than the pulse length of the beam, which is generally of the order of 1 μsec. During the beam pulse, electrons are continuously emitted from the thermionic cathode, and then the electrons are filled in a diode during the beam pulse. The current of the beam is limited due to the space-charge effects in a diode. And then the beam current I_0 in the conventional klystron is defined in terms of the applied voltage V_0 and the perveance k as

$$I_0 = k\, V_0^{3/2} \quad . \tag{1}$$

The beam impedance Z_b decreases with square root of the accelerating voltage as

$$Z_b = k^{-1}\, V_0^{-1/2} \quad . \tag{2}$$

The beam power P_b depends on the accelerating voltage and is given by

$$P_b = k\, V_0^{5/2} \quad . \tag{3}$$

The rf power is, therefore, obtained by multiplying the conversion efficiency η_{rf} of the beam power to the rf output as

$$P_{rf} = k\, \eta_{rf}\, V_0^{5/2} \quad . \tag{4}$$

As the perveance k increases, the space-charge effect becomes more severe, which makes it more difficult to obtain the small mono-energetic bunches at the gap of the rf output cavity. The efficiency η_{rf} of the conventional klystrons, therefore, decreases with increasing perveance.[7] If an efficiency greater than 60 % is required, the perveance should be less than 2×10^{-6} A / $V^{-3/2}$. When the rf power on the order of 1 GW is to be generated, the applied voltage V_0 should be increased to the range between 1 - 2 MV. At such high beam voltage, more rf input power or a longer drift distance is required to modulate the high-current electron beam.

3. LASERTRONS

In the LASERTRON , the photocathode is irradiated by a mode-locked laser modulated at the rf frequency f_0. As shown in Fig. 2-a, the burst of the laser consists of many fine structure pulses with the time interval of $1/f_0$. The number of photons in a fine structure pulse is given by

$$n_{ph} = \frac{\lambda\, P_1}{h\, C\, f_0} \quad , \tag{5}$$

where P_1 is a peak power averaged in the burst in W, λ is the wavelength of the laser and h is Plank's constant.

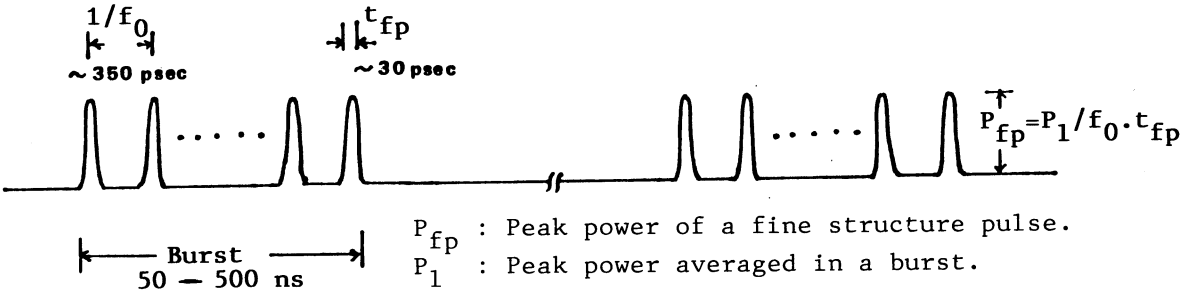

Fig. 2-a Laser required for LASERTRON.

The quantum efficiency η_e is not saturated at the laser power required for the LASERTRON , and then the number of electrons generated on the photocathode is proportional to the number of photons. The shape of the bunch might be equal to the shape of the fine structure pulses of the mode-locked laser. The charge Q_e of photoelectrons produced on the photocathode is, therefore, given by,

$$Q_e = e\,\eta_e\,n_{ph} \ . \tag{6}$$

And then the current of the photoelectrons is given by,

$$I_e = f_0\,Q_e \ . \tag{7}$$

However, the number of electrons, which can be accelerated by the applied voltage V_0 between cathode and anode, is limited by space-charge effects. The pulse width of the fine structure pulse of the mode-locked laser is on the order of 10 ps, and then the transit time of electrons between cathode and anode is longer than the pulse width of the bunch. The bunch length is quite shorter than the cathode--anode distance. When a bunch travels through the cathode-anode gap, bunched electrons exist only in a fraction of the space in the cathode-anode gaps as shown in Fig. 2-b. In this respect, the LASERTRON differs entirely from the conventional klystron .

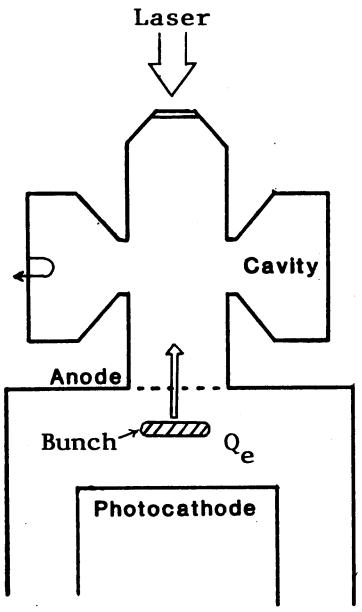

Fig. 2-b Bunch exists in a fraction of the space in the diode.

When the laser power is sufficiently intense, the maximum charge of a bunch is determined not by the charge Q_e but by the limited charge Q_c, which is equal to the surface charge Q_s on the photocathode induced by the applied voltage. The surface charge Q_s is obtained both by the applied voltage V_0 and by the capacitance C between cathode and anode as

$$Q_s = C V_0 \quad . \tag{8}$$

In a planar diode, the capacitance C is obtained by

$$C = \epsilon_0 S / d \quad , \tag{9}$$

where S is the surface area of the photocathode and d is the distance between anode and cathode.

The bunches are emitted at the repetition rate equal to the rf frequency f_0, so that the average beam current I_0 is also limited by the surface charge Q_s. Therefore, I_0 should be smaller than the limited current I_c, which is given by

$$\begin{aligned} I_c &= f_0 Q_s \\ &= f_0 C V_0 \quad . \end{aligned} \tag{10}$$

The limited current I_c is proportional to the applied voltage V_0, and then the beam impedance Z_b is independent of V_0 as

$$\begin{aligned} Z_b &= V_0 / I_c \\ &= 1 / f_0 C \quad . \end{aligned} \tag{11}$$

The beam power P_b is given by

$$P_b = f_0 C V_0^2 \quad . \tag{12}$$

The rf power is, therefore, obtained by multiplying the conversion efficiency η_{rf} of the beam to the rf power as

$$P_{rf} = f_0 C \eta_{rf} V_0^2 \quad . \tag{13}$$

The rf power depends on V_0^2 in the LASERTRON while on $V_0^{5/2}$ in the klystrons. It is the dependence of rf power on the applied voltage that makes difference between LASERTRONS and klystrons.

4. PROTOTYPE LASERTRON Mk-I

4.1 Mode-Locked Laser System

The laser system consists of a passive and active mode-locked YAG laser. After increasing the laser power by two amplifiers, the wavelength is converted from 1.06 to 0.53 μm with a KD^*P crystal in order to shift the wavelength to the sensitive region of the photocathode material. The pulse width of the burst is 50 ns, and the total energy per burst is 50 μJ. The laser output from the amplifier consists of the fine structure pulses with

the frequencies of 169.6 MHz. In order to obtain the frequencies in S-band, an etalon is utilized to multiply the frequency to 2884 MHz, which is 17 times 169.9 MHz. The shape of the each fine structure pulse of the laser is measured by a streak camera and the pulse width is estimated to be 35 ps, while the time interval between pulses is 347 ps. As the peak power averaged in a burst is 1 kW, the peak power of each fine structure pulse is estimated to be about 10 kW.

4.2 LASERTRON Mk-I

Figure 3 shows the crosssectional drawing of the LASERTRON Mk-I. It was fabricated by modifying a photo-diode[8] which is commercially obtained for the detection of the light pulse on subnanosecond time scale. The LASERTRON Mk-I consists of an electron gun and a cylindrical rf output cavity.

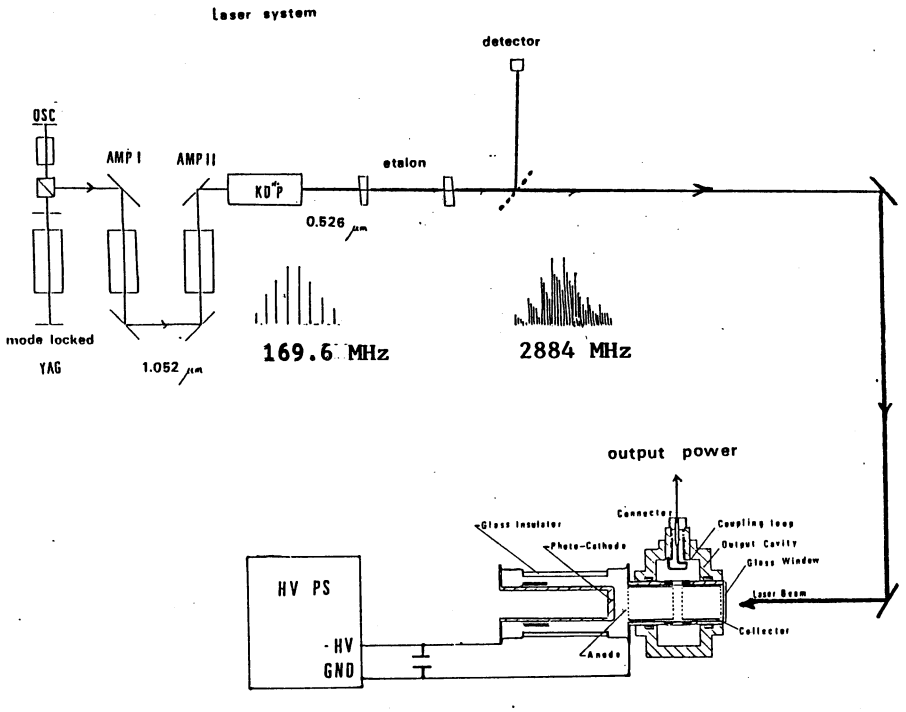

Fig. 3 A crosssectional view of the LASERTRON Mk-I and the experimental arrangement.

The photocathode material is made of bi-alkali and the effective area of the photocathode is 1.33 cm^2. The gap distance between the cathode and the anode mesh is 0.75 cm. The cavity is mounted on a glass tube after chipping off the tube, and then the inside of the cavity is in the atmosphere. The resonant frequency of the cavity is adjusted to the frequency of 2884 MHz, and the rf loss factor Q is estimated to be 75. The rf power is picked up by a coupling loop with the coupling efficiency of 0.3. Two meshes are set at the cavity gap in the drift tube in order to improve the transit angle even if the accelerating voltage is low. The gap

distance between these meshes is 5 mm. The beam collector consists of a mesh on the glass window so that the laser light penetrates from the outside of the LASERTRON Mk-I to the photocathode. A high DC-voltage was supplied to the cathode through a charging coaxial-line in order to supply charges with fast time-response.

5. EXPERIMENTAL RESULTS AND DISCUSSIONS

Experiments have been performed with a prototype LASERTRON Mk-I to obtain the fundamental data required for development of next LASERTRON. As a function of applied voltage V_0, the beam current I_0 is shown in Fig. 4 and the rf power P_{rf} is shown in Fig. 5. At the maximum applied voltage of 30 kV, which is the limited voltage due to breakdown, both the beam current I_0 of 10 A and the rf power of 1.6 kW have been observed. The power of the present laser is sufficiently intense since the current of photoelectrons I_e is estimated to be 12 A, which is higher than the maximum beam current of 10 A at 30 kV. If the beam current is lower than I_e, it is expected that the beam current I_0 increases in proportion to the applied voltage V_0 and that the rf power increases with square of the applied voltage. The experimental results show that the rf power increases with $V_0^{2.8}$. It seems that the conversion efficiency η_{rf} depends on the applied voltage V_0, since the transit angle of the bunched beam in the cavity gap depends on the non-relativistic velocity of the bunches.

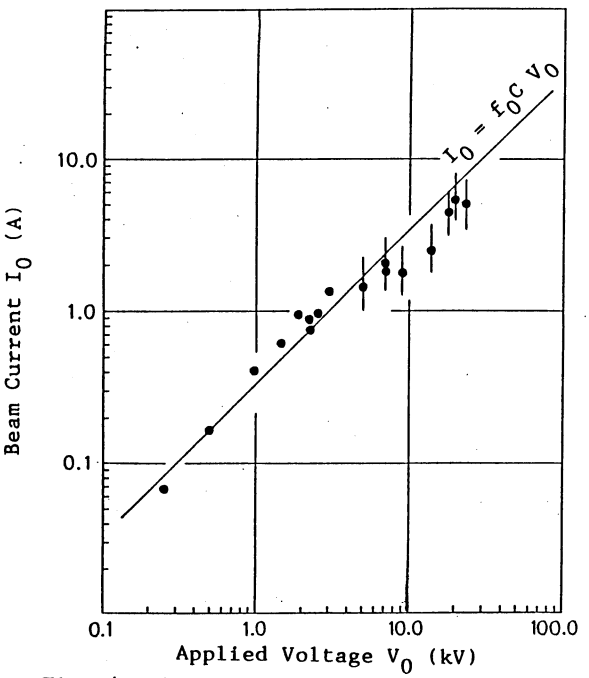

Fig. 4 The average beam current I_0 per burst of laser.

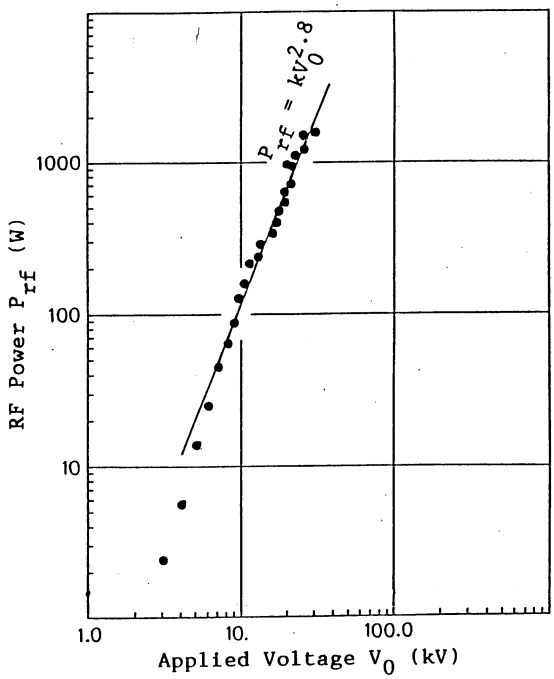

Fig. 5 The rf power as the function of applied voltage.

6. CONCLUSION

An rf power of 1.6 kW has been generated at the rf frequency of 2884 MHz by applying the accelerating voltage of 30 kV. A new prototype of the LASERTRON is now being studied in order to increase the applied voltage. Several kinds of cathode materials with negative electron affinity are also being studied to obtain high current beam and to realize the demountable photocathode gun.

Acknowledgements

The authors wish to express their thanks to S. Ozaki, H. Sugawara, K. Takahashi, K. Yokoya and Y. Yamazaki of National Laboratory for High Energy Physics, S. Kato and H. Okuno of the University of Tokyo, and C. Yamanaka, M. Kawanishi, Y. Cho and K. Tsumori of Osaka University for their helpful suggestions and encouragements. They also thanks to S. Asaoka, T. Morimoto, K. Norimura and Y. Tanaka of the University of Tokyo for their help of the present experiment.

REFERENCES

1) H. Hirabayashi (ed.), Proc. of the First Tristan Phase II Workshop, KEK Report (1982).
2) T. Sato (ed.), Proc. of the Workshop on the Future Accelerator and Physics, KEK Report 84-16 (1984).
3) P. B. Wilson, IEEE Trans. Nucl. Sci. NS-28, No.3, 2742 (1981).
4) T. Shidara et al, Proc. 5th Symp. on Accelerator Science and Technology (held at KEK, Sept. 1984) 130 (1984).
5) H. Nishimura, Proc. of the 1984 Linear Accelerator Conference, Darmstadt, 1984.
6) T. Shintake, Proc. of the 1984 Linear Accelerator Conference, Darmstadt, 1984.
7) P. J. Tallerico, IEEE Trans. Nucl. Sci. NS-26, No.3, 3877 (1979).
8) K. Oba (Hamamatsu Photonics Inc.), The quantum efficiency of the photocathode measured by Hamamatsu Photonics Inc. is 3 % for the wavelength of 530 nm.

Discussion

J. Rees, SLAC

At the end of your talk you mentioned plans for a Lasertron Mk II, operating at 300 kV to give a peak power of ~ 50 MW. What are the radio-frequency, pulse length and repetition rate?

Answer

The linear collider group propose a disc and washer accelerating structure operating at 2.8 GHz, so this is the frequency for the lasertron. The pulse length is 70 ns and the repetition rate 200 Hz.

L. Funk, Chalk River

What is the efficiency of your lasertron, and what do you expect will be the upper limit of achievable efficiency?

Answer

We expect about 50%.

SWITCHED POWER LINAC

W. Willis
CERN, Geneva, Switzerland

ABSTRACT

The proposed linac is powered by switched pulses instead of radio frequency power, using distributed photodiodes driven by short pulses of light. If the required photodiode and light source requirements can be met, this device will have the following advantages; 1) Very short pulses can be produced by the high pervaence photodiodes, leading to a small stored energy; 2) The distribution of the power source over the whole accelerator surface allows a high density which can produce a large gradient; 3) The short pulse reduces the heating of accelerator structure and other gradient limitations; 4) The power switching can be highly efficient; 5) It is straightforward to recover most of the energy in the pulse, raising the overall efficiency or allowing the beam loading to be lowered for fixed efficiency. Alternatively, multiple pulse schemes can be used to maintain high efficiency; 6) The high gradient and low beam loading give low wake field effects, and good output emittance.

The proposal can be understood by reference to Figs. 1 to 5. The accelerating structure consists of copper disks of radius R and thickness d, with a central aperture of radius r, spaced by a distance s. Near the outer radius is a wire photocathode of radius r_c, at a distance of g from the nearest copper surface. These wires are supported to form an octagon, and charged through an "external" photodiode as shown in Fig. 3.

The operation proceeds by charging the wire photocathode through the external photodiode in a moderately short time ~ 0.5 ns. (See the waveforms in Fig. 2a.) The charge then has time to distribute uniformly on the wire. Next a short light pulse discharges the wire photodiode in a much shorter time onto the disk structure, generating a pulse which travels inward at increasing voltage until it is reflected from the central aperture. At that time the particle bunch passes through the gap and feels the accelerating field. Most of the energy in the pulse is reflected and travels back out to the outer radius of the structure, where the energy is recovered by another photodiode switch.

An approximate quantitative analysis of this device will now be given. One has to put the analysis in a parametric form to realize certain matching conditions, but for brevity only a numerical example which satisfies these conditions is shown, with parameters given in Table 1. Derived

Table 1

Parameters

R	Outer radius	60 mm
S	Disk spacing	1 mm
d	Disk thickness	0.6 mm
r	Inner radius	0.15 mm
g	Photodiode gap	0.5 mm
r_c	Photodiode radius	50 μm
V	Charging voltage	40 kV
τ_e	Light pulse length	1 ps
C_x	External photodiodes cap.	1 pF
τ_x	Charging time	400 ps
E_γ	Light photon energy (wavelength)	9.5 eV (135 nm)

Table 2

Derived Quantities

Photodiode capacitance	8 pF
Photodiode charge	0.32 μC
Stored energy	6.4 mJ
Discharge time	10 ps
Power	0.64 GW
Outer radius impedance Z_r	1.3 ohm
Inner radius impedance Z_I	~ 30 ohm
Current	32 KA
Current/mm^2 at photocathode	2000 A/mm^2
Space charge limit (Child's law)	0.8×10^5 A
Line voltage at external feed	40 kV
Voltage at reflection	~ 1.6 MV
Accelerating field	~ 1.6 GV/m
Average gradient	~ 1 GV/m
Surface resistivity of Cu	0.06 ohm
Ohmic energy dissipation	0.1 mJ
Ohmic loss at inner radius	15 MW/cm^2
Energy deposit in skin volume	3 J/cm^3
No. particles to exhaust stored energy	2.5×10^{10}
Accelerator efficiency for 10% beam load	~ 30 %
Light power, 9.5 eV and 10% photocathode eff.	3 MW
Power density	240 KW/mm^2
Light energy	31 μJ
Length for 1 TeV	1 km
Beam stored energy/pulse of 2.5×10^9 C	400 J
Wasted energy lost in accelerator	933 J
Power required for 10^4 Hz	13 MW
Beam power	4 MW
Light power	63 KW
Light source power, if 1% eff.	6.3 MW

quantities are given in Table 2. The scale was chosen to match the stored energy to the required value and to push the accelerating field toward the limits given by field emission. The plate thickness is a structural choice. The diode characteristics were chosen to match the impedance of the structure, for efficient power transfer.

The copper disk structure driven at the edge looks like a transmission line of impedance 1.3 ohms. It is essential that the photodiode current into that produces a potential drop matched to that on the photocathode, V, so that the photoelectrons give up all the stored energy in their passage across g and arrive at the anode with small energy. For an accurate calculation of the photodiode performance one must consider the motion of the electrons taking into account their space charge and magnetic field, and the radiation in the structure. Since ours is a two dimensional problem, a numerical solution adapting existing programmes is perhaps possible, but for an approximate solution we ignore space charge and use the transmission line approximation, then check the current we obtain against the space charge limit.

It is important to keep the time constant of the electron motion short, in order to keep the power high and stored energy low. We may assume the light pulse itself is sufficiently short. The cylindrical geometry of the cathode wire is favourable in this respect, since the electrons acquire most of their energy in a short distance. The voltage assumed gives a surface field on the wire of 400 MV/m, well below the point where field emission would be a problem. This voltage is maintained for less than 1 ns, so that breakdown processes which depend on ion motion cannot be effective. A breakdown process dependent on photon feedback is not favoured because of the small solid angle subtended by the photocathode.

The risetime of the photocurrent pulse based on free electron motion is about 2.5 ps. The completion of the current pulse is dependent on the reaction of the electromagnetic field in the structure. One way to see a qualitative analysis is to note that in the first phase of charging the copper structure, its transmission line character is not relevant, and we may consider that we are charging a capacitor large compared to that of the photocathode. This is our justification for computing the risetime slope using the static field. Next, the structure looks like two transmission lines, one going inward and one outward, with a total impedance of 1.3/2 ohms. Then the reflection from the open outward line arrives, several ps later. By then, the electrons have fallen through most of the potential drop, the energy stored has been transferred, and the motion of the electrons will be stopped on the average or slightly reversed. A number of parameters are available for detailed timing of this condition. It seems that one should not lose more than a few percent of the stored energy in this process.

On the basis of this discussion, we take the full width of the current pulse to be 10 ps. The average value of the current is then 3.2×10^4 A, which develops a voltage in the transmission line equal to that originally on the photocathode. We note that this current is considerably smaller than that of a space charge limited diode (again noting that magnetic field is not considered) $i = 14 \times 10^{-6}(2\pi R/g)V^{3/2} = 0.052\ V^{3/2}$ A.The use of the "external photodiode" to apply the short high voltage pulse is very important in allowing an increase in V, and thus a big increase in the space charge limit through the $V^{3/2}$.

As the pulse travels inward, the impedance of the line rises with the inverse of the radius. Near the centre, where the inner aperture is reached and the pulse is reflected, $(1/r)^{1/2}$ has increased by a factor 20. Upon reflection, there is a doubling of the voltage, leading to an ideal transformer ratio of 40. The resulting acceleration field in the gap is 1.6 GeV/m, close to the field emission limit, though the computed field emission current is small. Note that the field is only maintained for 10 ps at any given point, eliminating breakdown mechanisms based on regeneration. As the voltage rises in the transformer, the current falls, being 'only' 1600 A near the centre. Consequently, the heating due to the current at the inner edge of the copper disk, is not sufficient to cause a problem.

The beam bunch length must be smaller than the length of the field pulse, probably about 1 mm. There is an opportunity to shape the electric field pulse, within the constraints determined by keeping the photodiode losses small, in order to compensate for longitudinal wake field.

The reflected pulse arriving back at the outer radius of the structure has lost ~ 1% of its energy in ohmic dissipation and about 10% to the beam. Allowing for photodiode losses, 2/3 remain to be recovered, which is well worthwhile. This is done by illuminating the other side of the photocathode, on a ridge provided on the copper disk, with a photocathode surface. The charge is transferred back to the wire and through the external diode into the power supply.

The use of the external photodiode solves two problems. It is essential to keep the total capacitance of the primary photocathode low, to match the stored energy to the desired value. With the coupling only through the very low capacitance of the external photodiode, the capacitance of the primary photocathode is determined essentially by its active portion. Also we wish to charge or discharge the photocathode line very quickly, in order to prevent breakdown. It would be difficult to find another charging mechanism on this time scale, and to transport pulses of this length involves undesirable ohmic losses. In this system, the short

pulses travel a very small distance. Further local filtering of the reactive power associated with the repetition rate (~ 10^4 Hz for example) means that the power distribution in the system is essentially continuous current, with very low losses. If the switch efficiency is high, the overall efficiency of the accelerator could be 25%, for 10% beam loading, with the important exception of the light source power.

The optics must focus light on the 100 μm wire, not a difficult requirement for the short wavelengths which will be used. The light wave front must have cylindrical symmetry to preserve the isochrony, but the photocathodes can be polygonal, as in Fig. 5. The alignment should be within 10 μm, not too difficult with a short focal length cylindrical lens or mirror mounted on the accelerator structure. The pathlength tolerance is ~ 0.1 mm, which is not very severe. The most difficult part seems to be the distribution of the light over the whole surface of a long accelerator, and the initial set-up.

The light source has to provide very large power in ~ 1 ps pulses at the repetition rate of the machine. One gap of this machine needs, for 9.5 eV photons and 10% cathode efficiency, about 2×10^6 W, or ~ 1 GW/m, 1 TW/km. This is large, but not unreasonable. Presumably an FEL is the way to do it at high repetition rates. Its power consumption may be an appreciable fraction of the total power used.

The photocathode is the element which presents the fundamental uncertainty. All photocathodes used in current practical devices are based on semiconducting layers, and usually on very special surface conditions. The surfaces are very easily damaged, and even the bulk properties of the semiconductors can easily change as the defects alter under high current loads or bombardment by energetic particles, unless they are already in an amorphous highly doped condition. Worse, in the particular design described here, the diode is driven both ways, so that each electrode receives electron bombardment as well as emitting electrons. (In fact, a design with two wire photocathodes can avoid this particular aspect.) It seems that we would prefer a photocathode which is a nominally pure, intrinsic conductor with a surface which is not special. Then its properties can be expected to remain stable. Work functions of decent metals are all more than 3.5 eV. Consequently, they are photo-emitters only in the far UV. Their quantum efficiency is found experimentally and theoretically to be of the form

$$QE = \frac{5 \times 10^{-4}}{\cos \theta} (h\nu - w)^2$$

where θ is the incident angle with respect to the normal. For w = 3.5 (thorium)hv = 9.5 eV (CaF_2 or MgF_2 optics) and θ = 75°, the QE = 7.2%. These values apply even though the surface is not atomically clean. This is a solution without fundamental uncertainties, though the use of floride optics (albeit in tiny pieces) or mirrors is not too pleasant, and the efficiency is a bit low. Quartz optics are much nicer, restricting use to hv ≤ 7 eV, but the efficiency is correspondingly lower.

We must also note the effect of the strong electrical field on the primary photodiode. The effect of this field is to lower the effective work function by more than 0.5 V, from the Schottky formula.

The method of single pulses with energy recovery is elegant, but demands very high peak power and the provision of photodiodes working in both directions seems rather tricky. Other schemes based on the same basic structure can easily be devised. For example, we can consider operation with multiple pulses spaced by the time of a round trip reflection, ~ 1/2 ns. Since the ohmic dissipation is less than the probable beam loading, the efficiency could be quite high. The echoing pulse strength could be built up over several cycles before the first beam bunch arrives, and the photodiode used to replace lost energy on each subsequent cycle. The dispersion in the structure is one limit in this scheme. Also, the intersection region design must cope with bunches with this separation. The laser must provide multiple pulses, but each one has lower power. The electron optics in the diode is less problematic because of the lower peak current. The waveforms are shown in Fig. 2b.

Another idea is to generate an rf field in the structure, which is modified by introducing some copper posts between the sheets, near the centre, so as to create a resonant cavity coupled to the transformer structure. The photodiode is then switched at a ~ 10 ps period, as shown in Fig. 2c, and the field builds up in the cavity and multiple beam pulses pass through, as close spaced as the intersection region design will allow, perhaps 100 ps as shown. This design has attractive features, but there must be compromise between the spacing of the multiple bunches and the heating of the copper surface in the central cavity, which will limit the allowable gradient.

Last, an aside on the transverse wake field. This effect and its damaging effects on emittance growth, is the source of limits on the allowed beam loading. We note that the open structure used in this accelerator allows an interesting attack on this problem, which can be reduced if the alignment of the beam with the inner aperture in the structure is improved. As shown in Fig. 3, antennae are provided in four orthogonal directions outside the accelerator structure, to pick up the wake field

radiation escaping from the slots at the outer radius. This is done on each accelerator pulse in 1% of the sections which are left unpowered for that purpose. The radiation from opposed pairs of antennae is subtracted and then detected, to obtain a check of symmetry of the radiation. This method looks at the effect to be suppressed directly, so that no separate alignment is necessary. These signals are Fourier analysed and give, and every 100 machine pulses, an indication of steering corrections. There can be feedback with a time constant of ~ 0.01 s, so that even earth motion can be servoed out. To first order, then, the transverse wake field problem can be suppressed.

These ideas were developed in collaboration with R. Palmer, J. Claus, V. Radeka and I. Stumer.

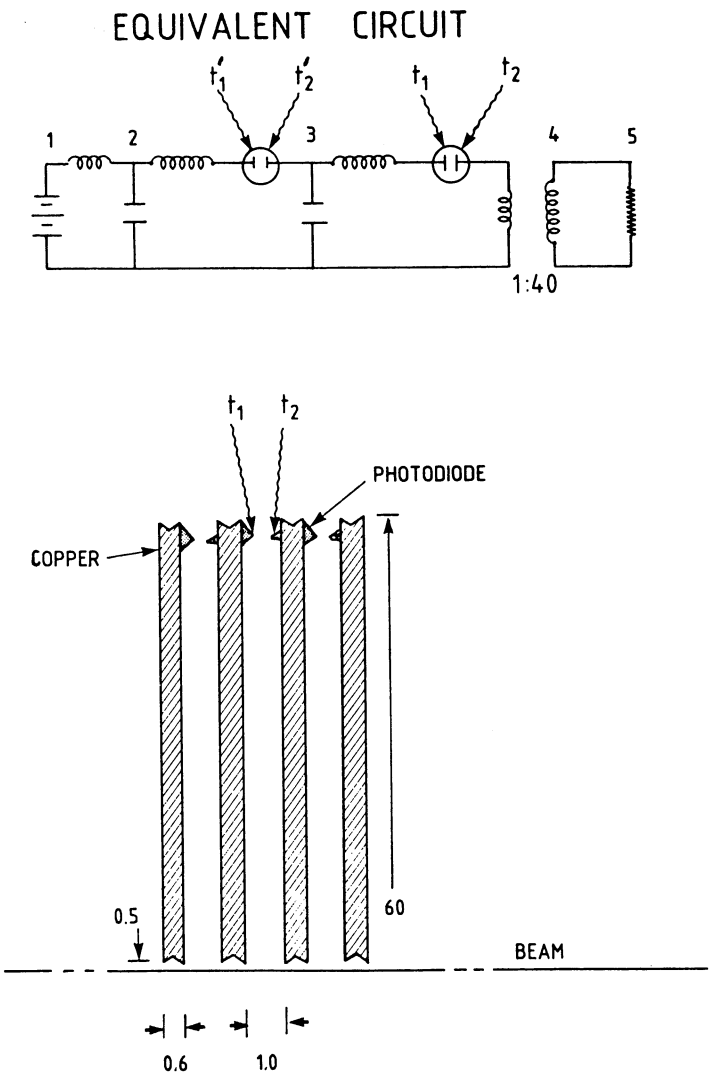

Fig. 1 Cross-sections through the accelerator structure, and equivalent circuit.

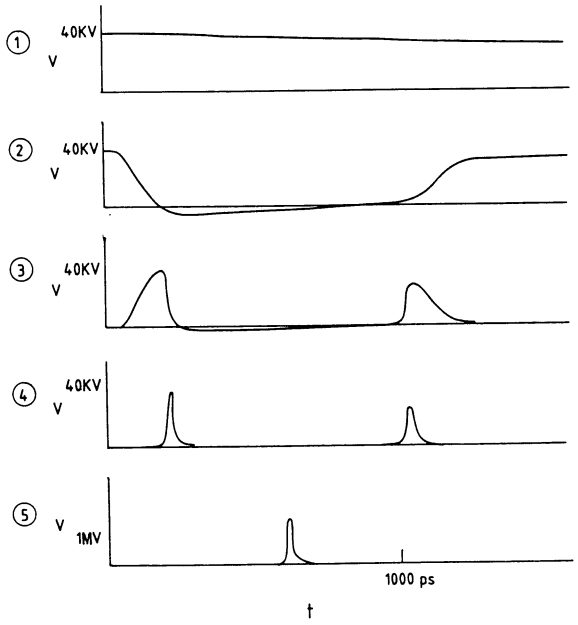

Fig. 2(a) Wave forms at the numbered points in the equivalent circuit.
1. At storage capacitor before external photodiode.
2. At external photodiode.
3. At primary photodiode.
4. At exterior of copper disk.
5. At centre of copper disk.

Scheme of single pulse with energy recovery.

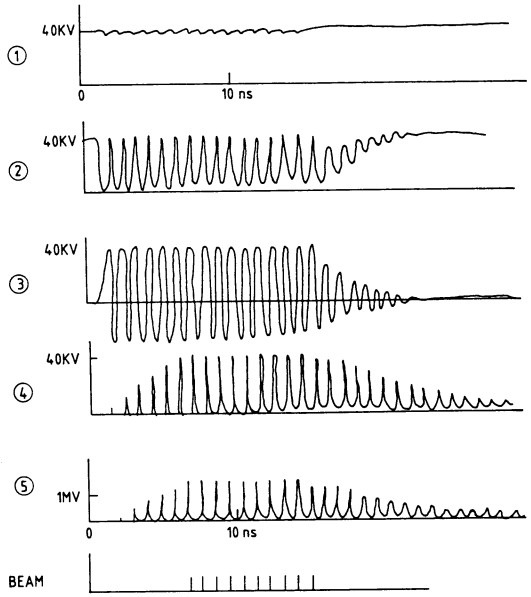

Fig. 2(b) Wave forms at the numbered points in the equivalent circuit.
1. At storage capacitor before external photodiode.
2. At external photodiode.
3. At primary photodiode.
4. At exterior of copper disk.
5. At centre of copper disk.

Scheme of multiple pulses echoing in disk structure.

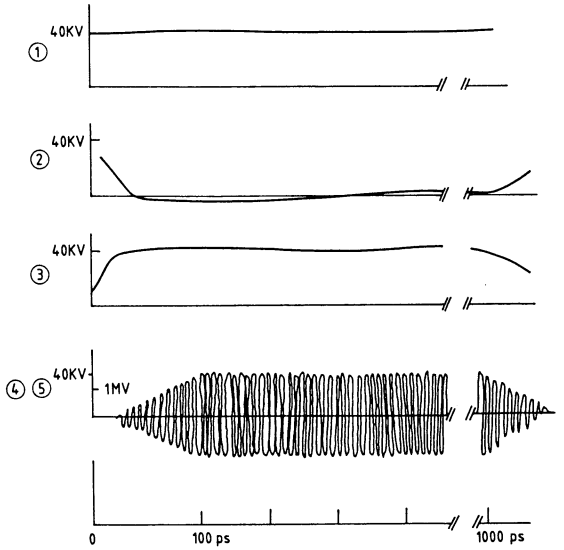

Fig. 2(c) Wave forms at the numbered points in the equivalent circuit.
1. At storage capacitor before external photodiode.
2. At external photodiode.
3. At primary photodiode.
4. At exterior of copper disk.
5. At centre of copper disk.

Scheme of rf generation to excite resonant cavity at centre of copper disk.

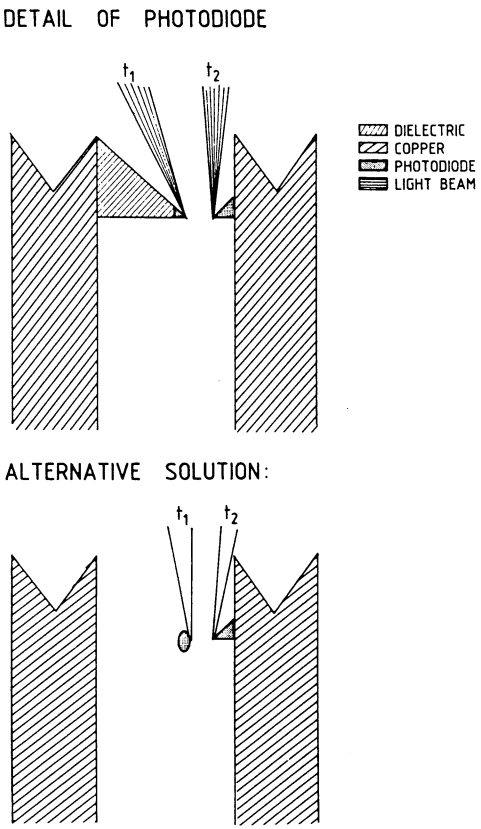

Fig. 3 Details of photodiode, for dielectric supported and wire alternatives.

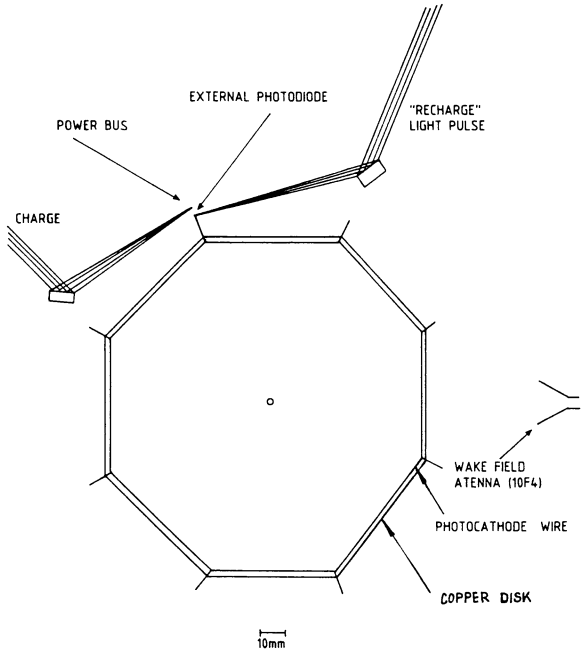

Fig. 4 View transverse to beam

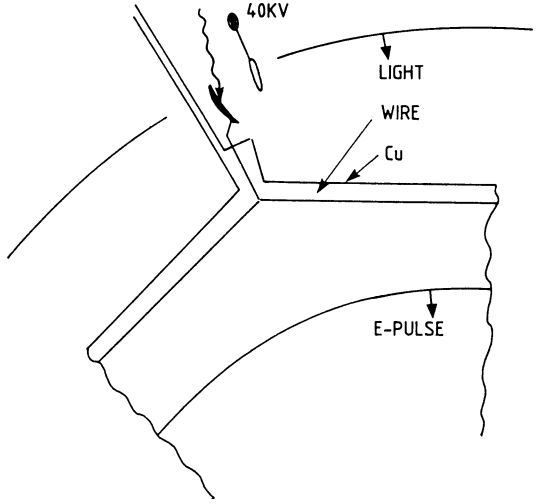

Fig. 5 Illustration of cylindrical wave front of light transformed to cylindrical electrical pulse on photodiodes formed of a polygonal wire array.

SUMMARY REPORT OF THE WORKING GROUP 3 ON PLASMA ACCELERATORS

C. Joshi
University of California, Los Angeles, CA 90024, USA

Participants in Working Group

D. Bailey, R. Bingham, J. Bobin, P. Bryant, R.A. Cairns, S. Chattopadhyay, K. Chen, D. Cline, E. Colton, A.E. Dangor, J. Dawson, M. Dupont, A. Dymoke-Bradshaw, R. Evans, W. Fischer, G. Grossetête, C. Joshi, J. Jowett, G. Korschinek, S. Karttunen, E. Laing, J. Lawson, J. LeDuff, F. Mills, B. Montague, M. Pabst, M. Querrou, R. Sudan, T. Tajima, E. Wilson, P. Wilson

I. INTRODUCTION

The plasma accelerators group, comprised of the participants listed above, considered two particular particle accelerator schemes: the Plasma Beat-Wave Accelerator (PBWA) and the Plasma Wake-Field Accelerator (PWFA). There has been intense activity in exploring both of these schemes since the Los Alamos Workshop on Laser Acceleration of Particles[1]. At this Workshop the participants of the study group on Plasma Acceleration heard of the progress that has been made since the Los Alamos Workshop in this area. In both of the above schemes mentioned, very large longitudinal fields ($E_z > 1$ GeV/m) of space-charge density waves in high density plasmas are used to accelerate particles. In the former case (PBWA) laser beams are used to drive the space-charge wave, whereas in the latter case (PWFA) bunches of relativistic electrons are used to drive the space-charge plasma wave. There are several groups engaged in this work and wherever appropriate we mention their contribution in this report.

An obvious question that comes to mind is, "Why should the accelerator builders consider plasma waves to accelerate particles?" After all a plasma accelerator is truly a collective accelerator and no such device has

ever been shown to work. Also, plasmas are known to be notoriously unstable, which should deter anyone but the most optimistic person from suggesting it as a medium for accelerating particles. But consider this: since a plasma is already ionized, there is no problem of breakdown which ultimately limits the maximum accelerating gradient that can be achieved in a conventional structure. Even more important, the maximum electric field of a space-charge plasma wave propagating close to c simply scales as $\sim \sqrt{n_e}$ (cm^{-3}) V/cm. Thus for plasmas with density in the range 10^{16} $cm^{-3} < n_e < 10^{20}$ cm^{-3}, the maximum field is in the range 10^{10} V/m $< E_z < 10^{12}$ V/m; orders of magnitude greater than that achievable in a conventional structure. For this reason alone, plasma wave accelerators are worth a study.

II. PROGRESS ON PBWA SINCE LOS ALAMOS WORKSHOP

The PBWA concept was introduced to the accelerator community at the Los Alamos Workshop[1]. In this concept, invented by T. Tajima and J.M. Dawson[2], two laser beams, (ω_0, k_0) and (ω_1, k_1), are injected into a plasma such that their frequency difference $\omega_o - \omega_1$ equals the plasma frequency ω_p. This generates a plasma wave (Fig. 1) which propagates with a phase velocity v_p that is equal to the group velocity of the light waves $v_g = \left(1 - \frac{\omega_p^2}{\omega^2}\right)^{1/2} c$. Although the longitudinal electric field of such a wave can be spectacularly high, the total energy gained by a trapped particle $\int \underline{E_z} \cdot d\underline{z}$ is finite because the wave propagates somewhat slower than c and relativistic particles soon outrun the wave. At the time of the Los Alamos Workshop it was thought that multistaging was necessary to reach ultrahigh energies.

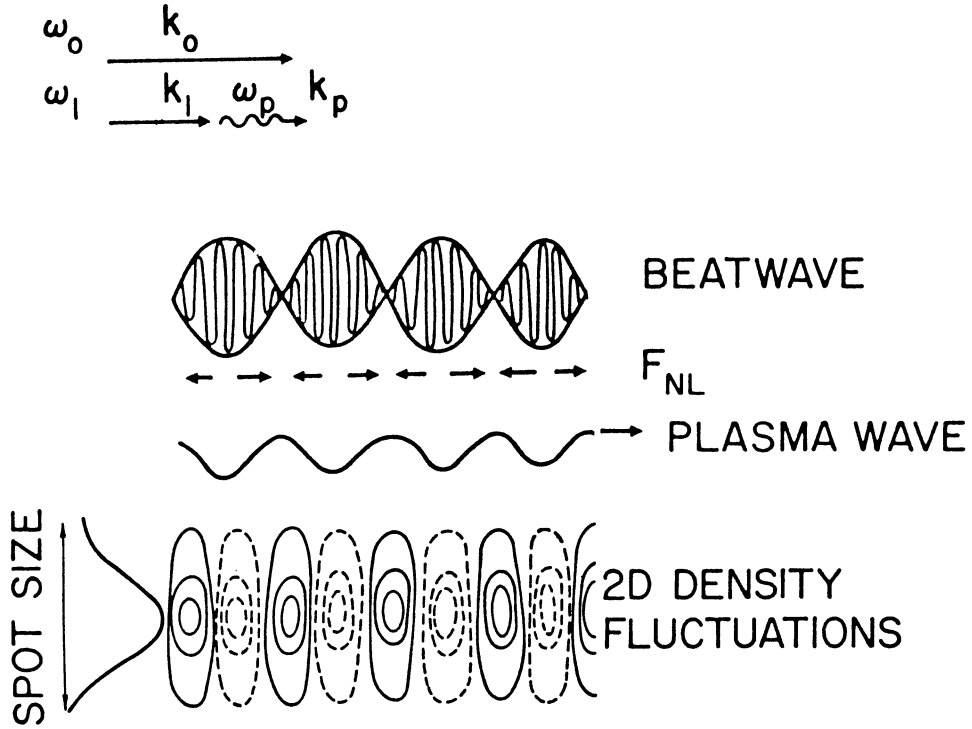

FIGURE 1.

The optimism in the PBWA to accelerate particles to ultrahigh energies was based mainly on the results of 1D particle simulations of T. Tajima[3] and D. Sullivan and B. Godfrey[4] and an experiment by C. Joshi, C.E. Clayton and F.F. Chen[5] which showed that even at very low laser intensities a beat-wave-driven plasma wave could be set-up in a quasi-homogeneous plasma. However, the experiment was done at intensities 10^9-10^{10} W/cm^2 for a CO_2 laser 50 ns (FWHM) such that most of the competing instabilities (which have a threshold) could not occur and therefore this experiment could not be regarded as scalable. Also two-dimensional, finite beam computer simulations were necessary in order to locate a window in the parameter space where the competing instabilities did not occur.

It is in this latter area that greatest progress has been made in the last two years. The competing phenomena can be categorized in two: those occurring on ω_p^{-1} timescale and those which occur on ω_{pi}^{-1} timescale. In the

former class are Raman sidescatter, magnetic field generation, Weibel instability, relativistic self-focusing and in the latter class are Brillouin scattering, ponderomotive self-focusing and resonant self-focusing. Extensive 2D simulations have been carried out by W. Mori, J.M. Kindel and D.W. Forslund[6,7] using the fully relativistic, electromagnetic code WAVE. These simulations show (Fig. 2) that provided a laser pulse of a short enough duration (10-20 ps) is used, results obtained with 1D simulations can be reproduced in 2D simulations. Namely, the growth and saturation of the plasma wave is consistent with the fluid theory results of Rosenbluth and Liu[8]. Also the energy gain by particles is in agreement with the predictions of single particle theory[2].

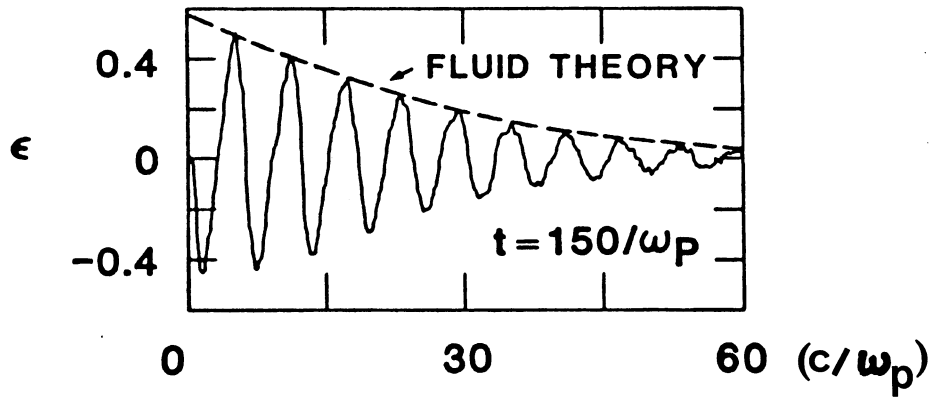

FIGURE 2.

2D particle simulations are extremely expensive and it is useful to have a compilation of thresholds and growth rates of the various instabilities that might occur using fluid theory so that a back-of-the-envelope estimate can be made of the input parameters (laser pulselength, intensity and laser frequency to plasma frequency ratio) for both computational work and designing experiments. This has been done by R. Bingham in a recent Rutherford Laboratory report[9].

Although the optimum pulsewidth is probably in the 10's of picosecond range, the current or planned experiments have laser pulselength considerably longer than this. For instance, Los Alamos uses or plans to use[10] a CO_2 laser with pulsewidth in 300 ps-600 ps range whereas experiments at UCLA again use a CO_2 laser with pulsewidth in the 1 ns range. The working group was also informed of a planned experiment by the Imperial College Group[11] at Rutherford Laboratory's Laser Facility which will employ 1 μm laser pulses of 100 ps-1 ns duration.

So what are the objectives of the current and planned experiments? There are several rather crucial issues regarding the excitation of the plasma wave that can be addressed with longer laser pulses. The first of these is the question of resonance. It is important to know what the tolerance is on the exact resonance condition $\omega_0-\omega_1 = \omega_p$. Any real plasma is going to have density inhomogeneities and these could degrade the plasma wave. Second, the growth and saturation of the plasma wave can be more easily diagnosed with longer and less intense laser pulses than those eventually needed for a proof of principle experiment. For instance for a linear risetime pulse the plasma wave grows and reaches saturation in a time t_s[12]

$$\omega_p t_s = 3.68\ (\omega p\tau)^{4/7}(\alpha_1\alpha_2)^{-2/7} \qquad (1)$$

where τ is the risetime of the laser pulse and $\alpha_{1,2} = \frac{v_{os}}{c}(1,2)$ is the normalized oscillatory velocity of the two pump beams. Substituting τ = 1 ns and $\alpha_1 = \alpha_2 = 0.02$, parameters typical of the UCLA experiment, we find that in a 10^{17} cm^{-3} density plasma the plasma wave reaches saturation in 400 ps. If this is indeed the case then using time resolved, collective Thomson scattering technique[13] it should be possible to 'watch' the growth and saturation of the plasma wave. On the other hand 400 ps is perhaps too long a

time for the plasma to stay undisturbed without any other instabilites; only experiments can resolve this. The saturation amplitude is[12]

$$\frac{E_{z,sat}}{E_{z,max}} \alpha \frac{n_1}{n_e} = 4.15\ (\alpha_1\alpha_2)^{1/7}(\omega_p t)^{-2/7} \qquad (2)$$

where $E_{z,max} = mc\omega_p/e$ is the wavebreaking amplitude in a cold plasma. For the UCLA experiment the saturated amplitude turns out to be 9% which gives an electric field of 3 GeV/m, quite a respectable value. In the above example, we see that although the laser has a risetime of 1 ns, the saturation is reached at 400 ps, well before the peak electric field is reached. This is because as the plasma wave amplitude grows, the relativistic effects lead to a phase mismatch between the plasma wave and the driving beam. For efficient energy transfer from the laser to the plasma wave, one clearly wants to choose τ and α_1, α_2 such that saturation occurs towards the back of the laser pulse. This situation is schematically shown in Fig. 3.

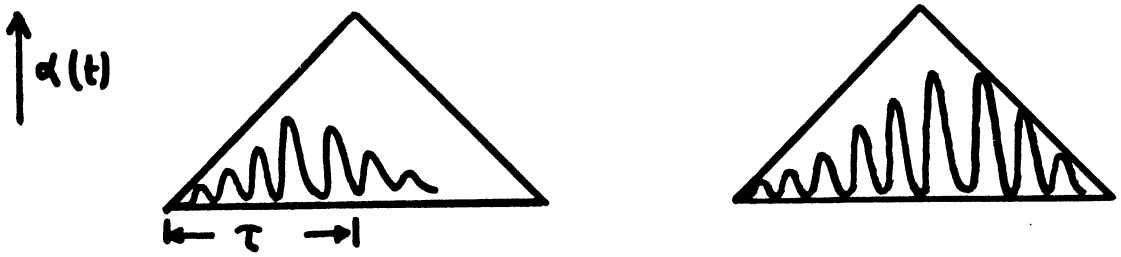

Figure 3.

There is one curious two-dimensional effect that is peculiar to the beat excitation of the plasma wave. This is the effect of the transverse beam

profile on the plasma wave build-up. In a conventional nonlinear amplifier, once saturation is reached the amplitude of the signal remains constant. For example in laser amplifiers, when a gaussian pulse, $\exp-(r/r_o)^2$ is injected, the beam center reaches saturation energy density before the 'wings' allowing the wing intensity to be amplified and 'catch up' with the center intensity. This leads to an amplified profile that is 'top hat', $\exp-(r/r_o)^n$ $n>2$. In beat wave excitation, if the laser beams have an intensity profile that is more intense in the center than it is at the edge, then the center indeed saturates first but once the saturation is reached the on axis amplitude actually begins to decrease, while the plasma wave amplitude on the edge is still building up. This can lead to a plasma wave that has a minimum on the center. This was pointed out by W. Mori and 2D simulations indeed show this to be the case (Fig. 4). Clearly this situation must be avoided in practice.

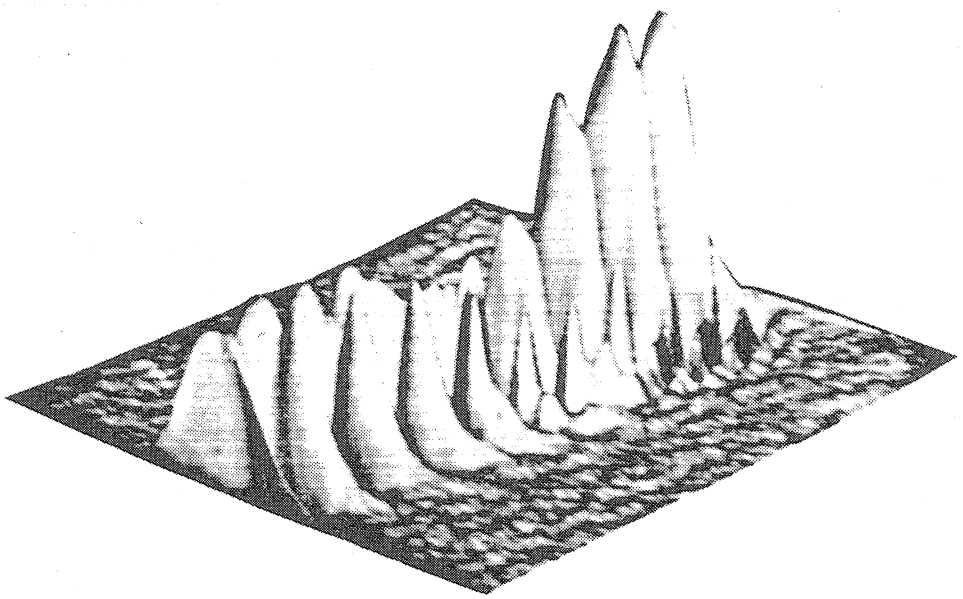

Figure 4.

The working group also reviewed the progress made on the theoretical front since Los Alamos. Of most significance is the proposal for phase

locking the particles in the accelerating bucket by T. Katsouleas and J.M. Dawson[14]. This concept called the SURFATRON is described elsewhere[30] and in this workshop by John Dawson, so it will not be discussed further here. Several groups[15,16] have been looking into the problem of laser beam trapping and/or self-focusing. Since there is an obvious interest in being able to keep the laser beams focused over distances much greater than the Rayleigh length, it is important to find out whether beams can be self-trapped such that self-focusing just balances diffraction and whether such self-trapped channels are stable[17,18].

Analytical and numerical work is being done by Tang et al.[19], Evans[20], Bingham[21], Katsouleas[22] and Noble[23], on the question of growth and saturation of highly non-linear plasma waves. Tang et al. find that if one starts off with a fractional frequency mismatch (1%) then plasma wave saturates at a much higher amplitude. In reality laser beams have a bandwidth and the plasma a variation in density. It is not clear whether the effect described in Ref. 19 is significant in real life.

W. Horton and T. Tajima[24] have considered the effect of plasma noise on the beat wave. The problem of emittance growth in a plasma as a result of multiple scattering is treated by B. Montague in these Proceedings.

III. DESIGN OF A 1 TeV PBWA

The working group was asked by the accelerator group to come up with a design for a 1 TeV accelerator based on the PBWA principle, however tentative such a design might be. It is obviously too early to come up with any meaningful design and in any case there are two reports[25,26] which outline a design philosophy. Nevertheless here we show some numbers which fall out naturally if we take the accelerator parameters specified by L. Hand and J. Rees.

Following the parameters given by L. Hand and J. Rees[27] we take:

Luminosity	10^{32} cm^{-2}s^{-1}
Frequency	4000 Hz
Particles per macrobunch	1.5×10^{9}
Bunch length	3 mm
Injection energy	1 GeV

The design parameters are:

Beam Loading	> 10%
$\Delta\phi/2\pi$	0.05
Minimum gradient	1 GeV/m

The variable parameters are:

plasma density	$10^{16} < n_e(cm^{-3}) < 10^{18}$
laser wavelength	$1 < \lambda\ (\mu m) < 10$

We choose λ = 0.25 μm (KrF) and use $E_z = 0.1\ E_{z\ max}$.

Plasma Density (cm^{-3})	E_z (GeV/m)	Length (m)	Energy Gain (GeV)
10^{16}	1	180	180
10^{17}	3	5.4	16.2
10^{18}	10	0.18	1.8

We consider the case of a 10^{17} cm^{-3} plasma, where the gain per stage limited by phase slip is 16 GeV. Thus we need roughly 62 stages to reach 1 TeV. Now we carry out a one-dimensional calculation. We neglect radial variation of the fields and assume that both the laser beams and the plasma wave are plane waves. In such a case the parameters turn out to be the following:

Plasma wave wavelength	100 μm
No. of bunchlets	30
Particles per bunchlet	5×10^7
Bunch density/Plasma density	1%
Bunch diameter	100 μm
Plasma wave diameter	500 μm
Plasma volume	1 cm^3
Plasma wave energy	16.65 Joules
Total energy gained by electrons	3.9 Joules
Beam loading	23%
Laser beam diameter	500 μm
Laser pulse width (square-pulse)	15 ps
Laser energy per pulse	2 kJ
$\alpha = V_{os}/c$	0.04
Build-up time of the plasma wave	15 ps
Laser-plasma wave coupling efficiency	1%

These are extremely approximate numbers and the error bars could easily turn out to be a factor of 3 to 5.

Technological issues such as whether or not a KrF laser firing at 4000 Hz and delivering a beam giving 2000 J in a 15 ps pulse can be produced are not considered. Also beam handling and optical transport problems are not addressed.

Since the laser to plasma wave coupling efficiency is rather low, beam depletion turns out not to be a problem. It's not clear if the 'left-over' energy in the laser beams can be used again or not at present. The working group did not evaluate the SURFATRON concept but it may be that SURFATRON is better able to utilize the energy in the laser beams.

IV. ISSUES NEEDING FURTHER STUDY (PBWA)

1) Multiple scattering

2) Laser to plasma wave coupling efficiency

3) Proper calculation done in Section 3 including transverse effects.

4) Issue of positron acceleration

5) Parametric decay of the plasma wave

6) Laser beam guiding in controllable plasma channels

7) Staging

V. THE PLASMA WAKE FIELD ACCELERATOR

The plasma wake field accelerator is so called because the idea is similar to other wake field schemes with plasma playing the role of the cavity or accelerating structure. The attraction of using a plasma once again is the very high accelerating gradients that might be achieved with no breakdown problem.

The idea due to J.M. Dawson and followed up by P. Chen[28] and R. Ruth et al.[29] is as follows: A bunch or bunches of electrons (appropriately spaced) excite a plasma wave or a wake field. A second beam or more precisely a bunch, trailing the driving bunch or bunches is accelerated by the wake field provided that it is at the correct phase on the plasma wave. As do all wake field schemes, this scheme suffers from the limitation that the total energy gain per particle is less than twice the initial energy per driving beam.

The idea is still in an embryonic stage and none of the 2D beam plasma effects have been investigated. Nonetheless the authors of Ref. 28 do give a conceptual design of a 1 TeV accelerator based on the PWFA principle. The efficiency of the device seems rather low but this is a very interesting scheme and further work is obviously needed.

VI. CONCLUSIONS

Considerable progress has been made in the last two years on understanding the physics of the PBWA.

Experiments are under way which should verify these issues. The laser pulse durations of the current experiments are probably too long but the intensities are adequate for what might be considered a proof-of-principle experiment which should be carried out in the near future.

The PWFA has interesting possibilities but 2D problems need to be tackled.

ACKNOWLEDGEMENTS

We wish to thank M. Tigner, L. Hand, and B. Willis for their contributions to our study group.

REFERENCES

1. Laser Acceleration of Particles, AIP Proceedings No. 91, Ed. P. Chanell (1982).
2. T. Tajima and J.M. Dawson, Phys. Rev. Lett. 43, 267 (1979).
3. T. Tajima, AIP Conference Proceedings No. 91, Ed. P. Chanell (1982).
4. D. Sullivan and B. Godfrey, Ref. 1, p. 43.
5. C. Joshi, C.E. Clayton and F.F. Chen, Phys. Rev. Lett. 48, 874 (1982).
6. D.W. Forslund, et al., Phys. Rev. Lett. (to be published).
7. C. Joshi, et al., Nature 311, 525 (1984).
8. M.N. Rosenbluth and C.S. Liu, Phys. Rev. Lett. 29, 701 (1972).
9. R. Bingham, Rutherford Laboratory Report RL-83-053, November 1983.
10. P. Goldstone, Private communication.
11. B. Dangor, Private communication.

12. W. Mori, M.S. Thesis, University of California, Los Angeles (1984), unpublished.

13. C.E. Clayton, C. Joshi and F.F. Chen, Phys. Rev. Lett. 51, 1656 (1983).

14. T. Katsouleas amd J.M. Dawson, Phys. Rev. Lett. 51, 392 (1983).

15. G. Schmidt and W. Horton, Private communication.

16. F. Felber, Private communication.

17. R. Bingham and H. Cairns, Private communication.

18. J. Dawson, Private communication.

19. C.M. Tang, et al., Appl. Phys. Lett. 45, 375 (1984).

20. R. Evans, Rutherford Laboratory Report RAL-84-086 (1984).

21. R. Bingham, Private communication.

22. T. Katsouleas, Private communication.

23. R. Noble, Private communication.

24. W. Horton and T. Tajima, submitted to Phys. Rev. A.

25. R. Ruth and A. Chao, Ref. 1, p. 94.

26. J.D. Lawson, Rutherford Laboratory Report RAL-83-057 (1983).

27. L. Hand and J. Rees, proceedings of this workshop.

28. P. Chen, et al., submitted for publication to Phys. Rev. Lett..

29. R. Ruth, et al., submitted for publication to Particle Acceleration.

30. C. Joshi, W.B. Mori, T. Katsouleas, J.M. Dawson, J.M. Kindel and D.W. Forslund, Ultrahigh gradient particle acceleration by intense laser-driven plasma density waves, Nature Vol. 311, 11 October 1984, p. 525.

Discussion

R. Palmer, BNL

This is a strictly leading question, but for looking at laser-grating and laser-droplet accelerators one needs a high power 3 to 30 ps laser at the CO_2 wavelength and we would need an electron source which was bright so that we could investigate beam-loading. If such a facility were built, would you be interested in doing beatwave experiments with it?

Answer

The answer to that is yes, but I feel that we are probably several years away from investigating questions of beam loading and efficiency of transfer from laser to particles and so forth. We would do the next phase of experiments just to look at the physics issues, but certainly at some stage we need to go to very short pulses and look at these problems.

J. Nation, Cornell

When you were discussing your 1 TeV concept you discussed a stage that would give you 30 GeV or whatever. Did you spend any time at all addressing any of the problems relating to staging?

Answer

No, not really. My feeling is, that the energy coming out of a stage is much, much larger, than the initial energy, so the problem associated with the edge effects of the plasma are probably not too severe and therefore you can just go from one stage into the next stage, as long as the lasers are properly phased.

R. Palmer

In the case of the surfatron, you bring the wave in at a finite angle to the path of the particle and in that way obtain synchronisation which will go on for ever. A suggestion, which I have been mulling over, is instead of using a magnetic field to generate the sideways motion, if you can bring the wave in from one side, you could also bring the wave in from the other side, and if you can bring it in from the other side you can also bring it from above and below providing the slip angle is always maintained. If you do that all the way round, then you get essentially an inverse Cerenkov cone of incoming light and obtain synchronisation along the axis for ever. You obtain a lot of other things too because the intensity is now greatest along the axis. There will be transverse

focusing because these buckets will fall away in intensity sideways. The question is, I suppose, why doesn't that become considered the standard way of doing it?

Answer

That obviously would be the way to go and that is the first thing we thought of. The problem is that if you bring in lasers from outside at an angle, then there are other coupling modes from laser to plasma, more dominant than the one you want.

THE BEAT-WAVE ACCELERATOR : TWENTY QUESTIONS

J D Lawson
Rutherford Appleton Laboratory, Chilton, Oxon OX11 0QX

ABSTRACT

Many questions in the fields of accelerator physics, plasma physics and laser technology need to be addressed if a useful accelerator based on the beat-wave principle is to be constructed. Many of these must be considered together rather than sequentially. An attempt has been made to set out a number of the more important questions in a logical manner.

It has been conjectured that it may be possible one day to build an accelerator useful for high energy physics research that is based on the 'beat-wave' principle. Two intense laser beams with frequency difference $\omega_1 - \omega_2 = \omega_p$ are fired simultaneously into a plasma to produce a longitudinally polarized plasma wave at the plasma frequency ω_p with phase velocity not much less than c.

A particle accelerator is a complicated 'system', and if such an enterprise is ever to come to fruition many parameters must simultaneously be accomodated within a set of constraints, physical, technical and financial. In principle these constraints can be represented in n-dimensional parameter space as n-1 dimensional bounding 'surfaces' between 'allowed' and 'disallowed' regions. We must enquire whether a volume exists in which all parameters have allowed values; if it does, we must locate it.

Of course the nature of the constraints is not yet known. Further, they are all interdependent, and cannot be considered singly. Nevertheless, it is important early on to try to identify all the major parameters and form some idea of how they are related. To begin with, it is of course necessary to look at the relationship between limited groups of parameters. The overall relationship of all the groups must be kept in mind; optimization within one group without reference to others is highly inefficient! To start with, a list of questions is often helpful; this must not be too long and detailed, but should include all the main features of the accelerator and not just questions of beat-wave physics. The attached list, based on experience in the RAL study, is suggested for consideration. Statements are designated S, questions Q. An attempt has been made to arrange the questions in a logical order. Guessed answers to some of them are in square brackets.

S1. Two questions may be asked:

Q1. Is it possible that a useful accelerator based on laser light can be built?

Q2. Can laser accelerators contribute to research in high energy physics?

S2. We consider only the second.

S3. We must therefore ask:

Q3. What is the minumum energy worth considering a) for electrons and b) for protons? [1 TeV and 30 TeV?]

Q4. Machines will be linear, and operate in colliding beam mode. What is the minimum acceptable luminosity a) for electrons and b) for protons [10^{32}?]

Q5. High energy and luminosity implies high beam power. What limit do we impose as a credible upper limit to P in the whole installation? [1GW?]

Q6. The beam power is then ηP. What value of η can we hope for? [5%?]

S4. The luminosity is defined as $L=N^2f/A$ where N is number of particles in bunch, f=frequency and A is beam area. The beam power $P=Nf\ \gamma m_0c^2$. This gives two relations to define the three parameters N,f,A. A set of curves or table of acceptable values would be useful here.

S5. These curves should include also luminosity enhancement due to pinch effect. From the two equations in S3 $L\propto P^2/fA$; this implies small A small f and high N. Limits to N arising from disruption and beamstrahlung should be indicated on the curves.

Q7. These curves will indicate a very small value of A, of order $10^{-6}cm^2$. What is the implication for emittance?

Q8. What is the permissible energy spread in the beam? (There are two considerations 1) requirements for experiments, [10%?] 2) requirements for focusing of beam). [1%?]

S6. ENOUGH BASIC REQUIREMENTS HAVE NOW BEEN STATED TO MAKE THE FIRST ATTEMPTS AT ASSESSING THE BEAT WAVE CONCEPT AS AN ACCELERATOR.

S7. Basic parameters for BWA are:

a) Plasma density n, $\propto\omega_p^2$, this controls maximum E_z.

b) Laser frequency ω_1

c) ω_p/ω_1, this controls wave velocity.

Q9. What are the relations between these and related parameters, and over what conceivable range of practical values could a BWA operate?

Q10. What pulse lengths are required a) to set up wave b) to accelerate enough particles?

Q11. Where do accelerated particles come from initially? How is the very low emittance that is required obtained? How is bunching achieved? What is phase width of bunch?

Q12. What can be assumed about laser optics? Is the light beam gaussian or are self-focusing effects important? What is the diameter of the beam channel?

Q13. What is the transverse size and physical nature of the plasma or gas channel? For how long a pulse can the channel be sustained with resonant plasma?

Q14. Clearly many stages are required; what determines the stage length?

Q15 Taking into account power and breakdown considerations, how are the lasers, mirrors etc configured in a practical system?

Q16. In particular, how are the stages arranged so that laser beams through different stages do not interfere? Can this be done without magnets? If not, can suitable achromatic benders be designed?

Q17. What are the power, pulselength, and repetition rate needed to satisfy the requirements defined in questions 1 - 8?

Q18. What transverse focusing and defocusing forces associated with the finite channel size are there?

Q19. How is focusing maintained between stages?

Q20. What effect do random transverse forces, arising from a) multiple scattering and b) plasma noise have on the beam emittance?

S8. Most of these questions (and many others) were thought about, but not satisfactorily answered, in the RAL study. There seem to be three alternatives for continuing the studies.

1) Try to resolve the problems.
2) Guess that they cannot be resolved and seek an alternative scenario.
3) Adopt the view that it is too early to think about accelerators, and concentrate on such physics as is considered interesting.

ANALYTICAL AND NUMERICAL STUDIES OF PLASMA BEAT WAVES

R. Bingham, R.A. Cairns*) and R.G. Evans
Rutherford Appleton Laboratory, Chilton, Didcot, OX11 0QX

ABSTRACT

We analyze the saturation mechanism for the electrostatic plasma wave excited by two electromagnetic waves, and show that the level is determined not only by the relativistic frequency shift but also by the frequency shift produced by second harmonics of the electrostatic plasma wave. The frequency shift due to the higher harmonics dominates, with the frequency increasing rather than decreasing with amplitude. The positive frequency shift makes the wave stable to the development of strong turbulence. The analytical results are directly checked by numerical simulations carried out using a 1-D particle in cell code showing excellent agreement between the two approaches.

Recently, there has been considerable interest in the nonlinear excitation of large amplitude plasma waves by beating two laser beams in an underdense plasma[1,2] as a particle accelerator for high energy physics, proposed by Tajima and Dawson[1] and known as the "Plasma beat wave accelerator". The scheme depends on the generation of a large amplitude plasma wave with a phase velocity close to the velocity of light. Such a wave can be produced by beating two colinear laser beams, with frequencies and wavenumbers (ω_1, k_1) and (ω_2, k_2) in a plasma where the frequency and wavenumber of the plasma wave satisfy the following resonance conditions.

$$\omega_p = \omega_1 - \omega_2 \qquad \ldots.(1)$$

$$k_p = k_1 - k_2$$

The laser beams exert a periodic force (the ponderomotive force) on the electrons and resonantly drive the plasma wave which consists of regions of space charge. If $\omega_p << \omega_{1,2}$ then the phase velocity of the plasma wave

---

*) Mathematical Institute, University of St Andrews, St Andrews KY16 9SS, Fife, Scotland.

$v_{ph} = \omega_p/k_p$ is equal to the group velocity of the laser beams $v_g = c(1-\omega_p^2/\omega_{1,2}^2)^{\frac{1}{2}}$ equal to the speed of light c in an underdense plasma. Particles which are injected into the beat wave region with a velocity comparable to v_{ph} can gain more energy from the longitudinal electric field of the plasma wave.

Previous studies[3,4] on the nonlinear behaviour of the large amplitude plasma wave have concentrated on the relativistic effects being the only saturation mechanism for the plasma wave. The relativistic mass increase of the plasma electrons has the effect of reducing the natural frequency of oscillation of the wave which ultimately destroys the phase locking and hence provides a saturation mechanism. In this paper we will not only include the relativistic correction factor but also the effect of second harmonic perturbations having frequency $2\omega_p$, these terms provide not only a much larger frequency shift than the relativistic term but also one of opposite sign. The correction due to these terms increases the natural frequency of oscillation rather than decreasing it which makes the wave stable to modulational instabilities.

Results from a numerical simulation using particle in cell methods agree well with the analytical theory.

We consider an unmagnetised plasma with two parallel propagating electromagnetic waves with electric fields given by

$$\frac{1}{2}\left(\underline{E}_j(\underline{x},t) \exp i(\underline{k}_j.\underline{x} - \omega_j t) + c.c.\right) , \; j = 1,2 \qquad - (2)$$

with polarization electric field along the y-axis with frequencies ω_j much greater than the plasma frequency ω_p. The normalized quiver velocities are $\alpha_j = e\,E_j/m_e\omega_j c$.
The equations describing the behaviour of the electrons are the relativistic fluid equations and Poissons equation,

$$\frac{\partial n_e}{\partial t} + \nabla.(n_e \underline{v}_e) = 0 \qquad -(3)$$

$$\left(\frac{\partial}{\partial t} + \underline{v}_e.\nabla\right)\gamma v_e + \frac{3KT_e}{n_o m_e}\nabla n_e = -\frac{e}{m_e}\left(\underline{E} + \underline{v}\times\underline{B}\right) \qquad -(4)$$

$$\nabla.\underline{E} = \frac{e}{\epsilon_o}(n_o - n_e) \qquad -(5)$$

where $\gamma = (1-(v_e/c)^2)^{-\frac{1}{2}}$ and n_o is the plasma density. The ions cannot respond to forces acting at the electron plasma frequency and are therefore neglected. However, if we wish to study the stability of the large amplitude plasma wave with respect to wave decay and modulational instabilities due to the ponderomotive force of the plasma wave the ion dynamics must be included.

Using equations (3)-(5) and assuming $v_e^2/c^2 \ll 1$ in the Lorentz factor we obtain the equation describing the electron density perturbation n_e

$$\left(\frac{\partial^2}{\partial t^2} - 3v_{Th}^2\frac{\partial^2}{\partial x^2} + \omega_{pe}^2\right)n_e = \frac{3}{2}\omega_{pe}^2\frac{v_e^2}{c^2}n_e + \frac{n_o e}{m_e}\frac{\partial}{\partial x}(\underline{v}_{1,2}\times\underline{B}_{2,1})$$

$$+ n_o\frac{\partial}{\partial x}\left(v_e\frac{\partial}{\partial x}v_e\right) - \frac{\partial}{\partial t}\frac{\partial}{\partial x}(n_e v_e) \qquad -(6)$$

where v_{Th}^2 is the electron thermal velocity, $v_{1,2}$ is the electron velocity in the transverse laser fields and $B_{1,2}$ is the magnetic field. The first term on the right hand side of equation (6) comes from the expansion of the relativistic Lorentz factor the second term represents the nonlinear coupling to the two high frequency laser beams. The last two terms represent the coupling between the fundamental and the second harmonic of the plasma wave which gives rise to a plasma response at the ω_p, these two terms have been neglected in previous work[3,4].

We assume $n_e = n_e^{(1)} + n_e^{(2)} + \ldots$, and $v_e = v_e^{(1)} = v_e^{(1)} + v_e^{(2)} + \ldots$

where the superscripts refer to first and second harmonic terms such that

$$n_e^{(m)} = \frac{1}{2}\left(N_m(x,t) \exp im(k_p x - \omega_p t) + c.c. \right) \qquad -(7)$$

where $N_m(x,t)$ is a slowly varying amplitude describing the nonlinear behaviour of the wave linear phase. From the fluid equations we can write expressions for $v_e^{(1)}$, $v_e^{(2)}$ and $n_e^{(2)}$ in terms of $n_e^{(1)}$

$$v_e^{(1)} = \frac{\omega_p}{k_p}\frac{n_e^{(1)}}{n_o}$$

$$v_e^{(2)} = \frac{k_p}{2\omega_p}\frac{n_e^{(1)} n_e^{(1)}}{n_o^2} \qquad -(8)$$

$$n_e^{(2)} = \frac{k_p}{\omega_p}\left(n_o v_e^{(2)} + n_e^{(1)} v_e^{(1)} \right)$$

Using (7) and (8) in (6) and expressing the transverse wave variables $v_{1,2}$ and $B_{1,2}$ in terms of the electric field given by equation (2) and separating the slow and fast times scales we obtain the following equation for the slowly varying amplitude $N_1(x,t)$

$$i\left(\frac{\partial}{\partial t} + v_{pg}\frac{\partial}{\partial x}\right)N + \frac{1}{2}\frac{\partial^2 \omega_p}{\partial k_p}\frac{\partial^2 N}{\partial x^2} + \frac{\omega_p^3}{n_o^2 k_p^2 c^2}\left(\frac{3}{16} - \frac{1}{2}\frac{k_p^2 c^2}{\omega_p^2}\right)|N|^2 N$$

$$= \frac{n_o e^2 k_p^2}{4 m_e^2 \omega_1 \omega_2 \omega_p} E_1 E_2^* \exp(-i\delta t) \qquad -(9)$$

where v_{pg} $(=v_{Th}^2 k_p/\omega_p)$ and δ is a frequency mismatch ($\delta = \omega_1 - \omega_2 - \omega_p$), we have also dropped the subscript on N.

Equation (9) is a nonlinear Schrodinger equation with a cubic nonlinearity and a driving term. The cubic nonlinearity is composed of two competing parts, the first comes from the relativistic correction and the second is the contribution due to the presence of harmonics. These two terms produce a frequency shift of the plasma wave. For the beat wave where $k_p = \omega_p/c$ the frequency shift due to the presence of the harmonic terms is greater than the relativistic term, the resultant shift is given by

$$\Delta\omega = \frac{5}{16}\omega_p \frac{|N|^2}{n_o}$$

This nonlinear frequency shift increases the plasma wave frequency, whereas the relativistic term decreases the frequency by $-3\omega_p|N|^2/16n_o^2$

The dispersion relation for the plasma wave can be written as

$$\omega(k,\delta n) = \omega_o(k) + \frac{5}{16}\omega_p\delta n^2 \qquad \ldots\ldots(11)$$

where $\omega_o(k)$ is the linear dispersion and δn $(=|N|/n_o)$ is the normalized wave amplitude.

The nonlinear frequency shift given by the cubic nonlinearity in equation (9) has important consequences regarding the self-modulation of the plasma wave. Self modulation leads to strong turbulence, generating multiple sidebands, broadening the wave spectrum, destroying its coherence and hence its accelerating efficiency. A simple test for self modulation is given by Whitham[5], who has shown that if $\Delta\omega>0$ the wave is stable, therefore any long wavelength perturbations will tend to be smoothed out. Self-modulation due to ponderomotive effects have been neglected since they occur on the ω_{pi}^{-1} time scale.

Setting $N(t)/n_o = A(t)e^{i\phi(t)}$, we find in the linear approximation the wave amplitude grows according to[3] $A(t) = A(0)+\alpha_1\alpha_2\omega_p t/4$ until $A(t)=1$ ie when the electron quiver velocity in the longitudinal wave equals c. The amplitude however will saturate well before reaching this level as a

result of the nonlinear frequencyshift. Including this frequency shift and a frequency mismatch and consider only the time dependent case equation (9) becomes

$$\frac{dA}{dt} = \lambda \sin\phi \qquad -(12)$$

$$\frac{d\phi}{dt} = \beta A^2 + \frac{\lambda}{A}\cos\phi - \delta \qquad -(13)$$

where $\lambda = \omega_p \alpha_1 \alpha_2/4$ and $\beta = 5\omega_p/16$. A constant of motion associated with Eqs. (12) and (13) is

$$A\left[A^3 - 2\delta A/\beta + 4\lambda\cos\phi/\beta\right] = C \qquad -(14)$$

where C = 0 since A(t=0)=0. Using (14) equation (12) becomes

$$\left(\frac{dA}{dt}\right)^2 = 1 - \left(\frac{\beta A^3}{4\lambda} - \frac{\delta A}{2\lambda}\right)^2 \qquad -(15)$$

Wave growth stops when dA/dt =0, and for δ=0 ie perfect phase matching the saturation amplitude is

$$A = \left(\frac{16}{5}\alpha_1\alpha_2\right)^{\frac{1}{3}} \qquad -(16)$$

for $\delta \neq 0$ the maximum amplitude A_{MAX} at saturation for fixed $\alpha_1\alpha_2$ is obtained from the cubic equation

$$A^3 - \frac{32}{5}\frac{\delta}{\omega_p}A - \frac{16}{5}\alpha_1\alpha_2 = 0 \qquad -(17)$$

resulting in

$$A_{MAX} = 4\left(\frac{\alpha_1\alpha_2}{5}\right)^{\frac{1}{3}} \qquad -(18)$$

for a frequency mismatch δ given by

$$\frac{\delta}{\omega_p} = \frac{3}{4}\left(\frac{\sqrt{5}}{\sqrt{8}}\alpha_1\alpha_2\right)^{2/3} \qquad -(19)$$

The maximum plasma wave amplitude A_{MAX} given by eqn (18) is larger than that given by eqn (16) where $\delta=0$. This is easily explained by the increase of the plasma wave frequency, given by eqn. 11, reducing the mismatch as the amplitude increases. A relativistic 1D electrostatic particle in cell code described in ref. 6 was used to confirm the accuracy of the analytical treatment. The results of a typical run with $\omega_{1,2}/\omega_p$ = 100 are shown in Fig 1. The electric field is plotted at two different times showing the growth and saturation of the field. The field is initially sinusoidal and develops a strong sawtooth before saturation. The saturation amplitude agrees well with the analytic result given by eqn (16) as shown in fig 2. As shown in the analytic treatment the main mechanism for detuning is the frequency shift introduced by the net effect of relativistic mass increase and second harmonic generation at large amplitude. This effect is overcome partially by driving the plasma wave slightly off resonance causing the wave to saturate at higher values. This is also found in the simulations, an example for fixed $\alpha_1\alpha_2$ (=0.013) being illustrated in Fig 3. For perfect resonance ie δ = 0 the wave amplitude saturates close to the value given by eqn 16 as expected, but a small reduction in the plasma frequency, δ/ω_p = 0.015 causes the wave to grow slightly more slowly in the initial stages, but maintain growth for a longer time. The maximum amplitude reached is about 1.6 times the "resonant" (δ=0) value. Since the saturated field is proportional to the one third power of the laser intensity it is equivalent to an increase in pump power of nearly a factor of four. Again there is excellent agreement between the analytic result obtained from eqn (17) and the simulations.

In conclusion we have shown that the effect of harmonic terms is to produce a frequency shift which is larger than that due to relativity and of the opposite sign. This has the important consequence that the beat wave is stable against self-modulation and strong turbulence. On a time scale when ion motion is important other instabilities may develop and may necessitate short laser pulses.

REFERENCES

1. T. Tajima and J. M. Dawson, Phys Rev Lett., 43, 267 (1979).

2. C. Joshi, T. Tajima, J. M. Dawson, H. A. Baldis and N. A. Ebrahim Phys Rev Lett. 47, 1285 (1981).

3. M. N. Rosenbluth and C. S. Liu, Phys Rev Lett. 29, 701 (1972).

4. C. M. Tang, P. Sprangle and R. N. Sudan, App Phys Lett. 45, 375 (1984).

5. G. B. Whitham, Linear and Nonlinear Waves John Wiley and Sons, New York (1973).

6. R. G. Evans, Rutherford Appleton Laboratory Report, RAL-84-086 (1984).

Note added in proof

The difference between the frequency shift calculated in this paper and by Rosenbluth and Liu (Ref. 3) has been found to be due to the drift induced in an infinite plasma by a longitudinal plasma wave. The drift velocity is $v_{D/C} = 1/2(v_0^2/c^2)$ and makes the laser frequency appear less in the moving frame of the plasma electrons.

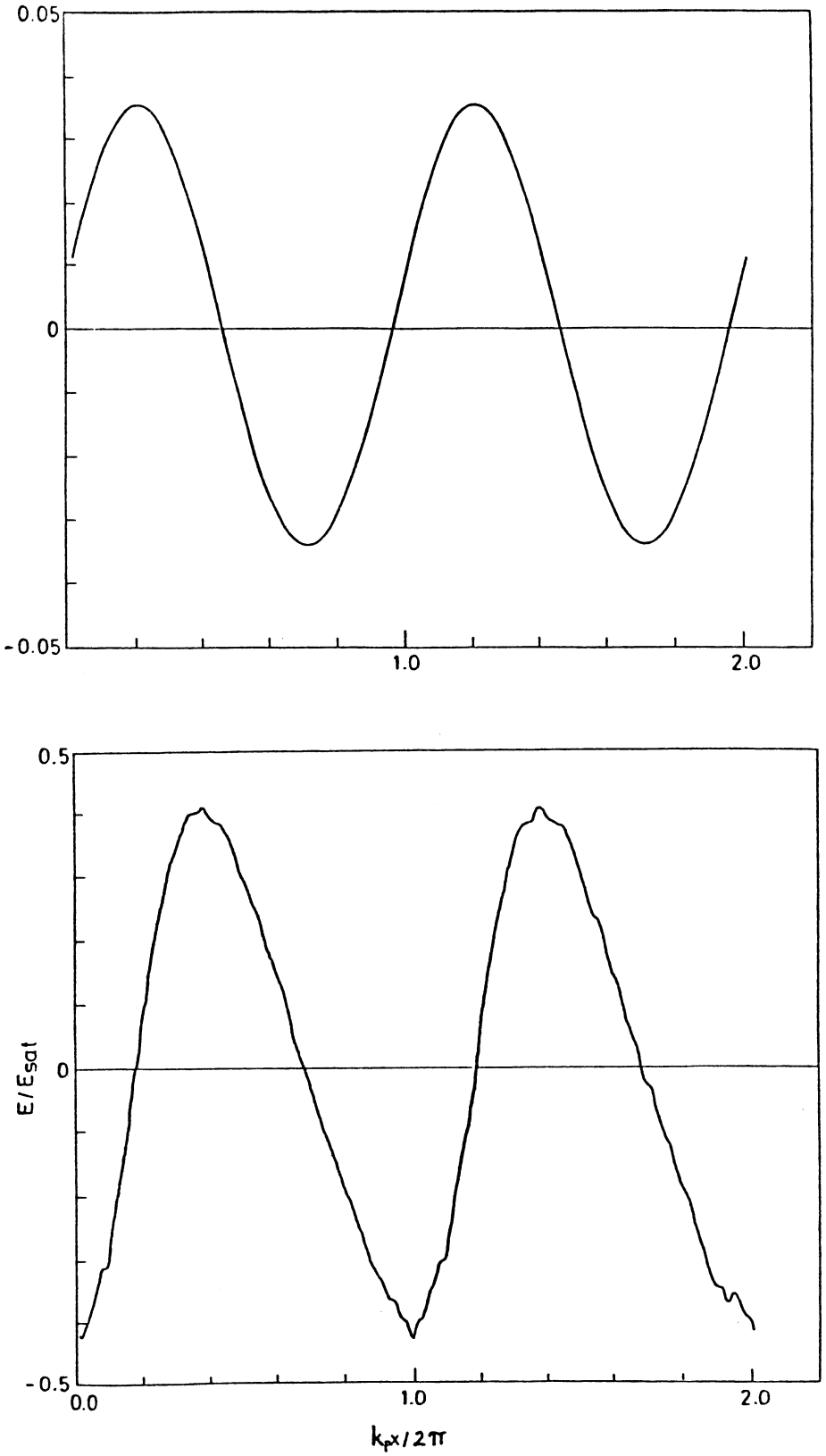

Fig 1 Electric field profiles at $(t/\tau_p) = 1$ and 13 for a pump strength of $\alpha_1\alpha_2 = 0.013$

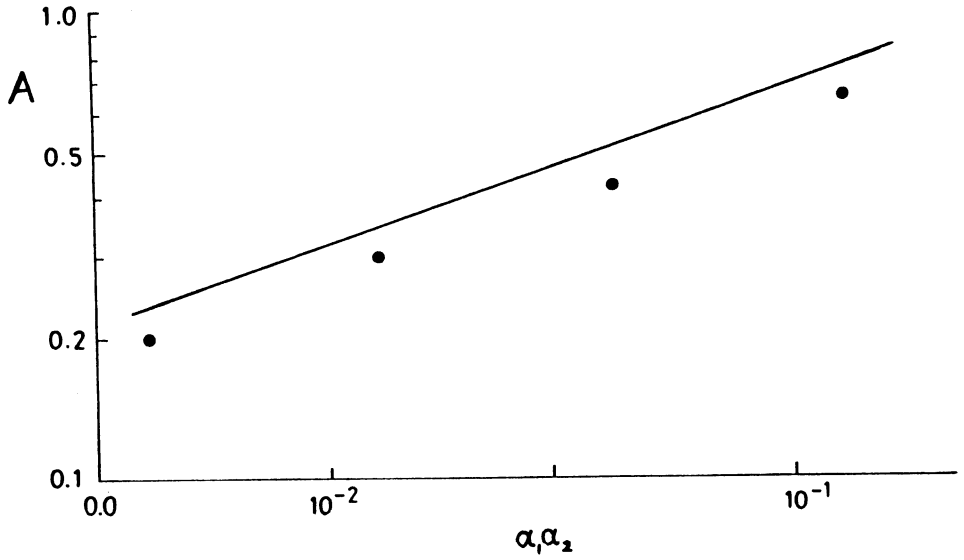

Fig 2 Saturated wave amplitudes as a function of pump intensity, dots simulation data, solid line theoretical result from equ 16.

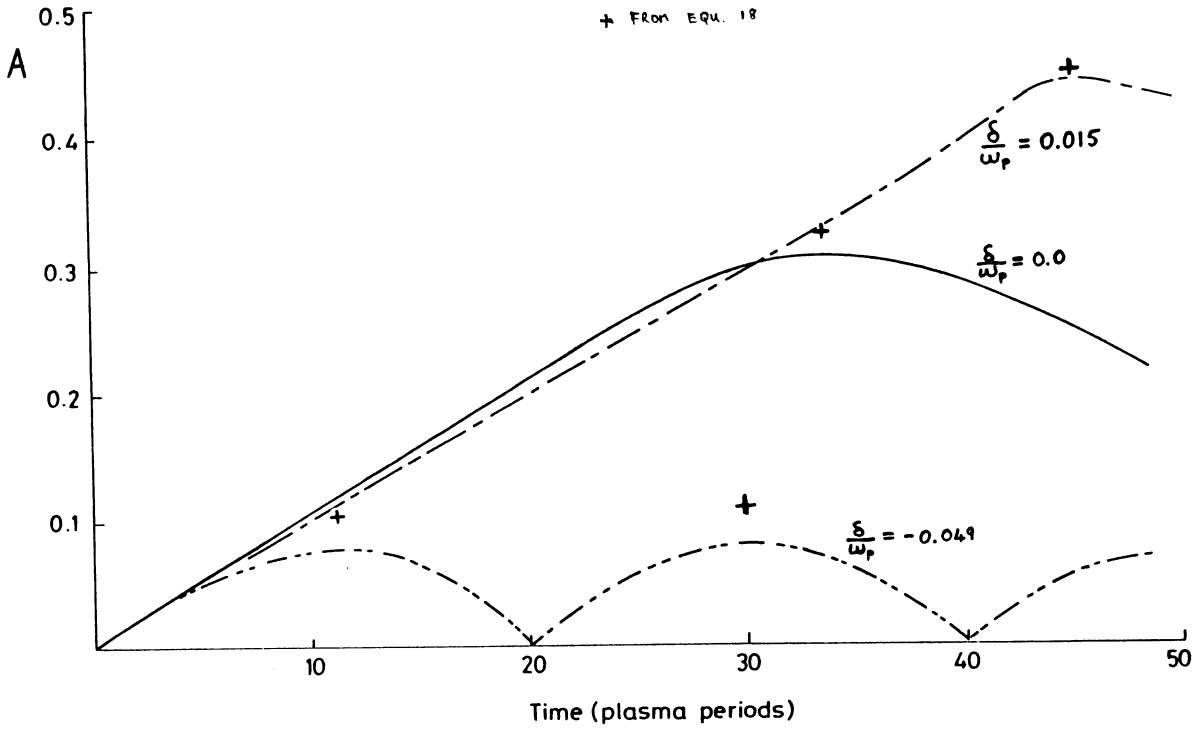

Fig 3 Wave amplitude as a function of time for different mismatch frequencies δ . The crosses represent the theoretical result obtained from equ 17.

RADIAL ELECTRIC FIELDS IN THE BEAT-WAVE ACCELERATOR

R.G. Evans
Rutherford Appleton Laboratory, Chilton, United Kingdom

ABSTRACT

The DC pondermotive force of the laser beams in the beat-wave accelerator causes a small but significant difference in the radial focusing of positive and negative charged particles.

Due to the finite width of the laser pump beams the electric fields generated in the "beat-wave accelerator"[1] will not be purely longitudinal. The effects of the radial dependence of plasma wave amplitude have been analysed by J.D. Lawson[2]. It is assumed that the longitudinal wave amplitude has a quadratic dependence on radius, r

$$E_z(r) = E_z\left(1 + \frac{r^2}{r_0^2}\right) \tag{1}$$

where r_0 is the laser beam radius.

The radial electric field is then found to be

$$\frac{E_r}{E_z} = \frac{2r}{k_p r_0^2} \tag{2}$$

where k_p is the wavenumber of the plasma wave. The longitudinal field E_z is given in terms of the plasma density fluctuation as

$$eE_z = m\,c\omega_p \cdot \frac{\delta n}{n} .$$

Thus

$$eE_r = \frac{2mc^2}{r_0^2} \cdot \frac{\delta n}{n} \cdot r \tag{3}$$

since $\omega_p/k_p = c$

and if $\delta n/n$ is limited by detuning at large amplitude then

$$\frac{\delta n}{n} = \frac{16}{5} \left(\frac{v_0}{c}\right)^{2/3} . \qquad (4)$$

The radial electric field E_r is 90° out of phase with the longitudinal field E_z so that one half of the accelerating cycle is radially focusing and one half is radially defocusing.

A second, and hitherto neglected effect is the radial field induced by the DC component of the ponderomotive force. This force results in the expulsion of plasma electrons from the intense parts of the laser beam and thus tends to focus injected negative charges and defocus injected positive charges. It introduces an asymmetry between the betatron wavelengths in the two halves of a linear collider.

The ponderomotive potential is conveniently expressed in terms of the oscillating velocity of the electrons in the laser fields

$$e = \frac{1}{4} m \left(v_{01}^2 + v_{02}^2\right) \quad ; \quad v_0 = \frac{eE}{m\omega} .$$

For conveniience we assume that $v_{01} = v_{02}$.

If the plasma potential is assumed to be parabolic and to build up at the boundary $r = r_0$ to just compensate the ponderomotive potential then

$$eE_r^{DC} = \frac{mv_0^2}{r_0^2} \cdot r . \qquad (5)$$

Since the injected particles are moving close to the phase velocity of the electromagnetic waves they do not see the ponderomotive force of the pump waves, but they are affected by the potential built up by the ponderomotive force acting on plasma electrons.

The ratio of DC to AC electric fields is given by (3) and (5) as

$$\frac{E_r^{DC}}{E_r^{AC}} = \frac{5}{32\xi} \left(\frac{v_0}{c}\right)^{4/3}$$

where ξ is the ratio of $\delta n/n$ achieved in practice to the value of $\delta n/n$ given by the detuning limit. Unless ξ is very small the DC field will

introduce a small, but noticeable difference in the focusing properties for positive and negative particles.

ACKNOWLEDGEMENTS

This work arose out of discussions in the media working group and thanks are particularly due to J.D. Lawson, W. Willis, B.W. Montague and P.B. Wilson.

* * *

REFERENCES

1) T. Tajima and J.M. Dawson, Phys. Rev. Lett. 43, 267 (1974).

2) J.D. Lawson, Rutherford Appleton Laboratory Report RL-83-057 (1983).

3) R. Bingham, R.A. Cairns and R.G. Evans, "Saturation of Plasma Beat Waves", submitted to Phys. Rev. Lett.

EMITTANCE GROWTH FROM MULTIPLE SCATTERING IN THE PLASMA BEAT-WAVE ACCELERATOR

Bryan W. Montague
CERN, Geneva, Switzerland.

ABSTRACT

Linear colliders for very high energies will require beams of extremely small emittance. In the plasma Beat-Wave Accelerator, multiple scattering from the plasma ions can cause emittance growth. A calculation of this growth is given for an example of a 1 TeV BWA.

1. INTRODUCTION

The plasma Beat-Wave Accelerator (BWA) proposed by Tajima and Dawson[1] offers a possibility of obtaining the extremely high accelerating fields that will be necessary in order to build, within an acceptable size and cost, linear colliders in the energy range of 1 to 10 TeV. Such intense fields can in principle be obtained in a highly-ionised plasma from charge separation induced by two laser beams, whose difference freqency resonates with the plasma frequency. The details of this process are described in Refs. 2, 3 and 4, which contain more extensive bibliographies.

So far no fundamental objection to the principle has appeared, and the BWA remains a serious contender for high-field generation. However, much theoretical and experimental work will be required before the feasibility can be properly assessed, and many questions remain to be resolved.

One of these questions, which is the subject of this report, concerns multiple scattering of the accelerated beam by the particles in the plasma. To obtain high luminosity within reasonable limits of beam power requires very small beam dimensions at the collision point and hence low beam emittance. Appreciable enhancement of the emittance by collisions with plasma particles would degrade the performance of the machine. This consideration was evoked by the RAL Study Group[4] and has been further discussed at this Workshop, from which it is apparent that a more precise estimate is needed.

Scattering of accelerated particles by the residual gas in a synchrotron is a familiar problem in accelerator physics which was already treated in 1948 by Blachman and Courant[5], and subsequently by many others. The situation in a BWA, though similar in principle, differs in detail for two main reasons. Firstly, we are dealing with an ionised plasma rather than neutral atoms or molecules, which has an influence on the effective range of the Coulomb force. Secondly, the transverse focusing of the accelerated beam in the BWA will in general be a function of energy which will influence the rate of emittance growth along the machine. It is therefore appropriate to derive scattering formulae which take into account these features.

As a basis for the calculation we take the conceptual design of a BWA elaborated at this Workshop. It consists of an e^+-e^- linear collider of 1 TeV per beam, with injection energy assumed to be about 10 GeV. The accelerated electrons are therefore highly relativistic over the whole energy range. A plasma of density $n = 10^{17}cm^{-3}$ yields an accelerating field of 6 GeV m^{-1} with a stage length of 5.4 m, giving a total length per linac of about 170 m. We assume a fully-ionised hydrogen plasma. In line with most of the references cited, c.g.s. units will mainly be used, though with energies in electron-volts.

2. SMALL-ANGLE SCATTERING

In the approximation of small angles $\theta \ll 1$, elastic scattering by a Coulomb central force is well described by the simplified Rutherford formula :

$$\theta = \frac{\Delta p}{p} \simeq \frac{2zZe^2}{pvb} \qquad (1)$$

where p, v, ze are respectively the momentum, velocity and charge of the incident particle, Ze is the charge of a stationary nucleus, Δp is the momentum transfer in the collision and b is the impact parameter, i.e. the perpendicular distance from the nucleus to the initial trajectory of the incident particle. For a point Coulomb field in the absence of screening, the Rutherford formula is exact quantum mechanically for the statistical distribution of scattering angles, even under conditions where classical trajectories cannot strictly be defined. Since we are considering highly relativistic incident particles we put $v = c$ in Eq.(1) which, for unit charge of both beam and plasma particles, becomes :

$$\theta = \frac{\Delta p}{p} \simeq \frac{2e^2}{pcb} \quad . \qquad (2)$$

Deviations from Eq.(2) occur both for very close collisions (small b) and for distant collisions (large b). Outside these limits the momentum transfer Δp is less than that given by a point Coulomb field, due to saturation or screening. This is taken into account to a good approximation by imposing limits b_{min} and b_{max}, corresponding to θ_{max} and θ_{min} respectively, on the range of integration of the scattering cross-section. The precise evaluation of these limits depends on the system in question and may be governed by either quasi-classical or strictly quantum-mechanical constraints. A very lucid and detailed discussion of these questions appears in a famous review by Bohr[6].

Scattering by neutral atoms or molecules has been extensively studied[7] and the results are widely applied as approximate formulae based on theoretical models of atoms adjusted by experimental observations. The minimum impact parameter b_{min} is governed by the effective radius of the nucleus, whilst b_{max} is determined by the shielding effect of the atomic electron shells. In a fully-ionised plasma, however, the electrons are not bound by individual nuclear charges but rather by the aggregate of Coulomb fields from

many nucleons. The cut-off of the Coulomb field will then be determined by the Debye shielding distance, which is generally much greater than atomic radii. In the following we therefore examine multiple scattering in the BWA from basic principles, using a number of results from Jackson[8] and applying cut-offs appropriate to a hydrogen plasma. For highly energetic incident particles we need only consider scattering from the protons, since the plasma electrons contribute very little to the momentum transfer. Also, spin effects can be neglected.

2.1 Minimum impact parameter b_{min}

For highly-relativistic incident electrons, b_{min} and therefore θ_{max} are governed by one of two quantum-mechanical limits, both related to the de Broglie wavelength $\lambda\!\!\!^{-} = \hbar/p$ of the electrons. The first of these requires that, for the impact parameter b to be definable,

$$b > \lambda\!\!\!^{-}$$

which leads to the approximate cut-off

$$b_{min} \approx \frac{\hbar}{p} \quad . \tag{3}$$

It is shown in ref. 8), by considering the situation in the reference frames of both the lighter and the heavier particle, that it is the de Broglie wavelength of the lighter particle which applies. From Eq.(2) the maximum scattering angle is then

$$\theta_{max} \approx 2e^2/\hbar c = 2\alpha \tag{4}$$

where $\alpha \approx 1/137$ is the fine structure constant.

The second quantum condition relates to diffraction of the de Broglie wavefront by an object of non-vanishing radius R. This sets an upper limit to the scattering angle such that

$$\theta < \frac{\lambda\!\!\!^{-}}{R}$$

and hence

$$\theta_{max} \approx \frac{\hbar}{pR} \tag{5}$$

with the corresponding impact parameter

$$b_{min} \approx 2\alpha R \quad . \tag{6}$$

The stronger condition corresponds to the larger of the two values of b_{min} given by Eqs.(3) and (6). Since $p = mc\gamma$, the two values are equal for

$$\gamma = \frac{\hbar}{2\alpha Rmc} = \frac{\lambda\!\!\!^{-}_C}{2\alpha R} \tag{7}$$

where $\lambda\!\!\!^{-}_C = \hbar/(mc) = 3.862 \times 10^{-11}$cm is the electron Compton wavelength.

The quantity R is the effective radius of the proton for electromagnetic interactions, and is related to the flattening of the Coulomb potential in the vicinity of the proton. It has a value of about 0.7×10^{-13}cm (0.7 fermi) and is thus close to the value of the classical electron radius. Putting the numbers into Eq.(7) we find

$$\gamma \approx 3.8 \times 10^4$$

for equal b_{min} in Eqs.(3) and (6). This corresponds to an electron energy of about 19 GeV, which is not much above that assumed for injection into the BWA.
At higher energies the cut-off is determined by Eqs.(5) and (6), and since this appears only in the Coulomb logarithm we can use these equations for the whole energy range as a good approximation.

2.2 Maximum impact parameter b_{max}

For relativistic particles the minimum scattering angle also is determined by quantum-mechanical conditions. To some given impact parameter b corresponds an uncertainty δp in the momentum transfer given by

$$b\delta p \geq \hbar \quad . \tag{8}$$

If we choose the minimum momentum transfer to be $\Delta p = \delta p$ we then have

$$\theta_{min} = \frac{\Delta p}{p} = \frac{\hbar}{pb}$$

and putting $b = \lambda_D$, the Debye distance in the plasma, yields

$$\theta_{min} = \frac{\hbar}{p\lambda_D} \quad . \tag{9}$$

Assuming that Eq.(2) is valid down to this cut-off angle we have, with the previous assumptions

$$b_{max} \approx \frac{2e^2}{pc\theta_{min}} = 2\alpha\lambda_D \quad . \tag{10}$$

2.3 Mean-square scattering angle

Since Eq.(5) can be expressed as :

$$\theta_{max} \approx \frac{\hbar}{mc\gamma R} = \frac{\lambda\!\!\!^{-}_C}{\gamma R} \quad ,$$

it is evident that, for $\gamma > 10^4$, $\theta_{max} \ll 1$ and we can use small-angle approximations with good accuracy. The differential cross-section for a cut-off Coulomb potential can then be written in the form[8]

$$\frac{d\sigma}{\delta\Omega} = \left(\frac{2e^2}{pc}\right)^2 \cdot \frac{1}{(\theta^2+\theta_{min}^2)^2} \quad . \tag{11}$$

The total cross section σ is obtained by integrating Eq.(11) from 0 to some suitably large angle θ_0. Since the small angles will dominate we can write

$$d\Omega = 2\pi \sin\theta d\theta \approx 2\pi\theta d\theta$$

and hence

$$\sigma = \int_0^{\theta_0} \frac{d\sigma}{d\Omega}\, d\Omega = 2\pi \left(\frac{2e^2}{pc}\right)^2 \int_0^{\theta_0} \frac{\theta d\theta}{(\theta^2+\theta_{min}^2)^2}$$

$$= \pi \left(\frac{2e^2}{pc}\right)^2 \left[\frac{1}{\theta_{min}^2} - \frac{1}{\theta_0^2}\right]$$

and for $\theta_0 \gg \theta_{min}$ we have

$$\sigma = \pi \left(\frac{2e^2}{pc\theta_{min}}\right)^2 \quad . \tag{12}$$

The mean-square scattering angle $\langle\theta^2\rangle$ is then

$$\langle\theta^2\rangle \approx \frac{1}{\sigma} \int_0^{\theta_{max}} \theta^2 \frac{d\sigma}{d\Omega}\, d\Omega$$

whence, using Eqs.(11) and (12), with $\theta^2_{max} \gg \theta^2_{min}$,

$$\langle\theta^2\rangle \approx 2\theta^2_{min}\left[\ln\left(\frac{\theta_{max}}{\theta_{min}}\right) - \frac{1}{2}\right] \quad . \tag{13}$$

Now from Eqs.(5) and (9),

$$\frac{\theta_{max}}{\theta_{min}} = \frac{\lambda_D}{R}$$

and, since λ_D is typically of order 10^{-6}cm or more and $R \approx 10^{-13}$cm, we can use the stronger assumption $\ell n(\theta_{max}/\theta_{min}) \gg 1$, approximating Eq.(13) to

$$\langle\theta^2\rangle \approx 2\theta^2_{min}\, \ell n \left(\frac{\theta_{max}}{\theta_{min}}\right) . \qquad (14)$$

2.4 Multiple scattering

Eq.(14) gives the mean square angle for individual scatterings. For incident particles undergoing a large number N of collisions in a distance ℓ, the angular distribution will be approximately Gaussian with a mean square angle $\langle\theta^2\rangle = N\langle\theta^2\rangle$. The number of collisions occuring over a distance ℓ in a medium with n scattering centres per unit volume is

$$N = n\sigma\ell$$

and, with σ given by Eq.(12), the increase in angular divergence from the multiple scattering is

$$\langle\theta^2\rangle = 2\pi n\ell \left(\frac{2e^2}{pc}\right)^2 \ell n\left(\frac{\theta_{max}}{\theta_{min}}\right) . \qquad (15)$$

Using Eqs.(5) and (9) respectively for θ_{max} and θ_{min} yields

$$\langle\theta^2\rangle = 2\pi n\ell \left(\frac{2e^2}{pc}\right)^2 \ell n\left(\frac{\lambda_D}{R}\right) . \qquad (16)$$

In Eq.(16), $\langle\theta^2\rangle$ is the spatial angular divergence; we shall in fact use the projection on to one plane $\langle\theta^2\rangle_p = {}^1/_2\langle\theta^2\rangle$, expressed in differential form instead of for a finite length ℓ, which results in

$$\frac{d}{dz}\langle\theta^2\rangle_p = \pi n \left(\frac{2e^2}{pc}\right)^2 \ell n\left(\frac{\lambda_D}{R}\right) . \qquad (17)$$

3. EMITTANCE GROWTH IN A FOCUSED SYSTEM

When a beam of particles undergoes multiple scattering in the presence of transverse focusing the effect of the random collisions is to excite betatron oscillations, leading to a growth in the beam emittance. Scattering by the residual gas in a synchrotron is a well-understood phenomenon and the established theory can readily be adapted to the situation in a plasma.

We adopt here the emittance definition normally used for electron storage rings, that is, measured at one standard deviation of an approximately Gaussian distribution. In an electron linac, in contrast to an electron storage ring, synchrotron radiation is weak and is assumed here to have a negligible effect on the beam emittance. Consequently, we distinguish between the absolute emittance E given by the product of the beam radius and angular divergence, and the invariant emittance $\varepsilon = \gamma E$ (for $v = c$) which is conserved if there is no multiple scattering or other random process.

In the absence of collision phenomena, the conservation of invariant emittance under acceleration implies

$$\frac{d\varepsilon}{dz} = \frac{d}{dz}(\gamma E) = 0$$

and hence

$$\left(\frac{dE}{dz}\right)_{ad} = -\frac{E}{\gamma}\frac{d\gamma}{dz} \quad . \tag{18}$$

This so-called adiabatic damping arises from the use of co-ordinates x, x' which are not canonically conjugate, resulting in the absolute emittance E decreasing with increasing energy. This is an important consideration in obtaining high luminosity in a high-energy linear collider.

Emittance growth due to multiple scattering is in competition with adiabatic damping and results in an increase in the (otherwise) invariant emittance ε. A convenient formulation of such growth produced by gas scattering in a synchrotron has been given by Hardt[9]. From the Fokker-Planck equation for a Gaussian distribution in a 4-dimensional phase space he obtains a diffusion equation in each of the two transverse space projections. Using the conventional definition of electron-beam emittance at one standard deviation σ_x

$$E = \frac{\sigma^2_x}{\beta_x} \quad . \tag{19}$$

where β_x is the betatron focusing function, the diffusion equation for one plane can be written in terms of the emittance growth rate

$$\left(\frac{dE}{dz}\right)_{diff} = \frac{\beta_x}{2}\frac{d}{dz}\langle\theta^2\rangle_p,$$

and adding the adiabatic damping term, Eq.(18), yields

$$\frac{dE}{dz} = \left(\frac{dE}{dz}\right)_{diff} + \left(\frac{dE}{dz}\right)_{ad}$$

$$= \frac{\beta_x}{2}\frac{d}{dz}\langle\theta^2\rangle_p - \frac{E}{\gamma}\frac{d\gamma}{dz} \quad .$$

It follows immediately that

$$\frac{d\varepsilon}{dz} = \frac{d}{dz}(\gamma E) = \frac{\gamma\beta_x}{2}\frac{d}{dz}\langle\theta^2\rangle_p \quad ,$$

which, from Eq.(17) with $p = mc\gamma$ results in

$$\frac{d\varepsilon}{dz} = \frac{\pi\beta_x n}{2\gamma}\left(\frac{2e^2}{mc^2}\right)^2 \ell n\left(\frac{\lambda_D}{R}\right) \quad . \tag{20}$$

Transverse focusing of the accelerated beam can occur due to radial fields in the plasma, which arise because of the finite lateral extent of the laser beams, and therefore of the plasma beat wave. The consequent radial dependence of the accelerating field E_z is associated, through Maxwell's equations, with a radial field which is focusing over a certain range of phase.

The corresponding betatron focusing function β_x has been derived in Ref.4 and is given by

$$\beta_x = \left[\frac{-\pi\sigma_0^2\, mc^2\gamma}{\lambda_p e E_{zo}\cos\phi}\right]^{1/2} \tag{21}$$

where σ_0 is the standard deviation of the laser-beam cross-section, λ_p is the wavelength of the plasma beat-wave and ϕ is the accelerating phase angle. It is assumed that both the laser beam and the resultant beat-wave have the same Gaussian distribution transversely. The accelerating field on the axis is given by $E_{zo}\sin\phi$. As discussed in Ref.4 the phase angle ϕ is constrained to the range

$$\frac{\pi}{2} < \phi < \frac{13\pi}{16}$$

because of acceleration, radial stability and phase slip between accelerated bunches and beat wave.

In Eq.(20) we replace β_x from Eq.(21), write $r_e = e^2/mc^2$ for the classical electron radius and obtain

$$\frac{d\varepsilon}{dz} = F/\sqrt{\gamma} \quad , \tag{22}$$

where

$$F = 2\pi r_e^2\, n\left[\frac{-\pi\sigma_0^2\, mc^2}{\lambda_p e E_{zo}\cos\phi}\right]^{1/2} \ell n\left(\frac{\lambda_D}{R}\right) \tag{23}$$

has no explicit energy dependence. Assuming a constant acceleration rate $eE_{zo}\sin\phi$ we can write

$$\gamma = \gamma_i + \gamma' z$$

where γ_i corresponds to injection energy and

$$\gamma' = \frac{d\gamma}{dz} = \frac{eE_{zo}\sin\phi}{mc^2} \quad . \tag{24}$$

Integrating Eq.(22) from γ_i to the final energy γ_f leads to a growth of emittance $\Delta\varepsilon$ given by

$$\Delta\varepsilon = \frac{2F}{\gamma'} \left[\sqrt{\gamma_f} - \sqrt{\gamma_i} \right] \tag{25}$$

where, by rearranging the factors

$$\frac{2F}{\gamma'} = 4\pi\, r_e^2\, \sigma_0\, n \left[\frac{mc^2}{eE_{zo}\sin\phi} \right]^{3/2} \left[\frac{-\pi\tan\phi}{\lambda_p} \right]^{1/2} \ln \left(\frac{\lambda_D}{R}\right) \quad . \tag{26}$$

To evaluate Eq.(26) we take the following parameters adopted at this Workshop :

$$\begin{aligned} n &= 10^{17}\text{cm}^{-3} \\ eE_{zo}\sin\phi &= 60\ \text{MeV cm}^{-1} \\ \lambda_p &= 10^{-2}\ \text{cm} \\ \sigma_0 &= 2.5 \times 10^{-2}\ \text{cm}. \end{aligned}$$

The Debye wavelength is given by

$$\lambda_D = \left[\frac{kT}{4\pi ne^2} \right]^{1/2} = \left[\frac{kT}{4\pi n mc^2 r_e} \right]^{1/2}$$

where k is Boltzmann's constant and T the temperature of the plasma electrons. Assuming a relatively cool plasma of 5 eV ($\sim 5.8 \times 10^4\ ^0$K) and with

$$\begin{aligned} r_e &= 2.818 \times 10^{-13}\text{cm} \\ mc^2 &= 0.511 \times 10^6\ \text{eV}, \end{aligned}$$

we have :

$$\lambda_D = 5.26 \times 10^{-6}\text{cm}.$$

Taking $R = 0.7 \times 10^{-13}$cm for the effective radius of the proton leads to

$$\ln \left(\frac{\lambda_D}{R} \right) = 18.13.$$

For ϕ we choose the average over the phase slip between $\pi/2$ and $13\pi/16$ for a single stage of the BWA, i.e. $\phi = 10.5\ \pi/16$, and find that Eq.(26) evaluates to

$$\frac{2F}{\gamma'} = 8.62 \times 10^{-10}\text{cm}.$$

Then, with $\gamma_f = 1.96 \times 10^6$ (1 TeV) and $\gamma_i = 1.96 \times 10^4$ (10 GeV),

$$\Delta\varepsilon = 1.086 \times 10^{-6} \text{ cm} = 1.086 \times 10^{-8} \text{ m}.$$

This can be compared with the nominal invariant emittance $\varepsilon = 3 \times 10^{-5}$m of the SLAC Linear Collider leading to

$$\frac{\Delta\varepsilon}{\varepsilon} = 3.62 \times 10^{-4}.$$

This is a very small emittance growth and gives no cause for concern with the parameters assumed.

4. DISCUSSION

The above results are rather insensitive to the injection energy since reducing γ_i even to 1 in Eq.(25) only increases $\Delta\varepsilon$ by about 10%. In fact, this increase would be somewhat less, because at lower injection energies we should use θ_{max} from Eq.(4) rather than Eq.(5). The logarithm in Eq.(26) would then be replaced by

$$\ell n \left(\frac{2\alpha \lambda_D \gamma}{\lambda_C} \right)$$

which decreases with decreasing energy.

If we use the SLC emittance as a reference there is considerable freedom in the choice of BWA parameters without appreciable degradation of performance due to multiple scattering in the plasma. This also implies that, if injected beams of appreciably lower emittance were available with the required intensity, there are potential benefits to be obtained in terms of luminosity and beam power before emittance growth becomes a serious constraint.

In the present evaluation no account has been taken of possible fluctuations of plasma density and focusing forces, nor of the influence of contamination of the plasma by high-Z impurities. With the comparison used here it is unlikely that such effects will be significant, but it may be necessary to scrutinise them more carefully if extremely low-emittance beams were contemplated. Furthermore, the assumption that the quantum fluctuations of synchrotron radiation produced by the focusing fields have a negligible influence on emittance growth requires proper verification.

REFERENCES

1) T. Tajima and J.M. Dawson, Phys. Rev. Lett. 43 (1979) 267.

2) The Challenge of Ultra-High Energies, Proc. ECFA-RAL meeting, Oxford, Sept. 1982. ECFA 83/68 (Rutherford Appleton Laboratory).

3) R.D. Ruth and A.W. Chao, AIP Conf. Proc. No.91, New York (1982).

4) J.D. Lawson, Report of the RAL Study Group, RL-83-057 (1983).

5) N.M. Blachman and E.D. Courant, Phys. Rev. 74 (1948) 140.

6) Niels Bohr, Kgl. Videnskab. Selskab. Math.-fys. Medd. XVIII, 8. København (1948).

7) Yung-Su Tsai, Rev. Mod. Phys. 46 (1974) 815.

8) J.D. Jackson, Classical Electrodynamics, 2nd Ed., John Wiley and Sons, New York 1975.

9) W. Hardt, Rpt. CERN ISR-300/GS/68-11 (1968).

SYNCHROTRON RADIATION DUE TO TRANSVERSE FOCUSSING IN A VERY HIGH ENERGY ELECTRON LINAC

W. Schnell, CERN, Geneva, Switzerland

Electron linear accelerators of 1 TeV or more final energy are now being discussed. At these energies the synchrotron radiation due to the unavoidable transverse focussing system may be of concern. The following simple expressions for the radiation loss per unit length (eqs. 5b and 14 below) may be well-known but I have not seen or heard them quoted so far.

Smooth focussing

In a beat-wave plasma accelerator the transverse focussing (primarily due to the transverse gradient of the accelerating force) will be continuous, i.e. the amplitude function β will not vary over an oscillation period; and even in a conventional alternating gradient system this assumption gives an interesting basis for comparison with what is treated in the next section. Thus

$$x = a \sin \frac{z}{\beta}$$

where x is the transverse displacement, a the amplitude, z the longitudinal coordinate and $2\pi\beta$ the oscillation wavelength. The curvature ρ^{-1} of any curve x(z) is given by

$$\rho^{-1} = \frac{x''}{(1+x'^2)^{\frac{3}{2}}} \qquad (1)$$

where the dashes denote differentiation with respect to z. Clearly $x'^2 \ll 1$ in any high energy accelerator. Hence

$$\rho^{-2} = \frac{a^2}{\beta^4} \sin^2 \frac{z}{\beta} \qquad (2)$$

and the average value over half an oscillation is given by

$$\langle \rho^{-2} \rangle = \frac{a^2}{2\beta^4} \quad . \qquad (3)$$

The radiation loss per unit length is given by

$$eU' = \frac{2 r_e m_0 c^2}{3} \frac{\gamma^4}{\rho^2} \qquad (4)$$

where U is the particle energy over elementary charge, r_e is the classical electron radius, m_0c^2 the rest energy and γ the Lorentz factor. Substituting eq. (2) for ρ^{-2} yields

$$\langle U' \rangle = 4.79\times10^{-10}\ a^2\left(\frac{\gamma}{\beta}\right)^4 \qquad [eVm^{-1}] \tag{5a}$$

for the average energy loss per unit length.

A particle whose amplitude equals σ of the distribution suffers an energy loss given by

$$\langle U' \rangle_\sigma = 4.79\times10^{-10}\ (\gamma\varepsilon)\left(\frac{\gamma}{\beta}\right)^3 \qquad [eVm^{-1}] \tag{5b}$$

where $\gamma\varepsilon = \gamma\sigma^2/\beta$ is the normalized emittance. At $\gamma = 2 \times 10^6$ (1 TeV) and with $\gamma\varepsilon = 3.5 \times 10^{-5}$ m (the SLC specification) one finds

Table 1, $\gamma\varepsilon = 3.5 \times 10^{-5}$ m

β	$\langle U' \rangle_\sigma$
10 m	134 eV m^{-1}
1 m	134 keV m^{-1}
0.1 m	134 MeV m^{-1}

Particles with amplitude $n\sigma$ will suffer n^2 times this energy loss. For higher energies the radiation loss will increase with $\gamma^3/2$, provided any emittance blow-up is avoided and the focussing strength is kept constant so that $\beta \propto \gamma^1/2$.

This result looks quite favourable but it must be remembered that equation (5b) is based on the assumption that the beam centre coincides exactly with the zero-field line of the focussing system. If, for any reason (e.g. misalignment) the beam oscillates with amplitude a around the zero-field eq. (5a) has to be used. For a = 0.1 mm, say, and 1 TeV one finds

Table 2, a = 0.1 mm

β	$\langle U' \rangle$
10 m	7.7 keV m^{-1}
1 m	76.6 MeV m^{-1}
0.1 m	766 GeV m^{-1}

Clearly this has to be avoided by using the radiation emitted as diagnostics for aligning the system.

Alternating gradient focussing

In an alternating gradient system the radiation must be expected to be much stronger because of the uneven distribution of the deflecting forces including outward bends. Generally (in the absence of driving terms!)

$$\rho^{-2} = \left[\frac{d^2x}{dz^2}\right]^2 = [K(z)x(z)]^2 \qquad (6)$$

where

$$K(z) = \frac{e\partial B}{p\partial x} \qquad (7)$$

is the normalized gradient (p: particle momentum).

A thin-lens FODO structure with period length L and amplitude functions β_F, β_D in the quadrupoles may be taken for deriving an analytical formula. In the quadrupoles, of length ℓ and focal length $\pm f$ one has $K = (f\ell)^{-1}$ and hence

$$\rho^{-2} = \frac{x^2}{(f\ell)^2} \quad . \qquad (8)$$

The distribution of displacements x of a particle at successive quadrupoles of same sign is sinusoidal. Hence, the average of ρ^{-2} over all F-quadrupoles (all D-quadrupoles) is

$$\langle\rho^{-2}\rangle_{F,D} = \frac{a_{F,D}^2}{2(f\ell)^2} \qquad (9)$$

where $a_{F,D}$ is the peak amplitude observed at any F(D) position. For a particle at one σ of the distribution of amplitudes within the beam

$$\langle\rho^{-2}\rangle_{F,D} = \frac{\varepsilon}{2(f\ell)^2}\,\beta_{F,D} \qquad (10)$$

where $\varepsilon = \sigma_F^2/\beta_F = \sigma_D^2/\beta_D$ is the emittance. As there is no radiation outside the quadrupoles the overall average is given by

$$\langle\rho^{-2}\rangle = \eta\,\frac{\varepsilon}{2(f\ell)^2}\,\beta \qquad (11)$$

where $\eta = 2\ell/L$ is the filling factor and $\beta = (\beta_F+\beta_D)/2$. Introducing the phase advance per period μ_0 with

$$\frac{L}{f} = 4 \sin \frac{\mu_0}{2} \tag{12}$$

$$L = \beta \sin \mu_0 \tag{13}$$

and inserting the overall average ρ^{-2} into eq. (4) finally gives

$$\langle U' \rangle_\sigma = 4.79\times10^{-10} \frac{64}{\eta} \frac{\left(\sin \frac{\mu_0}{2}\right)^2}{(\sin \mu_0)^4} (\gamma\varepsilon)\left(\frac{\gamma}{\beta}\right)^3 \quad [\text{eV m}^{-1}] \tag{14}$$

to be compared with eq. (5b). For $\mu_0 = 60^\circ$, $\eta = 0.1$ the factor

$$\frac{64}{\eta} \frac{\left(\sin \frac{\mu_0}{2}\right)^2}{(\sin \mu_0)^4}$$

by which the radiation is increased compared with smooth focussing at the same β-value amounts to 284! The factor of 64 $\sin^2(\mu_0/2)\sin^{-4}\mu_0$ has a minimum at $\mu_0 = 70.5^\circ$ where it amounts to 27.0.

Conclusions

The radiation loss due to transverse a.g. focussing along an electron linear collider is quite tolerable up to and beyond 1 TeV, provided the beam is steered precisely along the zero-field line. The following example shows this:

Energy (e^+, e^-)	1.02	TeV
Invariant emittance $\gamma\sigma^2/\beta$	3.5×10^{-5}	m
Amplitude function $\beta = (\beta_F+\beta_D)/2$	10	m
Phase advance per period μ_0	70.5°	
Filling factor with quadrupoles	10%	
Energy loss per unit length for particles at $\mathbf{3\sigma}$ $\langle U' \rangle_{3\sigma}$	326	keV m^{-1}

With continuous focussing (as in a beat-wave plasma accelerator?) the radiation is even lower by more than two orders of magnitude so that lower values of β could be tolerated in spite of the β^{-3}-dependence of the radiation loss per unit length.

Acknowledgement

I am very grateful to S. Myers for discussions, comments and corrections.

SPACE CHARGE WAVE ACCELERATORS

John A. Nation
Laboratory of Plasma Studies and School of Electrical Engineering, Cornell University, Ithaca, NY 14853

INTRODUCTION

Various novel schemes have been described to produce very high field gradient accelerators. In this report we briefly summarize some of the features associated with one proposal, the space charge wave accelerator. In this device we grow space charge waves on a weakly relativistic electron beam; the beam to be accelerated is then injected into the electron beam supported wave, and the wave phase velocity changed at a rate commensurate with the ion acceleration obtained in the electric field in the wave. Changes in the wave phase velocity may be achieved, either by expanding the beam or by converging the waveguide. In either case the effective plasma frequency is reduced and the wave phase velocity increased.

In the following sections we present an account of experimental observations showing control of the wave phase velocity for a slow wave, measurements of the wave electric field, and indicate how these results might apply to an ion accelerator. An interesting and new possibility is also indicated, namely the use of fast waves for electron accelerators. In this case preliminary estimates indicate that comparable field gradients to those already obtained in the slow wave scheme should be obtainable in fast waves and that these field gradients can be maintained at phase velocities close to the speed of light. The most likely wave for this application would appear to be the upper hybrid mode of the low energy, high current electron beam.

EXPERIMENTAL RESULTS

Space charge waves have been grown on weakly relativistic electron beams (200-400 keV, 500-2000 A, 50-500 nsec) by propagating the magnetically confined electron beam through a slow wave structure consisting of a series of disk loaded, coupled cavities excited in the TM010 mode. The slow space charge wave couples to either a forward or to a backward wave of the disk loaded structure depending on the experimental parameters used. Following wave growth the beam is extracted into a waveguide which is beyond cut off for the wave frequency chosen. In the experiments reported here the wave frequency was 1.067 GHz and the guide dimension was varied from 10 to 5 cm over relatively short distances, i.e. over distances comparable to or slightly greater than a guide wavelength[1]. The object

of the experiments was to compare the measurements of the wave phase velocity with linear theory predictions. The linear theory utilized describes slow space charge wave propagation on a pencil electron beam in a uniform guide. The converging guide was modelled in these calculations by using the results for different diameter guides and assuming that the changes in the guide dimensions were adiabatic at the wave frequency. This is obviously a poor approximation but nonetheless forms a convenient reference. A second goal was the measurement of the time resolved electric field. The electric field was inferred from measurements of the wave radial electric and azimuthal magnetic fields. From these measured values, and using the experimentally determined value of the wave phase velocity, we calculate the axial electric field of the wave at the beam edge. This measurement requires an accurate determination of the wave phase velocity with an estimated accuracy in the normalized phase velocity of 0.02 c resulting in a 10% accuracy for the axial electric field strength.

Results for the wave phase velocity (determined by measuring the phase shift of the wave between two adjacent ports) and the axial electric field are shown for a typical shot in Fig. 1. At a phase velocity of 0.2 c the electric field approaches 300 kV/cm. This field strength is typical of the results found in these experiments. Figure 2 shows a summary of the experimental results for the variation of the phase velocity with the drift tube size for various values of the electron beam current. The solid line represents the results of the linear theory calculation of the wave phase velocity. As can be seen from the figure we can control the wave phase velocity over a range of values up to the electron velocity.

It is interesting to note that we have on some occasions observed fast waves propagating on the beam. The mechanism leading to the fast waves generation is not completely clear but is believed to be associated with mismatches in the wave impedance in the structure at the boundary between the wavegrowth region and the uniform guide section.

DISCUSSION OF RESULTS

The wave electric fields measured are very competitive with those achievable using standard accelerator technology. They have certain other features which make them more attractive, namely:

(i) The field is a maximum at the beam location and becomes weaker close to the conducting walls and,

(ii) The fields measured are low estimates of the actual field since they are calculated on the basis of linear theory.

In practice the waves are non-linear[2,3] and the actual field strength may be larger by an order of magnitude. Simulations demonstrating this phenomenon have been reported elsewhere. Note that the non-linear wave steepening occurs after growth so that the fields at the walls of the wave-growth structure may be significantly lower than those in the accelerating structure.

The available electric fields are limited by self trapping of the primary beam electrons in the space charge wave. The onset field for self trapping is of order[4]

$$E_t = \frac{\alpha k_z}{\gamma_\phi} (\gamma_r - 1) \frac{m_0 c^2}{e}$$

where γ_r is the electron relativistic factor measured in the wave frame of reference, and α is a numerical factor of order 3 reflecting the fact that one can operate above the self trapping onset level in at least short accelerator sections. Estimates indicate that one can obtain acceleration field gradients of 200 MV/m with a 2.0 MeV electron beam and a wave frequency of 7.5 GHz.

The results shown in Fig. 2 show deviations from the linear theory results, especially at low phase velocities. The difference is outside the experimental error in the measurement and is associated with the non-linear reduction in the wave phase velocity. Non-linear effects have been confirmed, although not quantitatively determined, by observations of strong signals at the second harmonic of the wave frequency. The deviations from the linear theory at the small tube diameters are probably associated with inaccuracies in the modelling, especially the errors associated with ignoring the axial component of the wave electric field at the tube wall.

APPLICATION TO ACCELERATORS

The space charge wave accelerator scheme is applicable to ion acceleration and is in principle applicable for ion acceleration up to an energy equal to the mass ratio (accelerated particle to electron) times the electron beam energy. Perhaps a more severe limitation is the decrease in the self trapping field strength as one approaches the electron drift velocity. It appears at present that it is possible to grow waves at sufficiently high field strengths and to control the wave phase velocity sufficiently well that one could build a test section of an accelerator based on this principle. For ease of testing the injector should have an energy of at least 50 MeV.

A variation on the converging guide accelerator has been proposed and tried at Cornell University[5]. In this device we grow a large amplitude space charge wave on the beam using the techniques described earlier. The slow space charge wave supported by the electron beam is then propagated through a quasi-periodic rippled magnetic field. If the local wavenumber of the field ripple is K and that of the wave k then beat waves are generated with phase velocities of

$$v_B = \frac{v_\phi k}{k + K}$$

where v_ϕ is the phase velocity of the space charge wave. The velocity of these waves is unbounded and hence this configuration can be used for acceleration of particles to velocities up to the speed of light. This principle has been demonstrated on a statistical basis by accelerating protons through 2 MeV at an average gradient of about 4 MeV/m. The proton injection energy was 5 MeV. This configuration may also be used, in principle at least, for electron acceleration.

Finally we reiterate our earlier comments regarding fast waves. These waves do not grow naturally on beams and require that external work be done on the system to grow the waves. We have observed fast space charge waves on beams and have recently initiated experiments to deliberately excite this mode. There appear to be a number of ways of exciting this mode, and the upper hybrid mode, which seem feasible. These modes appear to be especially attractive for possible electron accelerators.

ACKNOWLEDGMENTS

This work was supported by the Department of Energy.

* * *

REFERENCES

1) A. Anselmo, G. Kerslick, J.A. Nation and G. Providakes, "Space Charge Wave Propagation in Inhomogeneous Waveguides", accepted for publication in Physics of Fluids.

2) T.P. Hughes and E.E. Ott, Physics of Fluids, Vol. 23, pp. 2265 (1980).

3) D.L. Fenstermacher and C.E. Seyler, Physics of Fluids, 27 (4) (1984).

4) P. Sprangle, A.T. Drobot and W.W. Manheimer, Phys. Rev. Letters 31, pp. 1234 (1973).

5) Electron Beam Wave Accelerators. A. Anselno et al. Proc. 5th International Topical Conference on High Power Electron and Ion Beam Research and Technology (San Francisco 1983).

SUMMARY REPORT OF THE WORKING GROUP 4 ON ACCELERATOR CONSIDERATIONS

W. Willis
CERN, Geneva, Switzerland

Participants in Working Group

J. Buon, G. Coignet, L. Hand, D. Keefe, J. Lawson, S. Myers, J. Rees, S. Ruggiero, D. Sutter, M. Tigner, J. Willis, J. Warren

Our Working Group addressed questions of accelerator designs. It was decided that the summary of our work would be included in M. Tigner's general summary talk, with a short account of the joint work of the group presented here.

We set ourselves the goal of understanding the parameters of the general case of linear colliders and aimed to produce skeleton parameter lists at the broadest conceptual level, for each of the accelerating mechanisms proposed. Our notions of physics requirements suggested that we needed to consider only colliding beams. The introductory talk of C. Rubbia emphasized that point, with a specific goal of 10 TeV e^+e^- collisions with a luminosity of 10^{34} s^{-1} cm^{-2}. We decided to consider also 1 TeV and lower luminosities.

P. Wilson, J. Rees and L. Hand presented approaches to the optimization of colliding beams, which are summarized, with numerical examples, in the paper of Hand and Rees. The classical formula for beamstrahlung is not always valid in these cases, and several members of the group worked on evaluating the importance of the quantum corrections, reported in the paper by J. Buon and G. Coignet.

The parameter list for the two-beam accelerator was given by A. Sessler and edited by S. Myers. A parameter list for a laser-droplet accelerator was given by R. Palmer. Parameter lists for the wakefield and beat-wave accelerators were not available at the time of the Workshop, but can be found in part in other sections of the Proceedings.

There were also contributions on other accelerator concepts: the "proton klystron" by A. Ruggiero and the "switched power linac" by myself, which are to be found in the section of these proceedings devoted to Working Group 2.

CHOICE OF BASIC PARAMETERS FOR TEV LINACS

L.N. Hand
Cornell University, Ithaca, NY 14853, USA

J.R. Rees
SLAC, PO Box 4349, Stanford, CA. 94305, USA

VARIABLES

Particle Physics:

Beam Energy	γm_0^2	
Luminosity	L	
Energy Spread	δ	(after collision)

Feasibility/Cost:

Beam Power	P_{beam}	(one beam)
Repetition Frequency	f	(Hz)
Bunch Population	N	
Effective Colliding Area	A	
Disruption Parameter	D	
Beta Function at Collision Point	β^*	
RMS Beam Size at Collision Point	σ^*	
Beam Emittance	ε	(definition, $\varepsilon = \sigma^{*2}/\beta^*$)
Bunch Length (rms)	σ_L	

BASIC FORMULAE FOR CYLINDRICAL BEAMS (Gaussian Distribution)

$$L = \frac{fN^2}{A} \qquad D = \frac{2\pi r_0 \sigma_L N}{\gamma A}$$

$$P_{beam} = f N \gamma m_0 c^2 \qquad \delta = \frac{4\pi r_0^3 N^2 \gamma}{3\sqrt{3} A \sigma_L}$$

$$A = 4\pi \sigma^{*2}$$

FORMULAE

Our procedure (perhaps not the best)

1. Choose Particle Physics parameters γ, L
   Feasibility/cost parameter P_{beam}

$$fA = \frac{P_{beam}^2}{L(\gamma m_0 c^2)^2}$$

2. The product "fA" is now fixed independent of any later choices. Next we choose "f"

$$A = fA/f \qquad \text{of course}$$

$$N = \frac{P_{beam}}{f\ \gamma m_0 c^2}$$

3. Then we set D = 1 which is somewhat arbitrary, but reasonable for orders of magnitude.

$$\sigma_L = \frac{\gamma\ A\ D}{2\pi\ r_0\ N}$$

4. Next we check to determine if δ is acceptable.

5. Finally we find the product "$\beta^*\varepsilon$" and compare it with SLC values scaled to the energy in question.

$$\beta^*\varepsilon = \frac{A}{4\pi} \qquad \text{(cylindrical beam)}$$

For comparison, the SLC produces a normalized emittance, $\gamma\varepsilon = 3 \times 10^{-5}$ m

$$\varepsilon_{SLC}(\gamma) = \frac{3 \cdot 10^{-5} m}{\gamma}$$

TABLES OF fA IN μ^2Hz

$L = 10^{32}\ cm^{-2}\ s^{-1}$

E \ P_b	1 MW	3 MW	10 MW
1 TeV	40	350	4000
10 TeV	0.4	3.5	40
100 TeV	$4 \cdot 10^{-3}$	$3.5 \cdot 10^{-2}$	0.4

fA in μ^2Hz

$L = 10^{34}\ cm^{-2}\ s^{-1}$

E \ P_b	1 MW	3 MW	10 MW
1 TeV	0.4	3.5	40
10 TeV	$4 \cdot 10^{-3}$	$3.5 \cdot 10^{-4}$	0.4
100 TeV	$4 \cdot 10^{-5}$	$3.5 \cdot 10^{-4}$	$4 \cdot 10^{-3}$

fA in μ^2Hz

$\mu^2 = (1\ \text{micrometer})^2 = 10^{-12}\ m^2$

TYPICAL PARAMETERS

Case A

$$\begin{cases} L = 10^{32}\ cm^{-2}\ s^{-1} \\ P_{beam} = 1\ MW \quad \text{(one beam)} \\ E = 1\ TeV \end{cases}$$

These parameters imply that

$$fA = 4 \times 10^{-11}\ m^2$$

Choosing

$$f = 4000\ Hz \quad \text{(Arbitrary choice)}$$

implies

$$A = 10^{-14}\ m^2 \qquad \sigma^* \sim 0.03\ \mu m = 300\ \text{Å}$$
$$N = 1.5 \times 10^9 \ \text{particles per bunch}$$

Also choosing

$$D = 1 \qquad \text{(Arbitrary choice)}$$

implies

$$\sigma_L = 0.35\ mm$$

which implies

$$\delta = 8\%$$

σ_L could be smaller

Comparison of spot size with SLC experience:

Using invariant emittance $\gamma\varepsilon = 3 \times 10^{-5}$ m from SLC, we get $\varepsilon = 1.5 \times 10^{-11}$ m at 1 TeV. If we used $\beta^* = 5$ mm (as at SLC) our spot area would be 94×10^{-14} m^2, about 100 times too big. Since β^* cannot be much reduced (on account of σ_L) the emittance must be reduced to 100 times lower than the present SLC value.

Case B

$$\begin{cases} L = 10^{32}\ \text{cm}^{-2}\ \text{s}^{-1} \\ P_{\text{beam}} = 3\ \text{MW}\ \ \text{(one beam)} \\ E = 10\ \text{TeV} \end{cases}$$

These parameters imply that

$$fA = 3.5 \times 10^{-12}\ \text{m}^2$$

Choosing

$f = 4000$ Hz (Arbitrary choice)

implies

$A = 0.9 \times 10^{-15}\ \text{m}^2$ $\quad\quad$ $\sigma^* \sim 83$ Å

$N = 0.5 \times 10^{9}$ particles per bunch

Also choosing

$D = 1$ (Arbitrary choice)

implies

$\sigma_L = 1.0$ mm (reduced somewhat by quantum correction)

which implies

$\delta = 26\%$

Comparison of spot size with SLC experience:

Using invariant emittance $\gamma\varepsilon = 3 \times 10^{-5}$ from SLC, we get $\varepsilon = 1.5 \times 10^{-12}$ m at 10 TeV. If we used $\beta^* = 5$ mm (as at SLC) our spot area would be 24×10^{-15} m^2, about 25 times too big. Since β^* cannot be much reduced (on account of σ_L) the emittance must be reduced. Spot size is extremely small.

Case C

$$\begin{cases} L = 10^{32}\ \text{cm}^{-2}\ \text{s}^{-1} \\ P_{beam} = 10\ \text{MW}\ \ \text{(one beam)} \\ E = 1\ \text{TeV} \end{cases}$$

$$fA = 4 \times 10^{-9}\ \text{m}^2$$

Choosing

$$f = 4000\ \text{Hz}$$

implies

$$A = 10^{-12}\ \text{m}^2$$

$$N = 1.5 \times 10^{10}\ \text{particles per bunch}$$

Then for

$$D = 1 \qquad \text{(Arbitrary choice)}$$

$\sigma_L = 3.5$ mm

$\delta = 0.8\%$

σ_L could be smaller, e.g.

($\sigma_L = 0.8$ mm

$\delta = 0.1\%$)

Emittance comparison:

ε (1 TeV) $= 1.5 \times 10^{-11}$ m (SLC). If we use $\beta^* = 5$ mm (SLC), spot area would be $0.24 \times 10^{-12}\ \text{m}^2$ so we may increase β^* and we need no improvement in emittance.

BEAMSTRAHLUNG IN HIGH ENERGY - HIGH LUMINOSITY COLLISIONS

J. Buon,
LAL, Orsay, France.

G. Coignet
LAPP, Annecy-le-Vieux, France

ABSTRACT
This paper gives rough estimates of the beamstrahlung from colliding beams for cases considered by the Workshop, including the quantum corrections to the classical treatment.

The beamstrahlung is the synchrotron radiation emitted when two e^+, e^- bunches collide. It results from the interaction between each particle and the electromagnetic field generated by the opposite bunch.

For a bunch of N particles with transversal area $A = \pi\sigma_x^2$ and longitudinal dimension σ_z, beamstrahlung leads to a beam energy spread $\Delta E/E$ during the collision. In the classical treatment of synchrotron radiation, it is defined[1] by the beamstrahlung parameter

$$\delta = \frac{1}{3\sqrt{3}} \frac{r_o^3 N^2 \gamma}{\sigma_x^2 \sigma_z}$$

which increases when energy and luminosity increase.

At high electron energy, that is when the critical energy E_c of the emitted photon is comparable with the beam energy, quantum corrections have to be applied; they tend to reduce the energy spread computed with classical formulae but $\Delta E/E$ has to be estimated for each particular case. Useful formulae and curves have been taken from Refs. 2) and 3). An average value of the magnetic field $B^{av} = B^{max}/2$ has been used.

The following table summarizes rough estimates of beamstrahlung for two cases which have been considered in this workshop.

For a 1 TeV x 1 TeV e^+e^- collider with $L = 10^{32} cm^{-2} s^{-1}$ the breamstrahlung produces an energy spread still relatively small (< 1%).

On the contrary for a 5 x 5 TeV e^+e^- collider with very high luminosity ($10^{34} cm^{-2} s^{-1}$), the critical energy becomes larger than 1 TeV and the beamstrahlung emission leads to a large energy spread, even for moderate values of the disruption factor D. It can be reduced by decreasing the number N of particles per bunch and the beam spot size, at the expense of a higher repetition rate, but keeping the total beam power constant.

1) See for example Report of Group 1 of Proceedings of the Second ICFA Workshop on Possibilities and Limitations of Accelerators and Detectors, Les Diablerets, Switzerland, 4-10 October 1979, p. 3.

2) T. Erber et al., Proceedings of the 12th International Conference on High Energy Accelerators, Fermilab, August 11-16, 1983, p. 372.

3) R. Noble, Talk given at Big Collider Study Group, SLAC, June 26, 1984.

	L.Hand + J.Rees case A	C.Rubbia's case		
E	1	5		TeV
L	10^{32}	10^{34}		$cm^{-2}s^{-1}$
P	1	10		Mw
$f A^{eff} = f \frac{A}{H(D)} = \frac{P^2}{L^2}$	$4\times(.1)^2$	$64\times(.005)^2$	$16\times(.01)^2$	$Khz\times\mu m^2$
$N = \frac{P}{fE}$	1.5×10^9	2×10^8	8×10^8	
σ_z	3	3	3	mm
$D.H(D) = \frac{\pi r_o N \gamma_z}{2\gamma A^{eff}}$	1×1	2×5	2×5	
$B^{av} = \frac{50\ N(10^{10})}{\sigma_x \ell}$ $R = \sqrt{A^{eff}/\pi}\ ;\ \ell = 2\sigma_z$	22	60	118	Tesla
$\rho = \frac{10^3\ E}{0.3\ B}$	150	280	140	m
$E_c = \frac{4.44\ E^3}{\rho}$	.029	2	4	TeV
$T = \gamma \frac{B^{av}}{4.4\times10^9}$	.01	.135	.27	
$g(T) = \begin{cases} T^2(1-5.953\ T) & T \ll 1 \\ 0.5563\ T^{2/3} & T \gg 1 \end{cases}$	10^{-4}	.01	.03	
$\Delta E^{QM} = 6.4\times10^3\ g(T)\ 2\sigma_z$	4	380	1200	GeV
$\Delta E^{QM}/\Delta E^{clas}$	.94	.35	.40	
$\Delta E/E$	.4	8	23	%

Table 1

Beamstrahlung estimates

POSSIBLE PARAMETERS OF 1 TeV × 1 TeV TWO-BEAM ACCELERATOR

S. Myers
CERN, Geneva, Switzerland

ABSTRACT

The attached parameters are suggested by the Two-Beam Accelerator group for a 1 TeV × 1 TeV collider with luminosity 10^{33} cm^{-2} s^{-1}.

Nominal Particle Energy	1	TeV
Total length of the Electron LINAC	4.5	km
Gradient of the Conventional LINAC	25	MeV/m
Gradient in the Two-Beam Accelerator	250	MeV/m
Average Power Consumption	125 + 125	MW
Overall Efficiency (P_{beam}/P_{mains})	8	%
Repetition Rate	10	kHz
Energy of Driving Beam	3	MeV
Driving Beam Bunch Length	25	ns
Driving Beam Current	1	kA
Number of High Energy Particles	6.25×10^9	
Length of High Energy Bunch	1.6	mm
β^*	0.5	cm
Disruption Parameter	0.5	
Beamstrahlung Parameter	0.8	%
Luminosity	10^{33}	cm^{-2} s^{-1}
Single Beam Power	10	MW
Transverse Beam Radius $\sigma_{x,y}$	0.17	μm
Emittance/SLC Emittance	0.41	

PARAMETERS FOR A LASER-DROPLET LINAC

R. Palmer
BNL, Upton, NY 11973, USA

ABSTRACT

Parameters are presented for a LINAC using an "ink-jet" droplet structure powered by CO_2 laser light, giving $\sqrt{s}$ = 10 TeV e^+ and e^- collisions at a luminosity of 10^{34} s^{-1} cm^{-2}.

Beam Parameters

Energy	5	TeV
Luminosity	10^{34}	cm^{-2} s^{-1}
Power, beam	2 × 5	MW
R, aspect ratio	1	
N/ε	10^{14}	cm^{-1}
$d = 2\sigma_z$	2	mm
Note, $L \propto (N/\varepsilon)(1/Rd)$		
β^*	2	mm
Disruption	12	
Enhancement (D)	6	
f	10^4	s^{-1}
N macro-bunch	3×10^8	
δ beamstrahlung	50	%
E normalized	3×10^{-8}	
σ^*	1	nm

Laser Parameters

λ	10	μm
Acc. field	20	GeV/m
Laser energy	2 × 1000	J
Laser power	$2 \times 1.7 \times 10^{14}$	watt
Length	2 × 250	m
Electron number to extract all	1.6×10^8	
N micro-bunch	1.5×10^6	
Acc. efficiency	50	%
Laser av. power	2 × 10	MW
Laser efficiency	10	%
Matching efficiency	50	%
Wall power	400	MW

THE CAS-ECFA-INFN WORKSHOP ON THE GENERATION OF HIGH FIELDS FOR PARTICLE ACCELERATION TO VERY HIGH ENERGIES: A SUMMARY

M. Tigner
Cornell University, Ithaca, New York, U.S.A.

ABSTRACT

The Workshop reviewed several of the various approaches to very high energy linear colliders which are now being pursued. Needed beam parameters were discussed as were the particular characteristics and unresolved problems of these approaches. Most recent experimental data bearing on some of the linac schemes were presented.

INTRODUCTION

Our basic objective is to provide accelerators for pushing back the frontiers of particle physics. The consensus is that this will require accelerators producing "elementary" reactions at energies significantly beyond those now available. For this colliding beams are needed. It is believed that high gradient linear colliders will be necessary, particularly for electrons because of synchrotron radiation. They may also be needed for pp, $\bar{p}p$ or ep where the colossal scale and synchrotron radiation will become dominant features at energies beyond those now planned.

It is likely that sometime in the next decade hadron collisions between beams of 10-20 TeV will become available through use of "standard" accelerator methods. They will provide hadronic "elementary" interactions of 2-4 TeV or more in the center of mass thereby setting the time and energy scale for the needed new technology. Thus the first window of opportunity for a major new facility employing one of the new technologies will be for an e^+e^- machine of approximately 1 TeV beam energy, complementary to the precited hadron collider. To achieve pioneering status on the energy frontier, an e^+e^- machine of 5-10 TeV per beam would be required.

While there are many "ifs, ands, and buts" in consideration of needed luminosity, a conservative approach based on physics we know demands a luminosity of at least $10^{32}cm^{-2}sec^{-1}$ for 1 TeV elementary interactions. At least some of the important elementary cross-sections we want to study will decrease as the inverse square of the beam energy so that their investigation at 10 TeV would require a luminosity of 10^{34}. Accordingly it is incumbent on us to explore the technical and economic consequences of providing such luminosities at the higher energies.

In principle one could explore possibilities for linear colliders for e^+e^-, pp, $\bar{p}p$, and ep at multi-TeV energies. At the Workshop we chose to concentrate on e^+e^- colliders for several reasons: no economical way to achieve TeV collisions with these "elementary particles" now exists; at least superficially, multi-TeV e^+e^- interactions promise to be relatively clean; beam energy needed for pioneering work with e^+e^- is about one tenth that required for protons. (Naturally a low cost linac producing more than a few hundred MV per meter would also compete favorably with the synchrotron in acceleration of protons, as has often been observed.)

Our challenge is to find technically feasible means for constructing linear colliders at energies beyond those now achievable. They must produce high luminosity and be more cost effective than current technology.

GENERAL RULES FOR e^+e^- COLLIDERS

Independent of the type of accelerator device there are certain basic relations among beam parameters which must be maintained. These put certain engineering constraints on the overall collider design.

The basic particle physics parameters are:

Beam Energy	$\gamma m_0 c^2$
Luminosity (Reaction Rate = L x Reaction Cross-section)	L $[cm^{-2}sec^{-1}]$
Fractional Energy Spread (Accumulated during collision due to "beamstrahlung")	δ

The associated accelerator parameters which influence technical feasibility and cost are:

Beam Power	P_b (power)
Repetition Rate	f (Hertz)
Bunch Population	N (number)
Bunch Area at Collision	A $(\text{length})^2$
Disruption Parameter	D (number)
Focusing Parameter at Collision	β^* (length)
RMS Beam Size at Collision	σ^* (length)
Beam Emittance	ϵ (length x angle)

$$\epsilon = \frac{\sigma^{*2}}{\beta^*}$$

RMS Bunch Length	σ_l (length)

For a simple, cylindrical, gaussian beam without pinching or quantum corrections taken into account the basic relations are given below. More general and sophisticated versions of these relations can be found in Refs. 1, 2, 3.

$$L = \frac{f N^2}{A} \qquad D = \frac{2\pi r_o \sigma_\ell N}{\gamma A}$$

$$A = 4\pi\sigma^{*2}$$

$$P_b = fN\gamma m_o c^2 \qquad \delta = \frac{4\pi}{3\sqrt{3}} \frac{r_o^3 N^2 \gamma}{A\sigma_\ell}$$

NOTES

1. $P_{AC\ total} = \left[P_o + \frac{P_b}{\eta_{tot}}\right] \times 2$; η_{tot} = total conversion efficiency

   one usually assumes $P_o << P_b/\eta_{tot}$ but this must be checked for each type of accelerator.

2. $D > 1$ Self-pinch mode - may increase both L and δ by same factor. Desired regime of operation (see Ref. 1).

   $D << 1$ Inefficient use of beam.

   $D >> 1$ Self-focus unstable - not useful.

3. δ formula invalid when critical energy of "beamstrahlung" exceeds nominal beam energy (see Ref. 3) and contributed paper to this workshop by Buon and Coignet.

4. Since P_b will be closely connected with cost it must be kept as small as possible. For a fixed L we need to keep N small to control power. This means one must strive for the smallest possible A.

There are many ways to use these relations depending on the constraints which may be imposed. One rather straightforward way which is useful for illustrative purposes is given by the following algorithm:

1. Choose γ, L, P_b guided by physics needs and your best guess about economics. These choices above determine

$$f\,A = P_b^2/L\,(\gamma m_o c^2)^2$$

2. The product f A being now fixed, we might select f guided by hardware considerations. Now A and

$$N = P_b/f\gamma m_o c^2$$

are determined.

3. Set D = 1 (or something slightly larger - no experimental data yet) and determine

$$\sigma_L = \frac{\gamma A D}{2\pi r_o N}$$

4. Check $\delta = \dfrac{4\pi r_o^3 L\gamma}{3\sqrt{3}\,\sigma_\ell f}$ If not ok then iterate again.

5. As a measure of the difficulty in producing and focusing the beam described by the above calculations, find the product $\beta^*\varepsilon = A/4\pi$ and compare with the design value for the SLC, i.e.,

$$\beta^* = 5 \text{ mm}; \quad \varepsilon = \frac{3\times10^{-5}}{\gamma} \text{ meter.}$$

Maintenance of this small emittance in the face of various dilution effects will be a substantial technological challenge.

Some illustrative examples of the product f A are given in Tables 1 and 2 below. These are not parameters the accelerator will achieve. They are parameters it must be built to achieve. Some of the combinations shown in the tables may be technically impossible.

Table 1

$L = 10^{32}$

E_b(TeV) \ P_b (mw)	1	3	10
1	40 * 0.01	350	4000 * 1.0
10	0.4	3.5 * 0.01	40 * 0.1
100	4×10^{-3}	3.5×10^{-2}	0.4 * 0.01

f A in μ^2 Hertz

Table 2

$L = 10^{34}$

E_b(TeV) \ P_b (mw)	1	3	10
1	0.4	3.5	40 * 0.01
10	4×10^{-3}	3.5×10^{-4}	0.4 * 0.001
100	4×10^{-5}	3.5×10^{-4}	4×10^{-3} * 0.0001

Numbers with * are ratios of A required to A_{SLC} projected to the appropriate γ assuming $\varepsilon\gamma$ = const. Also assumed are β^* = 5 mm, independent of γ, and f = 4 kHz.

Note that only in the case of highest beam power and lowest energy and luminosity is the beam area needed as large as that projected for the SLC. The total AC power required for that machine will be

$$P_{AC} > \frac{10\ \text{MWx2}}{\eta_T} = \frac{2\ \text{GW}}{\eta_T(\%)}$$

One can summarize by saying that if we hope to make significant luminosities at energies significantly higher than now achieved without improbably high capital and power cost we need:

- higher accelerating fields
- less emittance dilution
- higher efficiency
- lower emittance sources
- stronger focusing

in comparison with current technological achievements.

PARTICULAR APPROACHES TO NEW ACCELERATOR DEVICES

A. Near Field Devices

As described in Lawson's introductory discussion of accelerator physics, these devices convert the energy of an EM wave into kinetic energy of beam particles near the surface of conductors (or dielectrics) arranged so that the EM wave velocity equals that of the particle. Four types of device fitting this category were discussed at the workshop.

1. "Normal" Linac

This time honored device is undergoing further development towards optimization for collider use in SLAC, Novosibirsk and by the Japanese Lasertron group. An iris loaded wave guide, manufactured carefully to avoid sparking at high fields is driven by some dc to microwave conversion device such as a klystron, lasertron, gyrocon, etc. operating at $\lambda \leq 10$ cm. So far peak surface fields of 200 MV/m (100 MV/m accelerating) have been achieved. The maximum practical value is not known and will depend on pulse length as well as surface conditions, being higher for shorter pulses. The peak power achieved by Klystrons of the type useful for accelerators is 50 MW with a short pulse conversion efficiency of about 25 percent. The lasertron is expected to be capable of much higher power and efficiency. So far the Japanese group, reporting to this workshop, has achieved 1.6 kW at $\lambda \sim 10$ cm. Expectations are that lasertron units producing power 100 MW, or much greater, of efficiencies

greater than 80 percent are possible. In addition to the Japanese work there is a lasertron development program at SLAC.

While it has yet to be demonstrated, expectations are that efficiencies of transfer of rf power to beam power of 25 percent may be achieved with derivatives of the traditional linac structure.

The technical challenges faced by developers of the traditional linac are

- measurement of maximum field value
- improved rf-beam energy transfer for collider style beams
- higher power and higher efficiency rf services
- cut component costs
- understanding of scaling laws to find optimum λ. Note that if we could vary all accelerator parameters (ε, f, β, ...) at will, reducing λ helps. There are, however, practical limits which alter scaling to rob us of advantage of reducing λ beyond source value. More thought and experiments are needed to understand this.

2. Two-Beam Accelerator

In this scheme the accelerating wave is supported by a loaded wave guide also and the low current, high energy beam being accelerated passes down this wave guide. Parallel to it in the same or in a closely coupled waveguide of special design, the high current, low energy beam which is the basic energy source travels. Its kinetic energy is converted to the wanted EM radiation by free electron laser action, the lost energy being periodically restored by passing the source beam through an induction accelerator unit.

This concept is being pursued by Sessler and coworkers of LBL and LLNL. A prototype FEL operating at $\lambda \simeq 1$ cm has produced about 100 MW peak power into a 1 percent bandwidth.

The technical challenges faced by developers of this approach are;

- high efficiency lasing with reacceleration of the source beam
- suitable accelerating structure matched to the bandwidth of the source and capable of supporting high gradient while providing high rf-beam energy transfer efficiency
- cost estimates for a complete accelerator
- method for accommodating the path length differences between the sinuous source beam and the straight high energy beam.

3. Conducting Droplet Linac

The gradient of the more traditional linacs is certainly limited by spark or melting induced destruction of the conducting surfaces. This limit is expected to be in the 100 to a very few hundred MV/m range. If the near field structure supporting the accelerating wave were disposable after each pulse then this limit might be raised substantially. With this in mind R. Palmer (BNL) has suggested the use of an array of liquid droplets as the near field structure. The droplet array would be produced by modulating the streams from micro nozzles such as those used in ink jet printers. Drive power would come from a laser. The droplets would be made conducting by ionizing their surfaces, perhaps with the driving laser itself. Current thought is to use 10 μ radiation to capitalize on the already extensive developments of high power CO_2 lasers. Technical challenges which must be met are;

- formulation of precision droplet streams of 1 μ droplets (required tolerances yet to be studied)
- formation of surface plasma for needed time duration
- development of a suitable feed method for laser to structure coupling
- understanding of beamloading and wake characteristics of the droplet structure.
- demonstration of superior peak field performance

- development of a 10 ps laser with high rep rate and good conversion efficiency.

Experiments using a copper grating as the near field structure will begin in 1985 as a collaboration of BNL and NRC and AECL in Canada.

In both the traditional linac two beam accelerator and the droplet accelerator, the accelerating wave is built up resonantly from a relatively narrow band power source. Broadband accelerators are also being studied:

4. Wakefield Accelerators

The kinetic energy of a bunched beam can be converted into broad band electromagnetic field energy in the form of a pulse on a transmission line by passing the beam through a periodic structure. This wake pulse can subsequently be used to accelerate other particles. A form of this accelerator being developed by Voss and Weiland at DESY is termed the Wakefield Transformer. Calculation shows that a low current high energy beam of particles each having 20 or more times the kinetic energy of the high current, low energy source beam particles should be possible. In the DESY device a ring of electrons is formed by laser photo excitation of a ring shaped cathode. The ring is subsequently accelerated in a conventional linac after which it is introduced into the wake field transformer where it gives up most of its energy to the wake fields. The wake energy, deposited near the perimeter of a cylindrical structure, is reflected from the perimeter and travels, in the form of a pulse on a parallel plate, radial transmission line, towards the center, being geometrically compressed as it propagates. The radial compression results in multiplication of the local field in the pulse. It is believed that effective accelerating fields of 100 mV/m or more can be achieved. When the pulse has reached the center, a low current beam pulse, the high energy beam, is shot through on the central axis,

extracting energy from the compressed pulse. At DESY the photo-cathode, drive linac for ring acceleration, solenoidal ring transport system and wake field transformer are all under construction for test in 1985.

Some work along similar lines in which an electron beam is used as the source of wake energy was reported at the workshop by researchers from the University of Osaka.

Technical challenges for the developers of the wake field transformer (WFT) are:

- stable ring formation of needed high current by photomodulated electron gun
- stable acceleration of the high current rings in the driver linac
- stable ring compression
- stable deceleration of the high current rings, in the WFT
- provision of sufficient focusing in high energy beam channel of WFT to counteract transverse wake forces due to ring misalignment.

As pointed out some years ago by workers at Novosibirsk, the kinetic energy of a proton beam such as might be accelerated in one of the big synchrotrons or storage rings can also be converted to wake energy in a periodic linac type structure. A following electron beam of lower current, propagating along the same axis could pick up a fraction of that total energy. In this coaxial version of the scheme the kinetic energies of the accelerated and source beam particles will be comparable although some small multiplication may be effected. (A possible arrangement for an electron collider driven by such a "proton klystron" is found in a workshop paper by A. Ruggiero.)

B. Far Field Devices

The only possibility known in this class is the inverse free electron laser. As far as we know now, synchrotron radiation will limit this

device to about 300 GeV. Perhaps a new idea in the future will show how to increase the limit.

C. Media Accelerators

Of several devices studied the plasma beat-wave genre of Tajima and Dawson seems most interesting. Both laser and beam excited versions have been discussed. The laser excited type is most studied and appears to be the more efficient from our current perspective. In it, a tightly focused, very short, two frequency, laser pulse organizes a plasma of carefully controlled density, exciting a longitudinal Langmuir wave capable of accelerating particles. It is predicted that effective accelerating fields of several GV/m can be achieved. The wave generated when the frequency difference of the two laser beam components is just the plasma frequency can be made very close to light velocity. In the most straightforward layout of such an accelerator the laser and particle beams are coaxial and the phase slip between wave and particle limits each accelerating stage to lengths of a few meters. In more sophisticated versions the beams travel at an angle to compensate for the phase slip. By such means it may be possible to increase the stage length. The most favorable operating wavelength appears to be in the 0.25 to 10 micron range. On the basis of limited information, the overall efficiency of such devices has been estimated to be in the 10^{-3} to 10^{-4} range.

In separate experiments the existence of the beat wave and the acceleration of particles by a Langmuir wave has been demonstrated. Current experimental work concentrates on elucidation of the physics of the beat wave. To be understood are such questions as;

- how exactly must $\Delta\omega = \omega_p$?
- what is rise time of beat wave?
- what is saturation amplitude of beat wave?

- how long can the coherent wake train be?
- what are competing processes (e.g., stimulated Brillouin scattering; stimulated Raman scattering, etc.)?
- is self-focusing of the laser possible and/or desirable under accelerator conditions?

Experiments to elucidate these issues are now under way at UCLA. Soon to start will be similar experiments at RAL with collaboration from from Imperial College and CERN. Work is also being carried out by LANL/WR, NRL/Cornell, FNAL/LANL/Wisconsin collaborations as well as at University of Texas and SLAC. The beam excited version is being studied at UCLA and SLAC.

Should the answers to all these questions turn out satisfactorily from the accelerator point of view there remain the issues of efficiency improvement, the need for short pulse, high efficiency lasers and the multiple scattering of the beam in the plasma.

D. Sources

Possible accelerator optimized sources in the microwave, millimeter, infrared and visible were discussed in conjunction with the various acceleration schemes. In some bands the needed peak powers have been achieved. In no case is the ideal source available today. In the lower frequencies, higher peak powers are still needed. In all frequency bands, there will need to be substantial developments to produce shorter pulse lengths of high coherence with at least multikilohertz repetition rate and good conversion efficiency.

Evidently such sources are needed only for accelerator work at the moment so it will be up to the accelerator community to press for their development.

E. Beam Handling

Common to all the schemes is the need to produce submicron beam spots at the collision point. Only by this means can one hope to achieve needed luminosity at acceptable power levels with the single pass electron linear collider method. Higher brightness beam sources, better control of brightness dilution and tighter focusing methods would all contribute improvement. Particularly helpful would be the development of focusing channels which can accommodate significant energy spreads. Basic to success in all of these will be methods of beam position and distribution measurement and control at the submicron level which can be used with TeV beam energies.

Experiments at the SLC will shed some light on these needs. Other precision beams such as that being readied for NA-34 at CERN could be extended to investigate beam handling and control problems, perhaps even at the 100Å level.

CONCLUSION

Good progress in developing the various single pass linac schemes so far mentioned is being made. While one has grounds for being optimistic it is not yet clear that any of these approaches will prove viable in the end. Some may not achieve the required cost effectiveness. Some may prove technically unfeasible. Some may have fundamental flaws not yet seen. Thus there is still plenty of room for completely new ideas about other approaches.

Some of the open questions we have about any of the proposed methods may hide other important questions. Thus it is most important to get on with pursuing the questions we know as soon as possible. Growth of interest in attacking these problems is encouraging. More active interest is needed.

Common to all schemes is the need for improvement in power sources, beam sources, confinement and control. By attacking these early on we can make clearer the full range of constraints on the accelerators themselves.

Progress in experiments over the past two years has been substantial. It is likely that results to be obtained in the next two years will have a profound influence on our understanding of these urgent matters.

* * *

REFERENCES

1) B. Richter, "SLC and Future Linear Colliders", 12th International Acc. Conf., FNAL 1983.

2) P. Wilson, "High Pulse Power rf Sources for Linear Colliders", 12th International Acc. Conf., FNAL 1983.

3) H. Wiedemann, "Linear Collider, A Preview", SLAC Pub 2849, Nov. 1981.

Discussion

J. Buon, Orsay

I think you were a little too pessimistic about the highest luminosity case, 10^{34} cm^{-2} s^{-1} at 1 TeV, regarding the disruption factor which is obtained from a "reasonable" bunch length. In fact, the disruption factor is inversely proportional to the unperturbed cross-section of the beam at the collision point and without taking into account the pinch effect. This gives a much lower disruption figure. G. Coignet and I have derived relatively reasonable parameters in this case and even at higher luminosity. In the Rubbia case we have 5 TeV with 10^{34} cm^{-2} s^{-1} of luminosity, with a bunch length of a few millimetres, a beam power of 10 MW and 10-60 kHz repetition rate, while maintaining a disruption factor of the order of 2.

Answer

I have to apologise. I was just giving an example of how that algorithm can go wrong if you just follow it blindly. I agree that there are reasonable solutions.

LIST OF PARTICIPANTS

BAILEY, D., CERN, Geneva, Switzerland
BARLETTA, W.A., Lawrence Livermore Nat. Lab., Livermore, Calif., USA
BELLETTINI, G., Univ. of Pisa, Italy
BIALOWONS, W., DESY, Hamburg, Fed. Rep. Germany
BINGHAM, R., Rutherford Appleton Lab., Didcot, United Kingdom
BIZZARI, U., Ente Naz. Energie Alternative, Frascati, Italy
BOBIN, J.L., Univ. Pierre et Marie Curie, Paris, France
BRYANT, P.J., CERN, Geneva, Switzerland
BUON, J., Lab. de l'Accélérateur linéaire, Orsay, France
CAIRNS, R.A., Univ. of St. Andrews, Fife, United Kingdom
CASTELLANO, M., Ist. Naz. di Fisica Nucleare, Naples, Italy
CHAN, D., Chalk River Nuclear Lab., Chalk River, Canada
CHATTOPADHYAY, S., CERN, Geneva, Switzerland
CHEN, K.W., Univ. of Texas, Arlington, Texas, USA
CLAUS, J., Brookhaven Nat. Lab., Upton, NY, USA
CLINE, D., CERN, Geneva, Switzerland
COIGNET, G., Lab. d'Annecy de Physique des Particules, Annecy-Le-Vieux, France
COLTON, E.P., Los Alamos Nat. Lab., Los Alamos, NM, USA
COURANT, E.D., Brookhaven Nat. Lab., Upton, NY, USA
CUTOLO, A., Univ. of Naples, Italy
DANGOR, A.E., Imperial College, London, United Kingdom
DAWSON, J.M., Univ. California, Los Angeles, Calif., USA
DOME, G., CERN, Geneva, Switzerland
DYMOKE-BRADSHAW, A.K.L., Imperial College, London, United Kingdom
DUPONT, M., Univ. Clermont-Ferrand II, Aubière, France
EVANS, R.G., Rutherford Appleton Lab., Didcot, United Kingdom
FISCHER, W., Swiss Inst. for Nuclear Research, Villigen, Switzerland
FRANK, K., Univ. Erlangen-Nuremberg, Erlangen, Fed. Rep. Germany
FUNK, L.W., Chalk River Nuclear Lab., Chalk River, Canada
GIRARDEAU-MONTAUT, J.P., Inst. de Physique nucléaire, Villeurbanne, France
GROSSETÊTE, B., Univ. Pierre et Marie Curie, Paris, France
HAND, L.N., Cornell Univ., Ithaca, NY, USA
HASEROTH, H., CERN, Geneva, Switzerland
HENKE, H., CERN, Geneva, Switzerland
JAMESON, R.A., Los Alamos Nat. Lab., Los Alamos, NM, USA
JOHNSEN, K., CERN, Geneva, Switzerland
JOSHI, C., Univ. California, Los Angeles, Calif., USA
JOWETT, J., CERN, Geneva, Switzerland
KARTTUNEN, S.J., Technical Research Centre of Finland, Helsinki, Finland
KAWASKI, S., Kanazawa Univ., Ishikawa, Japan
KEEFE, D., Lawrence Berkeley Lab., Berkeley, Calif., USA
KLEIN, H., Inst. of Applied Physics, Frankfurt-on-Main, Fed. Rep. Germany
KOLOMENSKY, A.A., Lebedev Physical Inst., Moscow, USSR
KORSCHINEK, G., Technische Univ. München, Garching, Fed. Rep. Germany
KREJCIK, P., Kernforschungsanlage, Jülich, Fed. Rep. Germany
LAING, E., Univ. of Glasgow, United Kingdom
LAWSON, J.D., Rutherford Appleton Lab., Didcot, United Kingdom
LE DUFF, J., Lab. de l'Accélérateur linéaire, Orsay, France
LENGELER, H., CERN, Geneva, Switzerland
MILLS, F., Fermi Nat. Lab., Batavia, Ill., USA
MÖHL, D., CERN, Geneva, Switzerland
MONTAGUE, B.W., CERN, Geneva, Switzerland

MULVEY, J., Univ. of Oxford, United Kingdom
MYERS, S., CERN, Geneva, Switzerland
NATION, J., Cornell Univ., Ithaca, NY, USA
PABST, M., Kernforschungsanlage, Jülich, Fed. Rep. Germany
PALMER, R.B., Brookhaven Nat. Lab., Upton, NY, USA
PALUMBO, L., Univ. 'La Sapienza', Rome, Italy
PEREZ Y JORBA, J., Lab. de l'Accélérateur linéaire, Orsay, France
PLACIDI, M., CERN, Geneva, Switzerland
PREGER, M., Lab. Naz. dell'INFN, Frascati, Italy
QUERROU, M., Univ. de Clermont-Ferrand, Aubière, France
REES, J.R., Stanford Linear Accelerator Center, Stanford, Calif., USA
RENIERI, A., Ente Naz. Energie Alternative, Frascati, Italy
RUBBIA, C., CERN, Geneva, Switzerland
RUGGIERO, A.G., Fermi Nat. Lab., Batavia, Ill., USA
RUSTAGI, K., École Polytechnique, Palaiseau, France
SACTON, J., Inter-University Inst. for High-Energy Physics, Brussels, Belgium
SCHNELL, W., CERN, Geneva, Switzerland
SESSLER, A.M., Lawrence Berkeley Lab., Berkeley, Calif., USA
SIGEL, R., Max-Planck-Institut für Quantenoptik, Garching, Fed. Rep. Germany
SUDAN, R.N., Cornell Univ., Ithaca, NY, USA
SUTTER, D., US Dept. of Energy, Washington, DC, USA
TAJIMA, T., Univ. of Texas, Austin, Texas, USA
TAKEDA, S., Osaka Univ., Osaka, Japan
TAZZARI, S., CERN, Geneva, Switzerland
TIGNER, M., Cornell Univ., Ithaca, NY, USA
VACCARO, V.G., Univ. of Naples, Italy
WARREN, J.B., TRIUMF, Vancouver, Canada
WEILAND, T., Deutsches Elektronen-Synchrotron, Hamburg, Fed. Rep. Germany
WILSON, P.B., Stanford Linear Accelerator Center, Stanford, Calif., USA
WILSON, E.J.N., CERN, Geneva, Switzerland
WILLIS, W., CERN, Geneva, Switzerland
WITTE, K.J., Max-Planck-Institut für Quantenoptik, Garching, Fed. Rep. Germany
WURTELE, J., Lawrence Berkeley Lab., Berkeley, Calif., USA
ZOTTER, B., CERN, Geneva, Switzerland
ZYNGIER, H., Univ. de Paris-Sud, Orsay, France